frontiers | Research Topics

Prognostic and predictive factors in autoimmune connective tissue disorders

Edited by
Francesca Wanda Rossi and Mohammed Osman

Coordinated by
Ilaria Mormile

Published in
Frontiers in Immunology

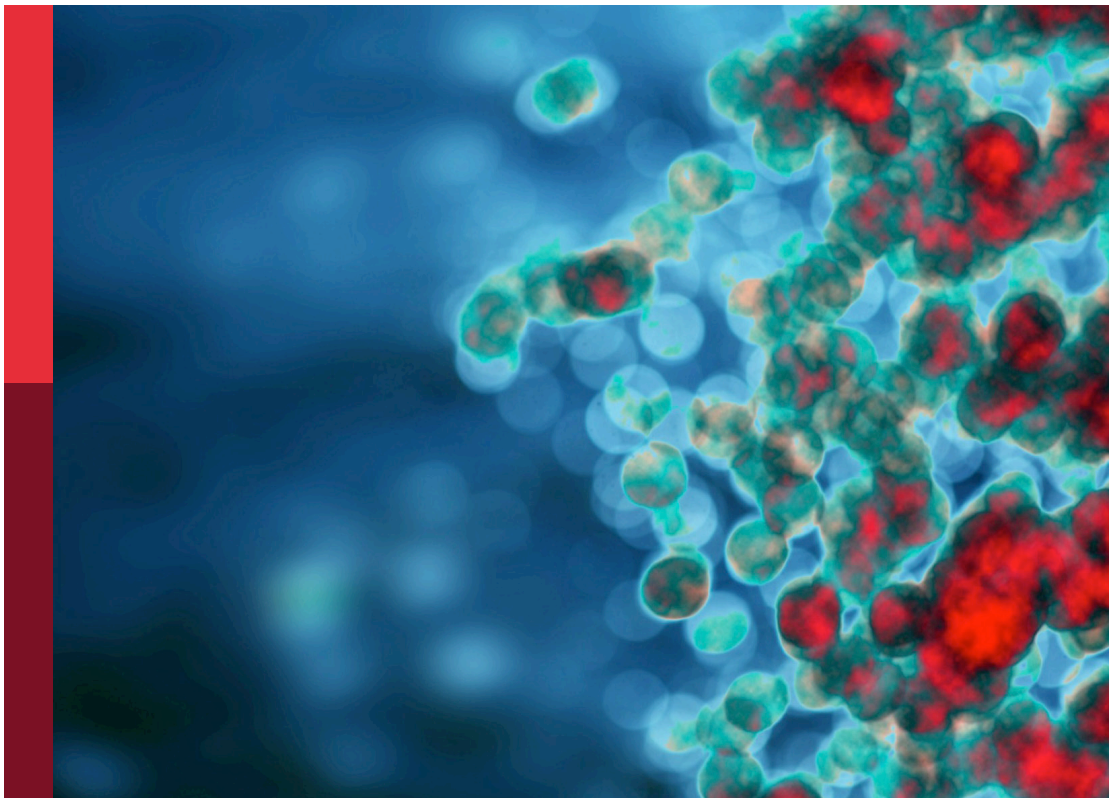

ISSN 1664-8714
ISBN 978-2-8325-5383-1
DOI 10.3389/978-2-8325-5383-1

About Frontiers

Frontiers is more than just an open access publisher of scholarly articles: it is a pioneering approach to the world of academia, radically improving the way scholarly research is managed. The grand vision of Frontiers is a world where all people have an equal opportunity to seek, share and generate knowledge. Frontiers provides immediate and permanent online open access to all its publications, but this alone is not enough to realize our grand goals.

Frontiers journal series

The Frontiers journal series is a multi-tier and interdisciplinary set of open-access, online journals, promising a paradigm shift from the current review, selection and dissemination processes in academic publishing. All Frontiers journals are driven by researchers for researchers; therefore, they constitute a service to the scholarly community. At the same time, the *Frontiers journal series* operates on a revolutionary invention, the tiered publishing system, initially addressing specific communities of scholars, and gradually climbing up to broader public understanding, thus serving the interests of the lay society, too.

Dedication to quality

Each Frontiers article is a landmark of the highest quality, thanks to genuinely collaborative interactions between authors and review editors, who include some of the world's best academicians. Research must be certified by peers before entering a stream of knowledge that may eventually reach the public - and shape society; therefore, Frontiers only applies the most rigorous and unbiased reviews. Frontiers revolutionizes research publishing by freely delivering the most outstanding research, evaluated with no bias from both the academic and social point of view. By applying the most advanced information technologies, Frontiers is catapulting scholarly publishing into a new generation.

What are Frontiers Research Topics?

Frontiers Research Topics are very popular trademarks of the *Frontiers journals series*: they are collections of at least ten articles, all centered on a particular subject. With their unique mix of varied contributions from Original Research to Review Articles, Frontiers Research Topics unify the most influential researchers, the latest key findings and historical advances in a hot research area.

Find out more on how to host your own Frontiers Research Topic or contribute to one as an author by contacting the Frontiers editorial office: frontiersin.org/about/contact

Prognostic and predictive factors in autoimmune connective tissue disorders

Topic editors
Francesca Wanda Rossi — University of Naples Federico II, Italy
Mohammed Osman — University of Alberta, Canada

Topic coordinator
Ilaria Mormile — University of Naples Federico II, Italy

Citation
Rossi, F. W., Osman, M., Mormile, I., eds. (2024). *Prognostic and predictive factors in autoimmune connective tissue disorders*. Lausanne: Frontiers Media SA.
doi: 10.3389/978-2-8325-5383-1

Topic Editor Dr. Mohammed Osman has an unrestricted research grant from Boehringer Ingelheim (BI) and have done advisory boards for BI and for Mallinckrodt pharmaceuticals in the last 2 years; The other Topic Editors declare no competing interests with regard to the Research Topic subject.

Table of contents

frontiers | Frontiers in Immunology

TYPE Editorial
PUBLISHED 29 July 2024
DOI 10.3389/fimmu.2024.1465572

OPEN ACCESS

EDITED AND REVIEWED BY
Betty Diamond,
Feinstein Institute for Medical Research,
United States

*CORRESPONDENCE
Mohammed Osman
mosman@ualberta.ca

RECEIVED 16 July 2024
ACCEPTED 18 July 2024
PUBLISHED 29 July 2024

CITATION
Mormile I, Osman M and Rossi FW (2024) Editorial: Prognostic and predictive factors in autoimmune connective tissue disorders. *Front. Immunol.* 15:1465572. doi: 10.3389/fimmu.2024.1465572

Editorial: Prognostic and predictive factors in autoimmune connective tissue disorders

Ilaria Mormile[1], Mohammed Osman[2]* and Francesca Wanda Rossi[1,3]

[1]Department of Translational Medical Sciences, University of Naples Federico II, Naples, Italy, [2]Division of Rheumatology, Department of Medicine, University of Alberta, Edmonton, AB, Canada, [3]Center for Basic and Clinical Immunology Research (CISI), University of Naples Federico II, World Allergy Organization (WAO) Center of Excellence, Naples, Italy

KEYWORDS

biomarkers, autoimmunity, autoimmune diseases, adaptive immunity, innate immunity, inflammation, connective tissue disorders

Editorial on the Research Topic
Prognostic and predictive factors in autoimmune connective tissue disorders

Autoimmune connective tissue diseases (CTD) are a complex group of diseases involving multiple organs and resulting in devastating visceral complications and even death. One of the most recognized challenges related to them is their variable disease courses that range from indolent ones to rapidly progressive clinical disease trajectories. This disease-associated heterogeneity is associated with differences in the severities of organ involvement, disease-specific damage accrual, autoantibody profiles, response(s) to treatment, and, ultimately, long-term survival. Hence, prognostic biomarkers that are ideally associated with the pathogenesis of these diseases are desperately needed.

In this Research Topic, "Prognostic and Predictive Factors in Autoimmune Connective Tissue Disorders", submissions were solicited for original research articles, brief research reports, and review papers with a particular emphasis on novel serological biomarkers of disease severity, evaluation of gene expression and protein levels of inflammatory mediators, adhesion proteins, cytokines, and pro-resolving molecules, recent applications of routinary laboratory parameters and instrumental techniques for assessing disease severity and systemic involvement, and development of new multi-parametrical disease activity score for autoimmune CTD. Since the Research Topic was open to submission, 39 manuscripts were submitted, of which 27 were rejected, and 12 were published. The Research Topic was viewed about 20,500 times, highlighting the scientific community's interest in the subject, and its relevance to patients.

An original research article by Atzeni et al. evaluated the soluble receptor for advanced glycation end products (RAGE) and its ligand high mobility group box 1 (HMGB1) as a potential predictor of pulmonary arterial hypertension (PAH) in systemic sclerosis (SSc). SSc (in general) and PAH (in particular) are characterized by a systemic progressive obliterative vasculopathy. Both interstitial lung disease (ILD) and PAH significantly impact the long-term survival of SSc patients. Early in the disease, SSc patients may develop pulmonary hypertension which may stem from ILD or PAH. Notably, there are no

biomarkers can preferentially identify patients developing these complications. The authors demonstrated that high systemic levels of sRAGE in SSc patients at baseline might be useful for predicting new-onset PAH. Indeed, sRAGE were much lower in patients who developed ILD, suggesting that elevated sRAGE may be more specific for PAH in SSc patients. Also, sRAGE levels were inversely proportional to patient survival. Future studies assessing a role for sRAGE in promoting vasculopathy (e.g., cardiovascular disease), or in resistant pulmonary arteries may provide added insights related to its role in the pathogenesis of SSc as both complications are more common in this group of patients (compared to age and sex-matched controls).

Zheng et al. focused on developing and validating a new diagnostic prediction model using machine learning and differential expression of ENHO and NOX4 for the progression of skin fibrosis in skin from patients with SSc. Increased ENHO and NOX4 are associated with immune cell activation and fibroblast, respectively, both of which play a pivotal role in the pathogenesis and progression of SSc. The goal set by the authors is valuable since patients with rapidly progressive forms of diffuse SSc have a small window for clinical intervention with immunomodulation. Hence, early identification of these patients may result in improved survival, whereas poor identification of these patients may result in increased disease-associated morbidity and poor outcomes.

Other notable contributions related to the development of predictive biomarkers were provided by Zhang et al. and Wang et al. Using peptidomics, Zhang et al. were able to identify three peptides (sequence: DSGEGDFLAEGGGVRGPR, NGFKSHAL, ISEQFTAMFR) in sera from patients with AS that promoted the proliferation of fibroblasts derived from patients with AS. This is highly relevant to the pathogenesis of AS, as fibroblasts in AS are known to promote one of the earliest changes related to new bone formation. Further to this, Wang et al. performed a two-sample Mendelian randomization and meta-analysis and found that elevated levels of serum lipid metabolites may contribute to the development of autoimmune diseases.

Other authors in this Research Topic focused on patients with severe outcomes related to dermatomyositis (DM). Rapidly progressive ILD (RP-ILD) is a major cause of death in patients with anti-melanoma differentiation-associated gene 5 positive DM (anti-MDA5+DM). Wang et al. used Cox proportional hazards models to identify risk factors of RP-ILD. In particular, the authors selected four independent risk factors and then created a new RP-ILD risk prediction model, which was designated as the CROSS score (comprised of elevated C-reactive protein (CRP) levels, anti-Ro52 antibody positivity, male sex, and short disease duration < 3 months from disease onset). Predictors of RP-ILD in anti-MDA5+ DM were also evaluated by Li et al., along with assessing prognostic factors. The analysis conducted in 73 MDA5+ DM patients showed that elevated lactate dehydrogenase (LDH) and elevated prognostic nutritional index (PNI) were independent prognostic factors. Moreover, an elevated LDH was an independent risk factor for RP-ILD (> 356 U/ml with a mortality rate of approximately 65% after 3 years). In another research article by Dong et al., the anti-carbamylation protein antibodies (anti-CarPA) assessment was proposed as a prediction biomarker for the development of ILD in patients with PM/DM, rheumatoid arthritis, and primary Sjögren's syndrome. Finally, Ji et al. compared clinical characteristics and risk factors for mortality between clinically amyopathic dermatomyositis (CADM) and classic DM (CDM) to clarify the distribution and impact of anti-MDA5 antibodies in patients with these conditions. The retrospective case-control study, which included 330 patients showed that CADM patients display higher anti-MDA5 antibody levels, worse symptoms, and worse prognosis, often requiring an earlier and more aggressive treatment than CDM.

In an intriguing study by Wang et al., the authors determined the probability of response to treatment in lupus nephritis by closely examining the tubulointerstitial macrophage infiltrations in 430 patients at the time of the renal biopsy. Importantly, the density of tubulointerstitial macrophage infiltration is a favorable independent predictor for treatment response (with an AUC of 0.78). Hence, this simple predictive biomarker could be added to the clinicopathological data at the time of biopsy for improved risk stratification. Renal involvement influences the prognosis of several other autoimmune conditions. Further to this, Uchida et al. found that the renal risk score (RRS), which is comprised of the percentage of normal glomeruli, the frequency of tubular atrophy/interstitial fibrosis, and the estimated glomerular filtration rate, is a reliable predictor of renal survival in Japanese patients with ANCA-associated glomerulonephritis.

This Research Topic also included novel observations relevant to patients with autoimmune CTDs. For instance, Maranini et al. presented the first case of a patient with eosinophilic granulomatosis with polyangiitis (EGPA) and middle lobe syndrome, which completely resolved through fiberoptic bronchoscopy, underlying the concept that the identification of this condition in EGPA patients may be essential to guide their management, treatment, and prognostication. Further to this, Xian et al. investigated the correlation between systemic erythematous lupus and Graves' disease. In their study, they suggested that the presence of SLE may potentially increase the risk of Grave's disease, highlighting a unifying common pathway related to immune dysregulation.

In conclusion, the articles published in this Research Topic have led to novel insights related to the prediction of autoimmune CTDs and their sequelae. They also linked previously unrelated clinical observations with laboratory ones to provide additional information related to the diagnosis and prognosis of patients with these diseases. Together, these developments may lead to personalized treatment strategies which may improve the care of patients with these devastating autoimmune diseases.

Author contributions

IM: Writing – original draft, Validation. MO: Writing – review & editing, Validation. FR: Writing – review & editing, Validation.

Conflict of interest

The authors declare that the research was conducted in the absence of any commercial or financial relationships that could be construed as a potential conflict of interest.

The author(s) declared that they were an editorial board member of Frontiers, at the time of submission. This had no impact on the peer review process and the final decision.

Publisher's note

frontiers | Frontiers in Immunology

TYPE Original Research
PUBLISHED 31 January 2023
DOI 10.3389/fimmu.2023.1104351

OPEN ACCESS

EDITED BY
Francesca Wanda Rossi,
University of Naples Federico II, Italy

REVIEWED BY
Saeed Mohammadi,
Golestan University of Medical Sciences, Iran
Zhigang Hu,
Wuxi Children's Hospital, China

*CORRESPONDENCE
Lei Jin
leijin1987@hotmail.com

SPECIALTY SECTION
This article was submitted to Autoimmune and Autoinflammatory Disorders : Autoimmune Disorders, a section of the journal Frontiers in Immunology

RECEIVED 21 November 2022
ACCEPTED 12 January 2023
PUBLISHED 31 January 2023

CITATION
Zhang G-n, Xu Y-j and Jin L (2023) Peptidomics analysis of plasma in patients with ankylosing spondylitis. *Front. Immunol.* 14:1104351. doi: 10.3389/fimmu.2023.1104351

Peptidomics analysis of plasma in patients with ankylosing spondylitis

Guo-ning Zhang[1], Ying-jia Xu[2] and Lei Jin[3]*

[1]Department of Orthopedics, Tongren Hospital, Shanghai Jiao Tong University School of Medicine, Shanghai, China, [2]Department of Laboratory Medicine, Tongren Hospital, Shanghai Jiao Tong University School of Medicine, Shanghai, China, [3]Department of Rheumatology and Immunology, Tongren Hospital, Shanghai Jiao Tong University School of Medicine, Shanghai, China

Background: This study aimed to explore the differential expression of peptides associated with ankylosing spondylitis (AS) patients, enabling identification of potential functional peptides to provide the basis for the novel intervention targets for AS.

Material and Methods: 3 AS patients and 3 healthy volunteers were enrolled in this study. The expression profiles for peptides present in the plasma of AS patients and the healthy individual were analyzed by liquid chromatography-tandem mass spectrometry (LC-MS/MS). The physicochemical properties and biological functions of identified peptides were further analyzed by bioinformatics. The results of peptide identification were verified by cell viability analysis, using CCK8 and Edu staining assay, and the differential peptides relevant to the disease were screened.

Results: 52 differential peptides were successfully identified using mass spectrometry. 44 peptides were up-regulated, while eight were down-regulated. FGA-peptide (sequences: DSGEGDFLAEGGGVRGPR), C4A-peptide (sequences: NGFKSHAL), and TUBB-peptide (sequences: ISEQFTAMFR) were screened out that could significantly promote the proliferation of fibroblasts in AS patients. Bioinformatics analysis showed these differentially expressed peptides might be associated with "MHC class I protein binding" and "pathogenic Escherichia coli infection" pathways, which might further affect the progression of AS.

Conclusion: This pilot study shows 3 differentially expressed peptides may have the potential function for the occurrence and development of AS, may provide novel insights into the underlying molecular mechanisms of AS based on peptide omics.

KEYWORDS

ankylosing spondylitis, peptidomics, LC-MS/MS, CCK8, edu

1 Introduction

Ankylosing spondylitis (AS) is one of the unsolved problems in the field of rheumatism, which finally results in bony ankylosis, discomfort, and impairment and mostly damages the lumbar spine as well as sacroiliac peripheral joints (1). As the disease progresses, the quality of life of AS patients gradually decreases. During the late stage, it might involve fusion of the spinal joint,

sacroiliac joint, hip joint, and other joints. Consequently, the patients completely lose the ability to work and self-care, adding a burden to society and patients' families. AS is one of the most intractable diseases with high occurrence, a great risk of impairment, as well as a significant cost of care. Its root cause of the "three high" lies in our insufficient understanding of the occurrence and development of AS. Although the "arthritogenic peptide" theory has been proposed on the mechanism of HLA-B27 induced AS in recent years (2), and some scholars have also proposed that AS and HLA-B27 may be related to deficiency gut immunity (3), however, the exact pathogenesis of AS remains unclear, so far it has not been effectively treated. Therefore, it is still necessary to conduct in-depth research on the pathogenesis of AS, open new directions for the development of more effective therapeutic drugs and promote the final victory over AS.

Plasma is a source of biomarkers that reflects physiological and pathological conditions in the body. A growing number of studies are focused on proteins and peptides, including a number of studies conducted as part of the Human Proteome Project (HPP) of the Human Proteome Organization (HUPO). It is becoming increasingly apparent that proteomics and peptidomics techniques can be used in the development of novel preventative measures in precision medicine. With the advent of plasma proteomics and peptidomics, it has become possible to study the pathogenesis of diseases (e.g., COVID-19 and cancer) to identify valuable biomarkers and improve the clinical management of these diseases (4). Peptidomics is an emerging field of proteomics (5). In general, it is a method that is widely used for the assessment of liquid chromatography-tandem mass spectrometry (LC-MS/MS) for the detection of peptides contained in diverse biological materials (6, 7). It can be used for systematic, qualitative, and quantitative assessment of the composition and content of endogenous peptides occurring in organisms under physiological or pathological conditions. Developments in the peptidomics field assisted in the identification of a group of small-molecule peptides of 3 to 50 amino acids that have a role in a number of biological processes, including cell differentiation (8), apoptosis (9), immune regulation (10), nervous system regulating (11), as well as reproduction regulation (12). It has been previously established that the variety and quantity of proteins and peptides mostly change even before the appearance of obvious symptoms or pathological changes of the disease (13). Therefore, the study of peptidomics exhibits great potential to explore the possible pathogenesis of various diseases.

In view of the effectiveness of peptideomics in exploring the underlying mechanisms of various diseases and few studies on peptideomics analysis related to AS so far, in this pilot study we perform peptidomic analysis of plasma in AS patients to explore the expressed peptides which may be involved in AS, could also provide fresh perceptions into the molecular pathways behind AS based on peptide omics.

2 Materials and methods

2.1 Subjects

A total of 6 subjects including 3 AS patients and 3 healthy volunteers were enrolled in this study. The patients with AS were recruited from the Orthopedic and Rheumatology Department at the Shanghai Tongren Hospital. The patients were required to meet the New York criteria for their inclusion (14). Patients with other chronic diseases such as hypertension or diabetes and those who have received treatment with a TNF inhibitor were excluded from this study. The Tongren Hospital's Ethics Committee gave their approval to this research. (IRB: 2021-006-01). All subjects in this study provided their signed informed consent. Their peripheral blood was sampled and centrifuged (maximum time intervals between venepuncture and serum separation 1h); the supernatant plasma samples were immediately stored in the refrigerator at -80°C until further processing (15).

2.2 Sample processing steps

To the plasma samples (500 μL), -20°C of pre-cooled methanol was added in the ratio of 1:2. The mixture was vortexed at 4°C and precipitated for 1hr at periodically rotated every ten minutes. At 4°C, the resulting supernatant was centrifuged at 12000 xg for 20 min. Its resultant supernatant was collected and dried by freezing using a centrifugal concentrator. Then, ultrafiltration was used to remove more fluid and high-molecular-weight solutes. Phosphate-buffered saline (PBS) was added to dissolve the dried sample, and the solution was transferred to a new 10-kDa ultrafiltration tube (RT-UFC501096-5; Millipore). The ultrafiltration device was Spin at 10000 xg for 30 min at 4°C. Collect the filtrate. next, HiPPR-derivative removal spin column kit (Thermo Scientific, cat log: Thermo Scientific) and C18 micro columns (Thermo Scientific, cat log: 89870) were used to remove potential contamination for the following mass spectrometry analysis (16).

2.3 Identification of peptides using LC-MS/MS

The peptides were identified using the nanoLC-MS/MS on the Fusion Lumo (Thermo Fisher Scientific, Inc.) in combination with the EASY-nano-LC1200. For chromatographic separation, MilliQ water was mixed with 2 percent acetonitrile and 0.1 percent formic acid as solvent A buffer, and 90 percent acetonitrile and 0.1 percent formic acid as solvent B buffer. The plasma samples were reconstituted in 20 μL of solvent A, processed through the nano-LC for separation, and then subjected to an online electrospray tandem MS analysis. Onto the analytical column (75×250 μm; Acclaim PepMap C18; Thermo Fisher Scientific, Inc.), 8L of the peptide sample were loaded. The peptides were then eluted with 5% of solvent B for 5 minutes, 5-40% of solvent B for 65 minutes, 40-80% of solvent B for 1 minute, 80% of solvent B for 4 minutes, and 5% of solvent B more than 20 minutes at 300 nL/min. The MS spectra were collected with a mass resolution of 120K across the mass range of 350-2,000 m/z.

The sample was analyzed by on-line nanospray LC-MS/MS on an Thermo Scientific™ Orbitrap Fusion Lumos ™ coupled to an EASY-nano-LC 1200 system (Thermo Fisher Scientific, MA, USA). 5L peptide was loaded (analytical column: Acclaim PepMap C18, 75 pm x 25 cm) and separated with a 60 min linear gradient, from 6% B (B: 0.1% formic acid in 80% ACN) to 60% B. The column flow rate was maintained at 400 nL/min with the column temperature of 40°C. The electrospray voltage of 2 kV versus the inlet of the mass spectrometer was used.

The mass spectrometer was run under data dependent acquisition mode, and automatically switched between MS and MS/MS mode. The parameters were: (1) MS: scan range (m/z) = 100-1500; resolution=120,000; AGC target=4e5; maximum injection time=50ms; include charge states=1-7; (2) HCD-MS/MS: resolution=15,000; isolation window=3; AGC target=5e4; maximum injection time=35 ms; collision energy=30.

Peptides were identified using PEAKS (17) search program across the Swissprot_human database (https://www.uniprot.org/taxonomy/9606) with the following search parameters: monoisotopic parent mass tolerance of 10 ppm; fragment mass tolerance of 0.5 Da; modifications – oxidation of methionine; unspecific peptide cleavage. The result filters were set as PSM FDR <1% (16).

2.4 Bioinformatics analysis

Label-free quantification was used to determine the peptides' intensity, whereas Peaks software was used to evaluate the MS/MS data. A fold change greater than 2 with P less than 0.05 (Student's t-test) was the selection criteria for the differentially expressed peptides. The programme MetaboAnalyst 5.0 was used to create the heat map. Online calculators were used to determine the peptides' molecular weight (MW) as well as isoelectric point (PI) (https://web.expasy.org/prot-param/). The UniProt database (http://www.uniport.org/) was used to evaluate the discovered peptides' progenitor proteins. According to the "Molecular Function," "Cellular Component," and "Biological Process" subcategories of the Gene Ontology (GO) (18), the putative functions of the precursor proteins derived from the discovered peptides were examined GO as well as Kyoto Encyclopedia of Genes and Genomes (KEGG) pathways (19) utilizing DAVID Bioinformatics Resources 6.8's Functional Annotation Tool (https://david.ncifcrf.gov). The protein interactions were analyzed using the STRING website (https://string-db.org/, version:11.0) and Cytoscape 3.5.1 software. The amino acid sequences of the different species were analyzed using the protein database on the NCBI website (https://www.ncbi.nlm.nih.gov/homologene/), and the results were compared with DNAMAN (version 9.0) software.

2.5 Screening and synthesis of peptides

We screened differential peptides according to the principles of high activity fraction of peptide ranker, large difference between groups and small difference within groups. The website also forecast the bioactivity of peptides(http://bioware.ucd.ie/), and the peptides with the top 10% activity were selected for preliminary functional evaluation. A total of 3 differential peptides were screened out. The physical and chemical properties were examined online using the website (https://web.expasy.org/protparam) and EMBL-EBI analysis (https://www.ebi.ac.uk/). These peptides were synthesized and the purity of peptides was >95%.

2.6 Cell viability analysis verification

2.6.1 Cell culture

The fibroblasts in patients with AS were obtained from the ligamentum teres of the hip during total hip arthroplasty. The ligament tissue samples were collected from the operating table and immediately placed into a sterile bottle containing DMEM/F-12 medium, stored at 4°C, and primary cultured within 2 hr. First, PBS was used to clean the ligament tissue samples thrice to remove the blood and other components. After centrifugation for five minutes, The supernatant was eliminated, and two times as much DMEM/F-12 solution containing type-I collagenase was added and digested at 37°C for 4 hr. Next, 0.25% trypsin was added to the tissues for 15 minutes. Following digestion, the cells were filtered *via* a 200-mesh screen for collection, centrifuged at 800 rpm for five minutes, and the supernatant was discarded. The cells were suspended in DMEM/F12 media supplemented with 20% foetal bovine serum (FBS), 100 μg/M1 penicillin, and 100 g/M1 streptomycin. Initially, the cells were cultured for 24 hours at 37°C with 5 percent CO_2 and saturated humidity after being injected at a density of $1\times103/cm^2$ in a 25-cm2 plastic culture container. Afterwards, 5 mL of new media was added to wash off the suspended contaminants, blood cells, as well as non-adherent cells after seeing the ligament fibroblasts under a microscope. The media was then changed to DMEM/F-12 with penicillin and 10% foetal bovine serum. Under the microscope, ligament fibroblasts were observed to grow in a dense monolayer. Meanwhile, the cells were subcultured. After washing the cells with PBS, 2 mL of 0.25% trypsin solution was added; the cells were observed to have shrunk into a single round cell under the microscope. The cells were gently blown to suspend them, and then DMEM/F-12 medium supplemented with 10% foetal bovine serum was given. The supernatant was then removed from the cell solution by centrifuging it for five minutes at 800 rpm in a sterile 15-mL tube. A fresh medium was added to re-suspend the cells, and the cell concentration was adjusted to $3\times103/cm^2$, after which the cells were inoculated into a new plastic cell culture bottle for further culture. In the experiment, the cells were subcultured in the ratio of 1:3. The third generation of fibroblasts in the patients with AS was used in this study.

2.6.2 CCK-8 assay

Fibroblasts from the AS patients were plated in a 96-well plate at a density of 1 × 104 cells per well and grown at 37°C in a 5 percent CO_2 environment. Cells were introduced at 70–80% confluency with varying amounts of the three produced peptides (50 μmmol/L), 5 compound wells per concentration,and each group was grown for 24 hours at 37°C with 5% CO_2. In the control group, no peptide was introduced. 10 μL CCK-8 (Beyotime) reagent was then used, and the plate was cultured for an additional 4 hours after that. To determine the cell viability, the absorbance was measured at 450 nm using a Tecan Infinite M1000 Pro microplate reader (San Jose, CA, US). Cell viability = (absorbance of experimental wells - absorbance of blank wells)/(absorbance of control wells - absorbance of blank wells)×100%. The experiment was repeated three times.

2.6.3 Edu staining assay

The fibroblasts in each group were inoculated into a 24-well plate with approximately 0.5×10^5 cells/well and cultured overnight. The cells were treated with 50 μmmol/L peptides the next day in a biosafety cabinet. The cells were washed three times with sterile 1×PBS after the cell culture supernatant was removed and discarded. The diluted peptides were added at the rate of 100 uL/well. No peptide was added in the control group. The proliferation was detected by Edu

10.3389/fimmu.2023.1104351

immunofluorescence staining at 24 hr. Cell proliferation rate = number of proliferating cells/total number of cells × 100%.

2.7 Statistical analysis

Every piece of data was represented as mean standard deviation (SD). To examine statistical differences, either a one-way analysis of variance (ANOVA) with Bonferroni's adjustment for multiple comparisons or an unpaired two-sided Student's t-test were used. The threshold for statistical significance was fixed at P less than 0.05.

3 Results

3.1 Process followed for peptidomics analysis

For peptidomics analysis, the plasma samples were collected from AS patients and healthy volunteers. The individuals were all of the same age. (30–40 years). All these subjects were male and presented no previous history of any other chronic diseases. The clinical characteristics of the subjects were shown in Table 1. Using LC-MS/MS, the expression patterns of peptides found in the plasma of AS patients and a healthy person was compared. In Figure 1, the schematic procedure can be seen.

3.2 Identification of peptide expression profiles

The results of MS analysis detected a total of 1559 peptides. Among these, 52 peptides exhibited differential expression in AS patients, against the control group (P less than 0.05 and fold change ≥2) (Table 2). Eight peptides were downregulated, whereas 44 were increased (Figure 2A). The heat map showed that the peptide profiles of AS patients and healthy people were significantly different from one another (Figure 2B). The distribution of 52 peptides in terms of length of the peptide revealed that these peptides were mainly concentrated in the range of 3–12 amino acids (Figure 2C). MW of these peptides was recorded to be in the range of 0.2–1.8 kDa, as well as PI scores were found to be between 3 and 10 (Figures 2D, E). Differentially expressed peptides' MW and PI distributions were correlated, and this connection showed that these peptides were mostly concentrated into four groups, particularly close to PIs 4, 5, 6, 9, and 10. (Figure 2F).

These differentially expressed peptides' C- and N-terminal cleavage sites were examined in the research. It's interesting to note that these peptides mostly had four cleavage sites: the N-terminal amino acid of the detected peptide, the C-terminal amino acid of the identified peptide, and the N-terminal amino acid of the next peptide. Notably, Leucine (L) and Lysine (K) were found to be the most prevalent amino acids at the N-terminus of the detected peptide,

TABLE 1 The clinical characteristics of the subjects.

	Patient 1	Patient 2	Patient 3	Normal subject 1	Normal subject 2	Normal subject 3
Gender	Male	Male	Male	Male	Male	Male
Age	34	36	33	33	36	34
Body mass index (Kg/m^2)	23.56	24.78	25.36	24.33	25.47	22.98
Disease duration (years)	2	1	2			
Blood routine leukocyte(g/L)	10.77×10^9	11.84×10^9	13.76×10^9			
Erythrocyte sedimentation rate(mm/h)	10	18	28			
C-Reactive Protein (mg/L)	15.18	22.25	16.14			
Bath Ankylosing Spondylitis Disease Activity Index (BASDAI)	4.9	4.5	4.8			
Bath Ankylosing Spondylitis Functional Index (BASFI)	4.1	4.9	4.4			
Visual analogue scale (VAS)	5	6	5			

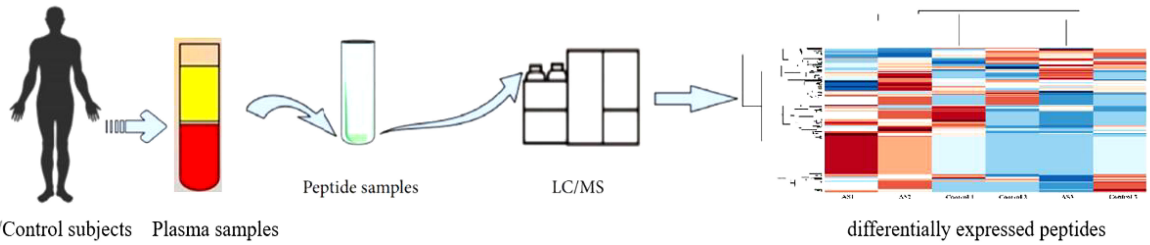

FIGURE 1
The process of peptide identificationin peripheral blood in patients with ankylosing spondylitis by LC/MS mass apectrometry.

10.3389/fimmu.2023.1104351

TABLE 2 The details of the 52 differentially peptides (AS group VS Control group).

Protein names	Protein Accession	Peptide sequence	Fold change	*P* Value*
Albumin	P02768	T.FTF.H	+7.093558743	0.02097
Collagen alpha-1	Q07092	G.NSGEKGDQGFQGQPGFPGPPGP.P	-4.311473151	0.039273
Ubiquitin-activating enzyme E1	P22314	L.KATL.P	-7.256112727	0.007996
Ubiquitin-activating enzyme E1	P22314	N.FAM.I	+3.223158229	0.027864
Nischarin	Q9Y2I1	L.PFT.C	+3.22315836	0.027864
Putative elongation factor 1-alpha-like 3	Q5VTE0	M.LEPS.A	+3.22315836	0.027864
Elongation factor 1-alpha 1	P68104	M.LEPS.A	+3.22315836	0.027864
Alpha-1 type I collagen	P02452	D.TTLK.S	+3.223158464	0.027864
Proline-rich protein 4	Q16378	D.FTF.T	+7.093558743	0.02097
Caveolae-associated protein 1	Q6NZI2	P.PFT.F	+3.22315836	0.027864
Caveolae-associated protein 1	Q6NZI2	P.FTF.H	+7.093558743	0.02097
Alpha-2-HS-glycoprotein	P02765	C.KATL.S	-7.256112727	0.007996
Alpha-actinin-1	P12814	F.KATL.P	-7.256112727	0.007996
Alpha-actinin-1	P12814	K.LVSIGAEEIVDGNVK.M	+3.223158453	0.027864
Alpha-actinin-2	P35609	F.KATL.P	-7.256112727	0.007996
Alpha-actinin-2	P35609	K.LVSIGAEEIVDGNVK.M	+3.223158453	0.027864
Myosin-6	P13533	R.LEEAGGATSVQIEMNK.K	+3.22315865	0.027864
Myosin-7	P12883	R.LEEAGGATSVQIEMNK.K	+3.22315865	0.027864
Dihydropyrimidinase-related protein 2	Q16555	R.DIGAIAQVHAENGDIIAEEQQR.I	+3.223157523	0.027864
ADP-ribosylation factor 5	P84085	R.HYFQNTQGLIFVVDSNDR.E	+3.223158596	0.027864
ATP synthase subunit alpha	P25705	K.LEPS.K	+3.22315836	0.027864
ATP synthase subunit alpha	P25705	R.NVQAEEMVEFSSGLK.G	+3.223158377	0.027864
NADH dehydrogenase	O95298	K.TYGEIFEKF.H	+3.22315853	0.027864
Filamin-A	P21333	G.LEPS.G	+3.22315836	0.027864
Filamin-A	P21333	I.PFT.I	+3.22315836	0.027864
Parathymosin	P20962	K.SVEAAAELSAK.D	+3.223158229	0.027864
Myosin-8	P13535	K.NDLQLQVQSEADSLADAEER.C	+3.22315843	0.027864
Myosin-8	P13535	K.EKNDLQLQVQSEADSLADAEER.C	+3.223158613	0.027864
Tubulin beta-3 chain (TUBB)	Q13509	R.ISEQFTAMFR.R	+3.223158132	0.027864
Tubulin beta-4B chain (TUBB)	P68371	R.ISEQFTAMFR.R	+3.223158132	0.027864
Tubulin beta-2A chain (TUBB)	Q13885	R.ISEQFTAMFR.R	+3.223158132	0.027864
Tubulin beta chain (TUBB)	P07437	R.ISEQFTAMFR.R	+3.223158132	0.027864
Tubulin beta-4A chain (TUBB)	P04350	R.ISEQFTAMFR.R	+3.223158132	0.027864
Tubulin beta-2B chain (TUBB)	Q9BVA1	R.ISEQFTAMFR.R	+3.223158132	0.027864
Hemoglobin subunit alpha	P69905	L.ASVSTVLTSK.Y	+3.223158483	0.027864
Alpha-2-antiplasmin	P08697	R.QLTSGP.N	+3.223157523	0.027864
Fibrinogen alpha chain (FGA)	P02671	A.DSGEGDFLAEGGGVRGPR.V	+3.223158996	0.027864
Complement C4-A (C4A)	P0C0L4	R.NGFKSHALQLNN.R	+3.223158111	0.027864
Complement C4-A (C4A)	P0C0L4	R.NGFKSHAL.Q	+3.223158539	0.027864
Complement C4-A (C4A)	P0C0L4	H.ALQLNNRQI.R	+3.223158413	0.027864

(Continued)

TABLE 2 Continued

Protein names	Protein Accession	Peptide sequence	Fold change	*P* Value*
Apolipoprotein L1	O14791	A.PFT.E	+3.22315836	0.027864
Collagen alpha-1	P20908	S.PSEI.G	+3.223158274	0.027864
Complement C3	P01024	R.IHWESASLL.R	+3.223158692	0.027864
Titin	Q8WZ42	S.KATL.F	-7.256112727	0.007996
Titin	Q8WZ42	P.PPPT.T	-2.186526157	0.048995
Titin	Q8WZ42	D.PSEI.L	+3.223158274	0.027864
Titin	Q8WZ42	K.LEPS.Q	+3.22315836	0.027864
Titin	Q8WZ42	R.TTLK.V	+3.223158464	0.027864
Titin	Q8WZ42	E.YAPP.K	-3.776166378	0.032523
Titin (EC 2.7.11.1)	Q8WZ42	I.ELSP.S	+3.223158437	0.027864
Titin (EC 2.7.11.1)	Q8WZ42	A.PFT.Y	3.22315836	0.027864
PDZ and LIM domain protein 1	O00151	M.PFT.A	3.22315836	0.027864

*The statistical significance level was set at $P < 0.05$.

whereas Arginine (R) was revealed to become the most abundant amino acid present at the C-terminus of the preceding peptide. Additionally, it was discovered that arginine (R) was the most prevalent amino acid at both the C-terminus of the detected peptide and the N-terminus of the next peptide (Figure 2G).

3.3 Bioinformatics analysis

The precursor proteins of these peptides were analyzed using the GO and KEGG pathways in the current investigation, to predict their potential functions. The results for GO analysis revealed enrichment of 10 'Molecular function' categories for these peptides, which included "GTPase activity", "GTP binding", "structural constituent of cytoskeleton", "Major histocompatibility complex (MHC) class I protein binding", et al. (Figure 3A). Among of these, the "MHC class I protein binding" has been proved to be relevant to the occurrence of AS. The most enriched 'cellular component' categories included "extracellular exosome", "blood microparticle", "platelet alpha granule lumen", et al. (Figure 3B). For these precursors, the 'Biological function' categories were mainly associated with "platelet degranulation", "microtubule-based process", "muscle filament sliding", "cytoskeleton organization", "striated muscle contraction", "muscle contraction", "sarcomere organization", "platelet activation", "ATP metabolic process", and "negative regulation of endopeptidase activity" (Figure 3C).

Additionally, the KEGG pathway analysis revealed that the precursor proteins were mostly linked to "Pathogenic Escherichia coli infection", "Phagosome", "Gap junction", et al. (Figure 3D). For the "pathogenic E. coli infection" signal pathway, some inflammatory factors that affect the process of AS, such as TNF α, IL-1 β, IL-1, IL-8 as well as NF-κB, are associated with this signal pathway. The STRING website was used to further examine the interaction network of these peptide precursor proteins. Figure 3E shows an illustration of a typical STRING network interaction.

3.4 Screening and synthesis of peptides

3 peptides from the differential peptides based on the activity fraction of peptide ranker, difference multiple, and P-value in this study were screened out. The FGA-peptide (sequences: DSGEGD FLAEGGGVRGPR), C4A-peptide (sequences: NGFKSHAL), and TUBB-peptide (sequences: ISEQFTAMFR) which be named according to their precursor proteins were screened out in this experiment. Table 3 displays the peptides' chemical and physical attributes.

3.5 Cell viability analysis

3.5.1 Cell culture

The cultured ligament fibroblasts, obtained from AS patients, were found/observed to be long and branched. Among these, few cells were flat and polygonal, with round or oval nucleus, and exhibited adherent growth patterns. When the bottom of the bottle became full, these fibroblasts got arranged in polar, indigo vortex, or radial shape, and the size of the cell body was observed to be the same.

3.5.2 CCK-8 assay

Additionally, a CCK-8 test was used to confirm the impact of 3 differentially expressed peptides, namely FGA-peptide, C4A-peptide, and TUBB-peptide, on cell viability. The results for the assay showed that these three differentially expressed peptides could significantly promote the rate of viability in fibroblasts at 24 hr ($P < 0.05$). Among of these, TUBB-peptide was the most significant difference of the rate of cell viability (%) (P less than 0.01) (Figure 4A).

3.5.3 Edu staining assay

The results for Edu staining showed that these three differentially expressed peptides could significantly promote the proliferation of fibroblasts at 24 hr, as compared to the control group ($P<0.05$). The CCK8 assay's findings and these results were in agreement (Figures 4B, C).

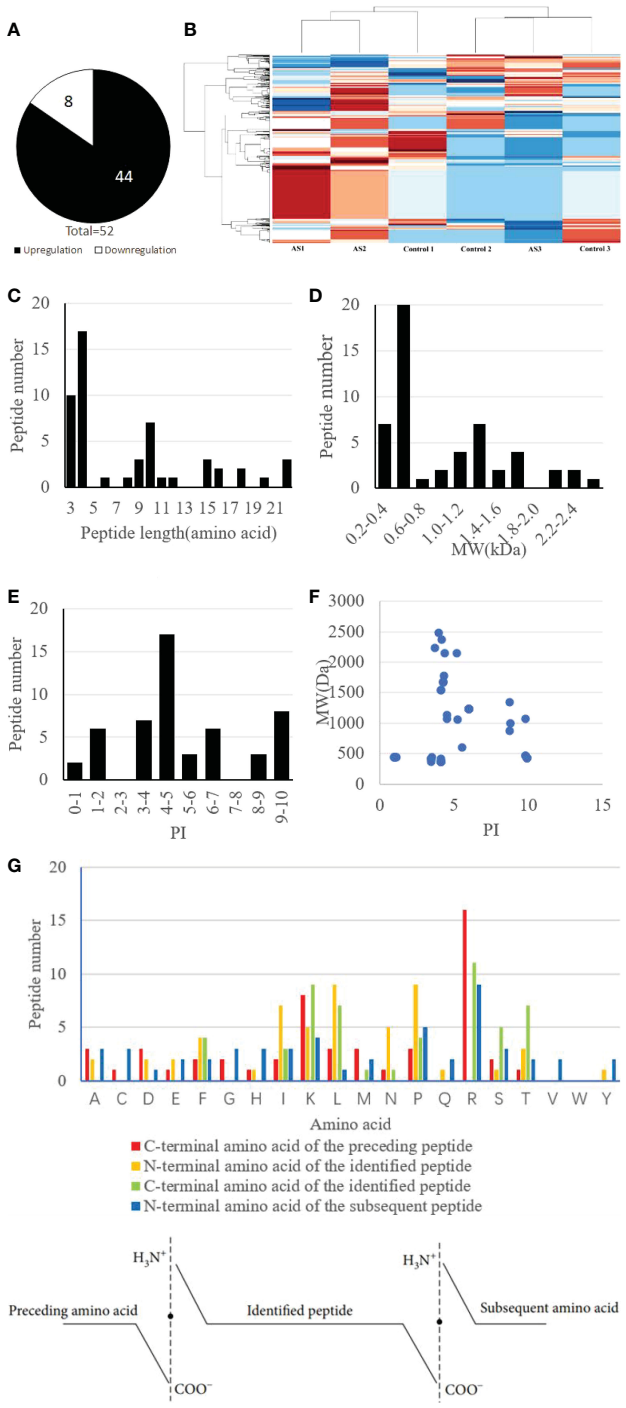

FIGURE 2
Identification and features of differentially expressed peptides. **(A)** Identification of the number of differentially expressed peptides. **(B)** Heat map of the differentially expressed peptides. **(C)** Distribution of the differentially expressed peptides by length. **(D)** Molecular weight (MW) of the differentially expressed peptides. **(E)** Isoelectric point (PI) of the differentially expressed peptides. **(F)** The correlation between the distribution of differentially expressed peptides by MW and PI. **(G)** Four cleavage sites of the differentially expressed peptides.

These results revealed that FGA-peptide (peptide sequences: DSGEGDFLAEGGGVRGPR), C4A-peptide (peptide sequences: NGFKSHAL), and TUBB-peptide (peptide sequences: ISEQFTAMFR) could significantly promote the proliferation of fibroblasts *in vitro*, which might be highly relevant to the occurrence and development of AS.

4 Discussion

As an immune-mediated chronic inflammatory disease, AS is the most prevalent type of spinal arthritis worldwide, occurring at a high rate. AS is characterized by persistent inflammation of the spinal joints as well as attachment sites along with spinal fusion due to he formation of new bone (20). The etiological mechanism of AS is complex and develops through the integration of genetic, microbial, environmental and immune factors (21–23). Peptidomystomics was used in the current work to thoroughly investigate alterations in the peptide profiles of AS patients, and differently expressed peptides were effectively found in the patients' plasma samples. The development of AS diagnosis and therapy will be aided by the possible bioactive peptides found in our investigation. The differently expressed peptides' physicochemical characteristics & bioinformatics research provided a fresh perspective on AS's mechanisms.

52 differentially expressed peptides that showed a change of more than 2 fold were found in this investigation. These peptides usually had 25 or fewer amino acids, and their molecular weights (MWs) were less than 3.0 kDa, indicating the validity of the peptides discovered in the current investigation. The same precursor protein served as the source of several of these peptides. Proteases are crucial in the process of protein cleavage, which produces the majority of peptides and necessitates the precise identification of cleavage sites. Importantly, the biological function of the resultant cleaved peptides would be greatly influenced by the proteases' identification of various cleavage sites (24). The process of protein cleavage by proteases often adheres to a set of guidelines. The choice of candidate peptides is aided by physicochemical characteristics including peptide length, MW, PI, and cleavage sites.

The results for GO analysis revealed that 'MHC class I protein binding' was one of the 10 leading categories under "Molecular function" that were found to be highly enriched with regard to these peptides. This suggested that MHC class I protein was one of the proteins that were associated with AS. These outcomes matched the results of Wang et al. (25) and Watad et al. (26). MHC Class I molecules are important for the initiation and propagation of immune responses (27, 28). AS is a chronic, progressive inflammatory diseases, which might result in the MHC class I presentation of viral peptides and is a chronic infection that finally clears up or persists for the whole life of the host (29). The "Pathogenic Escherichia coli infection" route was mostly linked to the precursor proteins, according to the KEGG pathway analysis. Importantly, among immune-mediated inflammatory illnesses, ankylosing spondylitis (AS), psoriatic arthritis (PsA), psoriasis, inflammatory bowel disease (IBD), and noninfectious uveitis form a separate category (30, 31). Interestingly, the "Pathogenic Escherichia coli infection" pathway might be associated with these immune-mediated inflammatory diseases, especially AS and IBD and genetic factors in these two diseases might also be related. Ergin et al. found that the E. coli-specific Th1 response was significantly reduced in Crohn's patients and to a lower extent also in AS patients (32), and

10.3389/fimmu.2023.1104351

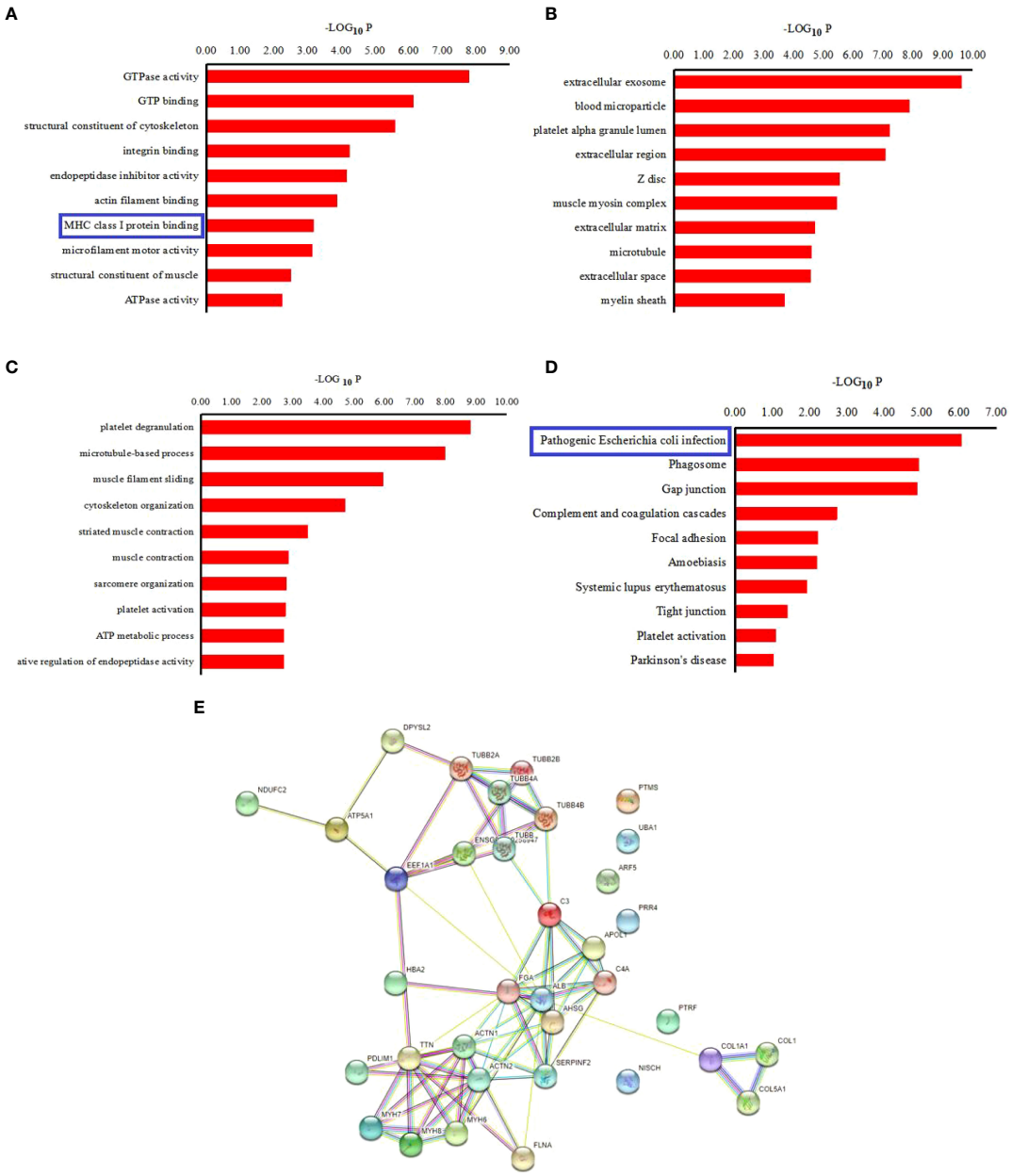

FIGURE 3
Bioinformatics analysis of pepetide precursor proteins: Gene ontology of 9 **(A)** Biological process of differentially expressed peptides precursor proteins. **(B)** Cellular components of differentialy expressed peptides precursor proteins. **(C)** Molecular function of differentially expressed peptides precursor proteins. **(D)** KEGG pathway analysis of the precursor proteins of the differentially expressed peptides. **(E)** Interaction network of precursor proteins of the differentially expressed peptides as determined with STRING (https://string-db.org/, version: 11.0). The confidence level: medium confidence 0.400.

TABLE 3 The physical and chemical properties of 3 differentially peptides.

Precursor protein	Peptide segment	Peptide ranker	Number of amino acids	Molecular weight	Theoretical PI	The instability index	Aliphatic index	Grand average of hydropathicity
FGA	DSGEGDFLAEGGGVRGPR	0.723607	18	1775.85	4.32	143.52	25.79	-1.974
C4A	NGFKSHAL	0.323976	8	872.98	8.76	-28.82	61.25	-0.425
TUBB	ISEQFTAMFR	0.656122	10	1229.42	6.00	39.98	49.00	0.080

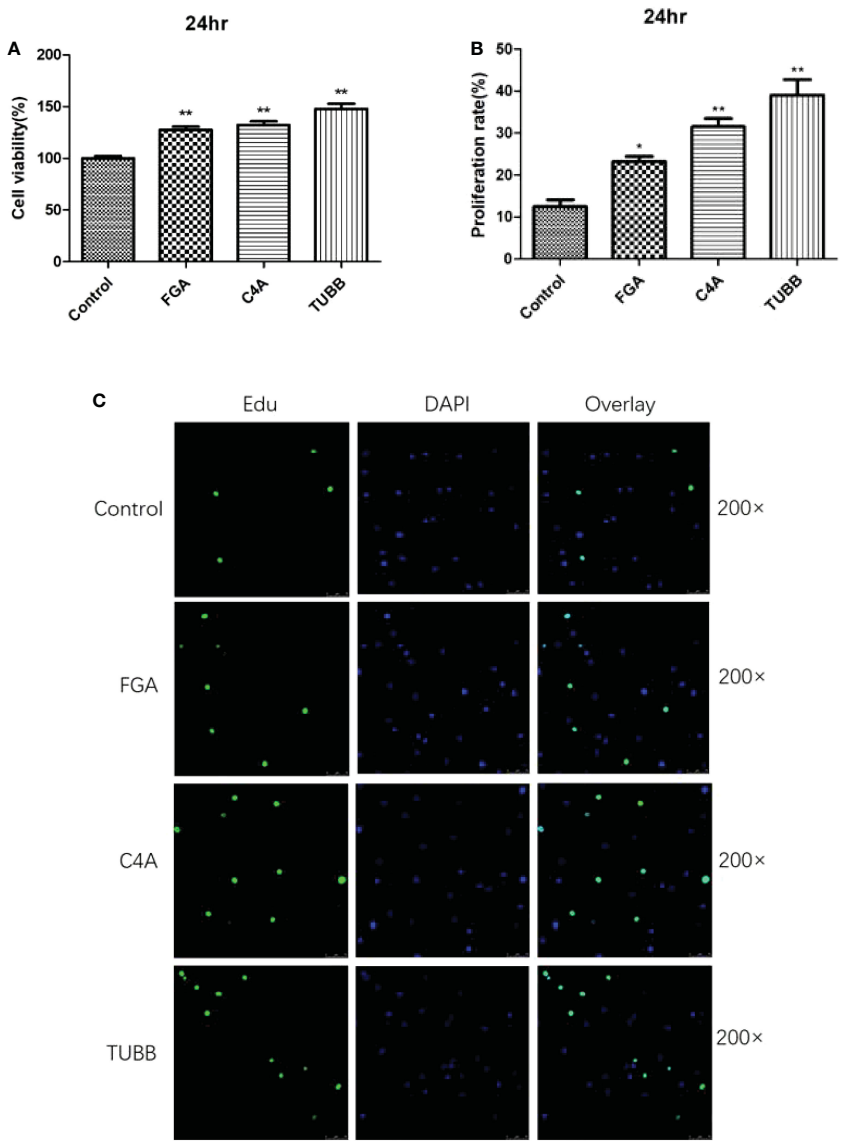

FIGURE 4
The results of Cell viability analysis verification by CCK8 and Edu staining: **(A)** The results of CCK8. **(B)** The results of Edu staining. **(C)** The 200x laser confocal microscope and photograph of Edu staining. * and ** indicates significant difference ($P < 0.05$) and extremely significant difference ($P < 0.01$) compared with the control group.

Syrbe et al. found that the high frequency and enrichment of E coli-specific CD4 T cells in the inflamed joints of patients with AS (33), which suggested that the "Pathogenic Escherichia coli infection" might be relevant to AS. For the "Pathogenic Escherichia coli infection" pathway, the study recognized some important inflammatory factors, such as TNF-α, IL-1β, IL-1, IL-8, and NF-κb, which were associated with different signaling pathways. These factors might affect the progression of the disease (31).

The most prevalent cell type in connective tissue, fibroblasts, are primarily in charge of producing and transforming the extracellular matrix, which contains a high concentration of collagen as well as other macromolecules (34). They exhibit osteogenic traits and could develop into osteoblasts that are crucial for pathological heterotopic ossification & wound healing (35). The majority of research has demonstrated that fibroblasts act as the starting point for AS ligament ossification (36). Thus, identifying target molecules that prevent fibroblasts from diffusing into osteoblasts could serve as a theoretical foundation for the therapy of AS, which is extremely crucial for enhancing the prognosis of AS patients. Numerous studies have concentrated on the various signaling pathways engaged in the ectopic ossification of AS (37), but there have been relatively few investigations on peptideomics evaluation in relation to this process. This study further screened out 3 up-regulated peptides from these differentially expressed peptides, according to activity fraction of peptide ranker, difference multiple, and P-value. These three peptides included FGA-peptide (sequence "DSGEGDFLAEGGGVRGPR"), C4A-peptide (sequence "NGFKSHAL"), and TUBB-peptide (sequence ISEQFTAMFR). These three synthesized peptides were added to the fibroblasts derived from the patients with AS. Further tests to confirm the impact of these differentially expressed peptides included CCK-8 and Edu

staining experiments. Synovial cell secretion could induce differentiation of fibroblasts into osteoblasts in ligaments, which might be one of the reasons for new bone formation in AS. Fibroblasts present in the granulation tissue of subchondral bone of hip joint and sacroiliac joint in AS patients proliferate abnormally, such that granulation tissue forms bone *via* the process of endochondral ossification, resulting in joint ossification and ankylosis (38). The results of the present study further revealed that these three differentially expressed peptides could significantly promote the proliferation of fibroblasts *in vitro* and verified the results of peptide identification. These results further suggested these peptides might be highly relevant for the occurrence and development of AS, provide new ideas for the prevention and treatment of as.

Precursor protein-encoding FGA-peptide (sequences: DSGEGDFLAEGGGVRGPR) is Fibrinogen alpha chain which associated with vascular endothelial growth factor (VEGF). FGA may activate the VEGFA-VEGFR2-FAK signalling pathway to promote angiogenesis (39). VEGF is a crucial regulator of angiogenesis, inflammation, vascular permeability, as well as tissue repair (40).Vascular endothelial growth factor (VEGF), which is typically elevated in axial spondyloarthritis, is associated to coagulation and fibrinolysis (axSpA) (41). VEGF plays a significant role in bone repair and regeneration by affecting angiogenesis and inflammation (42). Additionally, it has been mentioned as a predictive biomarker for axSpA, with greater VEGF levels being linked to an increased risk for the disease's radiographic progression (43). Ankylosing spondylitis, as a type of axSpA, characterized by the sacroiliac joint's spinal development on radiographs, the levels of VEGF can be elevated ≥600 pg/mL (41). Thus, in the current research *in vitro*, the FGA-peptide was speculated. FGA-peptide could increase the proliferation of fibroblasts with AS may contribute to inflammatory processes of AS by activating the VEGFA-VEGFR2-FAK signalling pathway.

Precursor protein-encoding C4A-peptide (sequence: NGFKSHAL) is Complement C4A. The complement system's traditional route includes C4A. Systemic lupus erythematosus and type 1 diabetes are both linked to C4A deficiency, whereas schizophrenia and bipolar illness are linked to C4A overexpression (44). An essential component of humoral and innate immunity is the complement system. Inhibiting the complement system in an animal model of AS might enhance therapy for the condition (45). Patients with systemic sclerosis, a musculoskeletal condition, have an active complement system (46). Ji-Hyun Lee et al. (47) has identified C4A as a potential biomarker for AS. Thus, we supposed that C4A-peptide might be related to the progress of AS by affecting the complement system.

Among these 3 peptides, the TUBB-peptide (sequence: ISEQFTAMFR) was associated with the most significant difference in cell proliferation. Precursor protein-encoding TUBB-peptide forms a dimer with α-tubulin and functions as a microtubule's structural component. TUBB serves as an aprotein-coding gene, which encodes for β-tubulin protein. Diseases associated with TUBB include cortical dysplasia, complex brain malformations, skin Creases, and congenital symmetric circumferential (48). GTP binding and structural molecular activity are two Gene Ontology (GO) annotations associated with TUBB. Signaling pathways related to TUBB include the development Slit-Robo signaling and the innate immune system (49). In a previous study, Chang et al. (50) revealed that TUBB exhibited higher expression in the synovial membranes of patients with rheumatoid arthritis. In fact, TUBB has been reported to be one of the differentially expressed genes in rheumatoid arthritis (51). TUBB might be associated with autoimmune diseases. In the present study, one of the peptides with differential expression in the plasma of AS patients was found to be the TUBB-peptide. It significantly increased the proliferation of fibroblasts *in vitro*. Therefore, the study conjectured that TUBB-peptide might be highly relevant for the occurrence and development of AS by influencing the Slit-Robo signaling pathway.

5 Conclusion

The present study reported the use of peptidomics for the first time for the analysis of the peptides present in the plasma of AS patients. The study identified 52 differentially expressed peptides using mass spectrometry. Further bioinformatics research revealed that these differently produced peptides maybe associated with "MHC class I protein binding" and "Pathogenic Escherichia coli infection" pathways, which might affect the progression of AS. Cell viability analysis verified the results of peptide identification and identified 3 peptides (sequence: DSGEGDFLAEGGGVRGPR, NGFKSHAL, ISEQFTAMFR) which might be highly relevant for the occurrence and development of AS, and may enhance this dangerous disease's clinical results. Overall, this research might provide fresh perspectives on the AS molecular mechanisms based on peptide omics.

It should be noted that this study has certain limitations. Firstly, due to the relatively small sample size, further data collection is still needed in future research. Secondly, the mechanism of the relationship between these differentially expressed peptides and AS would be explored in the future. Further cell function research, signal pathway research and animal experimental research will be carried out according to the results obtained.

Data availability statement

The original contributions presented in the study are included in the article/supplementary material. Further inquiries can be directed to the corresponding author.

Ethics statement

The studies involving human participants were reviewed and approved by The Ethics Committee of Tongren hospital. The patients/participants provided their written informed consent to participate in this study.

Author contributions

Collection of clinical data, Y-JX. Performed the experimental work and Cell viability analysis verification, G-NZ and LJ. Critically evaluated the study, LJ. Drafted the manuscript, G-NZ. Revision and

final approval of the manuscript, LJ. All authors contributed to the article and approved the submitted version.

Funding

This work was supported by the Program of Committee on science and technology of Shanghai Changning district [Grant number: CNKW2018Y09] and Shanghai Jiao Tong University "Star of Jiao Tong University" medical-engineering cross research fund [Grant number: YG2021QN142] and The Research Fund of Shanghai Tong ren Hospital, Shanghai Jiao tong University School of Medicine (nos. TRYJ2021LC14).

Acknowledgments

The authors thank all the patients and volunteers that participated in this study. Thanks are due to Keecloud (Shanghai) Biotechnology Ltd. and Zhong-Xiao Zhang for valuable discussion and formatting in this manuscript.

Conflict of interest

The authors declare that the research was conducted in the absence of any commercial or financial relationships that could be construed as a potential conflict of interest.

Publisher's note

References

1. Baeten D, Sieper J, Braun J, Baraliakos X, Dougados M, Emery P, et al. Secukinumab, an interleukin-17A inhibitor, in ankylosing spondylitis. *N Engl J Med* (2015) 373(26):2534–48. doi: 10.1056/NEJMoa1505066

2. Garrido-Mesa J, Brown MA. T Cell repertoire profiling and the mechanism by which HLA-B27 causes ankylosing spondylitis. *Curr Rheumatol Rep* (2022) 4(12):398–410. doi: 10.1007/s11926-022-01090-6

3. Song ZY, Yuan D, Zhang SX. Role of the microbiome and its metabolites in ankylosing spondylitis. *Front Immunol* (2022) 13:1010572. doi: 10.3389/fimmu.2022.1010572

4. He B, Huang Z, Huang C, Nice EC. Clinical applications of plasma proteomics and peptidomics: Towards precision medicine. *Proteomics Clin Appl* (2022) 16(6):e2100097. doi: 10.1002/prca.202100097

5. Dallas DC, Guerrero A, Parker EA, Robinson RC, Gan J, German JB, et al. Current peptidomics: Applications, purification, identification, quantification, and functional analysis. *Proteomics* (2015) 15(5-6):1026–38. doi: 10.1002/pmic.201400310

6. Slavoff SA, Mitchell AJ, Schwaid AG, Cabili MN, Ma J, Levin JZ, et al. Peptidomic discovery of short open reading frame-encoded peptides in human cells. *Nat Chem Biol* (2013) 9(1):59–64. doi: 10.1038/nchembio.1120

7. Rubakhin SS, Churchill JD, Greenough WT, Sweedler JV. Profiling signaling peptides in single mammalian cells using mass spectrometry. *Anal Chem* (2006) 78 (20):7267–72. doi: 10.1021/ac0607010

8. Chaturvedi LS, Basson MD. Glucagonlike peptide 2 analogue teduglutide: stimulation of proliferation but reduction of differentiation in human caco-2 intestinal epithelial cells. *JAMA Surg* (2013) 148(11):1037–42. doi: 10.1001/jamasurg.2013.3731

9. Dang LT, Feric NT, Laschinger C, Chang WY, Zhang B, Wood GA, et al. Inhibition of apoptosis in human induced pluripotent stem cells during expansion in a defined culture using angiopoietin-1 derived peptide QHREDGS. *Biomaterials* (2014) 35 (27):7786–99. doi: 10.1016/j.biomaterials.2014.05.018

10. Chimen M, McGettrick HM, Apta B, Kuravi SJ, Yates CM, Kennedy A, et al. Homeostatic regulation of T cell trafficking by a b cell-derived peptide is impaired in autoimmune and chronic inflammatory disease. *Nat Med* (2015) 21(5):467–75. doi: 10.1038/nm.3842

11. Zhu H, Wang X, Wallack M, Li H, Carreras I, Dedeoglu A, et al. Intraperitoneal injection of the pancreatic peptide amylin potently reduces behavioral impairment and brain amyloid pathology in murine models of alzheimer's disease. *Mol Psychiatry* (2015) 20(2):252–62. doi: 10.1038/mp.2014.17

12. Ivell R, Anand-Ivell R. Insulin-like peptide 3 (INSL3) is a major regulator of female reproductive physiology. *Hum Reprod Update* (2018) 24(6):639–51. doi: 10.1093/humupd/dmy029

13. Shin H, Markey MK. A machine learning perspective on the development of clinical decision support systems utilizing mass spectra of blood samples. *J BioMed Inform* (2006) 39(2):227–48. doi: 10.1016/j.jbi.2005.04.002

14. van der Linden S, Valkenburg HA, Cats A. Evaluation of diagnostic criteria for ankylosing spondylitis. a proposal for modification of the new York criteria. *Arthritis Rheum* (1984) 27(4):361–8. doi: 10.1002/art.1780270401

15. Padoan A. The impact of pre-analytical conditions on human serum peptidome profiling. *Proteomics Clin Appl* (2018) 12(3):e1700183. doi: 10.1002/prca.201700183

16. Zakharova NV, Shornikova AY, Bugrova AE, Baybakova VV, Indeykina MI, Kononikhin AS, et al. Evaluation of plasma peptides extraction methods by high-resolution mass spectrometry. *Eur J Mass Spectrom (Chichester)* (2017) 23(4):209–12. doi: 10.1177/1469066717720907

17. Tran NH, Zhang X, Xin L, Shan B, Li M. De novo peptide sequencing by deep learning. *Proc Natl Acad Sci U.S.A.* (2017) 114(31):8247–52. doi: 10.1073/pnas.1705691114

18. Ashburner M, Ball CA, Blake JA, Botstein D, Butler H, Cherry JM, et al. Gene ontology: tool for the unification of biology. the gene ontology consortium. *Nat Genet* (2000) 25(1):25–9. doi: 10.1038/75556

19. Kanehisa M, Goto S, Furumichi M, Tanabe M, Hirakawa M. KEGG for representation and analysis of molecular networks involving diseases and drugs. *Nucleic Acids Res* (2010) 38(Database issue):D355–60. doi: 10.1093/nar/gkp896

20. Hammoudeh M, Rahim Siam A, Khanjar I. Spinal stenosis due to posterior syndesmophytes in a patient with seronegative spondyloarthropathy. *Clin Rheumatol* (1995) 14(4):464–6. doi: 10.1007/BF02207683

21. Voruganti A, Bowness P. New developments in our understanding of ankylosing spondylitis pathogenesis. *Immunology* (2020) 161(2):94–102. doi: 10.1111/imm.13242

22. Hwang MC, Ridley L, Reveille JD. Ankylosing spondylitis risk factors: a systematic literature review. *Clin Rheumatol* (2021) 40(8):3079–93. doi: 10.1007/s10067-021-05679-7

23. Rath HC, Herfarth HH, Ikeda JS, Grenther WB, Hamm Jr Balish TE E, et al. Normal luminal bacteria, especially bacteroides species, mediate chronic colitis, gastritis, and arthritis in HLA-B27/human beta2 microglobulin transgenic rats. *J Clin Invest* (1996) 98(4):945–53. doi: 10.1172/JCI118878

24. Li F, Wang Y, Li C, Marquez-Lago TT, Leier A, Rawlings ND, et al. Twenty years of bioinformatics research for protease-specific substrate and cleavage site prediction: a comprehensive revisit and benchmarking of existing methods. *Brief Bioinform* (2019) 20 (6):2150–66. doi: 10.1093/bib/bby077

25. Wang G, Kim TH, Li Z, Cortes A, Kim K, Bang SY, et al. MHC associations of ankylosing spondylitis in East asians are complex and involve non-HLA-B27 HLA contributions. *Arthritis Res Ther* (2020) 22(1):8. doi: 10.1186/s13075-020-02148-5

26. Watad A, Bragazzi NL, Adawi M, Shoenfeld Y, Comaneshter D, Cohen AD, et al. FMF is associated with a wide spectrum of MHC class I- and allied SpA disorders but not with classical MHC class II-associated autoimmune disease: Insights from a Large cohort study. *Front Immunol* (2019) 10:7. doi: 10.3389/fimmu.2019.02733

27. Nguyen TT, Saridakis E, Stratikos E, Mavridis IM. Structural basis for antigenic peptide precursor processing by the endoplasmic reticulum aminopeptidase ERAP1. *Nat Struct Mol Biol* (2011) 18(5):604–13. doi: 10.1038/nsmb.2021

28. Yewdell JW. DRiPs solidify: progress in understanding endogenous MHC class I antigen processing. *Trends Immunol* (2011) 32(11):548–58. doi: 10.1016/j.it.2011.08.001

29. Sun S, Wang T, Pang B, Wei H, Liu G. Short peptide sequence identity between human viruses and HLA-B27-binding human 'self' peptides. *Theory Biosci* (2014) 133 (2):79–89. doi: 10.1007/s12064-013-0196-1

30. Bruner M, Dige A, Loft AG, Laurberg TB, Agnholt JS, Clemmensen K, et al. Spondylitis-psoriasis-enthesitis-enterocolitis-dactylitis-uveitis-periph eral synovitis (SPEED-UP) treatment. *Autoimmun Rev* (2021) 20(2):10. doi: 10.1016/j.autrev.2020.102731

31. Ashrafi M, Kuhn KA, Weisman MH. The arthritis connection to inflammatory bowel disease (IBD): why has it taken so long to understand it? *Rmd Open* (2021) 7(1):9. doi: 10.1136/rmdopen-2020-001558

32. Ergin A, Syrbe U, Scheer R, Thiel A, Adam T, Büssow K, et al. Impaired peripheral Th1 CD4+ T cell response to escherichia coli proteins in patients with crohn's disease and ankylosing spondylitis. *J Clin Immunol* (2011) 31(6):998–1009. doi: 10.1007/s10875-011-9575-x

33. Syrbe U, Scheer R, Wu P, Sieper J. Differential synovial Th1 cell reactivity towards escherichia coli antigens in patients with ankylosing spondylitis and rheumatoid arthritis. *Ann Rheum Dis* (2012) 71(9):1573–6. doi: 10.1136/annrheumdis-2012-201404

34. Lynch MD, Watt FM. Fibroblast heterogeneity: implications for human disease. *J Clin Invest* (2018) 128(1):26–35. doi: 10.1172/JCI93555

35. Claeys L, Bravenboer N, Eekhoff EMW, Micha D. Human fibroblasts as a model for the study of bone disorders. *Front Endocrinol (Lausanne)* (2020) 11:394. doi: 10.3389/fendo.2020.00394

36. Li DH, He CR, Liu FP, Li J, Gao JW, Li Y, et al. Annexin A2, up-regulated by IL-6, promotes the ossification of ligament fibroblasts from ankylosing spondylitis patients. *BioMed Pharmacother* (2016) 84:674–9. doi: 10.1016/j.biopha.2016.09.091

37. Zeng Y, Wang T, Liu Y, Luo T, Li Q, He Y, et al. Wnt and smad signaling pathways synergistically regulated the osteogenic differentiation of fibroblasts in ankylosing spondylitis. *Tissue Cell* (2022) 77:101852. doi: 10.1016/j.tice.2022.101852

38. Francois RJ, Gardner DL, Degrave EJ, Bywaters EG. Histopathologic evidence that sacroiliitis in ankylosing spondylitis is not merely enthesitis - systematic study of specimens from patients and control subjects. *Arthritis Rheumatism* (2000) 43(9):2011–24. doi: 10.1002/1529-0131(200009)43:9<2011::AID-ANR12>3.0.CO;2-Y

39. Li H, Cai E, Cheng H, Ye X, Ma R, Zhu H, et al. FGA controls VEGFA secretion to promote angiogenesis by activating the VEGFR2-FAK signalling pathway. *Front Endocrinol (Lausanne)* (2022) 13:791860. doi: 10.3389/fendo.2022.791860

40. Eming SA, Krieg T. Molecular mechanisms of VEGF-a action during tissue repair. *J Investig Dermatol Symp Proc* (2006) 11(1):79–86. doi: 10.1038/sj.jidsymp.5650016

41. Hoppe B, Schwedler C, Haibel H, Verba M, Proft F, Protopopov M, et al. Relation of alpha2-antiplasmin genotype and genetic determinants of fibrinogen synthesis and fibrin clot formation with vascular endothelial growth factor?level in axial spondyloarthritis. *Int J Mol Sci* (2020) 21(24):9383. doi: 10.3390/ijms21249383

42. Hu K, Olsen BR. Vascular endothelial growth factor control mechanisms in skeletal growth and repair. *Dev Dyn* (2017) 246(4):227–34. doi: 10.1002/dvdy.24463

43. Poddubnyy D, Conrad K, Haibel H, Syrbe U, Appel H, Braun J, et al. Elevated serum level of the vascular endothelial growth factor predicts radiographic spinal progression in patients with axial spondyloarthritis. *Ann Rheum Dis* (2014) 73 (12):2137–43. doi: 10.1136/annrheumdis-2013-203824

44. Ingram G, Hakobyan S, Hirst CL, Harris CL, Loveless S, Mitchell JP, et al. Systemic complement profiling in multiple sclerosis as a biomarker of disease state. *Mult Scler* (2012) 18(10):1401–11. doi: 10.1177/1352458512438238

45. Yang C, Ding P, Wang Q, Zhang L, Zhang X, Zhao J, et al. Inhibition of complement retards ankylosing spondylitis progression. *Sci Rep* (2016) 6:34643. doi: 10.1038/srep34643

46. Okroj M, Johansson M, Saxne T, Blom AM, Hesselstrand R. Analysis of complement biomarkers in systemic sclerosis indicates a distinct pattern in scleroderma renal crisis. *Arthritis Res Ther* (2016) 18(1):267. doi: 10.1186/s13075-016-1168-x

47. Lee JH, Jung JH, Kim J, Baek WK, Rhee J, Kim TH, et al. Proteomic analysis of human synovial fluid reveals potential diagnostic biomarkers for ankylosing spondylitis. *Clin Proteomics* (2020) 17:20. doi: 10.1186/s12014-020-09281-y

48. Romaniello R, Arrigoni F, Fry AE, Bassi MT, Rees MI, Borgatti R, et al. Tubulin genes and malformations of cortical development. *Eur J Med Genet* (2018) 61(12):744–54. doi: 10.1016/j.ejmg.2018.07.012

49. Isrie M, Breuss M, Tian G, Hansen AH, Cristofoli F, Morandell J, et al. Mutations in either TUBB or MAPRE2 cause circumferential skin creases kunze type. *Am J Hum Genet* (2015) 97(6):790–800. doi: 10.1016/j.ajhg.2015.10.014

50. Chang X, Zhao Y, Wang Y, Chen Y, Yan X. Screening citrullinated proteins in synovial tissues of rheumatoid arthritis using 2-dimensional Western blotting. *J Rheumatol* (2013) 40(3):219–27. doi: 10.3899/jrheum.120751

51. Zhu H, Xia W, Mo XB, Lin X, Qiu YH, Yi NJ, et al. Gene-based genome-wide association analysis in European and Asian populations identified novel genes for rheumatoid arthritis. *PloS One* (2016) 11(11):13. doi: 10.1371/journal.pone.0167212

frontiers | Frontiers in Immunology

TYPE Original Research
PUBLISHED 28 February 2023
DOI 10.3389/fimmu.2023.1141407

OPEN ACCESS

EDITED BY
Mohammed Osman,
University of Alberta, Canada

REVIEWED BY
Marisa Benagiano,
University of Florence, Italy
Edoardo Rosato,
Sapienza University of Rome, Italy

*CORRESPONDENCE
Kunihiro Ichinose
kichinos@nagasaki-u.ac.jp

SPECIALTY SECTION
This article was submitted to Autoimmune and Autoinflammatory Disorders : Autoimmune Disorders, a section of the journal Frontiers in Immunology

RECEIVED 10 January 2023
ACCEPTED 17 February 2023
PUBLISHED 28 February 2023

CITATION
Uchida T, Ichinose K, Yamashita A, Muta K, Kitamura M, Sato S, Iwamoto N, Nishino T and Kawakami A (2023) Evaluation of a renal risk score for Japanese patients with ANCA-associated glomerulonephritis in a multi-center cohort study.
Front. Immunol. 14:1141407.
doi: 10.3389/fimmu.2023.1141407

Evaluation of a renal risk score for Japanese patients with ANCA-associated glomerulonephritis in a multi-center cohort study

Tomohisa Uchida[1,2], Kunihiro Ichinose[2,3]*, Ayuko Yamashita[4], Kumiko Muta[4], Mineaki Kitamura[4], Shuntaro Sato[5], Naoki Iwamoto[2], Tomoya Nishino[4] and Atsushi Kawakami[2]

[1]Department of Rheumatology, National Hospital Organization Ureshino Medical Center, Ureshino, Japan, [2]Department of Immunology and Rheumatology, Division of Advanced Preventive Medical Sciences, Nagasaki University Graduate School of Biomedical Sciences, Nagasaki, Japan, [3]Department of Rheumatology, Shimane University Faculty of Medicine, Izumo, Japan, [4]Department of Nephrology, Nagasaki University Hospital, Nagasaki, Japan, [5]Clinical Research Center, Nagasaki University Hospital, Nagasaki, Japan

Background: In patients with anti-neutrophil cytoplasmic antibody (ANCA)-associated glomerulonephritis, prediction of renal survival should guide the choice of therapy, but a prediction of the histological classification has inconsistencies.

Objectives: To evaluate the usefulness of renal risk score (RRS) for Japanese patients with ANCA-associated glomerulonephritis (AAGN) and compare the prediction for end-stage renal disease (ESRD) between RRS and the histological classification.

Methods: We retrospectively analyzed 96 patients with AAGN who underwent a renal biopsy. Renal survival was categorized by RRS, and the histological classification was assessed separately. We compared the predictive values for RRS and the histological classification.

Results: The median observational period was 37.5 (interquartile range [IQR] 21.5–77.0) months. The median RRS point at the time of renal biopsy was 2 (IQR 0–7.8), and the patients were categorized into low- (n = 29), medium- (n = 43), and high-risk groups (n = 24) using RRS. As expected, the renal prognosis was the worst in the "high-risk" group and the best in the "low-risk" group. In the histological classification, the survival deteriorated progressively from "focal" (best) to "mixed," "crescentic," and "sclerotic" (worst) classes, different from the order in the original proposal for this system. Multivariable Cox regression analysis revealed that RRS was independently associated with ESRD. The difference in prediction for renal survival between RRS and the histological classification was not significant using area under receiver-operating-characteristic curves.

Conclusion: We evaluated the usefulness of RRS in Japanese patients with AAGN and found it a stable predictor of renal survival in such patients.

KEYWORDS

ANCA, ANCA-associated glomerulonephritis, end-stage renal disease, renal risk score, histological classification

Introduction

Anti-neutrophil cytoplasmic antibody (ANCA)-associated vasculitis (AAV) is a systemic vasculitis of small vessels accompanied by ANCAs (1). The major variants of AAV include eosinophilic granulomatosis polyangiitis (EGPA), granulomatosis polyangiitis (GPA), and microscopic polyangiitis (MPA) (2). Renal involvement is frequent in GPA and MPA, and 20-40% of cases develop the end-stage renal disease (ESRD) within 5 years (3–5). Renal involvement is also associated with a worse prognosis than AAV patients without impaired renal function (4, 6, 7). Clinicians need to perform prompt diagnosis and initiation of adequate immunosuppressive therapy to preserve patient and kidney outcomes, but avoidance of adverse events such as treatment-related complications, infection, cardiovascular diseases, and cancer is also a priority (8). Therefore, careful selection of patients who would benefit from intensive immunosuppressive therapy is highly required. Berden et al. proposed a histological classification to predict renal outcomes in patients with ANCA-associated glomerulonephritis (AAGN) in 2010 (9). However, several meta-analyses demonstrated that the histological classification did not accurately predict the renal prognosis of the mixed and crescentic classes (10–13). Recently, Brix et al. proposed another scoring system, a renal risk score (RRS), for predicting the renal prognosis (14). The RRS differs from the histological classification in that it is based on three parameters: percentage of normal glomeruli, tubular atrophy and interstitial fibrosis rate of the kidney, and estimated glomerular filtration rate (eGFR), which are scored according to the severity and classified into three groups with different prognoses. This scoring system has been validated in several studies and one meta-analysis (15–20). We aimed to validate the usefulness of the RRS for Japanese patients over a long-term observation period.

Patients and methods

Patients

The patients with ANCA-associated glomerulonephritis (AAGN) who underwent a renal biopsy at Nagasaki University Hospital and its associated hospitals between 1992 and 2019 were enrolled and assessed for eligibility in this study. The inclusion criteria were as follows: ANCA was detected in the sera; renal biopsy revealed necrotizing and/or crescentic glomerulonephritis; and follow-up of patients lasted at least 12 months (including patients who died or ESRD and required renal replacement therapy within 12 months). EGPA cases were not included because the biological and clinical presentation differed from GPA and MPA cases. Patients with secondary vasculitis or comorbid kidney disease were excluded. The baseline characteristics evaluated were the patient's age, sex, diagnosis, white blood cell count, hemoglobin, C-reactive protein (CRP), eGFR calculated as per the Japanese-based equation: eGFR (ml/min/1.73 m^2) = 194 × serum creatinine $^{-1.094}$ × age$^{-0.287}$ (if female, ×0.739) (21), proteinuria, hematuria, ANCA subtype determined by indirect immunofluorescence or enzyme-linked immunosorbent assay, use of antidiabetic drugs, smoking history, hypotensive drug, and immunosuppressive medication. The Birmingham Vasculitis Activity Score (BVAS) was used to assess the activity of the disease at the initial presentation (22). An opt-out strategy was chosen for the informed consent procedure; data from those who indicated an unwillingness to participate were excluded. This study was reviewed and approved by the Institutional Review Boards of Nagasaki University (approval no. 20021012).

Histopathologic evaluations

Biopsies were independently scored by two expert nephrologists blinded to clinical data (KM, MK). All specimens had at least five glomeruli per biopsy. Various calculations were performed for the RRS assessment, including the percentage of normal glomeruli, tubular atrophy/interstitial fibrosis, and renal function at the time of diagnosis (14). The histological classification was made according to the definition proposed by Berden et al. (9).

Outcome measures

The primary endpoint was the cumulative percentage of patients who developed ESRD over time censored by death. ESRD was defined as requiring long-term renal replacement therapy or renal transplantation. Renal survival time for each patient was calculated from the time of biopsy to the last time of follow-up or the time point of reaching ESRD.

Statistical analyses

Data are expressed as a median with an interquartile range (IQR) or n (%). Wilcoxon's rank sum test was used to compare the continuous variables, and Fisher's exact test to compare categorical variables. Renal survival was assessed using the Kaplan-Meier method, and differences between survival curves were compared with the log-rank test. Univariate and multivariable Cox proportional hazard regression analyses were performed to identify factors related to ESRD. Variables with p-values <0.15 and factors expected to be associated with the univariate Cox regression analyses were entered in the multivariable Cox regression analyses. Due to the collinearity between the explanatory variables and the RRS scoring system, eGFR was excluded. Discrimination capacity to predict dialysis dependency was assessed using the area under the receiver operating characteristic curve (AUC). We calculated differences using DeLong's test. P-values <0.05 were considered statistically significant.

Statistical analyses were performed using JMP® Pro 16 software (SAS Institute, Cary, NC) and RStudio version 2022.07.1, an integrated development environment for R version 4.1.2 (R Foundation for Statistical Computing, Vienna, Austria) (23).

Results

Baseline characteristics

Of the 128 patients, 96 patients with ANCA-associated renal vasculitis were enrolled (Figure 1). The patients included 83 with MPA, 10 with GPA, and 3 with renal-limited vasculitis. The mean BVAS was 14 (IQR 12–18). The baseline characteristics are summarized in Table 1, and the comparison of baseline characteristics between the patients who progressed to ESRD or not are summarized in Supplementary Table S1.

Evaluating the patients with RRS and histological classification

The median RRS at diagnosis was 2 (IQR 0–7.8), and the patients were categorized by RRS into low- (n = 29), medium- (n = 43), and high-risk groups (n = 24), respectively. The distribution of the RRS parameters is summarized in Table 2. Patients were also classified according to the histological classification (9) as focal (n = 12), crescentic (n = 18), mixed (n = 48), or sclerotic (n = 18). Comparisons of baseline characteristics by RRS and the histological classification are summarized in Supplementary Tables S2, S3, respectively.

Evaluating renal outcome with RRS and histological classification

The median length of the observation period was 37.5 (IQR 21.5–77.0) months. Fifteen (15.6%) patients progressed to ESRD and required renal replacement therapy. Kaplan-Meier curve of RRS-predicted risk demonstrated that renal prognosis was the worst in the "high-risk" group and the best in the "low-risk" group (Figure 2). There were significant differences in renal survival rates among the three groups (p<0.001). In the histological classification, the Kaplan-Meier curve showed that renal survival rates deteriorated in the order of "focal" (best) to "mixed," "crescentic," and "sclerotic" (worst), respectively (Figure 3). There were significant differences in renal survival rates among the four groups (p<0.001); however, the order of the classes differed from that of Berden et al. (9).

Risk factors related to ESRD

To identify risk factors associated with ESRD, we analyzed the baseline characteristics of the patients and the RRS using univariate

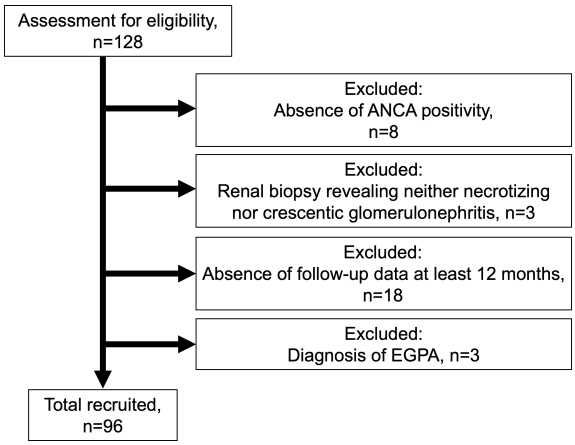

FIGURE 1
Flowchart summarizing the enrollment of the patient with ANCA-associated renal vasculitis ANCA, anti-neutrophil cytoplasmic antibody; EGPA, eosinophilic granulomatosis polyangiitis.

TABLE 1 Baseline characteristics of patients with ANCA-associated renal vasculitis.

Variables	Total (n = 96)
Male (n, %)	46 (47.9%)
Age, yrs†	70 (62.3-76.8)
Diagnosis (n, %)	MPA 83 (86.5%) GPA 10 (10.4%) RLV 3 (3.1%)
WBC (/μL)†	8450 (6600-11400)
Hb (g/dL)†	9.8 (8.63-11.08)
CRP (mg/dL)†	2.7 (0.27-8.86)
eGFR (mL/min/1.73m^2)†	27.6 (15.5-39.6)
Proteinuria (n, %)	95 (99%)
Hematuria (n, %)	97 (100%)
MPO-ANCA positivity (n, %)	92 (95.8%)
PR3-ANCA positivity (n, %)	6 (6.3%)
BVAS†	14 (12-18)
Use of hypotensive drugs (n, %)	37 (42.5%) n/a 9 patients
Smoking history (n, %)	35 (43.8%) n/a 16 patients
Use of diabetes mellitus (n, %)	8 (9.0%) n/a 7 patients
Use of Methylprednisolone pulse (%)	61 (63.5%)
Use of glucocorticoid (n, %)	94 (97.9%)
Glucocorticoid dose(mg/day)†	40 (30-50)
Plasmapheresis (n, %)	13 (13.5%)
Cyclophosphamide (n, %)	19 (19.8%)
Rituximab (n, %)	2 (2.1%)
ESRD (n, %)	15 (15.6%)

ANCA, anti-neutrophil cytoplasmic antibody; BVAS, Birmingham Vasculitis Activity Score; CRP, C-reactive protein; eGFR, estimated glomerular filtration rate; ESRD, end-stage renal disease; GPA, granulomatosis with polyangiitis; MPA, microscopic polyangiitis; MPO, myeloperoxidase; n/a, not available; PR3, proteinase-3; RLV, renal-limited vasculitis; WBC, white blood cell count
†Values are the median with IQR

and multivariable Cox regression analysis (Table 3). Univariate analysis showed that CRP and RRS were associated with ESRD. The multivariable analysis demonstrated that RRS was independently associated with ESRD among these factors.

Predictive values of RRS and histological classification

The AUC value of RRS was 0.890 (95%CI, 0.819–0.959) for developing ESRD. The AUC value of the histological classification for progression to ESRD was 0.857 (95% CI, 0.773–0.942). Two receiver operating characteristic (ROC) curves are shown in Figure 4 and did not show significant differences (p=0.474). We also calculated the AUC value using the points of RRS, which was 0.913 (95%CI, 0.833-0.994) for developing ESRD, and the cut-off value was 7.5 points (sensitivity: 86.7%, specificity: 86.6%) (Supplementary Figure S1).

TABLE 2 The distribution of the parameters of renal risk score in patients with ANCA-associated renal vasculitis.

Parameters of renal risk score	No. of patients, n (%)
Percentage of normal glomeruli (N)	
N0 (0 points) >25%	57 (59.4%)
N1 (4 points) 10%-25%	13 (13.5%)
N2 (6 points) <10%	26 (27.1%)
Tubular atrophy/interstitial fibrosis (T)	
T0 (0 points) ≦25%	41 (42.7%)
T1 (2 points) >25%	55 (57.3%)
Renal function at the time of diagnosis (eGFR; G)	
G0 (0 point) >15 mL/min/1.73m^2	76 (79.2%)
G1 (3 points) ≦15 mL/min/1.73m^2	20 (20.8%)

ANCA, anti-neutrophil cytoplasmic antibody; eGFR, estimated glomerular filtration rate

Discussion

Our present study demonstrated the usefulness of RRS for predicting renal survival among patients with AAGN in Japan. In 2010 Berden et al. devised a histological classification to predict renal outcomes in patients with AAGN (9). It categorized renal pathological findings into four groups: focal, crescentic, mixed, and sclerotic. Among their subjects, the focal group had the best renal survival, the crescentic class had the second-best, the sclerotic class had the worst renal prognosis, and the mixed class had the second-worst. However, several studies and meta-analyses have reported that the histological classification does not accurately predict the renal outcomes of the mixed and crescentic classes (10–13). Unlike the results of Berden et al. (9), our analysis found the mixed class had a better prognosis than that of the crescentic class. Several previous studies obtained similar results (24–26). We speculatively attributed these differences to the following considerations. First, in patients with AAGN in Japanese and Chinese patients, MPO-ANCA is more common than PR3-ANCA. Histological differences between MPO-AAV and PR3-AAV have been found in several reports (27–30): namely, more fibrotic changes, such as glomerulosclerosis, interstitial fibrosis, and tubular atrophy, are typically recognized in MPO-AAV than in PR3-AAV (28–30). Second, the rate of >25% normal glomeruli was lower in the crescentic class than in the mixed class (Supplementary Table S2). Hillhorst et al. showed that renal survival was significantly worse when the percentage of normal glomeruli was less than 25% (26).

Recently, Brix et al. proposed the RRS as another method to predict renal survival (14). We demonstrated that RRS was a stable predictor for ESRD in our analysis. In the baseline characteristics of our study, patient age was older, and MPO-ANCA positivity was higher than in the cohort of Brix et al. (14). Despite the differences in ANCA positivity between European and Asian cohorts

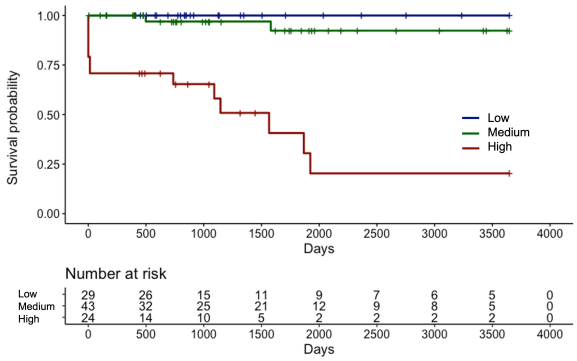

FIGURE 2
Kaplan-Meier curve demonstrating renal survival of Japanese patients with ANCA-associated renal vasculitis according to the renal risk score groups ANCA, anti-neutrophil cytoplasmic antibody.

mentioned above, the higher MPO-AAV rate did not degrade the ability of RRS to predict ESRD, not only in our cohort but in other Asian cohorts (19, 31). You et al. demonstrated that the prognostic value of RRS in Chinese patients with AAGN of the crescentic or mixed class was better than the histological classification (32). Saito et al. reported a validation study of RRS in Japanese patients with AAGN (19). They demonstrated that high-risk group patients had significantly poorer renal prognosis than other groups using the RRS, and that RRS was an independent renal prognostic factor in 86 Japanese biopsy-confirmed MPO-ANCA-positive GN patients. Our study likewise found the renal prognosis using RRS accurate in Japanese patients even when the histological classification was not predictive, and the rate of systemic AAV was higher than the report by Saito et al. (19).

In this study, we also evaluated how treatment for ANCA-associated renal vasculitis impacts the risk of ESRD. We found that the use of methylprednisolone pulse, dose of prednisolone, plasmapheresis, or cyclophosphamide did not significantly influence the risk of ESRD. Regarding the use of rituximab, only two patients were treated with it, and we did not include the analysis. We could confirm that RRS was the independent renal prognostic risk factor using multivariable Cox regression analyses, consistent with the previous report (19).

Next, we also analyzed the subgroup of patients with MPO-AAV and obtained the same results (data not shown).

We also compared the predictive value of RRS and histological classification using AUC values. In previous studies, An et al. compared the predictive values using ROC curves, and they showed that AUC values (95%CI) of RRS and histological classification were 0.742 (0.679–0.804) and 0.587 (0.515–0.659), respectively, with RRS having better performance (31). Saito et al. evaluated the AUC values (95%CI) of RRS and histological classification as 0.80 (0.69–0.91) and 0.74 (0.62–0.86), respectively (19). In our study, the AUC values of the RRS and the histological classification calculated based on the ROC for developing ESRD were 0.890 (95%CI, 0.819–0.959) and 0.857 (95% CI, 0.773–0.942), respectively. We found that the difference in prediction for renal survival between the RRS and the histological classification was insignificant. Assessment using the histological classification does not necessarily show a gradual deterioration in survival from "focal" (best) to "crescentic," "mixed," or "sclerotic" (worst), as was the case in our results. The evaluation results using the RRS were consistent across different cohorts, and we believe it is a highly reproducible prognostic tool.

There are several limitations to this study. First, this is a retrospective study, and the treatment regimen by clinicians changed over the years as new evidence came to light. Second, the

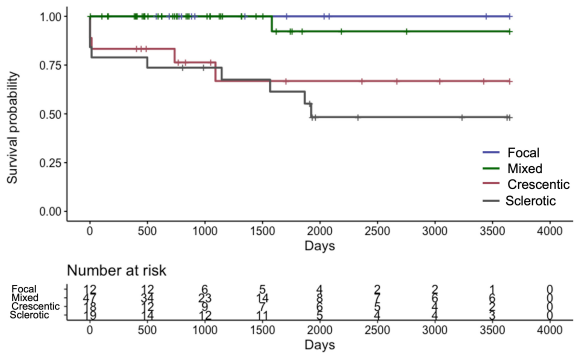

FIGURE 3
Kaplan-Meier curve demonstrating renal survival of Japanese patients with ANCA-associated renal vasculitis according to the histological classification ANCA: anti-neutrophil cytoplasmic antibody.

TABLE 3 Independent risk factors for end-stage renal disease in patients with ANCA-associated renal vasculitis.

Variables	Univariate analysis		Multivariable analysis	
	HR (95%CI)	P-value	HR (95%CI)	P-value
Sex, males/females	1.497 (0.539-4.152)	0.438		
Age, per 1-yr increase	0.982 (0.946-1.029)	0.421		
WBC, per 100/μL	0.998 (0.983-1.013)	0.881		
Hb, per 1 mg/dL	0.940 (0.712-1.219)	0.651		
CRP, per 1 mg/dL increase	0.898 (0.772-0.996)	0.040*	0.904 (0.774-1.016)	0.094
BVAS, per 1 unit increase	0.926 (0.818-1.034)	0.181		
renal risk score, per 1 unit increase	1.648 (1.366-2.087)	<.0001*	1.723 (1.387-2.302)	<.0001*
History of hypotensive drugs, yes/no	1.482 (0.518-4.241)	0.465		
Smoking history, yes/no	2.254 (0.659-7.709)	0.185		
Use of antidiabetic drugs, yes/no	1.485 (0.184-11.975)	0.724		
Use of methylprednisolone pulse, yes/no	1.225 (0.387-3.880)	0.726		
Dose of prednisolone, per 10 mg increase	1.121 (0.743-1.730)	0.600		
Plasmapheresis, yes/no	1.743 (0.491-6.182)	0.417		
Cyclophosphamide, yes/no	0.692 (0.156-3.078)	0.614		

*p < 0.05. BVAS, Birmingham Vasculitis Activity Score; CI, confidence interval; CRP, C-reactive protein; Hb, hemoglobin; HR, hazard ratio; WBC, white blood cell count

number of patients and events did not provide robust evidence. Third, we must consider that the patients may have had a period of undiagnosed AAGN before the diagnosis was made. Fourth, there may be a selection bias for the patients with AAGN in this cohort since a bias would have been introduced by excluding cases where the patients refused biopsy. Fifth, there was a variation in the induction therapy protocol in our cohort over the course of a long-term follow-up period. More extensive and prospective studies are needed in the future.

Conclusions

We demonstrated the stable predictive ability of the RRS for renal survival in Japanese patients over the long term, in contrast to

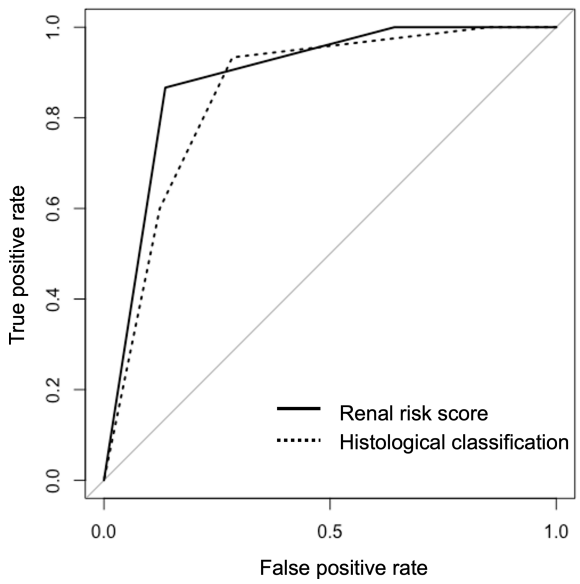

FIGURE 4
The receiver operating characteristic curves for predicting end-stage renal disease using the renal risk score and the histological classification.

the histological classification. However, further studies are necessary for validation.Abbreviations

AAV, anti-neutrophil cytoplasmic antibody-associated vasculitis; AAGN, anti-neutrophil cytoplasmic antibody-associated glomerulonephritis; ANCA, anti-neutrophil cytoplasmic antibody; AUC, area under the receiver operating characteristic curve; BVAS, Birmingham Vasculitis Activity Score; CRP, C-reactive protein; eGFR, estimated glomerular filtration rate; EGPA, eosinophilic granulomatosis polyangiitis; ESRD, end-stage renal disease; GPA, granulomatosis polyangiitis; IQR, interquartile range; MPA, microscopic polyangiitis; ROC, receiver operating characteristic; RRS, renal risk score.

Data availability statement

The raw data supporting the conclusions of this article will be made available by the authors, without undue reservation.

Ethics statement

The studies involving human participants were reviewed and approved by Institutional Review Boards of Nagasaki University. Written informed consent for participation was not required for this study in accordance with the national legislation and the institutional requirements.

Author contributions

TU, KI: Conception and design of the study, analysis and interpretation of data, and drafting of the article. TU, SS: Statistical analysis and interpretation of data. TU, KI, AY, KM, MK: Collection and assembly of data. TU, KI, KM, MK, SS, NI, TN, AK: analysis, and interpretation of data, critical revision of the manuscript. TN, AK, supervision of the project. All authors contributed to the article and approved the submitted version.

Conflict of interest

The authors declare that the research was conducted in the absence of any commercial or financial relationships that could be construed as a potential conflict of interest.

Publisher's note

Supplementary material

The Supplementary Material for this article can be found online at: https://www.frontiersin.org/articles/10.3389/fimmu.2023.1141407/full#supplementary-material

References

1. Nakazawa D, Masuda S, Tomaru U, Ishizu A. Pathogenesis and therapeutic interventions for ANCA-associated vasculitis. *Nat Rev Rheumatol* (2019) 15:91–101. doi: 10.1038/s41584-018-0145-y

2. Jennette JC. Overview of the 2012 revised international chapel hill consensus conference nomenclature of vasculitides. *Clin Exp Nephrol* (2013) 17:603–6. doi: 10.1007/s10157-013-0869-6

3. Sinico RA, Di Toma L, Radice A. Renal involvement in anti-neutrophil cytoplasmic autoantibody associated vasculitis. *Autoimmun Rev* (2013) 12:477–82. doi: 10.1016/j.autrev.2012.08.006

4. Berti A, Cornec-Le Gall E, Cornec D, Casal Moura M, Matteson EL, Crowson CS, et al. Incidence, prevalence, mortality and chronic renal damage of anti-neutrophil cytoplasmic antibody-associated glomerulonephritis in a 20-year population-based cohort. *Nephrol Dial Transplant* (2019) 34:1508–17. doi: 10.1093/ndt/gfy250

5. Sagmeister MS, Grigorescu M, Schönermarck U. Kidney transplantation in ANCA-associated vasculitis. *J Nephrol* (2019) 32:919–26. doi: 10.1007/s40620-019-00642-x

6. Binda V, Moroni G, Messa P. ANCA-associated vasculitis with renal involvement. *J Nephrol* (2018) 31:197–208. doi: 10.1007/s40620-017-0412-z

7. Flossmann O, Berden A, de Groot K, Hagen C, Harper L, Heijl C, et al. Long-term patient survival in ANCA-associated vasculitis. *Ann Rheum Dis* (2011) 70:488–94. doi: 10.1136/ard.2010.137778

8. Molnár A, Studinger P, Ledó N. Diagnostic and therapeutic approach in ANCA-associated glomerulonephritis: A review on management strategies. *Front Med (Lausanne)* (2022) 9:884188. doi: 10.3389/fmed.2022.884188

9. Berden AE, Ferrario F, Hagen EC, Jayne DR, Jennette JC, Joh K, et al. Histopathologic classification of ANCA-associated glomerulonephritis. *J Am Soc Nephrol* (2010) 21:1628–36. doi: 10.1681/ASN.2010050477

10. van Daalen EE, Wester Trejo MAC, Göçeroğlu A, Ferrario F, Joh K, Noël LH, et al. Developments in the histopathological classification of ANCA-associated glomerulonephritis. *Clin J Am Soc Nephrol* (2020) 15:1103–11. doi: 10.2215/CJN.14561119

11. Chen YX, Xu J, Pan XX, Shen PY, Li X, Ren H, et al. Histopathological classification and renal outcome in patients with antineutrophil cytoplasmic antibodies-associated renal vasculitis: A study of 186 patients and metaanalysis. *J Rheumatol* (2017) 44:304–13. doi: 10.3899/jrheum.160866

12. Huang S, Shen Q, Yang R, Lai H, Zhang J. An evaluation of the 2010 histopathological classification of anti-neutrophil cytoplasmic antibody (ANCA)-associated glomerulonephritis: a Bayesian network meta-analysis. *Int Urol Nephrol* (2018) 50:1853–61. doi: 10.1007/s11255-018-1941-7

13. Ge Y, Yang G, Yu X, Sun B, Zhang B, Yuan Y, et al. Outcome predictors of biopsy-proven myeloperoxidase-Anti-Neutrophil cytoplasmic antibody-associated glomerulonephritis. *Front Immunol* (2020) 11:607261. doi: 10.3389/fimmu.2020.607261

14. Brix SR, Noriega M, Tennstedt P, Vettorazzi E, Busch M, Nitschke M, et al. Development and validation of a renal risk score in ANCA-associated glomerulonephritis. *Kidney Int* (2018) 94:1177–88. doi: 10.1016/j.kint.2018.07.020

15. Gercik O, Bilgin E, Solmaz D, Cakalagaoglu F, Saglam A, Aybi O, et al. Histopathological subgrouping versus renal risk score for the prediction of end-stage renal disease in ANCA-associated vasculitis. *Ann Rheum Dis* (2020) 79:675–6. doi: 10.1136/annrheumdis-2019-216742

16. Bai X, Guo Q, Lou Y, Nie P, Zhu Y, Li B, et al. Validation of the renal risk score for anti-neutrophil cytoplasmic antibody-associated glomerulonephritis in a Chinese population. *Clin Rheumatol* (2021) 40:5009–17. doi: 10.1007/s10067-021-05862-w

17. Mejía-Vilet JM, Martín-Nares E, Cano-Verduzco ML, Pérez-Arias AA, Sedano-Montoya MA, Hinojosa-Azaola A. Validation of a renal risk score in a cohort of

ANCA-associated vasculitis patients with severe kidney damage. *Clin Rheumatol* (2020) 39:1935–43. doi: 10.1007/s10067-020-04936-5

18. Villacorta J, Diaz-Crespo F, Guerrero C, Acevedo M, Cavero T, Fernandez-Juarez G. Long-term validation of the renal risk score for vasculitis in a southern European population. *Clin Kidney J* (2021) 14:220–5. doi: 10.1093/ckj/sfaa073

19. Saito M, Saito A, Abe F, Imaizumi C, Kaga H, Sawamura M, et al. Evaluation of a newly proposed renal risk score for Japanese patients with ANCA-associated glomerulonephritis. *Clin Exp Nephrol* (2022) 26:760–9. doi: 10.1007/s10157-022-02217-w

20. Xia M, Yu R, Zheng Z, Li H, Feng J, Xie X, et al. Meta-analytical accuracy of ANCA renal risk score for prediction of renal outcome in patients with ANCA-associated glomerulonephritis. *Front Med (Lausanne)* (2021) 8:736754. doi: 10.3389/fmed.2021.736754

21. Matsuo S, Imai E, Horio M, Yasuda Y, Tomita K, Nitta K, et al. Revised equations for estimated GFR from serum creatinine in Japan. *Am J Kidney Dis* (2009) 53:982–92. doi: 10.1053/j.ajkd.2008.12.034

22. Mukhtyar C, Lee R, Brown D, Carruthers D, Dasgupta B, Dubey S, et al. Modification and validation of the Birmingham vasculitis activity score (version 3). *Ann Rheum Dis* (2009) 68:1827–32. doi: 10.1136/ard.2008.101279

23. R Core Team. R: A Language and Environment for Statistical Computing. R Foundation for Statistical Computing. Vienna, Austria (2022). Available from: https://www.R-project.org/

24. Chang DY, Wu LH, Liu G, Chen M, Kallenberg CG, Zhao MH. Re-evaluation of the histopathologic classification of ANCA-associated glomerulonephritis: a study of 121 patients in a single center. *Nephrol Dial Transplant* (2012) 27:2343–9. doi: 10.1093/ndt/gfr643

25. Muso E, Endo T, Itabashi M, Kakita H, Iwasaki Y, Tateishi Y, et al. Evaluation of the newly proposed simplified histological classification in Japanese cohorts of myeloperoxidase-anti-neutrophil cytoplasmic antibody-associated glomerulonephritis in comparison with other Asian and European cohorts. *Clin Exp Nephrol* (2013) 17:659–62. doi: 10.1007/s10157-012-0755-7

26. Hilhorst M, Wilde B, van Breda Vriesman P, van Paassen P, Cohen Tervaert JW. Estimating renal survival using the ANCA-associated GN classification. *J Am Soc Nephrol* (2013) 24:1371–5. doi: 10.1681/ASN.2012090912

27. Hilhorst M, van Paassen P, Tervaert JW. Proteinase 3-ANCA vasculitis versus myeloperoxidase-ANCA vasculitis. *J Am Soc Nephrol* (2015) 26:2314–27. doi: 10.1681/ASN.2014090903

28. Quintana LF, Peréz NS, De Sousa E, Rodas LM, Griffiths MH, Solé M, et al. ANCA serotype and histopathological classification for the prediction of renal outcome in ANCA-associated glomerulonephritis. *Nephrol Dial Transplant* (2014) 29:1764–9. doi: 10.1093/ndt/gfu084

29. Hakroush S, Kluge IA, Ströbel P, Korsten P, Tampe D, Tampe B. Systematic histological scoring reveals more prominent interstitial inflammation in myeloperoxidase-ANCA compared to proteinase 3-ANCA glomerulonephritis. *J Clin Med* (2021) 10:1231. doi: 10.3390/jcm10061231

30. Hauer HA, Bajema IM, van Houwelingen HC, Ferrario F, Noël LH, Waldherr R, et al. Renal histology in ANCA-associated vasculitis: differences between diagnostic and serologic subgroups. *Kidney Int* (2002) 61:80–9. doi: 10.1046/j.1523-1755.2002.00089.x

31. An XN, Wei ZN, Yao XY, Xu J, Qian WT, Pan XX, et al. Evaluating renal outcome of ANCA-associated renal vasculitis: Comparative study of two histopathological scoring systems. *Clin Exp Rheumatol* (2021) 39 Suppl 129:39–45. doi: 10.55563/clinexprheumatol/24ep0c

32. You X, Zhang J, Ding X, Zhang J, Zhou Q, Lu G. Predictors of renal outcomes in crescentic and mixed class of ANCA-associated glomerulonephritis. *Clin Nephrol* (2021) 95:81–6. doi: 10.5414/CN110221

frontiers | Frontiers in Immunology

TYPE Original Research
PUBLISHED 20 June 2023
DOI 10.3389/fimmu.2023.1189257

OPEN ACCESS

EDITED BY
Francesca Wanda Rossi,
University of Naples Federico II, Italy

REVIEWED BY
Vincent Sobanski,
INSERM U1286, France
Takemichi Fukasawa,
The University of Tokyo Hospital, Japan
Hayakazu Sumida,
The University of Tokyo, Japan

*CORRESPONDENCE
Douwe J. Mulder
d.j.mulder@umcg.nl

†These authors share first authorship

RECEIVED 18 March 2023
ACCEPTED 06 June 2023
PUBLISHED 20 June 2023

CITATION
Atzeni IM, Al-Adwi Y, Doornbos-van der Meer B, Roozendaal C, Stel A, van Goor H, Gan CT, Dickinson M, Timens W, Smit AJ, Westra J and Mulder DJ (2023) The soluble receptor for advanced glycation end products is potentially predictive of pulmonary arterial hypertension in systemic sclerosis. *Front. Immunol.* 14:1189257. doi: 10.3389/fimmu.2023.1189257

The soluble receptor for advanced glycation end products is potentially predictive of pulmonary arterial hypertension in systemic sclerosis

Isabella M. Atzeni[1†], Yehya Al-Adwi[1†], Berber Doornbos-van der Meer[2], Caroline Roozendaal[3], Alja Stel[2], Harry van Goor[4], C. Tji Gan[5], Michael Dickinson[6], Wim Timens[4], Andries J. Smit[1], Johanna Westra[2] and Douwe J. Mulder[1*]

[1]Department of Internal Medicine, Division of Vascular Medicine, University Medical Centre Groningen, University of Groningen, Groningen, Netherlands, [2]Department of Rheumatology and Clinical Immunology, University Medical Centre Groningen, University of Groningen, Groningen, Netherlands, [3]Department of Laboratory Medicine, University Medical Centre Groningen, University of Groningen, Groningen, Netherlands, [4]Department of Pathology and Medical Biology, University Medical Centre Groningen, University of Groningen, Groningen, Netherlands, [5]Department of Pulmonary Diseases and Tuberculosis, University Medical Centre Groningen, University of Groningen, Groningen, Netherlands, [6]Department of Cardiology, University Medical Centre Groningen, University of Groningen, Groningen, Netherlands

Introduction: Pulmonary arterial hypertension (PAH) and interstitial lung disease (ILD) are the leading causes of death in systemic sclerosis (SSc). Until now, no prospective biomarker to predict new onset of SSc-ILD or SSc-PAH in patients with SSc has reached clinical application. In homeostasis, the receptor for advanced glycation end products (RAGE) is expressed in lung tissue and involved in cell-matrix adhesion, proliferation and migration of alveolar epithelial cells, and remodeling of the pulmonary vasculature. Several studies have shown that sRAGE levels in serum and pulmonary tissue vary according to the type of lung-related complication. Therefore, we investigated levels of soluble RAGE (sRAGE) and its ligand high mobility group box 1 (HMGB1) in SSc and their abilities to predict SSc-related pulmonary complications.

Methods: One hundred eighty-eight SSc patients were followed retrospectively for the development of ILD, PAH, and mortality for 8 years. Levels of sRAGE and HMGB1 were measured in serum by ELISA. Kaplan-Meier survival curves were performed to predict lung events and mortality and event rates were compared with a log-rank test. Multiple linear regression analysis was performed to examine the association between sRAGE and important clinical determinants.

Results: At baseline, levels of sRAGE were significantly higher in SSc-PAH-patients (median 4099.0 pg/ml [936.3-6365.3], p = 0.011) and lower in SSc-ILD-patients (735.0 pg/ml [IQR 525.5-1988.5], p = 0.001) compared to SSc

patients without pulmonary involvement (1444.5 pg/ml [966.8-2276.0]). Levels of HMGB1 were not different between groups. After adjusting for age, gender, ILD, chronic obstructive pulmonary disease, anti-centromere antibodies, the presence of puffy fingers or sclerodactyly, use of immunosuppression, antifibrotic therapy, or glucocorticoids, and use of vasodilators, higher sRAGE levels remained independently associated with PAH. After a median follow-up of 50 months (25-81) of patients without pulmonary involvement, baseline sRAGE levels in the highest quartile were predictive of development of PAH (log-rank p = 0.01) and of PAH-related mortality (p = 0.001).

Conclusions: High systemic sRAGE at baseline might be used as a prospective biomarker for patients with SSc at high risk to develop new onset of PAH. Moreover, high sRAGE levels could predict lower survival rates due to PAH in patients with SSc.

KEYWORDS

PAH, sRAGE, predictability, SSc, scleroderma, ILD

Introduction

Interstitial lung disease (ILD) and pulmonary arterial hypertension (PAH) are the leading causes of death in systemic sclerosis (SSc) (1), a heterogeneous disease characterized by vasculopathy and immune activation, eventually leading to irreversible skin and internal organ fibrosis. Currently, no disease-modifying therapies are showing satisfactory results. Therefore, identifying disease markers that might help to predict the course of the disease is very useful. Some biomarkers have been identified for diagnosis, prognosis, and response to treatment in SSc-ILD (2). Other biomarkers were linked to SSc-PAH (3, 4),. However, no reliable prospective biomarker has been identified that can predict new onset of SSc-ILD or SSc-PAH in patients with SSc.

RAGE, a multi-ligand cell surface receptor that is expressed on a wide range of cell types, including fibroblasts, endothelial cells, and smooth muscle cells, has been implicated in numerous diseases (5, 6). Besides being the most important receptor for advanced glycation end products (AGEs), RAGE can bind exogenous and endogenous molecules, such as danger-associated molecular patterns (DAMPs) including S100A8, S100A9 and S100A12/calgranulin and high mobility group box 1 (HMGB1), leading to inflammation through NF-kB activation (7). Its soluble form (sRAGE) is established by alternative splicing of RAGE mRNA, or proteolytic cleavage of the membrane-bound form (mRAGE) by Matrix Metalloproteinase 9 (MMP9) or A-Disintegrin and Metalloprotease 10 (ADAM10) (8, 9). Although sRAGE may act as a decoy receptor for RAGE ligands which could lead to tissue damage (10), its exact role is still not completely clear.

RAGE is ubiquitously expressed in almost all tissues at relatively low levels. However, it is highly expressed in healthy lung tissue, especially on the alveolar type I cells, suggesting that RAGE may have a significant role in lung homeostasis, particularly in cell spreading and growth (11). While RAGE overexpression has been demonstrated in the fibrotic conditions in different organ systems, mRAGE and sRAGE expressions are strongly decreased in blood and lung tissue of patients with idiopathic pulmonary fibrosis (IPF) (11, 12). Also, in airway diseases such as chronic obstructive pulmonary disease (COPD) decreased sRAGE levels are described (12). In contrast, upregulation of (s)RAGE has been shown in serum and lung tissue of patients with PAH compared to healthy controls, giving rise to extracellular matrix accumulation, pulmonary artery smooth muscle cell proliferation, and apoptosis resistance (13, 14).

A potential role for HMGB1 has also been described in PAH development (14). HMGB1 is known to be released extracellularly in response to cellular injury or stress and functions as a DAMP that signals, as mentioned, through RAGE but also through the toll-like receptors (TLR4 and TLR2). The downstream processes of the HMGB1-RAGE/TLR4 axis are pro-inflammatory (15). Its serum and lung tissue levels have been reported to be increased in PAH patients and serum levels correlated with mean pulmonary arterial pressure (mPAP) (16). Similarly, serum HMGB1 is reported to be elevated in patients with SSc-ILD compared to SSc patients without ILD and healthy controls (17).

Thus, we hypothesized that high levels of sRAGE and/or HMGB1 would predict new onset of PAH and PAH-related mortality in patients with SSc while low levels would predict ILD. This may enable early identification of these devastating complications, and potentially set the stage for early intervention strategies in future studies.

Materials and methods

Patients

In the current study, a total of 188 SSc patients were included from 2013 to 2020. Patients were classified according to ACR/EULAR criteria for SSc (18). Demographic and disease data were

gathered retrospectively by screening medical records. Also, the use of medication was collected and divided into three groups: immunosuppression or antifibrotic therapy, glucocorticoids, and vasodilators. Pulmonary function tests (PFTs) and blood were collected from routine clinical care through our outpatient clinic. The date of first blood sampling was considered as baseline and all serum was stored at -20°C. PFTs were following ATS/ERS guidelines and were defined by diffusing capacity for carbon monoxide (DLCO), forced vital capacity (FVC), or forced expiratory volume in 1 second (FEV1). An abnormal DLCO was defined when the predicted value was < 80% and an abnormal FVC when the predicted value was < 70%. The FEV1/FVC ratio and medical history were used for the diagnosis of COPD. ILD was diagnosed by PFTs and high-resolution computed tomography (HRCT) using the diagnostic algorithm according to the British Thoracic Society guidelines (19). Patients underwent a right heart catheterization if echocardiography showed tricuspid regurgitant velocity > 2.8 and/or typical echocardiographic features of PH. PAH was diagnosed based on pulmonary arterial pressure ≥ 25 mmHg and pulmonary artery wedge pressure ≤ 15 mmHg at rest measured by right heart catheterization according to the ESC/ERS 2015 guidelines (20). Other pre-capillary causes of PH were excluded using a standardized work-up and discussion in a multidisciplinary expert team. Development of ILD, PAH, and mortality were assessed during follow-up, adjudicated by two investigators, reaching a consensus diagnosis. When a consensus diagnosis was not reached, patients were discussed in multidisciplinary consultations and a final diagnosis was concluded. According to Dutch law and University Medical Centre Groningen regulations, this type of study did not fall within the scope of Medical Research Involving Human Subjects Act. The local ethics committee provided approval with exemption from written informed consent. This study was registered in the research register of the University Medical Centre Groningen (201900260).

Enzyme-linked immunosorbent assays

HMGB1 and sRAGE serum concentrations were measured by enzyme-linked immunosorbent assays (ELISAs). HMGB1 was quantified using a commercial ELISA kit (TECAN, the Netherlands) while sRAGE was measured using a Duoset kit (R&D systems, United Kingdom), according to manufacturers' instructions. High-performance ELISA buffer (Sanquin, the Netherlands) was used during serum incubation to prevent non-specific reactions. ELISAs were read using a microplate reader at 450-575nm and analyzed using Softmax software.

Immunohistochemistry

For a pilot study, formalin-fixed paraffin-embedded human lung tissues obtained from two SSc-PAH patients were used for immunohistochemistry studies. Briefly, the lung tissues were cut at 3 microns sections, mounted on glass slides, and deparaffinized. For RAGE immunohistochemistry, antigen retrieval was performed with tris-HCl and EDTA. Mouse-anti-human RAGE (Santa Cruz, (A-9): sc-365154, Dallas, Texas, USA) was added overnight. Consecutively, samples were incubated with rabbit anti-mouse-HRP conjugate (Dako, 0260, Santa Clara, USA), and stained with diaminobenzidine as a substrate (Dako K4006, Santa Clara, USA). Negative control staining was performed by omission of RAGE antibody showing no aspecific binding. For determining RAGE localization, additional staining was performed on serial sections as follows. For comparison, standard histochemical Haematoxylin-Eosin and Verhoeff's elastin stains were performed, in addition to, immunohistochemical stains for CD31 (endothelial cells), alpha-smooth muscle actin ([α-SMA] myofibroblasts and smooth muscle cells), and desmin (smooth muscle cells). The latter immunohistochemical stains were performed using an automated Ventana Benchmark Ultra immunostainer (Roche Diagnostics Netherlands) in our ISO15189 accredited pathology department.

Statistical analysis

Statistical analysis was performed using IBM SPSS Statistics version 23. Patients were divided based on pulmonary involvement into four groups: no history of pulmonary involvement, ILD, PAH, or ILD and PAH. Data are presented as median and interquartile range (IQR) or as number (%). The Kruskal Wallis test and Mann-Whitney U test were used for comparison between groups. Spearman correlation coefficients were performed to measure associations. Kaplan-Meier survival curves were performed to predict lung events and mortality, and event rates were compared with log-rank test. Univariate analysis was used to identify factors potentially associated with PAH. In addition to age and gender, variables with significant associations were then used in the multivariate model. Multiple linear regression analysis was performed to examine the association between sRAGE and important clinical determinants at baseline. In our first model, we adjusted for age, gender, and PAH. Second, we added ILD and COPD. Third, anti-centromere antibody (ACA) positivity was added. Fourth, we added the presence of puffy fingers or sclerodactyly, and, finally, use of immunosuppression, antifibrotic therapy, glucocorticoids, or vasodilators were added. P-values < 0.05 were considered significant.

Results

Patient characteristics

The patient characteristics are shown in Table 1. At baseline, of the 188 included patients, 124 had no history of pulmonary involvement, 41 had ILD, 12 had PAH, and 11 had a history of both ILD and PAH. In all subgroups, the limited cutaneous form of SSc was most prevalent. As expected, the percentage of predicted FVC and DLCO was lower in ILD- and PAH- patients compared to SSc patients without pulmonary involvement. Moreover, treatment with immunosuppression was most often seen in ILD- and ILD+PAH- patients, while vasodilators were more prevalent in PAH- and PAH+ILD- patients.

10.3389/fimmu.2023.1189257

TABLE 1 Patient characteristics at baseline.

	SSc patients without pulmonary involvement (n=124)	SSc patients with ILD (n=41)	SSc patients with PAH (n=12)	SSc patients with ILD-PAH (n=11)	Kruskal Wallis Test
Age in years, median (IQR)	61 (54–72)	65 (53-72)	70 (66-78)	64 (58-72)	p = 0.102
Female, n (%)	102 (82.3)	28 (68.3)	9 (75.0)	6 (54.5)	p = 0.077
Extent of skin involvement, n (%)					p = 0.188
Limited Diffuse Other	114 (91.9) 9 (7.3) 1 (0.8)	35 (85.4) 6 (14.6) 0 (0.0)	10 (83.3) 2 (16.7) 0 (0.0)	8 (72.7) 3 (27.3) 0 (0.0)	
Puffy fingers or sclerodactyly, n (%)	103 (83.1)	35 (85.4)	10 (83.3)	10 (90.9)	p = 0.912
Pitting scars or digital ulcers, n (%)	66 (53.2)	17 (41.5)	3 (25.0)	7 (63.6)	p = 0.140
Telangiectasia, n (%)	83 (74.1) (ND: 12)	29 (78.4) (ND: 4)	9 (100.0) (ND: 3)	9 (90.0) (ND: 1)	p = 0.238
Raynaud's phenomenon, n (%)	124 (100.0)	40 (97.6)	11 (100.0) (ND: 1)	11 (100.0)	p = 0.313
Antibody profile, n (%)					p = 0.249
Anti-centromere Anti-topoisomerase I Anti-RNA polymerase III Other	74 (59.7) 10 (8.1) 1 (0.8) 39 (31.5)	8 (19.5) 8 (19.5) 0 (0.0) 25 (61.0)	8 (66.7) 1 (8.3) 1 (8.3) 2 (16.7)	3 (27.3) 2 (18.2) 2 (18.2) 4 (36.4)	
Calcinosis cutis, n (%)	40 (36.4) (ND: 14)	11 (32.4) (ND: 7)	4 (50.0) (ND: 4)	3 (50.0) (ND: 5)	p = 0.720
Gastrointestinal involvement, n (%)	88 (73.9) (ND: 5)	25 (62.5) (ND: 1)	6 (60.0) (ND: 2)	8 (72.7) (ND: 1)	p = 0.412
PFTs, median (IQR)					
% FVC	109.0 (95.5-120.0) (ND: 15)	94.5 (68.8-107.0)*** (ND: 3)	101 (83.8-116.8)	86.0 (65.0-107.0)***	p < 0.001
% DLCO	74.0 (62.0-83.5) (ND: 15)	54.0 (42.5-70.5) (ND: 9)	44.0 (42.0-61.0)* (ND: 3)	19.0 (17.3-35.5)** (ND: 12)	p < 0.001
% Tiffeneau index	78.0 (70.0-82.0) (ND: 13)	80.0 (74.5-84.5) (ND: 4)	73.0 (67.3-80.8)	79.0 (66.0-85.0)	p = 0.180
COPD, n (%)	28 (22.6)	6 (14.6)	3 (25.0)	3 (27.3)	p = 0.675
Medication, n (%)					
Immunosuppression Vasodilators Glucocorticoids	17 (13.7) 16 (12.9) 10 (8.1)	15 (36.6)** 3 (7.3) 7 (17.1)	0 (0.0) 9 (75.0)*** 0 (0.0)	5 (45.5)** 5 (45.5)** 3 (27.3)*	p = 0.001 p < 0.001 p = 0.065

SSc, systemic sclerosis; ILD, interstitial lung disease; PAH, pulmonary arterial hypertension; PFTs, pulmonary function tests; FVC, forced vital capacity; DLCO, diffusing capacity for carbon monoxide. *p<0.05, **p<0.01, ***p<0.001 vs no pulmonary involvement group (by Mann-Whitney U test). ND, not documented.

Baseline comparison of sRAGE and HMGB1 levels

At baseline, levels of sRAGE were significantly higher in SSc-PAH patients (4099.0 pg/ml [936.3-6365.3], p = 0.011) but significantly lower in SSc-ILD (median 735.0 pg/ml [IQR 525.5-1988.5], p = 0.001) compared to patients without pulmonary involvement (1444.5 pg/ml [966.8-2276.0]). Levels of sRAGE in patients with both ILD and PAH (1487.0 pg/ml [670.0-5319.0]) were comparable to those without pulmonary involvement. No differences in HMGB1 levels were present between the different patient subgroups (No lung involvement: 3.3 [1.7-5.2]; ILD: 3.6 [1.3-5.7]; PAH: 3.9 [2.0-5.1]; ILD+PAH: 3.9 [1.4-7.3]) (Figure 1).

In the entire cohort, levels of sRAGE correlated positively with age (r = 0.218; p = 0.003), FVC (r = 0.242; p = 0.002), FEV1 (r = 0.254; p = 0.001) but not with DLCO (r = -0.023; p = 0.769). sRAGE levels were significantly higher in females compared to males (p = 0.002), also in patients who were positive for ACA (p < 0.001)

10.3389/fimmu.2023.1189257

compared to ACA negative patients, and in patients with puffy fingers or sclerodactyly (p = 0.039) compared to patients with no puffy fingers or sclerodactyly. sRAGE did not differ between lcSSc- and dcSSc patients, pitting scars or digital ulcers, telangiectasia, Raynaud's phenomenon, calcinosis cutis, or intestinal involvement. HMGB1 levels were lower in patients with puffy fingers or sclerodactyly (p = 0.033) and higher in patients with telangiectasia (p = 0.027) compared to patients without puffy fingers or sclerodactyly, or telangiectasia.

Table 2 shows the results of the regression analyses between sRAGE and important clinical determinants. The model showed that baseline sRAGE levels remained independently associated with PAH after adjustment for age, gender, ILD, COPD, ACA positivity, puffy fingers or sclerodactyly, use of vasodilators, and use of immunosuppression, antifibrotic therapy, or glucocorticoids. Noticeably, the presence of ACAs (p < 0.001) and puffy fingers or sclerodactyly (p = 0.017) were significantly associated with sRAGE levels at baseline (model 5).

Follow-up

Follow-up data of 124 patients without pulmonary involvement identified 11 (9%) patients with newly developed ILD and 5 (4%) patients with newly developed PAH (Table 3). The total median time of follow-up was 50 months (25-81 months); 56 months (33-82

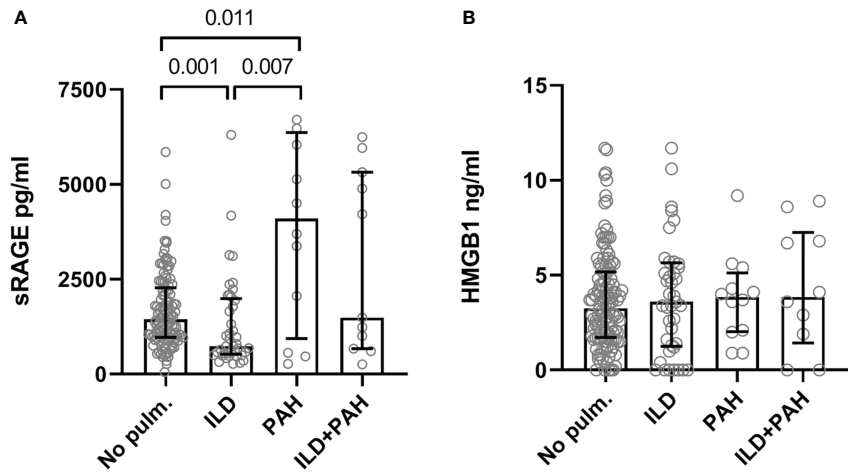

FIGURE 1
Serum levels of the sRAGE **(A)** and HMGB1 **(B)**. **(A)** Serum concentration levels are significantly elevated in SSc-PAH (PAH, N=12) patients compared to SSc-ILD (ILD, N=41) and SSc patients with no lung complications (No pulm., N=124). SSc-ILD patients had significantly lower concentration levels of serum sRAGE compared to SSc patients with no lung complications. SSc patients with PAH and ILD had serum sRAGE concentration levels comparable to SSc patients with no pulmonary complications. **(B)** Serum concentration levels of HMGB1 were comparable in all groups. Measurements are median values of sRAGE or HMGB1. sRAGE, soluble receptor for advanced glycation end products; HMGB1, high mobility group box 1; No pulm., no pulmonary involvement; ILD, interstitial lung disease; PAH, pulmonary arterial hypertension.

TABLE 2 Multiple linear regression models: sRAGE and important clinical determinants.

	Model 1 (R^2 = 0.172; p < 0.001) *St. ß (p = value)*	Model 2 (R^2 = 0.188; p < 0.001) *St. ß (p = value)*	Model 3 (R^2 = 0.261; p < 0.001) *St. ß (p = value)*	Model 4 (R^2 = 0.284; p < 0.001) *St. ß (p = value)*	Model 5 (R^2 = 0.287; p < 0.001) *St. ß (p = value)*
PAH	0.343 (< 0.001)	0.363 (< 0.001)	0.350 (< 0.001)	0.349 (< 0.001)	0.369 (< 0.001)
Gender	-0.142 (0.037)	-0.120 (0.081)	-0.048 (0.479)	-0.044 (0.508)	-0.046 (0.490)
Age	0.165 (0.016)	0.169 (0.016)	0.120 (0.078)	0.094 (0.168)	0.098 (0.153)
ILD		-0.128 (0.065)	-0.030 (0.664)	-0.026 (0.703)	-0.043 (0.557)
COPD		-0.023 (0.744)	-0.012 (0.854)	-0.008 (0.902)	-0.010 (0.879)
Anti-centromere			0.304 (< 0.001)	0.334 (< 0.001)	0.334 (< 0.001)
Puffy finger or sclerodactyly				0.155 (0.018)	0.158 (0.017)
Use of vasodilators					-0.040 (0.580)
Use of immunosuppression, antifibrotic therapy, or glucocorticoids					0.044 (0.511)

sRAGE, soluble receptor for advanced glycation end products; PAH, pulmonary arterial hypertension; ILD, interstitial lung disease; COPD, chronic obstructive pulmonary disease.

months) for the development of ILD and 57 months (35-83 months) for the development of PAH. In the subcohort without PAH at baseline, sRAGE levels in the highest quartile (4th quartile) predicted the development of PAH (p = 0.01) during follow-up (Figure 2A). Low sRAGE levels did not predict ILD development (p = 0.713). However, preliminary data from a small subset of 3 patients, in whom sequential samples were taken, showed that sRAGE levels decreased by approximately 250 pg/ml prior to ILD development. In this population, levels of HMGB1 did not predict PAH (p = 0.317) or ILD (p = 0.875).

Mortality

Overall mortality was in 38% of the cases related to PAH, 17% to ILD, and 21% to other SSc-related complications including gastro-intestinal complications and progressive disease. During follow-up, in the entire cohort, sRAGE (p = 0.126) or HMGB1 (p = 0.404) were not predictive of overall mortality. However, a trend was seen for sRAGE levels in the 1st and in 4th quartiles to predict overall mortality (not shown). PAH-related mortality was significantly predicted by sRAGE levels in the highest quartile (4th quartile) [p = 0.001 (Figure 2B)]. Mortality related to ILD was not predicted by low baseline sRAGE levels.

Immunohistochemical expression of RAGE

From our pilot immunohistochemical study, Figures 3, 4 show representative images of RAGE expression in primary lesions in small arterioles related to SSc vasculopathy, and in secondary lesions developed in due course in PAH in the pulmonary vasculature of SSc patients with PAH. The primary lesion (Figure 3) showed a clearly thickened media and a slightly thickened cellular intima, while the secondary lesion (Figure 4) showed clear, but irregular intima hyperplasia and a relatively normal surrounding media. In Figure 3B, expression of RAGE is seen most pronounced in the intima (inner layer; desmin negative), but also, somewhat less strong, in the thickened media, the surrounding, desmin positive layer. In Figure 4B, RAGE is located predominantly in the media and less in the intima. Comparing RAGE expression with desmin and α-SMA immunostains, the cells stained for RAGE are mainly smooth muscle cells in the media and are myofibroblasts in the intima. The endothelial layer appears

TABLE 3 Patient characteristics at follow-up.

	SSc patients without pulmonary involvement at follow-up (n=109)	SSc patients with ILD (n=11)	SSc patients with PAH (n=5)	Kruskal Wallis Test
Age in years, median (IQR)	61 (54-71)	75 (60-80)*	75 (52-79)	p = 0.048
Female, n (%)	89 (81.7)	9 (81.8)	5 (100.0)	p = 0.769
Death, n (%)	6 (5.5)	1 (9.1)	1 (20.0)	p = 0.441
Extent of skin involvement, n (%)				p = 0.450
Limited Diffuse Other	101 (92.7) 8 (7.3) 0 (0.0)	9 (81.8) 1 (9.1) 1 (9.1)	5 (100.0) 0 (0.0) 0 (0.0)	
Follow-up duration in months, median (IQR)	N/A	56 (33-82)	57 (35-83)	p = 0.793
Puffy fingers or sclerodactyly, n (%)	90 (82.6)	11 (100.0)	3 (60.0)	p = 0.149
Pitting scars or digital ulcers, n (%)	57 (52.3)	6 (54.5)	3 (60.0)	p = 0.551
Telangiectasia, n (%)	72 (74.2) (ND: 12)	8 (72.7)	4 (80.0)	p = 0.933
Raynaud's phenomenon, n (%)	109 (100.0)	11 (100.0)	5 (100.0)	p = 1.000
Antibody profile, n (%)				p = 0.627
Anti-centromere Anti-topoisomerase I Anti-RNA polymerase 3 Other	66 (60.6) 7 (6.4) 1 (0.9) 35 (32.2)	5 (45.5) 3 (27.3) 0 (0.0) 3 (27.3)	4 (80.0) 0 (0.0) 0 (0.0) 1 (20.0)	
Calcinosis cutis, n (%)	36 (37.9) (ND: 14)	3 (27.3)	1 (20.0)	p = 0.788
Gastrointestinal involvement, n (%)	74 (71.2) (ND: 5)	10 (90.9)	5 (100.0)	p = 0.322

SSc, systemic sclerosis; ILD, interstitial lung disease; PAH, pulmonary arterial hypertension; PFTs, pulmonary function tests; FVC, forced vital capacity; DLCO, diffusing capacity for carbon monoxide; N/A, not applicable. One patient had concomitantly ILD and PAH. *p<0.05 vs no pulmonary involvement group (by Mann-Whitney U test). ND, not documented.

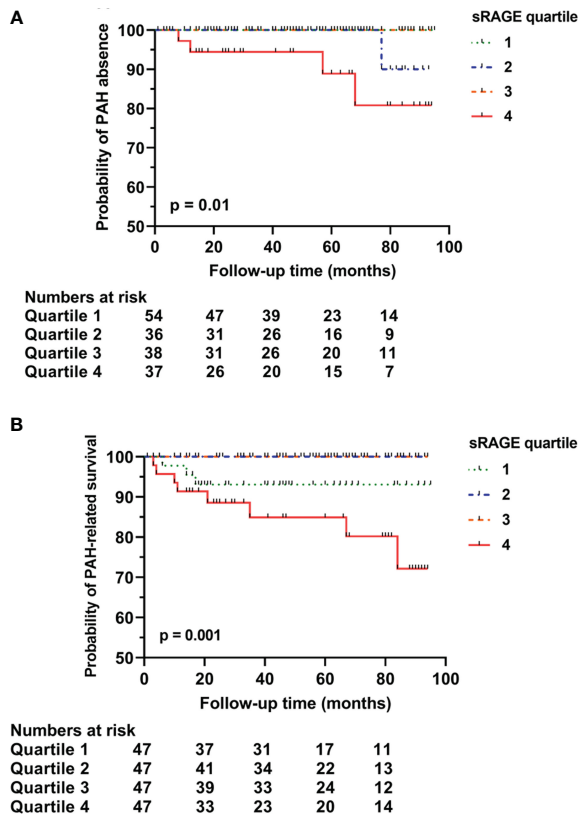

FIGURE 2
Predictive capacity of sRAGE for long-term pulmonary arterial hypertension rate **(A)**, and survival related to pulmonary arterial hypertension **(B)**. Survival curve of baseline sRAGE serum concentrations in SSc patients with no pulmonary involvement stratified into quartiles. **(A)** sRAGE concentration levels in the 4th quartile significantly predicted the development of PAH in SSc patients (p=0.01). **(B)** sRAGE concentration levels in the 4th quartile significantly predicted PAH-related mortality (p=0.001). sRAGE, soluble receptor for advanced glycation end products; PAH, pulmonary arterial hypertension.

negative for RAGE in the primary and secondary lesions. A summary of the IHC results is included in Table 4.

Discussion

PAH and ILD are severe complications in SSc patients, and early detection is still a challenge. Since (s)RAGE acts as a major mediator in pulmonary disease, we investigated the capacity of sRAGE and its ligand, HMGB1 to predict future incidence of SSc-related pulmonary complications. This study shows that sRAGE is significantly higher in sera of patients with SSc-PAH, while it is significantly lower in patients with SSc-ILD, when compared to SSc patients without pulmonary disease. Moreover, we show that high baseline sRAGE levels could potentially be predictive for development of PAH and PAH-related mortality in SSc.

sRAGE has been implicated in various pathological processes in the lung (5, 10, 20). Iwamoto et al. (21) showed that sRAGE was lower in patients with COPD. Similarly, another study showed that levels of sRAGE were lower in patients with IPF and other types of ILD compared to control subjects (22). This is in line with our data as we found lower levels of sRAGE in SSc-ILD patients. In *in vitro* experiments, blocking of RAGE resulted in cell-matrix adhesion impairment, and RAGE knockdown led to an increase in cell proliferation and migration of alveolar epithelial cells and lung fibroblasts (23). This implies that loss of RAGE can lead to fibrotic changes in lung tissues, of which ILD/IPF are important examples. Although in our current study we were not able to demonstrate a predictive value of low sRAGE levels for SSc-ILD, we did find in a small subset of patients (N=3) in whom sequential samples were taken that sRAGE decreased prior to ILD development. This is in line with the correlation of sRAGE with FVC, but not with DLCO, potentially indicating the decrease in sRAGE occurs in more advanced stages of ILD. This observation needs validation in a larger cohort with sequential measurements.

Recently, a group of scientists ran a panel of eight proteins to find a proteomic biomarker signature using a machine-learning approach to distinguish SSc patients with and without PAH (24). Serum samples of 77 patients with PAH and 80 patients without PAH underwent proteomic screening using a multiplex immunoassay. Among all proteins, RAGE turned out to be the most prominent protein to identify SSc-PAH patients. Moreover, a recent study by Nakamura et al. (25) demonstrated the potential role of RAGE in the proliferation of pulmonary artery smooth muscle cells in patients with PAH. This might implicate the pathogenetic role of RAGE and clarify its upregulation in sera of SSc-PAH patients. While these findings confirm the importance of RAGE in the classification and pathogenesis of PAH, our follow-up findings show that high baseline sRAGE levels may also be used to identify SSc patients who will develop PAH. Our results also show that sRAGE may be used to predict PAH-related mortality in SSc.

Our regression analysis shows that ACA presence is significantly correlated with sRAGE levels. Several studies have associated the presence of ACA with development and progression of PAH but could not define whether ACA has pathogenetic effects leading to development of PAH (26, 27). There is indeed a growing body of evidence that immune complexes of SSc-related autoantibodies have pathogenetic effects on skin fibroblasts and endothelial cells. However, to our knowledge, no study has investigated whether these effects lead to PAH development. Finding the primary pathogenetic factor, or possible RAGE-ACA interactions, should be subject to further studies.

In general, HMGB1 is released after cell injury. However, while some studies report increased HMGB1 levels in PAH and IPF, others report no differences between patients and controls (28, 29). We showed that levels of HMGB1 were not different between the subsets in our study and neither predicted pulmonary events nor mortality. This is in accordance with a previous study showing that sRAGE, but not HMGB1, was higher in patients with pulmonary hypertension, especially in PAH and chronic thromboembolic pulmonary hypertension (28). Based on this, we conclude that HMGB1 may not be an appropriate marker for pulmonary involvement and survival in SSc. This may implicate that the upregulation of RAGE in SSc lung tissue is not related to HMGB1 but is possibly due to other RAGE ligands. These include other DAMPs (AGEs and/or calgranulins) which have

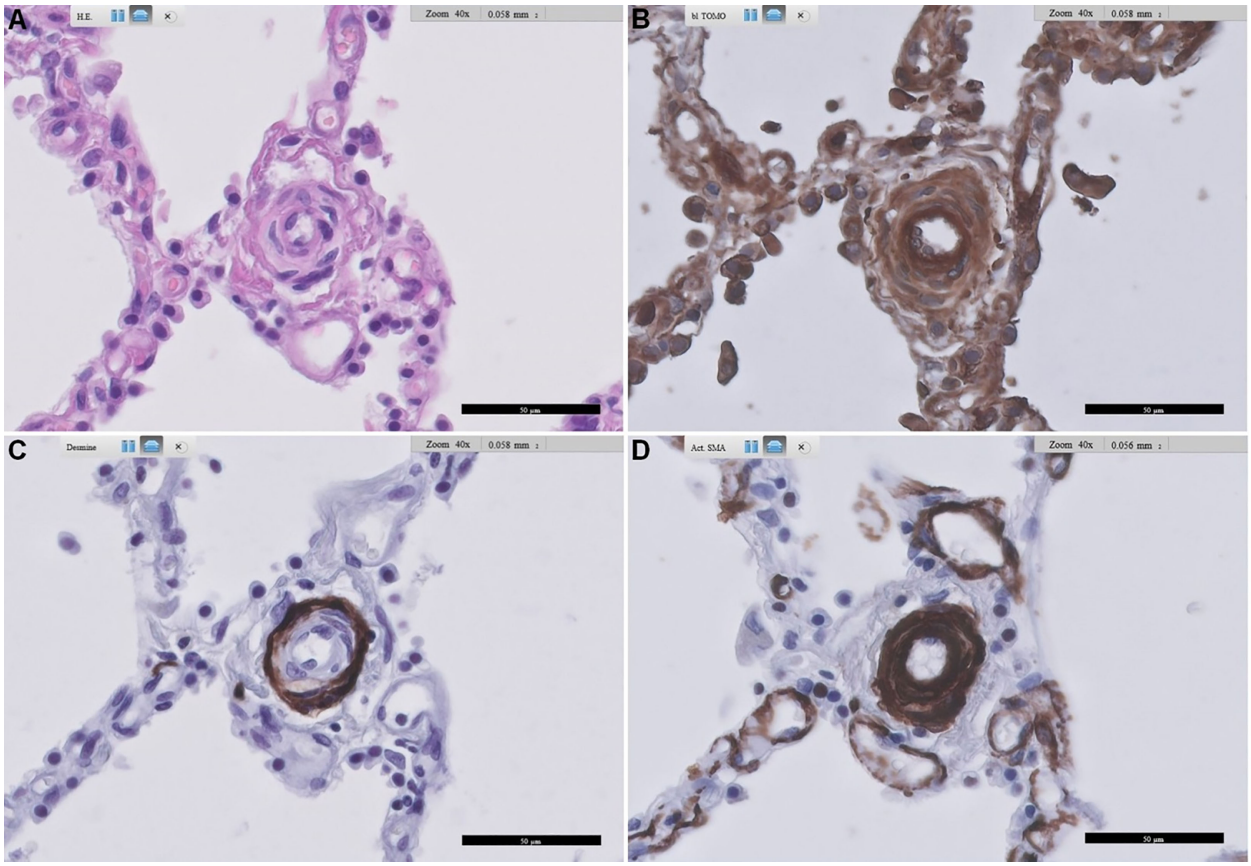

FIGURE 3
Representative images of RAGE staining in a primary pulmonary artery of a patient with SSc-related PAH. **(A)** shows standard Haematoxylin and Eosin-stained lung tissue, **(B)** shows RAGE staining, **(C)** shows desmin staining, and **(D)** shows alpha-smooth muscle actin staining. Arteriopathy in SSc is consistent with PAH with concentric thickening of the media and also concentric cellular increase in thickness of the intima. Scale bar, 50 µm. RAGE: receptor for advanced glycation end products; SSc: systemic sclerosis; PAH: pulmonary arterial hypertension.

previously been shown to be strongly associated with vascular disease and arterial wall remodeling and are increased in PAH (14, 30).

Taken together, it is plausible that the HMGB1 (or other DAMPs) and ACA-autoantibodies together are the actual pathogenetic factor forming immune complexes binding to RAGE in the lung and leading to the development of PAH in SSc patients. And the high sRAGE levels are a coping mechanism (decoy receptor) working to attenuate the overstimulated DAMPs-RAGE axis which, for unknown reasons, does not work in patients developing PAH. Page et al. (31) have demonstrated that co-stimulation of peripheral blood mononuclear cells (PBMCs, regulators of the immune system) with calgranulin leads to increased levels of proinflammatory cytokines (in a RAGE-dependent manner) in ANCA-associated vasculitides (AAV), a group of systemic autoimmune diseases with specific phenotypes. They also reported that DAMPs levels in the circulation vary according to the activity/subtype of the disease. Similarly, sRAGE levels were comparable except for active AAV patients where sRAGE levels were significantly lower. The reasons for these differences are unknown but the authors claim that this is due to disease-specific differences. Our data add considerable strength to what the authors reported by showing distinct levels of sRAGE in different disease subtypes.

Patients with IPF had worse survival rates after a 3-year follow-up when sRAGE levels were low at baseline (32). In our study, low sRAGE levels did not significantly show decreased ILD-related survival. This may have been due to that our study is underpowered, or it might be because while SSc-ILD and IPF pathogeneses could share some similarities, they are two distinct diseases. Importantly, SSc-ILD differs from IPF as it is a fibro-inflammatory disease complication, while the latter is predominantly fibrotic which might allow a divergent profile of sRAGE between both diseases (33).

Different therapies, like nifedipine, have the ability to downregulate the expression of RAGE (34). We were not able to investigate the association between sRAGE levels and calcium antagonists because no patient with SSc-PAH in our cohort used this type of medication. Nakamura et al. (25) reported that AS-1, an inhibitor of RAGE signalling, suppressed the proliferation of smooth muscle cells of patients with idiopathic and heritable PAH, showing that inhibition of RAGE signalling may be a new therapeutic target for PAH. Also, a recent study demonstrated inhibitory effects of a short and single-stranded DNA directed

10.3389/fimmu.2023.1189257

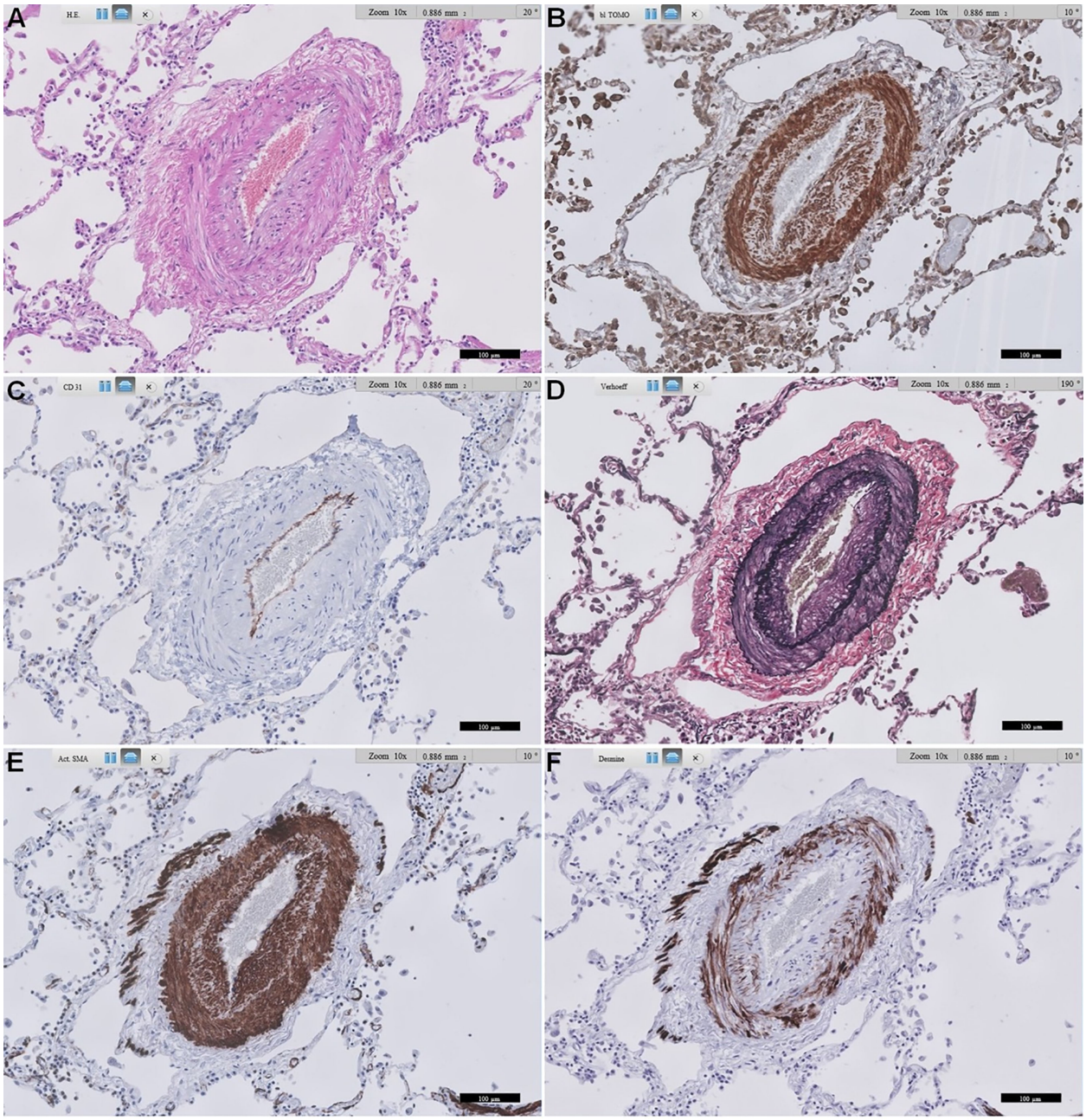

FIGURE 4
Representative images of RAGE staining in a secondary pulmonary artery of a patient with SSc-related PAH. **(A)** shows standard Haematoxylin and Eosin-stained lung tissue. **(B)** shows RAGE staining. **(C)** shows CD31 staining of endothelial cells. **(D)** shows Verhoeff's elastin staining, delineating the inner and outer arterial elastic membrane, and some more diffusely stained elastin in intima and media. **(E)** shows α-smooth muscle actin staining of the media, and also quite extensively in the irregularly thickened intima, likely mainly myofibroblasts. **(F)** shows desmin staining, mainly smooth muscle cells in the media, and some in the intima. Scale bar, 100 µm. This representative image of a SSc-related PAH patient shows predominant expression of RAGE in smooth muscle cells in the media, followed by prominent expression in likely mainly myofibroblasts in the intima. RAGE: receptor for advanced glycation end products; SSc: systemic sclerosis; PAH: pulmonary arterial hypertension.

against RAGE (RAGE aptamer) on the development of PAH in rats (35). This addresses a new therapeutic option for PAH which should be investigated in further studies.

Our pilot immunohistochemical data show expression of RAGE in the thickened intima of the primary arterial lesion related to SSc vasculopathy while the endothelium appears to be negative. Secondary arterial lesions developed in due course in PAH show also clear RAGE staining in the thickened intima. The thickening of the intima in both lesions may be due to infiltration by myofibroblasts since the intima is desmin negative and grossly α-SMA positive. Additionally, the media of both vascular lesions is clearly positive for RAGE, which has been reported before in other forms of PAH (25). Although speculative on these limited pilot data, we hypothesize that the higher systemic RAGE levels in SSc patients who develop PAH are associated with higher

TABLE 4 Summary of IHC studies.

	Primary PAH lesion	Secondary PAH lesion
Media region	Clearly thickened	Normal
Intima region	Slightly thickened	Clear and irregular hyperplasia
RAGE positive staining	Intima (strong), Media (weak)	Media (strong) Intima (weak)
RAGE in smooth muscle cells	In Media (α-SMA and desmin positive)	
RAGE in myofibroblasts	In Intima (α-SMA positive and desmin negative)	
RAGE in endothelial cells	Absent	Absent

RAGE expression in the intima. Possibly, the absence of RAGE staining on endothelial cells might indicate shedding of RAGE into circulation. Additionally, we cannot rule out the possibility that smooth muscle cell proliferation in the media could contribute to a certain extent to the development of other forms of pulmonary hypertension.

This study has some limitations. First, PAH is defined as mPAP > 20 mmHg in the most recent guideline of PAH (36). In this study, the 2015 ESC/ERS guideline for the diagnosis of PAH by Galiè et al. (20) was used to define PAH as mPAP > 25 mmHg as it was practised at our center. This may have resulted in missing patients. Second, measures of diagnostic accuracy have not been calculated due to the limited sample size of affected patients. Also, as a consequence, Cox regression and prediction of mortality in the subset of patients with PAH could not be calculated. Preferably, these measurements should be conducted in future, prospective larger studies and correction for potential confounders need to be performed. Third, the smoking status of the patients was not analyzed, which may have influenced levels of sRAGE. Fourth, we could not check the values of other ligands of RAGE such as AGEs or s100 proteins. Finally, due to the limited availability of PAH lung tissue sections, our immunohistochemistry studies left us with cautious conclusions regarding RAGE source and location. These preliminary data need further exploration in larger series, and this hypothesis needs to be confirmed in experimental studies.

Of importance, our data may be useful to design prospective, longitudinal, multi-center studies on early biomarkers in pulmonary involvement and mortality in SSc to improve and strengthen our observations. As mentioned above, preliminary data of sRAGE values in consecutive blood samples of a few patients with SSc showed a clear drop in sRAGE before the development of ILD. Therefore, it would be essential to repeat sRAGE measurements in longitudinal samples of SSc patients to investigate whether sRAGE levels follow the disease course on- and off-treatment, in order to qualify as a biomarker for SSc lung complications.

Nowadays, screening for PAH is performed by transthoracic echocardiogram and diagnosed by right heart catheterisation (20, 36). Our study stresses the importance of further investigations to establish this novel predictive “non-invasive” biomarker for the new onset of PAH in SSc. Ultimately if our results are replicated independently, this could mean that sRAGE levels may be used as a simple blood test to differentiate between low-risk and high-risk patients prone to developing PAH in practice, consequently with the possibility of earlier referral of high-risk patients to a cardiologist.

In conclusion, we show that high sRAGE levels, but not HMGB1, in patients with SSc at baseline may be used to predict new onset of PAH related to SSc. Moreover, high sRAGE levels may predict lower survival rates due to PAH in SSc. Future research should focus on including a larger cohort to correct for confounding factors and finding a cut-off value to calculate diagnostic accuracy. Finally, our findings suggest that sRAGE may function as a disease biomarker that identifies development of SSc-PAH and allows early intervention.

Data availability statement

The raw data supporting the conclusions of this article will be made available by the authors, without undue reservation.

Ethics statement

Ethical review and approval was not required for the study on human participants in accordance with the local legislation and institutional requirements. Written informed consent for participation was not required for this study in accordance with the national legislation and the institutional requirements.

Author contributions

Conceptualization and methodology, IA and DM; Formal Analysis, IA; Investigation, IA; Resources, YA-A, AS, BD-v, CR, HG, MD, CG, WT; Data Curation, IA, YA-A; Writing – Original Draft Preparation, IA; Writing – Review & Editing, AJS, AS, BD-v, CR, HG, JW, MD, CG, YA-A, WT, and DM; Visualization, IA; Supervision, AJS, JW, and DM; Project Administration, IA, YA-A. All authors contributed to the article and approved the submitted version.

Acknowledgments

We would like to thank Rita D.M. Varkevisser for her help with statistical analyses.

Conflict of interest

The authors declare that the research was conducted in the absence of any commercial or financial relationships that could be construed as a potential conflict of interest.

Publisher's note

References

1. Tyndall AJ, Bannert B, Vonk M, Airò P, Cozzi F, Carreira PE, et al. Causes and risk factors for death in systemic sclerosis: a study from the EULAR scleroderma trials and research (EUSTAR) database. *Ann Rheum Dis* (2010) 69(10):1809–15. doi: 10.1136/ard.2009.114264

2. Bonhomme O, André B, Gester F, de Seny D, Moermans C, Struman I, et al. Biomarkers in systemic sclerosis-associated interstitial lung disease: review of the literature. *Rheumatology* (2019) 58(9):1534–46. doi: 10.1093/rheumatology/kez230

3. Hickey PM, Lawrie A, Condliffe R. Circulating protein biomarkers in systemic sclerosis related pulmonary arterial hypertension: a review of published data. *Front Med (Lausanne)* (2018) 5(6):1–7. doi: 10.3389/fmed.2018.00175

4. Diekmann F, Chouvarine P, Sallmon H, Meyer-Kobbe L, Kieslich M, Plouffe BD, et al. Soluble receptor for advanced glycation end products (sRAGE) is a sensitive biomarker in human pulmonary arterial hypertension. *Int J Mol Sci* (2021) 22(16):8591. https://www.mdpi.com/1422-0067/22/16/8591. doi: 10.3390/ijms22168591

5. Oczypok EA, Perkins TN, Oury TD. All the "RAGE" in lung disease: the receptor for advanced glycation endproducts (RAGE) is a major mediator of pulmonary inflammatory responses. *Paediatr Respir Rev* (2017) 23:40–9. doi: 10.1016/j.prrv.2017.03.012

6. Schmidt AM, Du YS, Yan SF, Stern DM. The multiligand receptor RAGE as a progression factor amplifying immune and inflammatory responses. *J Clin Invest* (2001) 108(7):949–55. doi: 10.1172/JCI200114002

7. Nienhuis HLA, Westra J, Smit AJ, Limburg PC, Kallenberg CGM, Bijl M. AGE and their receptor RAGE in systemic autoimmune diseases: an inflammation propagating factor contributing to accelerated atherosclerosis. *Autoimmunity* (2009) 42(4):302–4. doi: 10.1080/08916930902831746

8. Hudson BI, Carter AM, Harja E, Kalea AZ, Arriero M, Yang H, et al. Identification, classification, and expression of RAGE gene splice variants. *FASEB J* (2008) 22(5):1572–80. doi: 10.1096/fj.07-9909com

9. Zhang L, Bukulin M, Kojro E, Roth A, Metz VV, Fahrenholz F, et al. Receptor for advanced glycation end products is subjected to protein ectodomain shedding by metalloproteinases. *J Biol Chem* (2008) 283(51):35507–16. doi: 10.1074/jbc.M806948200

10. Buckley ST, Ehrhardt C. The receptor for advanced glycation end products (RAGE) and the lung. *J BioMed Biotechnol* (2010) 2010:917108. doi: 10.1155/2010/917108

11. Mukherjee TK, Mukhopadhyay S, Hoidal JR. Implication of receptor for advanced glycation end product (RAGE) in pulmonary health and pathophysiology. *Respir Physiol Neurobiol* (2008) 162(3):210–5. doi: 10.1016/j.resp.2008.07.001

12. Miniati M, Monti S, Basta G, Cocci F, Fornai E, Bottai M, et al. Soluble receptor for advanced glycation end products in COPD: relationship with emphysema and chronic cor pulmonale: a case-control study. *Respir Res* (2011) 12:37. doi: 10.1186/1465-9921-12-37

13. Meloche J, Courchesne A, Barrier M, Carter S, Bisserier M, Paulin R, et al. Critical role for the advanced glycation end-products receptor in pulmonary arterial hypertension etiology. *J Am Heart Assoc* (2013) 2(1):1–14. doi: 10.1161/JAHA.112.005157

14. Jia D, He Y, Zhu Q, Liu H, Zuo C, Chen G, et al. RAGE-mediated extracellular matrix proteins accumulation exacerbates HySu-induced pulmonary hypertension. *Cardiovasc Res* (2017) 113(6):586–97. doi: 10.1093/cvr/cvx051

15. Watanabe H, Son M. The immune tolerance role of the hmgb1-rage axis. *Cells* (2021) Vol. 10:1–14. doi: 10.3390/cells10030564

16. Bauer EM, Shapiro R, Zheng H, Ahmad F, Ishizawar D, Comhair SA, et al. High mobility group box 1 contributes to the pathogenesis of experimental pulmonary hypertension *via* activation of toll-like receptor 4. *Mol Med* (2012) 18(12):1509–18. doi: 10.2119/molmed.2012.00283

17. Zheng JN, Li Y, Yan YM, Yu Y, Shao WQ, Wang Q. Increased serum calpain activity is associated with HMGB1 levels in systemic sclerosis. *Arthritis Res Ther* (2020) 22(1):110. doi: 10.1186/s13075-020-02195-y

18. van den Hoogen F, Khanna D, Fransen J, Johnson SR, Baron M, Tyndall A, et al. 2013 classification criteria for systemic sclerosis: an American college of Rheumatology/European league against rheumatism collaborative initiative. *Arthritis Rheum* (2013) 65 (11):2737–47. doi: 10.1002/art.38098

19. Wells AU, Hirani N. Interstitial lung disease guideline. *Thorax* (2008) 63 (Supplement 5):v1–58. doi: 10.1136/thx.2008.101691

20. Galiè N, Humbert M, Vachiery JL, Gibbs S, Lang I, Torbicki A, et al. ESC/ERS guidelines for the diagnosis and treatment of pulmonary hypertension. *Eur Heart J* (2015) 37(1):67–119. doi: 10.1093/eurheartj/ehv317

21. Iwamoto H, Gao J, Pulkkinen V, Toljamo T, Nieminen P, Mazur W. Soluble receptor for advanced glycation end-products and progression of airway disease. *BMC Pulm Med* (2014) 14(1):1–7. doi: 10.1186/1471-2466-14-68

22. Manichaikul A, Sun L, Borczuk AC, Onengut-Gumuscu S, Farber EA, Mathai SK, et al. Plasma soluble receptor for advanced glycation end products in idiopathic pulmonary fibrosis. *Ann Am Thorac Soc* (2017) 14(5):628–35. doi: 10.1513/AnnalsATS.201606-485OC

23. Queisser MA, Kouri FM, Königshoff M, Wygrecka M, Schubert U, Eickelberg O, et al. Loss of RAGE in pulmonary fibrosis: molecular relations to functional changes in pulmonary cell types. *Am J Respir Cell Mol Biol* (2008) 39(3):337–45. doi: 10.1165/rcmb.2007-0244OC

24. Bauer Y, de Bernard S, Hickey P, Ballard K, Cruz J, Cornelisse P. Identifying early pulmonary arterial hypertension biomarkers in systemic sclerosis: machine learning on proteomics from the DETECT cohort. *Eur Respir J* (2021) 57 (6):2002591. doi: 10.1183/13993003.02591-2020

25. Nakamura K, Sakaguchi M, Matsubara H, Akagi S, Sarashina T, Ejiri K, et al. Crucial role of RAGE in inappropriate increase of smooth muscle cells from patients with pulmonary arterial hypertension. *PloS One* (2018) 13(9):e0203046. doi: 10.1371/journal.pone.0203046

26. van Leeuwen NM, Wortel CM, Fehres CM, Bakker JA, Scherer HU, Toes REM, et al. Association between centromere- and topoisomerase-specific immune responses and the degree of microangiopathy in systemic sclerosis. *J Rheumatol* (2021) 48(3):402–9. doi: 10.3899/jrheum.191331

27. Kampolis C, Plastiras SC, Vlachoyiannopoulos PG, Moyssakis I, Tzelepis GE. The presence of anti-centromere antibodies may predict progression of estimated pulmonary arterial systolic pressure in systemic sclerosis. *Scand J Rheumatol* (2008) 37 (4):278–83. doi: 10.1080/03009740801978871

28. Suzuki S, Nakazato K, Sugimoto K, Yoshihisa A, Yamaki T, Kunii H, et al. Plasma levels of receptor for advanced glycation end-products and high-mobility group box 1 in patients with pulmonary hypertension. *Int Heart J* (2016) 57(2):234–40. doi: 10.1536/ihj.15-188

29. Hamada N, Maeyama T, Kawaguchi T, Yoshimi M, Fukumoto J, Yamada M, et al.

30. Farmer DGS, Kennedy S. RAGE, vascular tone and vascular disease. *Pharmacol Ther* (2009) 124(2):185–94. doi: 10.1016/j.pharmthera.2009.06.013

31. Page TH, Chiappo D, Brunini F, Garnica J, Blackburn J, Dudhiya F, et al. Danger-associated molecular pattern molecules and the receptor for advanced glycation end products enhance ANCA-induced responses. *Rheumatol (United Kingdom)* (2022) 61(2):834–45. doi: 10.1093/rheumatology/keab413

32. Machahua C, Montes-Worboys A, Planas-Cerezales L, Buendia-Flores R, Molina-Molina M, Vicens-Zygmunt V. Serum AGE/RAGEs as potential biomarker in idiopathic pulmonary fibrosis. *Respir Res* (2018) 19(1):1–9. doi: 10.1186/s12931-018-0924-7

33. Herzog EL, Mathur A, Tager AM, Feghali-Bostwick C, Schneider F, Varga J. Review: interstitial lung disease associated with systemic sclerosis and idiopathic pulmonary fibrosis: how similar and distinct? vol. 66, arthritis and rheumatology. *John Wiley Sons Inc* (2014) 66:1967–78. doi: 10.1002/art.38702

34. Prasad K. AGE-RAGE stress in the pathophysiology of pulmonary hypertension and its treatment. *Int J Angiology* (2019) 28(2):71–9. doi: 10.1055/s-0039-1687818

35. Nakamura K, Akagi S, Ejiri K, Yoshida M, Miyoshi T, Sakaguchi M. Inhibitory effects of RAGE-aptamer on development of monocrotaline-induced pulmonary arterial hypertension in rats. *J Cardiol* (2021) 78(1):12–6. doi: 10.1016/j.jjcc.2020.12.009

36. Simonneau G, Montani D, Celermajer DS, Denton CP, Gatzoulis MA, Krowka M, et al. Haemodynamic definitions and updated clinical classification of pulmonary hypertension. *Eur Respir J* (2019) 53(1):1801913. doi: 10.1183/13993003.01913-2018

frontiers | Frontiers in Immunology

TYPE Original Research
PUBLISHED 19 July 2023
DOI 10.3389/fimmu.2023.1197458

OPEN ACCESS

EDITED BY
Francesca Wanda Rossi,
University of Naples Federico II, Italy

REVIEWED BY
Claudia Azucena Palafox-Sánchez,
University of Guadalajara, Mexico
Scott A. Jenks,
Emory University, United States

*CORRESPONDENCE
Zhenzhen Ma
mazhenzhendz@163.com
Ling Zhu
zhuling7103@163.com

†These authors have contributed equally to this work

RECEIVED 31 March 2023
ACCEPTED 03 July 2023
PUBLISHED 19 July 2023

CITATION
Dong R, Sun Y, Xu W, Xiang W, Li M, Yang Q, Zhu L and Ma Z (2023) Distribution and clinical significance of anti-carbamylation protein antibodies in rheumatological diseases among the Chinese Han population.
Front. Immunol. 14:1197458.
doi: 10.3389/fimmu.2023.1197458

Distribution and clinical significance of anti-carbamylation protein antibodies in rheumatological diseases among the Chinese Han population

Rongrong Dong[1†], Yuanyuan Sun[2†], Wei Xu[1], Weizhen Xiang[1], Meiqi Li[3], Qingrui Yang[1,3], Ling Zhu[2*] and Zhenzhen Ma[1,3*]

[1]Department of Rheumatology and Immunology, Shandong Provincial Hospital, Cheeloo College of Medicine, Shandong University, Jinan, Shandong, China, [2]Department of Respiratory and Critical Care Medicine, Shandong Provincial Hospital Affiliated to Shandong First Medical University, Jinan, Shandong, China, [3]Department of Rheumatology and Immunology, Shandong Provincial Hospital Affiliated to Shandong First Medical University, Jinan, Shandong, China

Objective: Several studies have demonstrated that anti-carbamylation protein antibodies (Anti-CarPA) are persistent in patients with rheumatoid arthritis (RA), systemic lupus erythematosus (SLE), systemic sclerosis (SSC), primary Sjögren's syndrome (pSS), and interstitial lung disease associated with RA (RA-ILD). However, the relationship between anti-CarPA and other rheumatic diseases (RDs) and non-RA-ILD is not known till now. This study sought to examine the presence of anti-CarPA in Chinese Han patients with RDs and its clinical significance.

Methods: The study included 90 healthy controls (HCs) and 300 patients with RDs, including RA, SLE, polymyositis/dermatomyositis (PM/DM), pSS, SSC, spondyloarthritis (SpA), anti-neutrophil cytoplasmic autoantibodies associated with vasculitis (AAV), undifferentiated connective tissue disease (UCTD), and Behcet's disease (BD). Antibodies against carbamylated human serum albumin were detected using commercial enzyme-linked immunosorbent assay kits. Correlations between clinical and laboratory parameters were analyzed.

Result: Serum levels of anti-CarPA in RA (34.43 ± 33.34 ng/ml), SLE (21.12 ± 22.23 ng/ml), pSS (16.32 ± 13.54 ng/ml), PM/DM (30.85 ± 17.34 ng/ml), SSC (23.53 ± 10.70 ng/ml), and UCTD (28.35 ± 21.91 ng/ml) were higher than those of anti-CarPA in the HCs (7.30 ± 5.05 ng/ml). The concentration of serum anti-CarPA was higher in patients with rheumatic disease-related interstitial lung disease (RD-ILD), especially RA-ILD, PM/DM-ILD, and pSS-ILD. Patients with RD-ILD who tested positive for anti-CarPA were more likely to have a more severe radiographic classification (grades II, $p = 0.045$; grades III, $p = 0.003$). Binary logistic regression analysis suggested that anti-CarPA had an association with ILD in RA ($p = 0.033$), PM/DM ($p = 0.039$), and pSS ($p = 0.048$). Based on receiver operating characteristics (ROC) analysis, anti-CarPA cutoffs best discriminated ILD in RA (>32.59 ng/ml, $p = 0.050$), PM/DM (>23.46 ng/ml, $p = 0.038$), and pSS

(>37.08 ng/ml, p = 0.040). Moreover, serum levels of anti-CarPA were correlated with antibodies against transcription intermediary factor 1 complex (anti-TIF1) (R = −0.28, p = 0.044), antibodies against glycyl-transfer ribonucleic acid synthetase (anti-EJ) (R = 0.30, p = 0.031), and antibodies against melanoma differentiation-associated gene 5 (anti-MDA5) (R = 0.35, p = 0.011).

Conclusion: Serum anti-CarPA could be detected in patients with RA, PM/DM, pSS, SSC, and UCTD among the Chinese Han population. And it may also assist in identifying ILD in patients with RA, PM/DM, and pSS, which emphasized attention to the lung involvement in anti-CarPA-positive patients.

KEYWORDS

rheumatic diseases, autoantibodies, anti-carbamylation protein antibodies, interstitial lung disease, Chinese patients

Introduction

Rheumatic diseases (RDs) are characterized by long disease duration, diverse clinical manifestations, and various prognoses. The diagnosis of these diseases is primarily determined by the clinical manifestations and the presence of specific autoantibodies. In clinical practice, early diagnosis of RDs among some patients is challenging due to the absence of specific autoantibodies. Exploration of new antibodies is essential in the study of RDs. Anti-carbamylated protein antibody (anti-CarPA) is one of the new autoantibodies discovered in recent years. According to some studies, patients with RDs always have higher levels of anti-CarPA than healthy individuals. Indeed, antibodies to anti-CarPA are widely used in rheumatological research in RA and have been demonstrated to be associated with its diagnostic efficiency (1), risk stratification (2, 3), and treatment evaluation of RA patients (4), making it an ideal biomarker.

Carbamylation is a non-enzymatic process by which self-proteins are added to a cyanate group. In this process, lysine is converted to a homo-citrulline in the tertiary structure (5). Several proteins in the body, including albumin, low density lipoprotein, fibrinogen, enolase, 78 kDa glucose regulatory protein, vimentin, and α-1 antitrypsin, could be carbamylated (6–10). Many physiological and pathological processes, such as aging, cataracts, atherosclerosis, chronic kidney disease, and nervous system disorders, are also affected by carbamylated proteins (11). Additionally, some studies have suggested that the positive charge is inhibited after protein carbamylation, changing the interactions among ions on the protein surface. During these processes, the secondary and/or tertiary structure of proteins could be changed, exposing the abnormal region of the protein, thereby producing anti-CarPA (11, 12). Initially described in 2011 among patients with RDs, anti-CarPA could recognize homocitrullinated peptides (13). In subsequent studies, anti-CarPA was found in non-RA RDs, such as systemic lupus erythematosus (SLE), systemic sclerosis (SSC), and primary Sjögren's syndrome (pSS), with different outcomes (14–20). Studies on anti-CarPA have revealed that it is associated with poor disease outcomes, including increased disease activity, radiographic progression, and mortality in patients with RA (1–3, 21, 22). Recent studies have also linked anti-CarPA with RA associated interstitial lung disease (RA-ILD), which may explain the increased mortality rate among anti-CarPA-positive patients with RA (2, 23).

Rheumatic disease-related interstitial lung disease (RD-ILD) is a common complication in patients with RDs. Depending on the screening method and the sample population, ILD affects 3–70% of patients with RDs. Difficult diagnosis, poor prognosis, and lack of effective treatments made RD-ILD one of the main causes of death in patients with RDs, thus prompting greater efforts to detect the disease as early as possible. However, clinically effective biomarkers for RD-ILD are still lacking, and early detection is problematic. A number of risk factors have been identified in patients with RD-ILD; they include smoking, male gender, higher disease activity, longer disease duration, older age, positive rheumatoid factor (RF), and anticitrullinated protein antibodies (ACPAs) (23, 24). Several biomarkers have also been proposed for RD-ILD screening, but none has been universally accepted. Recent studies have identified anti-CarPA as a potentially useful biomarker for RA-ILD, but other RD-ILDs have not been studied yet. Besides, the clinical significance in RDs other than RA was still unclear. Therefore, we sought to determine the presence of anti-CarPA in Chinese Han patients with RDs and its clinical significance. In this study, serum anti-CarPA levels and the association between anti-CarPA and its clinical significance including RD-ILD were also investigated among a diverse population of patients with RDs.

Materials and methods

Study population

This retrospective study involved 300 patients and 90 healthy controls (HC) consecutively admitted to the Rheumatology Department, Shandong Provincial Hospital from November 2020

to January 2022. All of patients were Han population. The inclusion criterion was diagnosis of one of the RDs, defined according to the updated international classification criteria, which is as followed: RA (25): American College of Rheumatology/European League Against Rheumatism (ACR/EULAR) classification criteria in 2010; SLE (26): The Systemic Lupus International Collaborating Clinics (SLICC) criteria for SLE in 2012; PM/DM (27): diagnostic criteria proposed by Bohan and Peter in 1975; pSS (28): ACR classification criteria in 2012; AAV (29): ACR classification criteria in 1990; SSC (30): ACR/EULAR classification criteria in 2013; SpA (31):International Spondyloarthritis Assessment Association SpA classification criteria in 2009; UCTD (32): definition proposed by Marta Mosca in 2014; BD (33): International Criteria for Behçet's Disease in 2014. The exclusion criteria included (1) diagnosis of two or more kinds of RDs and (2) history of diagnosis and therapy for RDs (Figure 1). Furthermore, we divided the participants into subgroups based on whether they had ILD or not. The high-resolution computed tomography (HR-CT) was performed on all patients. If patients without ILD developed persistent symptoms, such as cough, chest distress or dyspneal, they would be suspected of ILD and repeated HR-CT. The patterns of ILD were classified by HR-CT, which was reviewed by two experienced radiologists according to the ATS/ERS International Multidisciplinary Consensus Classification of the Idiopathic Interstitial. According to the HR-CT manifestations of RD-ILD, patients were classified into three types: usually interstitial pneumonia (UIP), non-specific interstitial pneumonia (NSIP), and unclassifiable (34). The classification was based on clinical criteria for the definition of idiopathic interstitial pneumonia by the Japanese Ministry of Health and Welfare (35). The classifications included grades I (the lesion range does not exceed the peripheral lung field), II (the lesion range exceeds the peripheral lung field but does not exceed the medial lung field), and III (the lesion range exceeds the medial lung field). The local ethics committee of Shandong Provincial Hospital validated the study protocol, and all participants provided informed consent before enrolment (SZRJJ: NO.2021-438).

Detection of antibodies against carbamylated human serum albumin

Autoantibody status was measured in sera collected at study enrolment. We used a commercial human anti-CarPA enzyme-linked immunosorbent assay (ELISA) kit (Fine Test, Wu Han, China) to measure anti-CarPA levels in patients with RDs and HCs. This kit quantifies all isotypes of anti-CarPA. After dialyzing at 4°C against distilled water for 36 hours, all reaction mixtures were stored at 20°C. The manufacturer's instructions were followed, and the detailed procedure was as follows. ELISA microplates were coated with carbamylated human serum albumin and washed with the wash buffer. Sera were diluted with sample dilution buffer at a ratio of 1:2 and subsequently added to the ELISA wells (300 ul/well) for 90 minutes at 37°C. After washing with the wash buffer, biotinylated secondary antibodies were added to the ELISA wells (100 ul/well) for 60 minutes at 37°C. After additional washing with wash buffer, strept avidin-biotin complex (SABC) was added to the ELISA wells (100 ul/well) for 30 minutes at 37°C. The reaction was developed with tetramethylbenzidine (TMB) (90 ul/well) for 15 minutes at 37°C and then terminated with the stop solution (50 ul/well). Optical

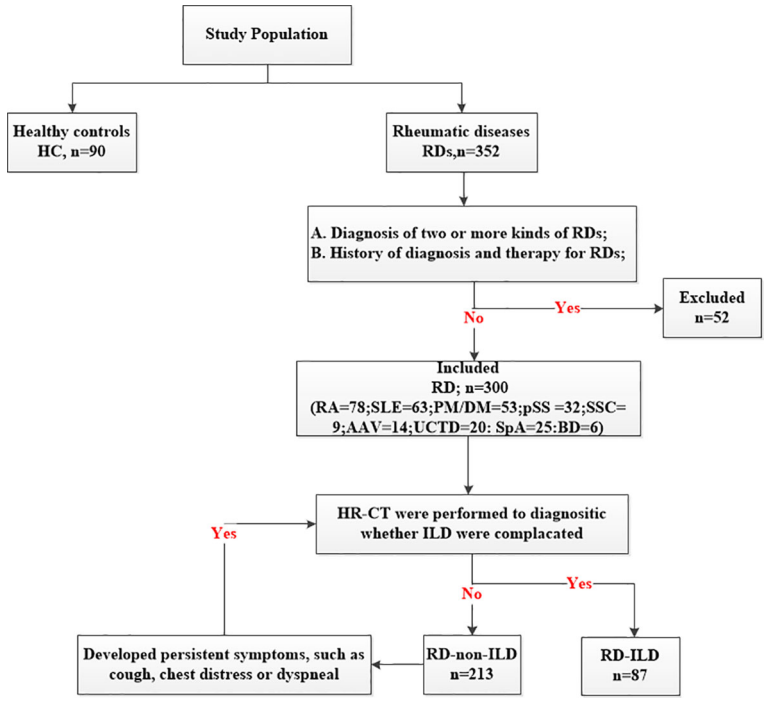

FIGURE 1
Study cohort.

density (OD) was measured at 450 nm using an ELISA spectrophotometer (ThermoMultiskan GO Type:1510). Serum anti-CarPA levels were expressed in ng/ml. The detection limit of anti-CarPA was 0.781-50ng/ml, and the sensibility was 0.469ng/ml.

Collection of clinical and laboratory indices

Beside the level of anti-CarPA, the following clinical information of RD patients was collected directly from the medical record (all of patients were hospitalized): rheumatoid factor (RF), anti-cyclic citrullinated peptide antibodies (CCP), antinuclear antibody (ANA), anti-Smith antibodies (SM),anti-double-stranded DNA antibody (dsDNA), antibodies reactive against the ribonucleoprotein antigens Ro/Sjögren's syndrome A antigen (SSA), antibodies reactive against the ribonucleoprotein antigens La/Sjögren's syndrome B antigen (SSB), and myositis-specific autoantibodies (MSAs). RF was detected by immune turbidimetry (0–20KU/L). SSA, SSB, and dsDNA were measured by ELISA with the normal range: SSA (0–20 RU/ml), SSB (0–20 RU/ml), and dsDNA (0–100 IU/ml). ANA was detected by indirect immunofluorescence. CCP and SM were measured by chemiluminescent immunoassay with the normal range: CCP (0–20 U/ml) and SM (0–20 CU). MSAs were detected using line blot techniques.

Statistical analysis

Data analyses were performed using SPSS 26 software for Windows (IBM SPSS Inc., Chicago, USA) and GraphPad Prism 9 for Windows (San Diego, CA, USA). Results from parametric data were expressed as mean SD, and differences between groups were analyzed using a student's T test. For nonparametric data, results were expressed as median (interquartile range) values, and differences between groups were analyzed using the Mann-Whitney test and Kruskal and Willis test. A correlation analysis between two continuous variables was performed using Spearman's analysis. Multivariable analysis was then used to compare variables that had a p-value <0.1 by single-variable analysis. For all statistical analyses, p-values <0.05 were considered statistically significant.

Results

Baseline characteristics of the study population

A total of 300 patients with RDs were enrolled in the main study. They included 78 patients with RA, 63 patients with SLE, 53 patients with PM/DM, 32 patients with pSS, 14 patients with anti-neutrophil cytoplasmic autoantibodies (ANCA)-associated vasculitis (AAV), 9 patients with SSC, 20 patients with undifferentiated connective tissue disease (UCTD), 6 patients with Behcet's disease (BD), and 25 patients with spondyloarthritis (SpA). The diseases were further grouped into ILDs and non-ILDs: RA (12 vs 66), SLE (14 vs 49), PM/DM (38 vs 15), pSS (7 vs 25), AAV (4 vs 10), SSC (5 vs 4), and UCTD (5 vs 15). There were no ILD patients in SpA group and BD group, so we didn't set up ILD sub-group in them. Patients in this study were predominantly female (230/300) with a gender ratio of 76.67%, mean age of 50.46 ± 15.75 years, disease duration of 12.00 (3.00, 60.00) months, and smoking percentage of 12.00% (36 patients). Ninety HCs, comprising 25 men and 65 women, were included; they had a mean age of 46.32 ± 15.74 years. No significant differences were observed between the patients and HCs at baseline (Table 1).

Clinical features of patients with RDs and the distribution of anti-CarPA

Consistent with findings from previous studies, our findings showed that the serum levels of anti-CarPA in patients with RA, SLE, and pSS were 34.40 ± 32.96 ng/ml (p <0.0001), 21.12 ± 22.23 ng/ml (p = 0.005), and 16.32 ± 13.54 ng/ml (p = 0.005), respectively, which were higher than those of HCs (7.30 ± 5.05 ng/ml). Moreover, the anti-CarPA titers were higher in patients with PM/DM (30.85 ± 17.34 ng/ml, p <0.0001), SSC (23.53 ± 10.70 ng/ml, p = 0.0019), and UCTD (28.35 ± 21.91 ng/ml, p <0.0001) than in HCs. No differences in the mean levels of anti-CarPA was observed between patients with AAV [8.85 (7.05, 32.15) ng/ml, p = 0.10], SpA (14.41 ± 10.70ng/ml, p=0.19), and BD [5.72 (2.73, 9.08) ng/ml, p >1.00] and HCs. As reported previously, the anti-CarPA levels in HCs were comparable (Figure 2A).

The clinical varieties of patients with RDs who are anti-CarPA negative and positive were compared. Compared to the RA patients without anti-CarPA, those with anti-CarPA had higher levels of WBC (6.39 $\times10^9$/L vs 5.53 $\times10^9$/L, p = 0.048), RF (145.50 vs 59.95 KU/ml, p = 0.004), and DAS28 (5.05 vs 4.69, p=0.047) (Table 2A). In SLE, patients who were anti-CarPA-positive had higher levels of ESR (55.24 vs 35.68 mm/h, p = 0.006), rRNP (58.65 vs 17.22 RU/ml, p = 0.006), U1RNP (464.60 vs 17.05 CU/ml, p = 0.048), and SLEDAI [6.50 (4.75, 8.00) vs 4.00 (3.00, 7.00), p=0.036] (Table 2B). Anti-CarPA-positive patients with PM/DM had a high prevalence of arthralgia (p = 0.034) (Table 2C). Among anti-CarPA-positive patients with pSS, PLT levels were not frequently decreased (275.29 $\times10^9$/L vs 193.05 $\times10^9$/L, p = 0.026) (Table 2D). Additionally, the levels of autoantibodies and inflammatory markers in patients with SSC and UCTD did not differ significantly between the anti-CarPA-positive and negative groups.

Association between anti-CarPA and RD-ILD

Eighty-seven patients with ILD were identified in this cohort. Compared to those without ILD, patients with ILD had higher serum levels of anti-CarPA (33.41 vs 22.51 ng/ml, p = 0.0002). Anti-CarPA was found to be higher in ILD groups of RA, PM/DM, and pSS (RA-ILD vs RA-non-ILD: 49.65 vs. 28.17 ng/ml, p = 0.014; PM/DM-ILD vs PM/DM-non-ILD 34.37 vs 23.81 ng/ml, p = 0.045; pSS-

TABLE 1 Demographic and clinical characteristics of the 300 patients with RDs and 90 Healthy controls.

Disease	Positive rate of anti-CarPA (%)	n	Gender F/M	Age(years) mean ± SD	Disease duration (month), median(IQR)/mean ± SD	Smoker (n(%))
RA	48.71	78	62/16	54.96 ± 14.47	9.50(3.00,60.00)	7/78(8.97%)
RA	+	38	29/9	54.71 ± 15.80	10.50(2.00,84.00)	4/38(10.53%)
RA	–	40	33/7	55.20 ± 13.29	9.50(4.00,48.00)	3/40(7.50%)
SLE	28.57	63	57/6	41.35 ± 16.07	12.00(5.00,60.00)	4/63(6.35%)
SLE	+	18	16/2	47.72 ± 15.20	30.00(2.75,126.00)	2/18(11.11%)
SLE	–	45	41/4	38.80 ± 15.85	12.00(6.00,36.00)	2/45(4.44%)
PM/DM	62.26	53	35/18	53.64 ± 12.73	6.00(2.00,12.00)	13/53(24.53%)
PM/DM	+	34	23/11	53.22 ± 10.54	8.00(2.00,24.00)	8/33(24.24%)
PM/DM	–	19	12/7	54.44 ± 16.50	3.50(2.00,12.00)	5/19(26.32%)
pSS	31.25	32	32/1	53.18 ± 13.84	30.00(6.00,84.00)	0
pSS	+	10	9/1	51.90 ± 12.92	12.00(6.00,93.00)	0
pSS	–	22	22/0	53.77 ± 14.50	36.00(5.00,84.00)	0
AAV	21.42	14	9/5	62.71 ± 9.90	6.00(4.75,9.50)	3/14(21.43%)
AAV	+	3	3/0	62.33 ± 11.50	5.67 ± 2.08	0
AAV	–	11	6/5	62.81 ± 10.04	6.00(5.00,12.00)	3/11(27.27%)
SSC	44.44	9	8/1	50.78 ± 12.59	73.89 ± 12.49	1/9(11.11%)
SSC	+	4	4/0	55.75 ± 15.88	75.00 ± 35.83	0
SSC	–	5	4/1	46.80 ± 9.15	73.00 ± 42.90	1/5(20.00%)
UCTD	55.00	20	14/6	50.10 ± 16.72	12.00(2.25,45.00)	4/20(20.00%)
UCTD	+	11	8/3	48.18 ± 18.07	6.00(1.70,24.00)	3/11(27.27%)
UCTD	–	9	6/3	52.44 ± 15.65	24.00(7.50,54.00)	1/9(11.11%)
SpA	24.00	25	9/16	44.08 ± 17.33	2.00(0.85,48.00)	4/25(16.00%)
SpA	+	6	4/2	43.00 ± 19.54	2.00(0.88,123.00)	1/6(16.67%)
SpA	–	19	5/14	44.42 ± 17.14	6.00(0.70,24.00)	3/19(15.79%)
BD	0	6	5/1	43.83 ± 7.44	60.00(0.88,174.00)	0
TOTAL	41.00	300	230/70	50.46 ± 15.75	12.00(3.00,57.00)	36/300(12.00%)
HC	–	90	65/25	46.32 ± 15.74	–	17/90(18.89%)

SD, standard deviation; IQR, interquartile range; RDs, Rheumatic diseases; RA, rheumatoid arthritis; SLE, systemic lupus erythematosus; PM/DM, polymyositis/dermatomyositis; pSS, primary Sjögren's syndrome; AAV, anti-neutrophil cytoplasmic autoantibodies associated vasculitis; SSC, systemic sclerosis; UCTD, undifferentiated connective tissue disease; BD, Behcet's disease; SpA, spondyloarthritis; HC, healthy controls.
Parametric data results were expressed as mean ± SD values; Nonparametric data results were expressed as median (IQR) values. Some values presented as n or n(%); n represents the number of people according with the criteria. Student's -test was used in comparison between parametric data. Mann-Whitney test was used in comparison between parametric data and nonparametric data or nonparametric data.

ILD vs. pSS-non-ILD, 26.15 vs 13.57 ng/ml, p = 0.027) than in the non-ILD group. In patients with SLE, SSC, AAV, and UCTD, however, anti-CarPA titers were not significantly different between the ILD and non-ILD groups (Figure 2B). Additionally, we examined the relationship between anti-CarPA and the radiographic features, including the image classification and image grading, in patients with RD-ILD. The image classification of RD-ILD seemed not to be significantly associated with anti-CarPA levels (UIP: 32.52 ng/ml, NSIP: 35.81 ng/ml, unclassifiable: 31.10 ng/ml, p = 0.62) (Figure 2C). Additionally, among the subgroups of ILD, differences in serum levels of anti-CarPA were observed (grade I: 21.90 ng/ml, grade II: 38.16 ng/ml, and grade III: 41.61 ng/ml, p = 0.0027). In pairwise comparisons, differences were observed between grade I and grade II (p = 0.045) and grade I and grade III (p = 0.003) (Figure 2D).

Association between anti-CarPA and RA-ILD

The differences in clinical and laboratory features between RA-ILD and RA-non-ILD patients are shown in our results. Patients

10.3389/fimmu.2023.1197458

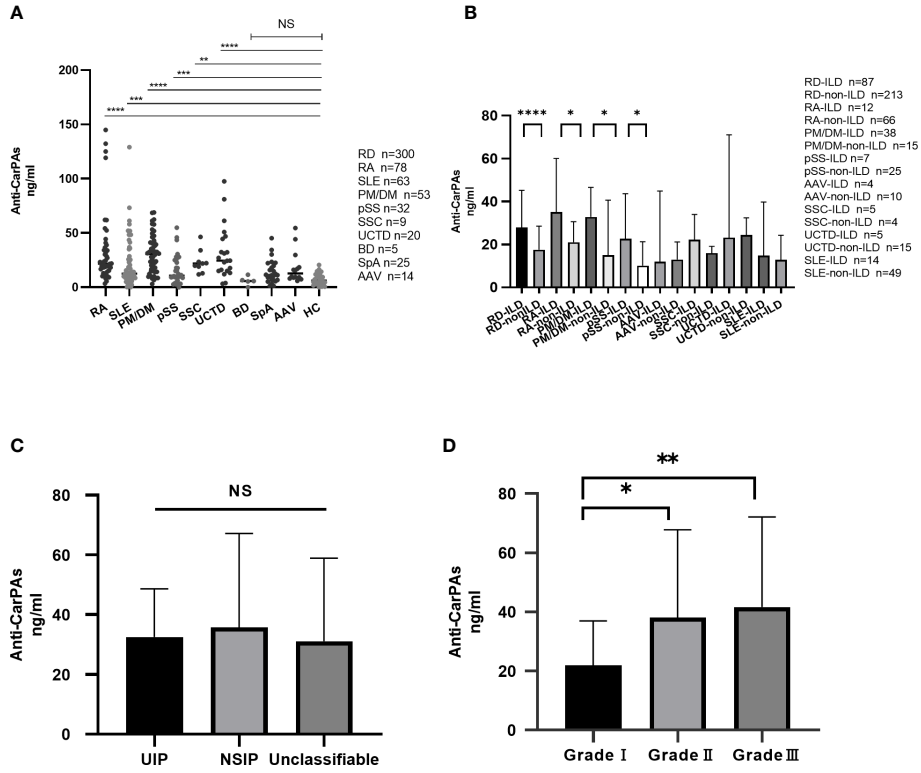

FIGURE 2
(A) Distribution of anti-CarPA in RDs. Serum sample obtained from 78 patients with rheumatoid arthritis (RA), 63 patients with systemic lupus erythematosus (SLE), 53 patients with polymyositis/dermatomyositis (PM/DM), 32 patients with primary Sjögren's syndrome (pSS), 14 patients with anti-neutrophil cytoplasmic autoantibodies associated vasculitis (AAV), 9 patients with systemic sclerosis (SSC), 20 patients with undifferentiated connective tissue disease (UCTD), 6 patients with Behcet's disease (BD), 25 patients with spondyloarthritis (SpA), and 90 healthy controls. Serum levels of anti-CarPA in RDs patients was measured by ELISA. Kruskal-Wallis rank sum test were used in multiple samples; Dunnett's multiple comparisons test was used for pairwise comparisons. **(B)** Distribution of anti-CarPA in RD-ILD. Mann-Whitney test used for pairwise comparisons. **(C)** Distribution of anti-CarPA in different image classifications of RD-ILD. Kruskal-Wallis rank sum test were used in multiple samples; Bonferroni adjustment used for pairwise comparisons. **(D)** Distribution of anti-CarPA in different image grades of RD-ILD. Kruskal-Wallis rank sum test were used in multiple samples; Bonferroni adjustment used for pairwise comparisons. ****p < 0.0001, ***p < 0.001, **p < 0.01, *p < 0.05, NS:p>0.05.

with RA-ILD had older age (67.67 vs 52.65 years, p=0.001) and a higher level of CRP than RA-non-ILD patients (53.63 vs 8.43 mg/ml, p = 0.004). In terms of other laboratory markers, such as disease duration, ESR, CCP, RF, and MCV, no significant difference was observed (Table 3A). To further exclude the effects of clinical confounders, single factor regression was performed. A factor could be added to a multi-factor regression with only p <0.1 in single factor regression. In this study, age, gender, smoking, and CRP were all considered covariates in RA. According to the logistic regression model adjusted for covariates, anti-CarPA was independently associated with RA-ILD (OR: 1.02, 95% CI: 1.00–1.04, p = 0.033) (Table 3B). Additionally, we examined the association between disease course and RA-ILD, ESR, RF, CCP, and MCV and found no significant association. The results of our study demonstrated no significant differences in CCP, MCV, or RF, depending on ILD status. The results were not altered after adjusting for clinical confounding factors. To determine whether serum anti-CarPA could act as a diagnostic biomarker of ILD among patients with RA, receiver operating characteristic (ROC) curve analysis was performed, resulting in an AUC of 0.860 for RA-ILD. The serum anti-CarPA >32.59 ng/ml was used as a cut-off value to diagnose ILD in patients with RA, with a sensitivity and specificity of 78.79% and 58.33%, respectively (Figure 3A).

Association between anti-CarpA and PM/DM-ILD

The differences in clinical and laboratory features between PM/DM-ILD and PM/DM-non-ILD patients are summarized in Table 4. Patients with PM/DM-ILD had older age (55.61 vs 49.00 years, p = 0.022), longer disease duration (8.00 vs 2.00 months, p = 0.005), and higher levels of CRP (7.32 vs 1.21 mg/ml, p = 0.012) than PM/DM-non-ILD patients (Table 4A). Age and smoking status, which were selected by a single factor regression and a previous study, were controlled as confounders in the PM/DM group. An analysis of multi-factor logistic regression demonstrated that anti-CarPA is independently associated with PM/DM-ILD (OR: 1.05, 95% CI: 1.00–1.10, p = 0.040) (Table 4B). However, ESR, CRP, and autoantibodies, including anti-threonyl-transfer

TABLE 2 Clinical and laboratory characteristics of patients with RDs.

A. Clinical and laboratory characteristics of patients with RA grouped by anti-CarPA.				
RA	Total	Positive	Negative	P
WBC(10^9/L(IQR))	6.09(5.12,8.15)	6.39(5.59,9.09)	5.53(4.76,7.91)	0.048*
CRP(median(IQR),mg/ml)	12.70(3.23,32.85)	17.15(4.49,62.05)	7.87(1.55,25.49)	0.086
ESR(mean ± SD,mm/h)	47.99 ± 31.35	52.68 ± 34.52	43.52 ± 27.73	0.20
RF(median(IQR),KU/ml)	85.00(36.45,333.00)	145.50(52.40,420.25)	59.95(3.20,194.50)	0.004*
CCP(median(IQR),U/ml)	195.10(47.48,200.00)	200.00(71.70,200.00)	172.55(27.50,200.00)	0.19
MCV(median(IQR),U/ml)	378.45(58.33,1000.00)	493.55(66.33,1000.00)	227.80(24.58,1000.00)	0.21
ILD(n(%))	12/78(15.38%)	8/38(21.05%)	4/40(10.00%)	0.18
DAS28(mean ± SD)	4.87 ± 1.00	5.05 ± 0.84	4.69 ± 1.12	0.047*
B. Clinical and laboratory characteristics of patients with SLE grouped by anti-CarPA.				
SLE	Total	Positive	Negative	P
WBC(median(IQR),10^9/L)	4.27(2.91,7.68)	4.06(2.72,8.44)	4.47(2.89,7.28)	0.58
Hb(mean ± SD,g/L)	106.76 ± 22.79	106.12 ± 17.78	107.05 ± 24.93	0.98
PLT(mean ± SD,10^9/L)	196.66 ± 99.02	226.41 ± 106.30	183.21 ± 93.98	0.090
ESR(mean ± SD,mm/h)	41.72 ± 25.82	55.24 ± 28.59	35.68 ± 22.32	0.006*
CRP(median(IQR),mg/ml)	6.07(0.87,22.10)	9.22(2.62,26.6)	3.61(0.66,19.32)	0.094
C3(median(IQR),g/L)	0.72(0.49,0.99)	0.72(0.56,1.04)	0.77(0.48,1.00)	0.94
C4(mean ± SD, g/L)	0.13 ± 0.11	0.13 ± 0.12	0.13 ± 0.10	0.96
dsDNA(median(IQR),IU/ml)	75.19(21.87,310.59)	219.89(56.78,455.12)	47.35(16.83,288.98)	0.11
SM(median(IQR),CU)	19.30(6.00,123.10)	39.30(6.80,428.05)	15.65(5.25,54.90)	0.13
AnuA(median(IQR),RU/ml)	14.77(4.78,59.18)	17.90(2.50,171.61)	12.95(4.46,49.34)	0.24
SSA(median(IQR),RU/ml)	75.14(6.95,175.33)	161.94(12.40,200.0)	67.01(5.22,153.96)	0.052
rRNP(median(IQR),RU/ml)	30.03 ± 56.34	58.65 ± 73.67	17.22 ± 41.73	0.006*
U1RNP(median(IQR),CU)	75.00(3.90,643.80)	464.60(45.10,643.80)	17.05(3.10,643.80)	0.048*
Skin rash(n(%))	18/63(28.57%)	4/18(22.22%)	14/45(31.11%)	0.35
Arthralgia(n(%))	34/63(53.96%)	11/18(61.11%)	23/45(51.11%)	0.33
Raynaud phenomenon(n(%))	16/63(25.39%)	3/18(16.67%)	13/45(28.89%)	0.25
Lupus nephritis (n(%))	14/63(22.22%)	5/18(27.77%)	9/45(20.00%)	0.36
ILD(n(%))	14/63(22.22%)	5/18(27.77%)	9/45(20.00%)	0.36
SLEDAI(median(IQR))	5.00(3.00,8.00)	6.50(4.75,8.00)	4.00(3.00,7.00)	0.036*
C. Clinical and laboratory characteristics of patients with PM/DM grouped by anti-CarPA.				
PM/DM	Total	Positive	Negative	P
CK(median(IQR),U/L)	179.00(48.00,865.00)	178.00(48.25,1163.50)	190.00(30.50,649.00)	0.63
CRP(median(IQR),mg/ml)	4.50(0.89,13.68)	4.41(0.78,12.15)	13.77(0.65,32.26)	0.56
ESR(median(IQR),mm/h)	29.00(8.00,56.00)	53.00(7.50,74.50)	26.00(8.75,47.75)	0.32
FER(median(IQR),ng/ml)	475.97(41.00,942.00)	482.52(137.25,1381.24)	246.66(94.41,765.95)	0.22
Skin rash(n(%))	30/53(56.60%)	18/34(52.94%)	12/19(63.16%)	0.39
Arthralgia(n(%))	20/53(37.74%)	17/34(50.00%)	3/19(15.79%)	0.034*
Skeletal muscle weakness(n(%))	32/53(60.38%)	22/34(64.71%)	10/19(52.63%)	0.56
ILD(n(%))	37/53(69.81%)	27/34(79.41%)	10/19(52.63%)	0.11

(Continued)

TABLE 2 Continued

D. Clinical and laboratory characteristics of patients with pSS grouped by anti-CarPA.				
pSS	Total	Positive	Negative	P
PLT(mean ± SD,10^9/L)	213.61 ± 95.97	275.29 ± 94.15	193.05 ± 89.44	0.026*
CRP(median(IQR),mg/ml)	1.26(0.48,1.93)	1.49(0.69,2.99)	1.04(0.41,1.72)	0.14
ESR(median(IQR),mm/h)	26.5(12.0,64.5)	36.00(12.00,98.00)	25.00(11.00,49.50)	0.10
SSA(median(IQR),RU/ml)	134.43(2.42,183.93)	168.40(48.89,184.34)	123.07(1.20,183.87)	0.59
SSB(median(IQR),RU/ml)	3.33(0.00,109.37)	3.99(2.50,19.83)	2.41(0.00,150.98)	0.86
Raynaud phenomenon(n(%))	8/32(25.00%)	3/10(30.00%)	5/22(22.73%)	0.68
Arthralgia(n(%))	12/32(37.50%)	6/10(60.00%)	6/22(27.27%)	0.12
ILD(n(%))	7/32(21.88%)	4/10(40.00%)	3/22(13.64%)	0.17

SD, standard deviation; IQR, interquartile range; WBC, white blood cell; Hb, hemoglobin; PLT, platelet; ESR, erythrocyte sedimentation rate; CRP, C reaction protein; RF, rheumatoid factor; CCP, anti-cyclic citrullinated peptide antibody; MCV, anti-mutated citrullinated vimentin antibody; ILD, Interstitial lung disease; DAS28, Disease Activity Score 28; C3, complement 3; C4, complement 4; dsDNA, anti-dsDNA antibody; SM , SM antibody; AnuA, anti-nucleosome antibody; SSA, antibodies reactive against the ribonucleoprotein antigens Ro/Sjögren's syndrome A; SSB, antibodies reactive against the ribonucleoprotein antigens La/Sjögren's syndrome B antigen; rRNP, anti-ribosomal antibody; U1RNP, anti-U1 small ribonucleoprotein antibody; SLEDAI, SLE Disease Activity Index; CK, creatine kinase.
Parametric data results were expressed as mean ± SD values. Nonparametric data results were expressed as median IQR values. Some values presented as n or n%; n represents the number of people with this clinical manifestation. T-test, Mann-Whitney U tests and Chi-square test are used. *p<0.05; Student's-test was used in comparison between parametric data. Mann-Whitney test was used in comparison between parametric data and nonparametric data or nonparametric data.

ribonucleic acid synthetase anti-body (anti-PL-7), anti-glycyl-transfer ribonucleic acid synthetase antibodies (anti-EJ), anti-histidyl-transfer ribonucleic acid synthetase antibody (anti-JO-1), anti-melanoma differentiation-associated gene 5 antibodies (anti-MDA-5), and antibodies of Ro-52 (anti-Ro-52), showed no significant difference in association with PM/DM-ILD. Following this, Spearman's correlation analysis was applied to determine if different MSAs were associated with anti-CarPA. According to our study, the levels of anti-CarPA were negatively correlated with anti-transcription intermediary factor 1 complex antibodies (anti-TIF1) ($R = -0.28$, $p = 0.044$), while positively correlated with anti-EJ ($R = 0.30$, $p = 0.031$), and anti-MDA-5 ($R = 0.35$, $p = 0.011$). No association between other MSAs and anti-CarPA were observed. Additionally, ROC of anti-CarPA was generated for patients with PM/DM-ILD, with serum anti-CarPA >23.46 ng/ml (AUC: 0.68, $p = 0.038$, sensitivity: 66.67%, specificity: 73.68%) being the optimal cutoff (Figure 3B).

Association between anti-CarPA and pSS-ILD

The clinical and laboratory characteristics of patients with pSS grouped by ILD show a higher level of PLT in the pSS-ILD patients than in the pSS-non-ILD patients (Table 5A). The binary logistic regression analysis showed a relationship between pSS-ILD and anti-CarPA. Single factor logistic regression suggested that anti-CarPA was independently associated with pSS-ILD (OR = 1.07, 95% CI: 1.00–1.10, $p = 0.048$). From single factor logistic regression, no risk factor could be adjusted (Table 5B). ROC curve of anti-CarPA in pSS-ILD showed that the best cut-off for anti-CarPA in pSS-ILD was a level >37.08 ng/ml (AUC: 0.773, $p = 0.040$, sensitivity: 33.33%, specificity: 96.00%) (Figure 3C).

Discussion

Anti-CarPA was shown to be widely distributed among patients with RDs in this study. Past studies have shown that anti-CarPA persists in parts of RDs: Verheul et al. (1) enrolled more than 5,000 patients with RA, and the positive rate of anti-CarPA was 34–53%. Nakabo et al. (14) included 241 patients with SLE in Japan, and the positive rate of anti-CarPA was 54.4%. Two studies from Europe showed that the positive rates of anti-CarPA in patients with pSS were 26.9% and 30%, respectively (15, 18). Riccardi et al. (17) included 448 French patients with SSC, and the positive rate of anti-CarPA was 14%. These studies showed that anti-CarPA were not the specific antibody for RA, which inspired us it may exist in various RDs. Besides, the clinical value of anti-CarPA in different RDs remained unclear, which should be identified whether it related to occurrence and development of some manifestations in RDs. Currently, the research object of previous studies were mainly among Caucasian, but the research on the distribution of anti-CarPA among the Chinese Han population remains insufficient. Therefore, we conducted this study among the Chinese Han population to explore the distribution and clinical significance of anti-CarpA. Our study confirmed the presence of anti-CarpA in several RDs, including RA, SLE, pSS, SSC, PM/DM, UCTD, SpA, and BD. In our study, anti-CarPA was detected in 48.70% of patients with RA, 28.57% of patients with SLE, 31.25% of patients with pSS, 62.26% of patients with PM/DM and 55.00% of patients with UCTD, further confirming and expanding these findings. As described above, preliminary results indicated that anti-CarPA antibodies are broadly distributed and have a low specificity in RDs. According to our observations, the serum titer of anti-CarpA was obviously higher in RA than in other RDs. Furthermore, anti-CarPA was proven to be detectable almost 14 years before RA appeared (36). Anti-CarPA seemed to play a significant role in the

TABLE 3 Analysis of the risk factors for patients with RA-ILD.

A. Clinical and laboratory characteristics of RA patients grouped by ILD.				
RA	Total	RA-ILD	RA-non-ILD	P
Gender(n,M/F)	16/62	5/7	11/55	0.063
Age(mean ± SD,years)	54.96 ± 14.47	67.67 ± 9.21	52.65 ± 14.09	0.001*
Disease duration(median(IQR),month)	9.50(3.00,60.00)	24.00(6.00,105.00)	8.50(3.00,51.00)	0.23
Smoker(n(%))	7/78(8.97%)	3/12(25.00%)	4/66(6.06%)	0.069
WBC(median(IQR),10^9/L)	6.09(5.12,8.45)	6.70(5.67,10.74)	5.93(5.08,8.05)	0.13
CRP(median(IQR)mg/ml)	12.69(3.23,32.85)	53.63(19.57,83.20)	8.43(2.60,27.94)	0.004*
ESR(mean ± SD,mm/h)	47.98 ± 31.35	57.25 ± 34.66	46.30 ± 30.70	0.27
CCP(median(IQR),U/ml)	195.10(47.48,200.00)	143.50(52.95,200.00)	200.00(44.68,200.00)	0.59
RF(median(IQR),KU/ml)	85.00(36.45,333.00)	52.45(18.43,485.50)	87.35(41.88,333.00)	0.45
MCV(median(IQR),U/ml)	378.45(58.33,1000.00)	232.95(59.43,1000.00)	408.00(54.73,1000.00)	0.81
Anti-CarPA(mean ± SD,ng/ml)	31.47 ± 28.04	49.65 ± 44.68	28.17 ± 22.84	0.014*

B. Binary logistic regression analysis of patients with RA-ILD.							
Single factor regression	OR	95%CI	P	Multi-factor regression	OR	95%CI	P
Anti-CarPA	1.02	1.00-1.04	0.028*	Anti-CarPA	1.02	1.00-1.04	0.033*
Age	1.11	1.04-1.23	0.003*	Age	1.14	1.04-1.25	0.010*
Gender	3.57	0.96-13.34	0.058	Gender	1.29	0.21-7.88	0.78
Disease duration	–	–	0.41	–	–	–	–
Smoke	0.41	0.70-2.41	0.32	Smoke	0.24	0.016-3.69	0.36
CRP	1.02	1.00-1.03	0.020*	CRP	1.01	0.99-1.02	0.24
ESR	–	–	0.27	–	–	–	–
RF	–	–	0.95	–	–	–	–
CCP	–	–	0.79	–	–	–	–
MCV	–	–	0.95	–	–	–	–

SD, standard deviation; IQR, interquartile range; WBC, white blood cell; ESR, erythrocyte sedimentation rate; CRP, C reaction protein; RF, rheumatoid factor; CCP, anti-cyclic citrullinated peptide antibody; MCV, anti-mutated citrullinated vimentin antibody; ILD, Interstitial lung disease; RA-ILD, interstitial lung disease associated with rheumatoid arthritis; 95%CI, 95% confidence interval.

Parametric data results were expressed as mean ± SD values. Nonparametric data results were expressed as median IQR values. Some values presented as n or n%; n represents the number of people with this clinical manifestation. T-test, Mann-Whitney U tests, Chi-square test and Logistic regression analysis are used. *p<0.05.

diagnosis and prediction of RA, especially among patients with RA-ILD.

In terms of clinical and laboratory variables, anti-CarPA-positive and negative patients were quite different in several aspects. Patients with anti-CarPA positive RA had younger onset ages and longer disease durations, which were consistent with previous observations (3, 22, 37). In spite of these findings, we observed that RA patients with positive anti-CarPA had higher levels of RF and DAS28, which potentially resulted in more severe joint damage (38, 39), and could indicate poor prognosis. A significant increase in ESR and SLEDAI were observed in SLE individuals with positive anti-CarPA in our study. Li et al. (19) observed that anti-CarPA was associated with high disease activity in SLE patients. It was consistent with our results, and suggested that anti-CarPA was associated with disease activity in patients with SLE. Massaro and Ceccarelli (40, 41) confirmed that anti-CarPA was associated with joint damage in patients with SLE. However, our results showed no significant difference between anti-CarPA and arthralgia. It could be accounted for that joint ultrasonography was not a regular examination for SLE patients in our department, so that patients with joint damage in early stage, especially patients with mild symptom, were prone to miss in this study. In the PM/DM group, we observed an association between anti-CarPA and arthralgia (p = 0.034). The most common finding in joint damage of idiopathic inflammatory myopathies (IIM) is active synovitis, which is similar to RA (42). Highly abundant neutrophils in synovium have been observed to be capable of forming neutrophil extracellular traps (NETs) that externalize carbamylated autoantigens to the extracellular space, resulting in an increase in the production of anti-CarPA (43, 44), which in turn causes joint inflammation. Anti-CarPA may play a role in arthritis associated with PM/DM in a manner similar to RA. However, further validation is required. The correlation between anti-CarPA and RA-ILD has been proposed in

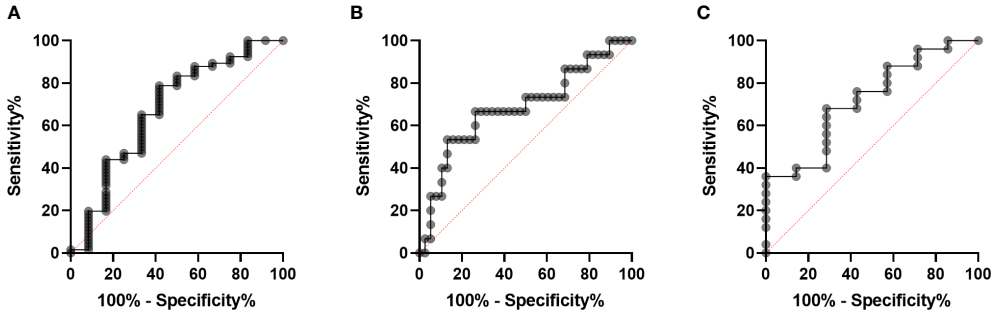

FIGURE 3
Diagnostic performance of serum anti-CarPA. **(A)** Receiver operating characteristic (ROC) curve analysis of serum anti-CarPA for diagnosis of RA-ILD [area under curve (AUC) 0.67, 95%CI 0.49-0.86)]; **(B)** ROC curve analysis of serum anti-CarPA for diagnosis of PM/DM-ILD (AUC 0.68, 95%CI 0.51-0.85); **(C)** ROC curve analysis of serum anti-CarPA for diagnosis of pSS-ILD (AUC 0.72, 95%CI 0.51-0.93).

TABLE 4 Analysis of the risk factors for patients with PM/DM-ILD.

A. Clinical and laboratory characteristics of PM/DM patients grouped by ILD.							
PM/DM	Total	PM/DM-ILD	PM/DM-non-ILD	P			
Gender (n,M/F)	19/34	3/12	16/22	0.13			
Age(mean ± SD,years)	54.24 ± 10.34	55.61 ± 9.51	49.00 ± 12.65	0.022*			
Disease duration(median(IQR),month)	6.00(2.00,12.00)	8.00(3.75,13.5)	2.00(1.00,3.00)	0.005*			
Smoker(n(%))	14/53(26.42%)	10/38(26.32%)	4/15(26.67%)	0.62			
CK(median(IQR),U/L)	190.00(48.00,956.00)	179.00(34.00,1019.00)	217.50(55.50,1155.75)	0.073			
CRP(median(IQR),mg/ml)	4.50(0.89,13.68)	7.32(1.60,15.60)	1.21(0.00,6.64)	0.012*			
ESR(median(IQR),mm/h)	29.00(8.00,56.00)	44.00(7.00,67.00)	17.00(8.25,24.5)	0.11			
FER(median(IQR)ng/ml)	475.97(120.17,1005.58)	578.06(182.45,1024.94)	153.93(96.06,583.74)	0.36			
Anti-CarPA(mean ± SD,ng/ml)	31.43 ± 2.41	34.37 ± 2.82	23.81 ± 4.24	0.045*			
B. Binary logistic regression analysis of patients with PM/DM-ILD.							
Single factor regression	OR	95%CI	P	Multi-factor regression	OR	95%CI	P
Anti-CarPA	1.00	1.00-1.09	0.052	Anti-CarPA	1.05	1.00-1.10	0.040*
Age	1.06	1.00-1.12	0.033*	Age	1.07	1.01-1.14	0.029*
ender	2.91	0.70-12.03	0.14	–	–	–	–
Disease course	1.00	1.00-1.00	0.33	–	–	–	–
Smoke	1.02	0.26-3.40	0.98	Smoke	0.87	0.20-3.90	0.85
Gender	1.04	0.98-1.10	0.20	–	–	–	–
ESR	1.01	0.99-1.04	0.27	–	–	–	–
Anti-PL-7	1.84	0.30-11.22	0.51	–	–	–	–
Anti-EJ	–	–	1.00	–	–	–	–
Anti-JO-1	–	–	1.00	–	–	–	–
Anti-MDA-5	1.86	0.86-4.01	0.12	–	–	–	–
Anti-Ro-52	1.45	0.86-2.43	0.16	–	–	–	–

SD, standard deviation; IQR, interquartile range; CK, creatine kinase; ESR, erythrocyte sedimentation rate; CRP, C reaction protein; FER, ferritin; anti-PL-7, anti-threonyl-transfer ribonucleic acid synthetase anti-body; anti-EJ, anti-glycyl-transfer ribonucleic acid synthetase antibody; anti-JO-1, anti-histidyl-transfer ribonucleic acid synthetase antibody; anti-MDA-5, anti-melanoma differentiation-associated gene 5 antibody; anti-Ro-52,anti-Ro52 antibody; ILD, Interstitial lung disease; PM/DM-ILD, interstitial lung disease associated with polymyositis/dermatomyositis; 95%CI, 95% confidence interval.
Parametric data results were expressed as mean ± SD values. Nonparametric data results were expressed as median IQR values. Some values presented as n or n%; n represents the number of people with this clinical manifestation. T-test, Mann-Whitney U tests, Chi-square test and Logistic regression analysis are used. *p<0.05.

10.3389/fimmu.2023.1197458

TABLE 5 Analysis of the risk factors for patients with pSS.

A. Clinical and laboratory characteristics of pSS patients grouped by ILD.				
pSS	Total	pSS-ILD	pSS-non-ILD	P
Gender (n,M/F)	31/1	1/6	0/25	0.22
Age(mean ± SD,years)	53.11 ± 13.06	55.50 ± 6.35	52.45 ± 14.40	0.052
Disease duration(median(IQR),month)	30.00(6.00,84.00)	24.00(6.00,36.00)	36.00(6.00,84.00)	0.71
PLT(mean ± SD,10^9/L)	213.61 ± 95.97	310.50 ± 83.07	187.18 ± 82.38	0.002*
CRP(median(IQR),mg/ml)	1.26(0.48,1.93)	1.36(0.38,3.37)	1.17(0.50,1.80)	0.39
ESR(median(IQR),mm/h)	26.50(12.00,64.50)	24.50(9.25,101.0)	26.50(12.00,55.50)	0.88
SSA(median(IQR),RU/ml)	134.43(2.43,183.93)	105.02(0.00,180.07)	134.43(2.47,184.52)	0.60
SSB((median(IQR),RU/ml)	3.33(0.00,109.37)	2.59(0.00,115.82)	5.08(0.00,117.28)	0.67
Anti-CarPA(mean ± SD,ng/ml)	16.30 ± 2.42	26.15 ± 6.61	13.57 ± 2.20	0.027*
B. Binary logistic regression analysis of patients with pSS-ILD.				
Single factor regression		OR	95%CI	P
Anti-CarPA		1.07	1.00-1.14	0.048*
Age		1.01	0.95-1.08	0.69
Gender		–	–	1.00
Disease course		1.00	1.00-1.00	0.64
CRP		1.28	0.71-2.30	0.41
ESR		1.00	0.99-1.03	0.52
SSA		1.00	0.99-1.01	0.64
SSB		1.00	0.99-1.01	0.71

SD, standard deviation; IQR, interquartile range; PLT, platelet; ESR, erythrocyte sedimentation rate; CRP, C reaction protein; SSA, antibodies reactive against the ribonucleoprotein antigens Ro/Sjögren's syndrome A; SSB, antibodies reactive against the ribonucleoprotein antigens La/Sjögren's syndrome B antigen; ILD, Interstitial lung disease; pSS-ILD, interstitial lung disease associated with primary Sjögren's syndrome; 95%CI, 95% confidence interval.
Parametric data results were expressed as mean ± SD values. Nonparametric data results were expressed as median IQR values. Some values presented as n or n%; n represents the number of people with this clinical manifestation. T-test, Mann-Whitney U tests and Chi-square test are used.*p<0.05.

recent years (23, 45, 46). Our study identified for the first time that serum anti-CarPA was upregulated in various patients with RD-ILD, not only RA but also PM/DM and pSS. This upregulation was associated with the severity of pulmonary fibrosis but not the image classifications of HR-CT. Anti-CarPA may act as a biomarker for predicting RA-ILD, suggesting more serious lung involvement.

An association seemed to exist between anti-CarPA and ILD in patients with PM/DM in our study. We found that PM/DM-ILD patients had higher levels of CRP than patients with PM/DM-non-ILD. Accordingly, CRP may be involved in the development and progression of PM/DM-ILD. Gono (47) developed a prediction model termed MCK (MDA5, CRP, and KL-6) to identify patients with PM/DM-ILD at low, moderate, or high risk of mortality, using CRP as a risk factor. In our study, we identified an association between anti-CarPA and PM/DM-ILD and proved a relationship between anti-CarPA and severer RD-ILD. Therefore, we speculate that anti-CarPA participates in PM/DM-ILD development and progression, whereas little evidence exists on how anti-CarPA contributes to PM/DM-ILD. In spite of this finding, anti-CarPA is positively correlated with anti-MDA5 and anti-EJ, while negatively correlated with anti-TIF-γ in patients with PM/DM. Several studies found that anti-MDA5 and anti-EJ were associated with more severe ILD in patients with PM/DM, whereas anti-TIF-γ was related to less lung involvement (48). Previous studies confirmed that NETs could participate in the development of ILD in IIM (49–51). Seto (51) identified that anti-MDA5 promotes the formation of NETs, in turn to induce epithelial cell injury and inflammatory cytokine release. In RA, NETs seem to play a role in the production of anti-CarPA, whereas in ILD, the neutrophils that contribute to the production of NETs increase near the lesion site (43). Anti-CarPA is believed to play an important role in the progression of PM/DM-ILD.

Bergum et al. (18) have confirmed that anti-CarPA was associated with the severity of pSS. Our study interestingly found that PLT was lower in anti-CarPA-negative subgroups of pSS. Wu et al. (52) have observed that patients with pSS without thrombocytopenia were more likely to have ILD. Our observations suggest rather that an association exists between them. Additionally, we showed that levels of anti-CarPA were correlated with pSS-ILD and it could predict pSS-ILD. Furthermore, our study found no significant difference in serum anti-CarPA levels between patients with SSC with and without ILD. In a recent study, Riccardi et al. (17) showed an association between anti-

CarPA with "fibrotic subset" in patients with SSC, including patients with diffuse cutaneous subset and/or interstitial lung disease. A study with a large sample size is needed to confirm these findings. The SLE-ILD and UCTD-ILD groups had no association with anti-CarPA, indicating that different pathogenetic mechanisms may be involved.

In this study, we extend the study of anti-CarPA to examine its widespread distribution in RDs among Chinese Han nationals. Moreover, it is the first study to examine the relationship between anti-CarPA and RD-ILD, especially non-RA-ILD. According to our results, anti-CarPA plays an important role in RD-ILD and could be used to identify patients with RDs who are at high risk of developing ILD. This study had two main limitations. First, the relative small number of patients enrolled was the main study limitation. Therefore, further studies on a larger population are mandatory to clarify the prognostic value of anti-CarPA in patients with RDs, especially for patients with RD-ILD. Second, the triage system in our country made it likely that our cohort would enroll patients with more severe diseases. However, a series of analyses have indicated that anti-CarPA is associated with several RDs and linked with ILD in patients with RA, PM/DM, and pSS.

Conclusion

For the first time, we demonstrated the presence of anti-CarPA in a Chinese cohort of patients with RDs, such as RA, SLE, PM/DM, pSS, and UCTD. Based on the results of our study, anti-CarPA may assist in the identification of ILD in patients with RA, PM/DM, and pSS. Further replicative investigations may confirm the pathologic role of anti-CarPA in patients with RDs. Serum anti-CarPA could be detected in patients with RA, PM/DM, pSS, SSC, and UCTD among the Chinese. And it may also assist in identifying ILD in patients with RA, PM/DM, and pSS, which emphasized attention to the lung involvement in anti-CarPA-positive patients.

Data availability statement

The raw data supporting the conclusions of this article will be made available by the authors, without undue reservation.

Ethics statement

The studies involving human participants were reviewed and approved by Shandong Provincial Hospital validated the study protocol (SZRJJ: NO.2021-438). Written informed consent to participate in this study was provided by the participants' legal guardian/next of kin.

Author contributions

RD and YS participated in the study design, literature review, and performed statistical analysis and presentation of the results and participated in the drafting and review of the manuscript. RD, WX, WZX, and ML collected serum samples. ZM, QY, and LZ participated in the study design, the drafting and review of the manuscript. All authors contributed to the article and approved the submitted version.

Funding

This work was supported by the National Natural Science Foundation of China (Youth fund project, Grant NO.82201994) and the Natural Science Foundation of Shandong Province (General Program, Grant No.ZR2022MH016, ZR2022MH138 and Youth fund project, Grant No. ZR2021QH043).

Acknowledgments

We are extremely grateful to all the patients and volunteers who took part in this study, as well as the helpful discussions with Professor Baoting Chao and her colleagues on the image classification and image grading on RD-ILD patients.

Conflict of interest

The authors declare that the research was conducted in the absence of any commercial or financial relationships that could be construed as a potential conflict of interest.

Publisher's note

References

1. Verheul MK, Böhringer S, Delft MAM, Jones JD, Rigby WFC, Gan RW, et al. Triple positivity for anti–citrullinated protein autoantibodies, rheumatoid factor, and anti–carbamylated protein antibodies conferring high specificity for rheumatoid arthritis: implications for very early identification of At-risk individuals. *Arthritis Rheumatol* (2018) 70:1721–31. doi: 10.1002/art.40562

2. Ajeganova S, Humphreys JH, Verheul MK, van Steenbergen HW, van Nies JAB, Hafström I, et al. Anticitrullinated protein antibodies and rheumatoid factor are associated with increased mortality but with different causes of death in patients with rheumatoid arthritis: a longitudinal study in three European cohorts. *Ann Rheum Dis* (2016) 75:1924–32. doi: 10.1136/annrheumdis-2015-208579

3. Humphreys JH, Verheul MK, Barton A, MacGregor AJ, Lunt M, Toes RE, et al. Anticarbamylated protein antibodies are associated with long-term disability and increased disease activity in patients with early inflammatory arthritis: results from the Norfolk arthritis register. *Ann Rheum Dis* (2016) 75:1139–44. doi: 10.1136/annrheumdis-2015-207326

4. Kumar R, Piantoni S, Boldini M, Garrafa E, Bazzani C, Fredi M, et al. Anti-carbamylated protein antibodies as a clinical response predictor in rheumatoid arthritis patients treated with abatacept. *Clin Exp Rheumatol* (2021) 39:91–7. doi: 10.55563/clinexprheumatol/g8xqxr

5. Wang Z, Nicholls SJ, Rodriguez ER, Kummu O, Hörkkö S, Barnard J, et al. Protein carbamylation links inflammation, smoking, uremia and atherogenesis. *Nat Med* (2007) 13:1176–84. doi: 10.1038/nm1637

6. Nakabo S, Hashimoto M, Ito S, Furu M, Ito H, Fujii T, et al. Carbamylated albumin is one of the target antigens of anti-carbamylated protein antibodies. *Rheumatol (Oxford).* (2017) 56:1217–26. doi: 10.1093/rheumatology/kex088

7. Apostolov EO, Basnakian AG, Ok E, Shah SV. Carbamylated low-density lipoprotein: nontraditional risk factor for cardiovascular events in patients with chronic kidney disease. *J Ren Nutr* (2012) 22:134–8. doi: 10.1053/j.jrn.2011.10.023

8. Sidiras P, Lechanteur J, Imbault V, Sokolova T, Durez P, Rasschaert J. Human carbamylome description identifies carbamylated a2-macroglobulin and hemopexin as two novel autoantigens in early rheumatoid arthritis. *Rheumatol (Oxford).* (2022) 61:2826–34. doi: 10.1093/rheumatology/keab838

9. Verheul MK, Yee A, Seaman A, Janssen GM, van Veelen PA, Drijfhout JW, et al. Identification of carbamylated alpha 1 anti-trypsin (A1AT) as an antigenic target of anti-CarP antibodies in patients with rheumatoid arthritis. *J Autoimmun* (2017) 80:77–84. doi: 10.1016/j.jaut.2017.02.008

10. Hörkkö S, Savolainen MJ, Kervinen K, Kesäniemi YA. Carbamylation-induced alterations in low-density lipoprotein metabolism. *Kidney Int* (1992) 41:1175–81. doi: 10.1038/ki.1992.179

11. Jaisson S, Pietrement C, Gillery P. Protein carbamylation: chemistry, pathophysiological involvement, and biomarkers. *Adv Clin Chem* (2018) 84:1–38. doi: 10.1016/bs.acc.2017.12.001

12. Trouw LA, Rispens T, Toes REM. Beyond citrullination: other post-translational protein modifications in rheumatoid arthritis. *Nat Rev Rheumatol* (2017) 13:331–9. doi: 10.1038/nrrheum.2017.15

13. Shi J, Knevel R, Suwannalai P, van der Linden MP, Janssen GMC, van Veelen PA, et al. Autoantibodies recognizing carbamylated proteins are present in sera of patients with rheumatoid arthritis and predict joint damage. *Proc Natl Acad Sci USA* (2011) 108:17372–7. doi: 10.1073/pnas.1114465108

14. Nakabo S, Yoshifuji H, Hashimoto M, Imura Y, Nakashima R, Murakami K, et al. Anti-carbamylated protein antibodies are detectable in various connective tissue diseases. *J Rheumatol* (2017) 44:1384–8. doi: 10.3899/jrheum.161432

15. Sidiras P, Spruyt D, Gangji V, Imbault V, Sokolova T, Durez P, et al. Antibodies against carbamylated proteins: prevalence and associated disease characteristics in Belgian patients with rheumatoid arthritis or other rheumatic diseases. *Scand J Rheumatol* (2021) 50:118–23. doi: 10.1080/03009742.2020.1798500

16. Favoino E, Prete M, Vettori S, Corrado A, Cantatore FP, Valentini G, et al. Anti-carbamylated protein antibodies and skin involvement in patients with systemic sclerosis: an intriguing association. *PloS One* (2018) 13:e0210023. doi: 10.1371/journal.pone.0210023

17. Riccardi A, Martinroche G, Contin-Bordes C, Avouac J, Gobeaux C, Cauvet A, et al. Erosive arthritis autoantibodies in systemic sclerosis. *Semin Arthritis Rheumatol* (2022) 52:151947. doi: 10.1016/j.semarthrit.2021.11.013

18. Bergum B, Koro C, Delaleu N, Solheim M, Hellvard A, Binder V, et al. Antibodies against carbamylated proteins are present in primary sjögren's syndrome and are associated with disease severity. *Ann Rheum Dis* (2016) 75:1494–500. doi: 10.1136/annrheumdis-2015-207751

19. Li Y, Jia R, Liu Y, Tang S, Ma X, Shi L, et al. Antibodies against carbamylated vimentin exist in systemic lupus erythematosus and correlate with disease activity. *Lupus* (2020) 29:239–47. doi: 10.1177/0961203319897127

20. Özdemir B, Erden A, Erten Ş, Yeşil TH, Alışık M, Kucuksahin O. Can anticarbamylated protein antibodies be used to support the diagnosis of systemic lupus erythematosus? *biomark Med* (2021) 15:1253–60. doi: 10.2217/bmm-2021-0037

21. Shi J, van de Stadt LA, Levarht EWN, Huizinga TWJ, Hamann D, van Schaardenburg D, et al. Anti-carbamylated protein (anti-CarP) antibodies precede the onset of rheumatoid arthritis. *Ann Rheum Dis* (2014) 73:780–3. doi: 10.1136/annrheumdis-2013-204154

22. Vidal-Bralo L, Perez-Pampin E, Regueiro C, Montes A, Varela R, Boveda MD, et al. Anti-carbamylated protein autoantibodies associated with mortality in Spanish rheumatoid arthritis patients. *PloS One* (2017) 12:e0180144. doi: 10.1371/journal.pone.0180144

23. Castellanos-Moreira R, Rodríguez-García SC, Gomara MJ, Ruiz-Esquide V, Cuervo A, Casafont-Solé I, et al. Anti-carbamylated proteins antibody repertoire in rheumatoid arthritis: evidence of a new autoantibody linked to interstitial lung disease. *Ann Rheum Dis* (2020) 79:587–94. doi: 10.1136/annrheumdis-2019-216709

24. Xie S, Li S, Chen B, Zhu Q, Xu L, Li F. Serum anti-citrullinated protein antibodies and rheumatoid factor increase the risk of rheumatoid arthritis–related interstitial lung disease: a meta-analysis. *Clin Rheumatol* (2021) 40:4533–43. doi: 10.1007/s10067-021-05808-2

25. Aletaha D, Neogi T, Silman AJ, Funovits J, Felson DT, Bingham CO, et al. Rheumatoid arthritis classification criteria: an American college of Rheumatology/European league against rheumatism collaborative initiative. *Arthritis Rheumatol* (2010) 62:2569–81. doi: 10.1002/art.27584

26. Petri M, Orbai AM, Alarcón GS, Gordon C, Merrill JT, Fortin PR, et al. Derivation and validation of the systemic lupus international collaborating clinics classification criteria for systemic lupus erythematosus. *Arthritis Rheumatol* (2012) 64:2677–86. doi: 10.1002/art.34473

27. Bohan A, Peter JB. Polymyositis and dermatomyositis (first of two parts). *N Engl J Med* (1975) 292:344–7. doi: 10.1056/NEJM197502132920706

28. Shiboski C, Criswell L, Baer A, Challacombe S, Lanfranchi H, Schiødt M, et al. American College of rheumatology classification criteria for sjögren's syndrome: a data-driven, expert consensus approach in the SICCA cohort. *Arthritis Care Res* (2012) 64:475–87. doi: 10.1002/acr.21591

29. Masi AT, Hunder GG, Lie JT, Michel BA, Bloch DA, Arend WP, et al. The American college of rheumatology 1990 criteria for the classification of churg-Strauss syndrome (allergic granulomatosis and angiitis). *Arthritis Rheumatol* (1990) 33:1094–100. doi: 10.1002/art.1780330806

30. van den Hoogen F, Khanna D, Fransen J, Johnson SR, Baron M, Tyndall A, et al. Classification criteria for systemic sclerosis: an American college of rheumatology/European league against rheumatism collaborative initiative. *Ann Rheum Dis* (2013) 72:1747–55. doi: 10.1136/annrheumdis-2013-204424

31. Sieper J, Rudwaleit M, Baraliakos X, Brandt J, Braun J, Burgos-Vargas R, et al. The assessment of SpondyloArthritis international society (ASAS) handbook: a guide to assess spondyloarthritis. *Ann Rheum Dis* (2009) 68:ii1-ii44. doi: 10.1136/ard.2008.104018

32. Mosca M, Tani C, Vagnani S, Carli L, Bombardieri S. The diagnosis and classification of undifferentiated connective tissue diseases. *J Autoimmun* (2014) 48-49:50–2. doi: 10.1016/j.jaut.2014.01.019

33. International Team for the Revision of the International Criteria for Behçet's Disease (ITR-ICBD), Davatchi F, Assaad-Khalil S, Calamia KT, Crook JE, Sadeghi-Abdollahi B, et al. The international criteria for behçet's disease (ICBD): a collaborative study of 27 countries on the sensitivity and specificity of the new criteria. *J Eur Acad Dermatol Venereol.* (2014) 28:338–47. doi: 10.1111/jdv.12107

34. Travis WD, Costabel U, Hansell DM, King TE, Lynch DA, Nicholson AG, et al. An official American thoracic Society/European respiratory society statement: update of the international multidisciplinary classification of the idiopathic interstitial pneumonias. *Am J Respir Crit Care Med* (2013) 188:733–48. doi: 10.1164/rccm.201308-1483ST

35. Homma Y, Saiki S, Doi O, Yoneda R, Mikami R, Tamura M. Clinical criteria for definition of idiopathic interstitial pneumonia (IIP). *Nihon Kyobu Shikkan Gakkai Zasshi.* (1992) 30:1371–7.

36. Alessandri C, Bartosiewicz I, Pendolino M, Mancini R, Colasanti T, Pecani A, et al. Anti-carbamylated protein antibodies in unaffected first-degree relatives of rheumatoid arthritis patients: lack of correlation with anti-cyclic citrullinated protein antibodies and rheumatoid factor. *Clin Exp Rheumatol* (2015) 33:824–30. doi: 10.1136/annrheumdis-2015-eular.5009

37. Brink M, Hansson M, Mathsson-Alm L, Wijayatunga P, Verheul MK, Trouw LA, et al. Rheumatoid factor isotypes in relation to antibodies against citrullinated peptides and carbamylated proteins before the onset of rheumatoid arthritis. *Arthritis Res Ther* (2016) 18:43. doi: 10.1186/s13075-016-0940-2

38. Lamacchia C, Courvoisier DS, Jarlborg M, Bas S, Roux-Lombard P, Möller B, et al. Predictive value of anti-CarP and anti-PAD3 antibodies alone or in combination with RF and ACPA for the severity of rheumatoid arthritis. *Rheumatol (Oxford).* (2021) 60:4598–608. doi: 10.1093/rheumatology/keab050

39. Šenolt L, Grassi W, Szodoray P. Laboratory biomarkers or imaging in the diagnostics of rheumatoid arthritis? *BMC Med* (2014) 12:49. doi: 10.1186/1741-7015-12-49

40. Massaro L, Ceccarelli F, Colasanti T, Pendolino M, Perricone C, Cipriano E, et al. Anti-carbamylated protein antibodies in systemic lupus erythematosus patients with articular involvement. *Lupus* (2018) 27:105–11. doi: 10.1177/0961203317713141

41. Ceccarelli F, Perricone C, Colasanti T, Massaro L, Cipriano E, Pendolino M, et al. Anti-carbamylated protein antibodies as a new biomarker of erosive joint damage in systemic lupus erythematosus. *Arthritis Res Ther* (2018) 20:126. doi: 10.1186/s13075-018-1622-z

42. Klein M, Mann H, Vencovský J. Arthritis in idiopathic inflammatory myopathies. *Curr Rheumatol Rep* (2019) 21:70. doi: 10.1007/s11926-019-0878-x

43. Khandpur R, Carmona-Rivera C, Vivekanandan-Giri A, Gizinski A, Yalavarthi S, Knight JS, et al. NETs are a source of citrullinated autoantigens and stimulate inflammatory responses in rheumatoid arthritis. *Sci Transl Med* (2013) 5:178ra40. doi: 10.1126/scitranslmed.3005580

44. O'Neil LJ, Barrera-Vargas A, Sandoval-Heglund D, Merayo-Chalico J, Aguirre-Aguilar E, Aponte AM, et al. Neutrophil-mediated carbamylation promotes articular damage in rheumatoid arthritis. *Sci Adv* (2020) 6:eabd2688. doi: 10.1126/sciadv.abd2688

45. Xue J, Hu W, Wu S, Wang J, Chi S, Liu X. Development of a risk nomogram model for identifying interstitial lung disease in patients with rheumatoid arthritis. *Front Immunol* (2022) 13:823669. doi: 10.3389/fimmu.2022.823669

46. Oka S, Higuchi T, Furukawa H, Shimada K, Okamoto A, Hashimoto A, et al. Serum rheumatoid factor IgA, anti-citrullinated peptide antibodies with secretory components, and anti-carbamylated protein antibodies associate with interstitial lung disease in rheumatoid arthritis. *BMC Musculoskelet Disord* (2022) 23:46. doi: 10.1186/s12891-021-04985-0

47. Gono T, Masui K, Nishina N, Kawaguchi Y, Kawakami A, Ikeda K, et al. Risk prediction modeling based on a combination of initial serum biomarker levels in Polymyositis/Dermatomyositis–associated interstitial lung disease. *Arthritis Rheumatol* (2021) 73:677–86. doi: 10.1002/art.41566

48. Gunawardena H. The clinical features of myositis-associated autoantibodies: a review. *Clinic Rev Allerg Immunol* (2017) 52:45–57. doi: 10.1007/s12016-015-8513-8

49. Khawaja AA, Chong DLW, Sahota J, Mikolasch TA, Pericleous C, Ripoll VM, et al. Identification of a novel HIF-1α-αMβ2 integrin-NET axis in fibrotic interstitial lung disease. *Front Immunol* (2020) 11:2190. doi: 10.3389/fimmu.2020.02190

50. Zhang S, Jia X, Zhang Q, Zhang L, Yang J, Hu C, et al. Neutrophil extracellular traps activate lung fibroblast to induce polymyositis-related interstitial lung diseases via TLR9-miR-7-Smad2 pathway. *J Cell Mol Med* (2020) 24:1658–69. doi: 10.1111/jcmm.14858

51. Seto N, Torres-Ruiz JJ, Carmona-Rivera C, Pinal-Fernandez I, Pak K, Purmalek MM, et al. Neutrophil dysregulation is pathogenic in idiopathic inflammatory myopathies. *JCI Insight* (2020) 5:e134189. doi: 10.1172/jci.insight.134189

52. Wu J, Chang X, Zhang J, Liu C, Liu M, Chen W. Clinical and laboratory features of primary sjögren's syndrome complicated with mild to severe thrombocytopenia. *Ann Transl Med* (2022) 10:300. doi: 10.21037/atm-22-162

frontiers | Frontiers in Immunology

TYPE Case Report
PUBLISHED 10 August 2023
DOI 10.3389/fimmu.2023.1222431

OPEN ACCESS

EDITED BY
Francesca Wanda Rossi,
University of Naples Federico II, Italy

REVIEWED BY
Sevim Bavbek,
Ankara University, Türkiye
Aikaterini Detoraki,
Federico II University Hospital, Italy

*CORRESPONDENCE
Beatrice Maranini
beatrice.maranini@edu.unife.it

RECEIVED 14 May 2023
ACCEPTED 17 July 2023
PUBLISHED 10 August 2023

CITATION
Maranini B, Guzzinati I, Casoni GL, Ballotta M, Lo Monaco A and Govoni M (2023) Case Report: Middle lobe syndrome: a rare presentation in eosinophilic granulomatosis with polyangiitis. *Front. Immunol.* 14:1222431. doi: 10.3389/fimmu.2023.1222431

Case Report: Middle lobe syndrome: a rare presentation in eosinophilic granulomatosis with polyangiitis

Beatrice Maranini[1]*, Ippolito Guzzinati[2], Gian Luca Casoni[2], Maria Ballotta[3], Andrea Lo Monaco[1] and Marcello Govoni[1]

[1]Division of Rheumatology, Department of Medical Sciences, University of Ferrara, Ferrara, Italy, [2]Pneumology Unit, Hospital of Rovigo, Rovigo, Italy, [3]Section of Anatomic Pathology, Azienda Ospedaliera Rovigo, Rovigo, Italy

Background: Antineutrophil cytoplasmic antibody (ANCA)-associated vasculitis (AAV) is a group of disorders characterized by necrotizing inflammation of small- and medium-sized blood vessels and the presence of circulating ANCA. Eosinophilic granulomatosis with polyangiitis (EGPA) is a systemic ANCA-associated vasculitis, characterized by peripheral eosinophilia, neuropathy, palpable purpuras or petechiae, renal and cardiac involvement, sinusitis, asthma, and transient pulmonary infiltrates. Middle lobe syndrome (MLS) is defined as recurrent or chronic atelectasis of the right middle lobe of the lung, and it is a potential complication of asthma.

Case presentation: Herein, we describe a case of MLS in a 51-year-old woman, never-smoker, affected by EGPA, presenting exclusively with leukocytosis and elevated concentrations of acute-phase proteins, without any respiratory symptom, cough, or hemoptysis. Chest computed tomography (CT) imaging documented complete atelectasis of the middle lobe, together with complete obstruction of lobar bronchial branch origin. Fiberoptic bronchoscopy (FOB) revealed complete stenosis of the middle lobar bronchus origin, thus confirming the diagnosis of MLS, along with distal left main bronchus stenosis. Bronchoalveolar lavage (BAL) did not detect any infection. Bronchial biopsies included plasma cells, neutrophil infiltrates, only isolated eosinophils, and no granulomas, providing the hypothesis of vasculitic acute involvement less likely. First-line agents directed towards optimizing pulmonary function (mucolytics, bronchodilators, and antibiotic course) were therefore employed. However, the patient did not respond to conservative treatment; hence, endoscopic management of airway obstruction was performed, with chest CT documenting resolution of middle lobe atelectasis.

Conclusion: To the best of our knowledge, this is the first detailed description of MLS in EGPA completely resolved through FOB. Identification of MLS in EGPA appears essential as prognosis, longitudinal management, and treatment options may differ from other pulmonary involvement in AAV patients.

KEYWORDS

eosinophilic granulomatosis with polyangiitis, EGPA, Churg–Strauss, asthma, middle lobe syndrome

Introduction

Antineutrophil cytoplasmic antibody (ANCA)-associated vasculitides (AAV) are composite disorders characterized by necrotizing inflammation, predominantly involving small blood vessels, usually associated with circulating myeloperoxidase (MPO)- or proteinase 3 (PR3)-ANCA (1). Medium-sized arteries may also be affected (1).

AAV include granulomatosis with polyangiitis (GPA, formerly Wegener granulomatosis), microscopic polyangiitis (MPA), and eosinophilic granulomatosis with polyangiitis (EGPA, formerly Churg–Strauss syndrome) (1). Taken together, the most commonly affected systems in AAV are the upper airways, lungs, kidneys, eyes, skin, and peripheral nerves. Presenting symptoms include chronic sinusitis, nasal discharge or crusting, hearing loss, ear fullness, tinnitus, cough, wheeze or hemoptysis, renal failure and proteinuria, purpuric rash, and peripheral neuropathy (2). Pulmonary involvement includes necrotizing granulomatous inflammation (nodules, masses, with or without cavitation), tracheobronchial inflammation, alveolar hemorrhage, interstitial lung disease (ILD), and asthma (3).

EGPA is histologically defined by eosinophil-rich, necrotizing granulomatous inflammation, primarily involving the respiratory tract, along with necrotizing vasculitis of small to medium size (4). ANCAs are detected in ~40%–60% of patients with EGPA typically directed against MPO (5).

Middle lobe syndrome (MLS) is a rare clinical entity, defined as chronic or recurrent atelectasis of the right middle lobe of the lung, although it can also involve the lingula of the left lung (6). First described in 1948 (7), it can present in patients of any age. The right middle lobe bronchus is susceptible to partial or total obstruction due to a smaller intraluminal diameter compared to other lobar bronchi (6).

Female patients present smaller intraluminal diameters compared to male counterparts, thus providing anatomical explanation for a female epidemiological predisposition (8).

Here, we report the case of a 51-year-old woman affected by EGPA, presenting exclusively with leukocytosis and elevated concentrations of acute-phase proteins, which turned out to present MLS diagnosis.

Case presentation

A 51-year-old woman, with an established diagnosis of EGPA, presented to our Rheumatology Clinic for a routine follow-up scheduled visit.

Diagnosis was determined in 2014, when she presented with asthma-like tracheobronchitis, for which she underwent high-resolution chest computed tomography (HRCT) revealing bronchial wall thickening and lung consolidations. MPO-ANCA positivity was evidenced. After pneumological examination, she was referred to bronchoscopy. Bronchoalveolar lavage (BAL) cell count showed 22% eosinophils, while peripheral eosinophilia was >10% on differential white blood cell count. Since IgG4-related disease (IgG4-RD) may cause lung manifestations in terms of interstitial pneumonitis, organizing pneumonia, and lymphomatoid granulomatosis, IgG4 was collected in both serum and tissues, and found within normal ranges. Bronchial mucosa histological samples described granulation tissue, neutrophilic and eosinophilic inflammatory infiltration, plurinucleate giant cells, and fibrinoid necrosis. No peripheral neuropathy or renal involvement was observed at the time. No ear–nose–throat manifestations were referred by the patient; however, and ENT specialist still evaluated her, excluding the presence of rhinological, otological, or other manifestations of EGPA. Finally, diagnosis was established following the 1990 ACR diagnostic criteria for EGPA. The patient's past medical history highlighted arterial hypertension, thyroid nodules with normal thyroid function, diverticulosis of the sigma, polycystic ovary syndrome (PCOS), and incomplete right bundle branch block. She had never smoked. At disease onset, she was treated with high doses of steroid (prednisone 1 mg/kg/day), gradually tapered until suspension after 6 months. During steroid-tapering, at week 12 from disease onset, therapy with azathioprine was introduced at the dosage of 150 mg and 100 mg every other day (because of moderate toxic myelosuppression at higher doses). The patient remained in remission for 8 years, with a Birmingham Vasculitis Activity Score (BVAS) of 0.

During follow-up visits, neither systemic nor localized symptoms emerged, particularly of the respiratory tract. Her asthma control was optimal with beclometasone-formoterol as maintenance and reliever treatment. However, blood tests showed mild leukocytosis and elevated levels of acute-phase proteins. Allergy, stress, injury, surgery, or thyroid problems were all excluded. Complete blood tests repeated in our clinic confirmed neutrophilic leukocytosis (leukocyte count 15.59×10^3 cell/mmc, normal value $<11 \times 10^3$ cell/mmc; neutrophil 10.84×10^3 cell/mmc, normal value $<7.2 \times 10^3$ cell/mmc) and elevated levels of C-reactive protein (CRP) (3.46 mg/dl, cutoff value < 0.50) and erythrocyte sedimentation rate (ESR) (81 mm/h, cutoff value < 28). No other relevant findings emerged (normal liver and kidney function, electrophoresis, and urine analysis). Eosinophils were normal. ANCA testing proved negative. Free light chains were present at normal ranges in the blood. After hematological consult, lympho-proliferative disease was excluded and laboratory alterations were ascribed to a reactive leukocytosis derived from rheumatological condition.

Because of persistent leukocytosis and elevated inflammatory markers, in the absence of alternative causes, and as the patient's last chest CT scan dated 2 years before, in agreement with the pulmonary specialist, an HRCT examination (Figures 1A–D) was scheduled again, highlighting complete bronchiectasis and atelectasis of the middle lobe (ML), on an obstructive basis because of stenosis at the origin of the ML bronchial branch (Figures 1A, B). Moreover, diffuse thickening of the proximal bronchial walls of the inferior ipsilateral lobar branch, the common bronchus of the left lobe, and the origin of the bronchial branches of the lingula were detected. A polypoid-like neoformation of the anterior wall of the left common bronchus was reported as well, measuring approximately 8 × 10 mm (Figures 1C, D). According to a radiologist and pneumologist consultant, these findings appeared worthy of endoscopic investigations to rule out differential diagnosis between granulomas and heterotoplastic tissue.

After fiberoptic bronchoscopy (FOB), stenosis at the origin of the middle lobar bronchus, associated with architectural stenosis of the distal section of the left main bronchus, was confirmed (Figure 2A). At BAL, no hypereosinophilia was detected and microbiological tests were all negative for infections.

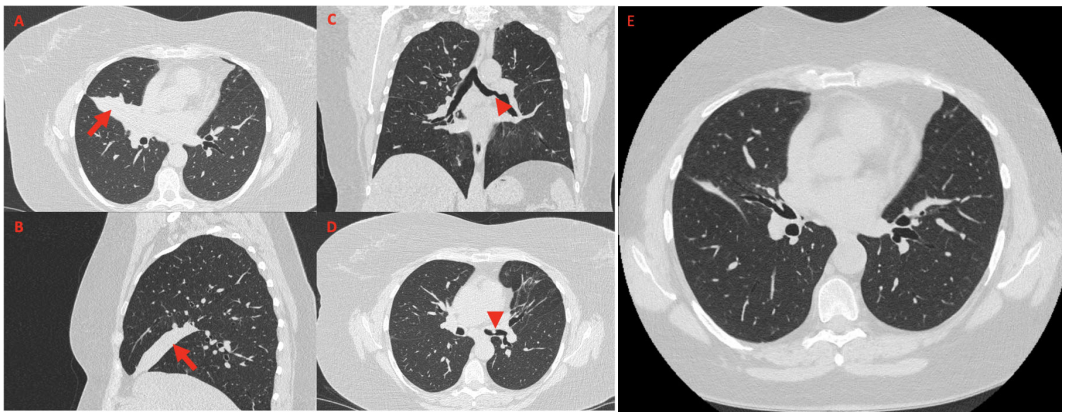

FIGURE 1
High-resolution chest CT showing a wedge-shaped density extending from the hilum anteriorly and inferiorly towards the chest wall, confirming the presence of middle lobe syndrome [red arrow in **(A)**, axial view, and **(B)**, sagittal view]. Coronal view **(C)** shows polypoid-like neoformation of the anterior wall of the left common bronchus (red arrowhead), confirmed in axial view (**D**, red arrowhead). High-resolution chest CT performed 15 days after the bronchodilation procedure documented regression of the middle lobe atelectasis (**E**, axial view).

Bronchial biopsies showed the prevalence of an infiltrate of plasma cells and neutrophils, with isolated eosinophils, in the absence of granuloma, fibrinoid necrosis, eosinophilic vasculitis, and neoplastic cells (Figure 3). Nonabundant interstitial IgG4 plasma cells by IgG4 immunoperoxidase stain were observed, the Tfh–plasmablast axis was not elevated, and no positive stains to CD138, CD38, MUM1, and CD79a were observed. Based on these features, the pneumologist concluded an MLS diagnosis. Anti-inflammatory therapy was attempted, with prednisone 25 mg daily for 35 days. Because of lack of response to conservative treatment, endoscopic attempt of middle lobar bronchus dilatation (by Fogarty 4 F balloon and tissue removal using flexible biopsy forceps) was scheduled (Figure 2B). At follow-up chest CT scan, reventilation of middle lobe was documented (Figure 1E). Repeated FOB confirmed improving middle lobar bronchus stenosis (Figure 2C). The patient completely recovered from the procedure, without any respiratory symptom. Complete blood count was repeated 20 days after the procedure, documenting a slowly lowering neutrophilic leukocytosis (leukocyte count 14.3×10^3 cell/mmc, normal value $<11 \times 10^3$ cell/mmc; neutrophil 9.9×10^3 cell/mmc, normal value $<7.2 \times 10^3$ cell/mmc), as well as CRP (1.71 mg/dl, cutoff value < 0.50) and ESR (72 mm/h, cutoff value < 28).

Discussion

Lung involvement is one of the most common clinical features in AAV (9). Airway involvement presents as tracheobronchial (TB) obstruction, sustained by inflammation, which occurs at any region of the tracheobronchial tree, including subglottic stenosis (SGS) and lower tracheal and bronchial stenosis (BS). Notably, BS is less frequently described, since it is more frequently asymptomatic and discovered accidentally, unlike SGS, which becomes rapidly symptomatic (voice changes, noisy breathing, dyspnea, etc.). Thus, BS is probably underdiagnosed among AAV patients (10). TB involvement is more frequent in GPA (15%–55% of patients, according to different cohorts in literature) (10–12), but it is rarely described even in MPA and EGPA (13).

MLS is a rare clinical entity, defined as chronic or recurrent atelectasis of the right middle lobe of the lung, and it is a potential

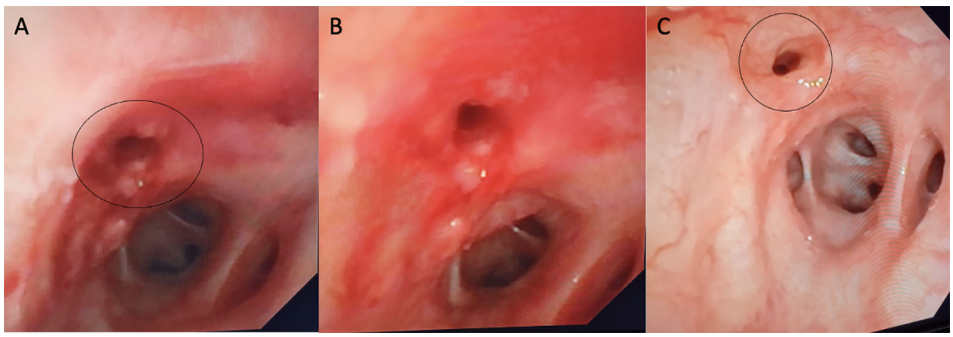

FIGURE 2
On bronchoscopy, the right main bronchus was partially obstructed by fibrotic stenosis **(A)**. **(B)** shows bronchoscopic images after dilatation and 1 month later showing complete healing of bronchial tear **(C)**.

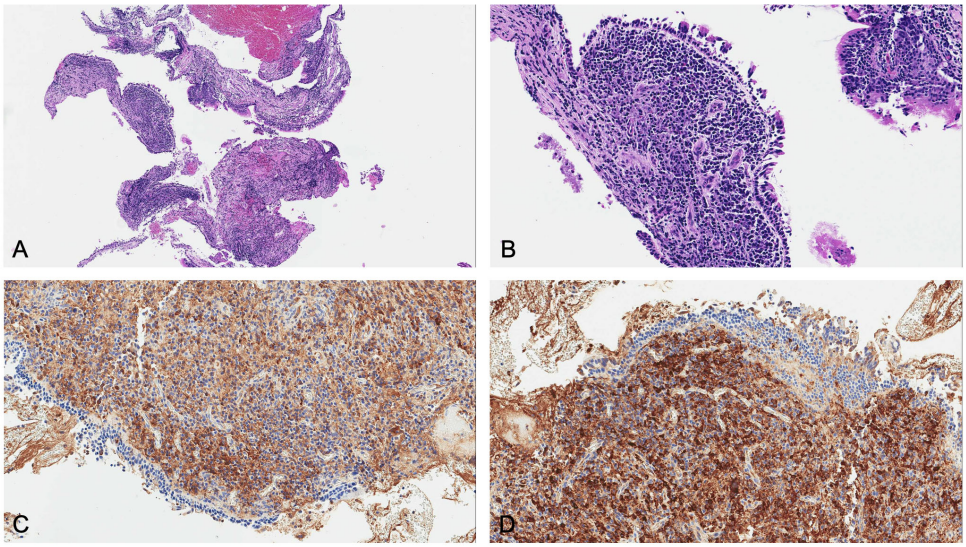

FIGURE 3
Microscopic examination revealed: **(A)** low magnification and **(B)** high magnification of hematoxylin and eosin staining, showing plasma cell infiltrate in the absence of eosinophils and vasculitis. Since main differential diagnosis includes lymphoma, kappa and lambda light chain immunostains were needed. Immunoglobulin free light chain (IgLC) levels in lung tissue were determined by immunohistochemistry, and no abnormalities were observed both at **(C)** low and **(D)** high magnification.

complication of asthma. In some cases, the lingula of the left lung may also be involved (6).

To the best of our knowledge, this is the first detailed description of MLS in EGPA. Although there is no established definition of MLS, it is fundamentally distinct into two pathophysiological pathways: a non-obstructive type (patent right middle lobe bronchus) and an obstructive type (documented airway occlusion), both caused by various etiologies. A history of atopy, asthma, or COPD has been reported in up to 50% of patients (14).

Recurrent infections and chronic airway inflammatory processes, as observed in asthma, may lead to parenchymal damage and bronchiectasis, and contribute to transient bronchial obstruction (15).

TB obstruction/stenosis differential diagnosis is thus mandatory. Infections, traumatic injuries, radiation, and extrinsic compression (e.g., lung malignancies) are the principal etiologies. Other rarer causes are rheumatoid arthritis (RA), sarcoidosis, amyloidosis, Behçet's disease, relapsing polychondritis (RP), and fibrosing mediastinitis due to autoimmune disorders such as IgG4-RD (16–25).

Nonetheless, histological sampling of tracheobronchial lesions is not always specific (10). It often shows necrotizing granulomas that alter the normal alveolar architecture, progressively impairing respiratory function and causing subsequent bronchial stenosis and fibrosis. However, also non-specific mucosal inflammation and ulcerations may be observed, and it has to be considered that vasculitis is much more rarely encountered compared to granuloma, such as in our case (26).

It is important that the bronchoscopist carefully inspects the airways, since the TB mucosal lesions may be easily missed as they are very tiny and possibly sparse (27).

Since BS should be considered a severe manifestation of AAV, eventually leading to marked functional and life-threatening risks, physicians should be aware of this complication.

It may present totally asymptomatic, showing solely raised leukocyte count and inflammatory markers, in the absence of other possible explanation, similarly to our reported case (9).

Commonly, asthma exacerbation should be ruled out, and BS diagnosis may therefore derive only from chest HRCT, scheduled to exclude the presence of asthma abnormalities, namely, air trapping, bronchiectasis, bronchial dilatation, and bronchial wall thickening (28–31). In BS, imaging reports chronic or recurrent lobe atelectasis, particularly involving ML, since ML's fissures insufflate the segment from collateral ventilation, reducing the likelihood of auto-correction of atelectasis (32), configuring MLS disease.

Findings from literature data suggest that BS involvement might be significantly more frequent than generally believed in patients being evaluated for possible eosinophilic lung diseases. In fact, chronic inflammation, as observed in recurrent asthma episodes and eosinophilic infiltrates, may lead to altered bronchus mucosal microarchitecture and fibrosis, thus causing BS (6). Therefore, careful asthma management in these patients is decisive to prevent airway stenoses and lobar collapse (33).

Figure 4 summarizes the main aspects discussed and to be considered in AAV patients at risk of MLS development.

Regarding management, TB disease may require treatment with high-dose systemic glucocorticoids and cyclophosphamide or rituximab. In a small cohort in literature, cyclophosphamide seemed to effectively treat BS, but not SGS, while rituximab appeared to be a promising therapy for tracheobronchial lesions (11, 34).

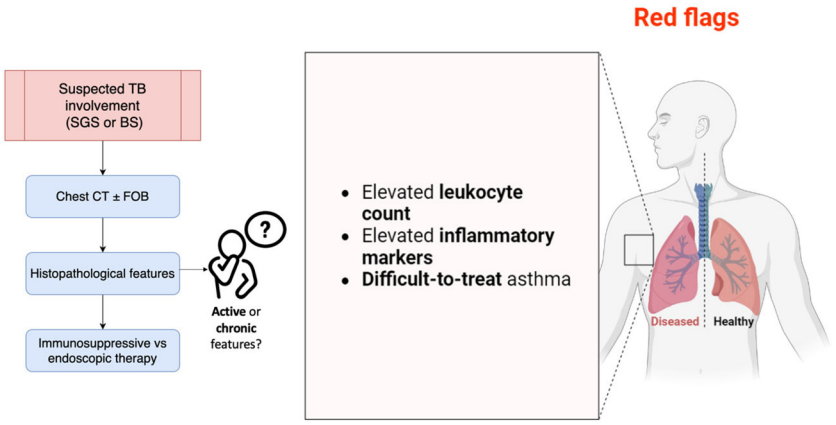

FIGURE 4
Main points to consider in AAV patients at risk of MLS development. BS, bronchial stenosis; CT, computed tomography; FOB, fiberoptic bronchoscopy; SGS, subglottic stenosis; TB, tracheobronchial. The image was created with BioRender.

When TB involvement does not respond to standard immunosuppressive treatment, particularly when the stenosis is severe or it is likely to be problematic in the future (e.g., potentially complicating intubation or decannulation), and especially in symptomatic patients, complementary endoscopic management may be considered (35).

Furthermore, TB disease evolves independently from other systemic AAV manifestations, and little is known in terms of therapeutic response or evolution, even if viral infection and autoimmune flares may play a role (36). ANCA autoantibodies and inflammatory markers could be useful in monitoring disease course (37); however, they may be non-specific, affected by other causes (e.g., infections, as above mentioned), and they fluctuate over time without effectively predicting disease flares (38). Moreover, TB stenosis relapses are common and mostly occur under immunosuppressant therapy, suggesting the absence of response to classical AAV treatment (10). Differentiating active inflammatory endobronchial involvement from damage (scarring resulting from post-inflammatory fibrosis, or restenosis) may be clinically challenging, especially in patients without any other active organ involvement or in patients with negative ANCA test results, like in our presented case. In such patients, enforcing an intensification of immunosuppressive therapy may prove ineffective, merely increasing the risk of infectious complications (3). The CRP trend in our patient was decreasing after operative bronchus dilatation, and we believe this may reflect chronic BS. Otherwise, ongoing inflammation and fibroblast activation may subtend active disease. Additionally, characterization of serial changes in inflammation in EGPA patients with lung involvement may provide information about disease progression, foster further imaging investigation, potentially allowing risk stratification, and finally helping clinicians through treatment plans. Managing other sources of inflammation that could accelerate or induce recurrence may be pivotal as well, even if, today, there are no guidelines supporting physicians in such cases, and the risk of recurrence remains undisclosed. In conclusion, the rationale for TB stenosis screening in AAV patients is based on clinical experience, since usually patients are completely asymptomatic. Laboratory markers are not helpful as disease biomarkers, but they could be considered "red flags", identifying patients needed to be closely monitored. Prompt evaluation with chest CT and FOB is required, even if histopathology may be inconclusive in defining acute rather than chronic disease features. Immunosuppressive therapy is the gold standard, but if worsening stenosis is confirmed, endoscopic restoration of airway patency is indicated (39).

To the best of our knowledge, this is the first detailed description of MLS in EGPA completely removed through FOB. Identification of MLS in EGPA appears imperative as prognosis, longitudinal management, and treatment options may differ from other pulmonary involvement in AAV patients.

Data availability statement

The original contributions presented in the study are included in the article/supplementary material. Further inquiries can be directed to the corresponding author.

Ethics statement

Ethical review and approval was not required for the study on human participants in accordance with the local legislation and institutional requirements. The patients/participants provided their written informed consent to participate in this study. Written informed consent was obtained from the participant/patient(s) for the publication of this case report.

Author contributions

Conceptualization, BM; methodology, BM, IG, GLC, MB, ALM, MG; investigation, BM, IG, GLC, MB, ALM; data curation, BM, IG, GLC, MB, ALM, MG; writing—original draft preparation, BM; writing—review and editing, BM, IG, GLC, MB, ALM, MG; supervision, MG. All authors contributed to the article and approved the submitted version.

Funding

The APC was funded by University of Ferrara.

Conflict of interest

The authors declare that the research was conducted in the absence of any commercial or financial relationships that could be construed as a potential conflict of interest.

Publisher's note

All claims expressed in this article are solely those of the authors and do not necessarily represent those of their affiliated organizations, or those of the publisher, the editors and the reviewers. Any product that may be evaluated in this article, or claim that may be made by its manufacturer, is not guaranteed or endorsed by the publisher.

References

1. Jennette JC, Falk RJ, Bacon PA, Basu N, Cid MC, Ferrario F, et al. Revised international chapel hill consensus conference nomenclature of vasculitides. *Arthritis Rheum* (20122013) 65(1):1–11. doi: 10.1002/art.37715

2. Hunter RW, Welsh N, Farrah TE, Gallacher PJ, Dhaun N. Anca associated vasculitis. *Bmj* (2020) 369:m1070. doi: 10.1136/bmj.m1070

3. Sacoto G, Boukhlal S, Specks U, Flores-Suárez LF, Cornec D. Lung involvement in anca- associated vasculitis. *Presse Med* (2020) 49(3):104039. doi: 10.1016/j.lpm.2020.104039

4. Grayson PC, Ponte C, Suppiah R, Robson JC, Craven A, Judge A, et al. American College of rheumatology/european alliance of associations for rheumatology classification criteria for eosinophilic granulomatosis with polyangiitis. *Ann Rheum Dis* (20222022) 81(3):309–14. doi: 10.1136/annrheumdis-2021-221794

5. Sablé-Fourtassou R, Cohen P, Mahr A, Pagnoux C, Mouthon L, Jayne D, et al. Antineutrophil cytoplasmic antibodies and the churg-strauss syndrome. *Ann Intern Med* (2005) 143(9):632–8. doi: 10.7326/0003-4819-143-9-200511010-00006

6. Gudbjartsson T, Gudmundsson G. Middle lobe syndrome: a review of clinicopathological features, diagnosis and treatment. *Respiration* (2012) 84(1):80–6. doi: 10.1159/000336238

7. Graham EA, Burford TH, Mayer JH. Middle lobe syndrome. *Postgrad Med* (1948) 4(1):29–34. doi: 10.1080/00325481.1948.11693655

8. Mi W, Zhang C, Wang H, Cao J, Li C, Yang L, et al. Measurement and analysis of the tracheobronchial tree in chinese population using computed tomography. *PloS One* (2015) 10(4):e0123177. doi: 10.1371/journal.pone.0123177

9. Cottin V, Bel E, Bottero P, Dalhoff K, Humbert M, Lazor R, et al. Respiratory manifestations of eosinophilic granulomatosis with polyangiitis (churg-strauss). (2016) 48(5):1429–41. doi: 10.1183/13993003.00097-2016

10. Taylor SC, Clayburgh DR, Rosenbaum JT, Schindler JS. Clinical manifestations and treatment of idiopathic and wegener granulomatosis-associated subglottic stenosis. *JAMA Otolaryngol Head Neck Surg* (2013) 139(1):76–81. doi: 10.1001/jamaoto.2013.1135

11. Girard C, Charles P, Terrier B, Bussonne G, Cohen P, Pagnoux C, et al. Tracheobronchial stenoses in granulomatosis with polyangiitis (wegener's): a report on 26 cases. *Med (Baltimore)* (2015) 94(32):e1088. doi: 10.1097/md.0000000000001088

12. Garcia-Valladares I, Espinoza LR. Subglottic stenosis is a form of limited wegener's granulomatosis. *J Rheumatol* (2011) 38(10):2268. doi: 10.3899/jrheum.110371

13. Polychronopoulos VS, Prakash UB, Golbin JM, Edell ES, Specks U. Airway involvement in wegener's granulomatosis. *Rheum Dis Clin North Am* (2007) 33(4):755–75. doi: 10.1016/j.rdc.2007.09.004

14. Einarsson JT, Einarsson JG, Isaksson H, Gudbjartsson T, Gudmundsson G. Middle lobe syndrome: a nationwide study on clinicopathological features and surgical treatment. *Clin Respir J* (2009) 3(2):77–81. doi: 10.1111/j.1752-699X.2008.00109.x

15. Soyer O, Ozen C, Cavkaytar O, Senyücel C, Dallar Y. Right middle lobe atelectasis in children with asthma and prognostic factors. *Allergology Int* (2016) 65(3):253–8. doi: 10.1016/j.alit.2015.12.002

16. Puchalski J, Musani AI. Tracheobronchial stenosis: causes and advances in management. *Clin Chest Med* (2013) 34(3):557–67. doi: 10.1016/j.ccm.2013.05.002

17. Illamperuma C, Reid J, Kanthan R. Chyloptysis with right middle lobe syndrome complicated postoperatively by chylothorax: an unusual cause of right middle lobe syndrome. *Can Respir J* (2009) 16(2):e1–2. doi: 10.1155/2009/370496

18. Yamasaki A, Tomita K, Chikumi H, Tatsukawa T, Shigeoka Y, Nakamoto M, et al. Lung cancer arising in association with middle lobe syndrome. *Anticancer Res* (2006) 26(3b):2213–6.

19. Keshishyan S, Harris K, Mohan A, Patil M. Bronchoscopic management of central airway obstruction secondary to rheumatoid arthritis. *J Bronchology Interv Pulmonol* (2018) 25(1):e9– e11. doi: 10.1097/lbr.0000000000000430

20. Teo F, Anantham D, Feller-Kopman D, Ernst A. Bronchoscopic management of sarcoidosis related bronchial stenosis with adjunctive topical mitomycin c. *Ann Thorac Surg* (2010) 89(6):2005–7. doi: 10.1016/j.athoracsur.2009.10.072

21. Milani P, Basset M, Russo F, Foli A, Palladini G, Merlini G. The lung in amyloidosis. *Eur Respir Rev* (2017) 26(145):170046. doi: 10.1183/16000617.0046-2017

22. Witt C, John M, Martin H, Hiepe F, Ewert R, Emslander HP, et al. Behet's syndrome with pulmonary involvement-combined therapy for endobronchial stenosis using neodym-yag laser, balloon dilation and immunosuppression. *Respiration* (1996) 63(3):195–8. doi: 10.1159/000196544

23. Rahman N, Senanayake E, Mascaro J, Situnayake D, Bishay ES, Patel AJ. Recurrent endobronchial occlusion and aorto-bronchial fistula formation in behcet's disease. *J Cardiothorac Surg* (2023) 18(1):22. doi: 10.1186/s13019-023-02145-0

24. de Montmollin N, Dusser D, Lorut C, Dion J, Costedoat-Chalumeau N, Mouthon L, et al. Tracheobronchial involvement of relapsing polychondritis. *Autoimmun Rev* (2019) 18(9):102353. doi: 10.1016/j.autrev.2019.102353

25. Ito M, Yasuo M, Yamamoto H, Tsushima K, Tanabe T, Yokoyama T, et al. Central airway stenosis in a patient with autoimmune pancreatitis. . *Eur Respir J* (2009) 33(3):680–3. doi: 10.1183/09031936.00051408

26. Schwarz MI, Brown KK. Small vessel vasculitis of the lung. *Thorax* (2000) 55(6):502–10. doi: 10.1136/thorax.55.6.502

27. Livi V, Cancellieri A, Patelli M, Trisolini R. Tracheobronchial involvement in churg-strauss syndrome. *J Bronchology Interv Pulmonol* (2012) 19(1):81–2. doi: 10.1097/LBR.0b013e3182422dd1

28. Gupta S, Siddiqui S, Haldar P, Raj JV, Entwisle JJ, Wardlaw AJ, et al. Qualitative analysis of high-resolution ct scans in severe asthma. *Chest* (2009) 136(6):1521–8. doi: 10.1378/chest.09-0174

29. Lin X, Lin Y, Lai Z, Wei S, Qiu M, Li J, et al. Retrospective comparison of high-resolution computed tomography of eosinophilic granulomatosis with polyangiitis with severe asthma. *Ann Transl Med* (2021) 9(12):983. doi: 10.21037/atm-21-2243

30. Baroni RH, Feller-Kopman D, Nishino M, Hatabu H, Loring SH, Ernst A, et al. Tracheobronchomalacia: comparison between end-expiratory and dynamic expiratory ct for evaluation of central airway collapse. *Radiology* (2005) 235(2):635–41. doi: 10.1148/radiol.2352040309

31. Stern EJ, Graham CM, Webb WR, Gamsu G. Normal trachea during forced expiration: dynamic ct measurements. *Radiology* (1993) 187(1):27–31. doi: 10.1148/radiology.187.1.8451427

32. Aquino SL, Shepard JA, Ginns LC, Moore RH, Halpern E, Grillo HC, et al. Acquired tracheomalacia: detection by expiratory ct scan. *J Comput Assist Tomogr* (2001) 25(3):394–9. doi: 10.1097/00004728-200105000-00011

33. Latorre M, Baldini C, Seccia V, Pepe P, Novelli F, Celi A, et al. Asthma control and airway inflammation in patients with eosinophilic granulomatosis with polyangiitis. *J Allergy Clin Immunol Pract* (2016) 4(3):512–9. doi: 10.1016/j.jaip.2015.12.014

34. Fowler NM, Beach JM, Krakovitz P, Spalding SJ. Airway manifestations in childhood granulomatosis with polyangiitis (Wegener's). *Arthritis Care Res (Hoboken)* (2012) 64(3):434–40. doi: 10.1002/acr.21565

35. Terrier B, Dechartres A, Girard C, Jouneau S, Kahn JE, Dhote R, et al. Granulomatosis with polyangiitis: endoscopic management of tracheobronchial stenosis: results from a multicentre experience. *Rheumatol (Oxford)* (2015) 54 (10):1852–7. doi: 10.1093/rheumatology/kev129

36. Shitrit D, Kuchuk M, Zismanov V, Rahman NA, Amital A, Kramer MR. Bronchoscopic balloon dilatation of tracheobronchial stenosis: long-term follow-up. *Eur J Cardiothorac Surg* (2010) 38(2):198–202. doi: 10.1016/j.ejcts.2009.11.056

37. Tian Y, Liu N, Yin H, Duan L. Relationship between c-reactive protein/serum albumin ratio, neutrophil/lymphocyte ratio, and anca-associated vasculitis activity: a retrospective single center cohort study. *Front Med (Lausanne)* (2022) 9:855869. doi: 10.3389/fmed.2022.855869

38. Monach PA, Warner RL, Lew R, Tómasson G, Specks U, Stone JH, et al. Serum biomarkers of disease activity in longitudinal assessment of patients with anca-associated vasculitis. *ACR Open Rheumatol* (2022) 4(2):168–76. doi: 10.1002/acr2.11366

39. Sheski FD, Mathur PN. Long-term results of fiberoptic bronchoscopic balloon dilation in the management of benign tracheobronchial stenosis. *Chest* (1998) 114 (3):796–800. doi: 10.1378/chest.114.3.796

frontiers | Frontiers in Immunology

TYPE Original Research
PUBLISHED 24 August 2023
DOI 10.3389/fimmu.2023.1209282

OPEN ACCESS

EDITED BY
Francesca Wanda Rossi,
University of Naples Federico II, Italy

REVIEWED BY
Takemichi Fukasawa,
The University of Tokyo Hospital, Japan
Yongzhe Li,
Peking Union Medical College Hospital (CAMS), China

*CORRESPONDENCE
Zhenzhen Ma
mazhenzhendz@163.com
Qingrui Yang
qryang720@163.com

†These authors have contributed equally to this work and share first authorship

RECEIVED 20 April 2023
ACCEPTED 08 August 2023
PUBLISHED 24 August 2023

CITATION
Li M, Zhao X, Liu B, Zhao Y, Li X, Ma Z and Yang Q (2023) Predictors of rapidly progressive interstitial lung disease and prognosis in Chinese patients with anti-melanoma differentiation-associated gene 5-positive dermatomyositis. *Front. Immunol.* 14:1209282. doi: 10.3389/fimmu.2023.1209282

Predictors of rapidly progressive interstitial lung disease and prognosis in Chinese patients with anti-melanoma differentiation-associated gene 5-positive dermatomyositis

Meiqi Li[1†], Xuli Zhao[2†], Baocheng Liu[1], Yaqi Zhao[3], Xinya Li[1], Zhenzhen Ma[1,3*] and Qingrui Yang[1,3*]

[1]Department of Rheumatology and Immunology, Shandong Provincial Hospital Affiliated to Shandong First Medical University, Jinan, Shandong, China, [2]Department of Pain Medicine, Shandong Provincial Hospital Affiliated to Shandong First Medical University, Jinan, Shandong, China, [3]Department of Rheumatology and Immunology, Shandong Provincial Hospital, Cheeloo College of Medicine, Shandong University, Jinan, Shandong, China

Background: Rapidly progressive interstitial lung disease (RP-ILD) is the most serious complication of anti-melanoma differentiation-associated gene 5-positive dermatomyositis (anti-MDA5$^+$ DM). This study was performed to assess the prognostic factors of patients with anti-MDA5$^+$ DM and the clinical characteristics and predictors of anti-MDA5$^+$ DM in combination with RP-ILD.

Methods: In total, 73 MDA5$^+$ DM patients were enrolled in this study from March 2017 to December 2021. They were divided into survival and non-survival subgroups and non-RP-ILD and RP-ILD subgroups.

Results: The lactate dehydrogenase (LDH) concentration and prognostic nutritional index (PNI) were independent prognostic factors in patients with anti-MDA5$^+$ DM: the elevated LDH was associated with increased mortality (p = 0.01), whereas the elevated PNI was associated with reduced mortality (p < 0.001). The elevated LDH was independent risk prognostic factor for patients with anti-MDA5$^+$ DM (HR 2.42, 95% CI: 1.02–4.83, p = 0.039), and the elevated PNI was independent protective prognostic factor (HR, 0.27; 95% CI, 0.08 - 0.94; p = 0.039). Patients who had anti-MDA5$^+$ DM with RP-ILD had a significantly higher white blood cell count and LDH concentration than those without RP-ILD (p = 0.007 and p = 0.019, respectively). In contrast, PNI was significantly lower in patients with RP-ILD than those without RP-ILD (p < 0.001). The white blood cell count and elevated LDH were independent and significant risk factors for RP-ILD (OR 1.54, 95% CI: 1.12 - 2.13, p = 0.009 and OR 8.68, 95% CI: 1.28 - 58.83, p = 0.027, respectively), whereas the lymphocyte was an independent protective factor (OR, 0.11; 95% CI, 0.01 - 0.81; p = 0.03).

Conclusion: The elevated LDH and elevated PNI were independent prognostic factors for patients with anti-MDA5$^+$ DM. The elevated LDH was independent risk

factor for RP-ILD. Patients with anti-MDA5$^+$ DM could benefit from the measurement of LDH and PNI, which are inexpensive and simple parameters that could be used for diagnosis as well as prediction of the extent of lung involvement and prognosis.

KEYWORDS

dermatomyositis, anti-melanoma differentiation-associated protein 5 antibody, rapidly progressive interstitial lung disease, lactate dehydrogenase, prognosis

Introduction

Idiopathic inflammatory myopathy (IIM), also referred to as myositis, is a heterogeneous autoimmune disease with distinctive characteristics of chronic inflammation of the muscles, progressive muscle weakness, and increased muscle enzymes. Dermatomyositis (DM) is one of the most common clinical subtypes of IIM (1, 2). Anti-melanoma differentiation-associated gene 5-positive DM (anti-MDA5$^+$ DM) refers to a rare and unique subtype of IIM. The clinical features of anti-MDA5$^+$ DM usually include a characteristic DM rash, inflammatory muscle involvement, interstitial lung disease (ILD), and rapidly progressive ILD (RP-ILD) (3, 4). Numerous studies worldwide have revealed obvious regional and ethnic differences in the incidence of anti-MDA5$^+$ DM, and it is mainly distributed in East Asia, especially among the Japanese and Chinese populations (5).The incidence of anti-MDA5$^+$ DM ranges from 10% to 20% in Japan, from 17.6% to 22.6% in China, and from 7% to 13% in the United States (6–9). The cumulative 100-month survival rate of patients with anti-MDA5$^+$ DM is 66%, and fatal outcomes occur very frequently within the first 6 months of diagnosis (10).

ILD is the most common and severe pulmonary manifestation of IIM patients, and the incidence of ILD in patients with IIM ranges from 5% to 80% (11). Patients with anti-MDA5$^+$ DM are prone to the development of ILD with a probability of 50% to 100%. A previous cohort study showed that the 6-month mortality rate of patients with anti-MDA5$^+$ DM was relatively high, ranging from 33% to 66% (12). Our previous study confirmed that the simultaneous presence of anti-MDA5$^+$ and RP-ILD is a risk factor for a poor prognosis in patients with DM (13). Another study also showed that among patients with anti-MDA5$^+$ DM, the mortality rate was significantly higher among those with than without RP-ILD, most patients died within 6 months of developing symptoms, and the 6-month survival rate was only 41% (14). The primary cause of death was respiratory failure caused by RP-ILD (10). Despite aggressive treatment with immunosuppressants and corticosteroids, patients with concurrent anti-MDA5$^+$ DM and RP-ILD have a high 6-month mortality rate of 50% to 70% after the development of symptoms (15, 16). RP-ILD is an important subtype of anti-MDA5$^+$ DM with ILD, and its prevalence is higher in East Asian populations (4). It progresses rapidly and has no effective treatment, making it an important cause of death in patients with anti-MDA5$^+$ DM. Few studies to date have focused on the predictive effect of the clinical features of anti-MDA5$^+$ DM with RP-ILD. Therefore, the present study was performed to identify the serological markers for anti-MDA5$^+$ DM complicated with RP-ILD to assist in the achievement of a definitive diagnosis, accurate assessment of the patient's condition, and improvement of the prognosis for patients with anti-MDA5$^+$ DM.

Abbreviations: 95% CI, 95% confidence interval; ALT, alanine transaminase; AST, aspartate transaminase; CRP, c-reactive protein; DM, dermatomyositis; ESR, erythrocyte sedimentation rate; LDH, lactate dehydrogenase; MDA5, melanoma differentiation-associated gene 5; PNI, prognostic nutritional index; RO52, tri-partite motif-containing 21; RP-ILD, rapidly progressive interstitial lung disease; WBC, white blood cell.

Materials and methods

Patients

This study involved 73 patients with newly diagnosed anti-MDA5$^+$ DM who were admitted to our hospital from March 2017 to December 2021. The inclusion criteria were as follows (1). The diagnosis of DM was based on the international standards established by Bohan and Peter (17, 18). (2) Anti-MDA5 antibody was positive in patients with anti-MDA5$^+$ DM. (3) The diagnosis of ILD was based on the results of high-resolution computed tomography of the chest, appearing as ground-glass opacity, consolidation, grid, and pulmonary interstitial lesions such as honeycomb peribronchovascular thickening or traction bronchiectasis changes (19–21). (4) The diagnostic criteria for RP-ILD were met; namely, the imaging manifestations and lung symptoms had worsened within 3 months or the lung function had markedly worsened since the previous test (e.g., the forced vital capacity decreased by >10% and the partial arterial oxygen pressure decreased by >10 mmHg) (22). (5) Complete long-term survival data were available. The exclusion criteria were (1) ILD caused by drug, environment, or microbial infection; (2) recent diagnosis and treatment of new tumors; (3) recent development of chronic or acute infection, metabolic disease, or chronic liver and kidney disease; and (4) the presence of other autoimmune diseases. The patient selection process is shown in Figure 1. The research process strictly followed established ethical principles. All patients or guardians provided written informed consent.

10.3389/fimmu.2023.1209282

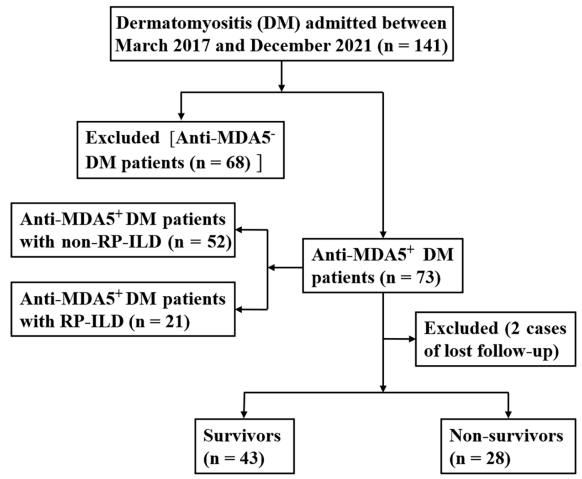

FIGURE 1
Study cohort.

Methods

The MDA5$^+$ DM patients were divided into a survival subgroup (n = 43) and non-survival subgroup (n = 28) as well as a non-RP-ILD subgroup (n = 52) and RP-ILD (n = 21) subgroup. The patients' clinical data, including age, sex, blood examination findings, and high-resolution computed tomography findings, were collected. The patients' survival status and time to death were provided by the hospital. The prognostic nutritional index (PNI) was calculated as follows: PNI = serum albumin (g/L) + 5 × absolute peripheral blood lymphocyte count ($\times 10^9$/L).

Statistical analysis

IBM SPSS version 25.0 (IBM Corp., Armonk, NY, USA) was used for data analysis. Continuous measurement data with a normal distribution are expressed as mean ± standard deviation, and the independent sample *t* test was used for comparison between groups. Data with a non-normal distribution are expressed as median (interquartile range), and the Mann–Whitney *U* test was used for comparison between groups. Count data are expressed as a percentage, and the x^2 test was used for comparison between groups. The risk factors for RP-ILD were analyzed by binary logistic regression. GraphPad Prism 9.0 (GraphPad Software, San Diego, CA, USA) was used to draw the receiver operating characteristic (ROC) curve for exploration of the sensitivity and specificity of the white blood cell (WBC) count and lactate dehydrogenase (LDH) concentration in predicting the occurrence of MDA5+ DM with RP-ILD and obtain the optimal critical values. In order to compare the predictive performance of LDH and PNI, ROC analysis was performed. We calculated alternative cut-off point by the Youden's index. The cut-off point was then converted into a dichotomous variable as the point of tangency. Finally, R statistical software 4.1.3 was used to analyze and compare the mortality of patients in the two groups. A *P* value of < 0.05 was considered statistically significant.

Results

Comparison of laboratory parameters between survivors and non-survivors in the anti-MDA5$^+$ DM group

All patients in the MDA5$^+$ DM group were followed up. They were then further divided into survivor and non-survivor subgroups based on the follow-up results. During the median follow-up period of 11.0 (2.0–20.0) months, approximately 58.90% patients survived (survival group, n = 43), 38.36% died (non-survival group, n = 28), and 2.74% were lost to follow-up. Thirteen of the 28 patients in the non-survival group had RP-ILD, and RP-ILD was correlated with mortality in patients with anti-MDA5$^+$ DM (p = 0.002). The LDH concentration was significantly higher in the non-survival group than in the survival group (p = 0.009), whereas the non-survival group had a lower albumin concentration (p = 0.001), lymphocyte count (p = 0.032), and PNI (p < 0.001) than survival group. Of the 73 patients with anti-MDA5$^+$ DM included in this study, all received glucocorticoid therapy. In the survival group, 35 (81.40%) patients received pulse steroid therapy, and in the non - survival group, all received pulse steroid therapy. Both in the survival and non - survival groups used calcineurin inhibitors, 58.14% and 71.43% in each. The remaining indicators were not significantly different between the two groups, as shown in Table 1.

Comparison between the PNI and clinical manifestations in patients with anti-MDA5$^+$ DM

Table 2 shows the correlation between clinical manifestations and PNI in patients with anti-MDA5$^+$ DM. PNI was negatively correlated with patients with anti-MDA5$^+$ DM with oedema (P = 0.014). PNI was negatively correlated with the occurrence of RP-ILD (P < 0.001), arthritis (P = 0.019) and Gottron rash (P = 0.028). However, there was no significant correlation between other clinical manifestations and PNI (Table 2).

Prognosis and Kaplan–Meier survival analysis of patients with anti-MDA5$^+$ DM

Based on the ROC curve, the critical value of the LDH concentration and PNI was 356.15 U/L and 34.1, respectively. The LDH concentration and PNI were then transformed into binary variables with 356.15 U/L and 34.1 as their tangent points, and the binary variables were subdivided into low and high subgroups. The results revealed 49 patients in the LDH < 356.15 U/L group and 22 patients in the LDH > 356.15 U/L group, with fatalities occurring in both groups [13 (27.7%) patients in the LDH < 356.15 U/L group and 15 (62.5%) patients in the LDH > 356.15 U/L group]. According to the Kaplan–Meier survival analysis, patients with anti-MDA5$^+$ DM who had a high LDH concentration had a lower survival rate (p = 0.01) (Figure 2A). In addition, the incidence of death within 1 to 5 years was significantly higher in the LDH > 356.15 U/L group than in

TABLE 1 Comparison of laboratory parameters between survivors and non-survivors in the anti-MDA5$^+$ DM group.

Parameter	Survivors	Non-survivors	*p*
Gender (male/female)	14/29	7/21	0.495
Age (years)	49.86 ± 9.86	51.32 ± 14.06	0.608
Course of disease (months)	6.00(3.00, 30.00)	2.00(1.00, 8.50)	0.002**
WBC (× 10^9/L)	4.83(3.58, 6.75)	5.93(3.91, 7.13)	0.223
Lymphocyte (× 10^9/L)	1.27(0.81, 1.83)	0.94(0.62, 1.24)	0.032*
ESR (mm/h)	32.00(17.75, 46.00)	33.00(25.50, 46.50)	0.367
CRP (mg/L)	2.30(1.07, 8.33)	4.79(2.43, 8.75)	0.178
AST (U/L)	47.00 (32.00, 70.54)	70.54(43.05, 80.50)	0.019*
ALT (U/L)	42.00(23.00, 59.00)	55.52(36.25,89.00)	0.050
Albumin (g/L)	33.05 ± 4.30	29.34 ± 4.80	0.001**
LDH (U/L)	323.54(232.61, 354.35)	359.56(302.22, 446.87)	0.009**
PNI	38.79 ± 4.87	33.85 ± 5.34	< 0.001***
Anti-RO52$^+$	28(66.70%)	24(88.90%)	0.074
RP-ILD	7(16.3%)	13(46.4%)	0.006**
Treatment of MDA5$^+$ DM (n, %)			
Glucocorticoids	43(100%)	28(100%)	
Pulse steroid therapy	35(81.40%)	28(100%)	
Calcineurin inhibitors	25(58.14%)	20(71.43%)	
Mycophenolate mofetil	4(9.30%)	0	

Values are presented as mean ± standard deviation (SD) or median and interquartile range (IQR), Mann-Whitney U test, inter-with t test and x^2 test were used. * $p < 0.05$; ** $p < 0.01$; *** $p < 0.001$.

the LDH < 356.15 U/L group, and the difference in patient mortality became more significant over time (Table 3). Similarly, after converting the PNI to a binary variable with a cutoff point of 34.1 into PNI < 34.1 and PNI > 34.1 groups, the Kaplan–Meier survival curves showed that survival was much higher in the PNI > 34.1 group than in the PNI < 34.1 group ($p < 0.001$) (Figure 2B). In addition to the LDH concentration and PNI being significantly associated with patient prognosis, the mortality rate increased along with the occurrence of RP-ILD ($p = 0.002$) (Figure 2C).

Mortality of patients with anti-MDA5$^+$ DM based on Cox regression analysis

Of the 73 patients with anti-MDA5$^+$DM, 20 died from exacerbation of ILD or infection during the follow-up period, 1 died from cardiovascular disease and the cause of death was unknown in 7 cases. A total of 19 patients (67.86%) died within 6 months of onset and 24 patients (85.71%) died within 1 year. To identify the independent prognostic factors, Cox proportional hazard regression analysis was applied to the clinical and laboratory data of patients with anti-MDA5$^+$ DM (Table 4). In deviation with MDA5$^+$ DM patients, the age and sex adjusted multivariate analyses showed that the elevated LDH (HR 2.42, 95% CI: 1.02–4.83, p = 0.039) was independent risk factors for the poor prognosis (Figure 3). Interestingly, the elevated PNI (HR, 0.27; 95% CI, 0.08 - 0.94; $p = 0.039$) was an independent protective factor for the prognosis (Figure 3).

Comparison of laboratory parameters between non-RP-ILD and RP-ILD groups

Patients with MDA5$^+$ DM were divided into RP-ILD and non-RP-ILD subgroups according to the presence or absence of RP-ILD. The non-RP-ILD group comprised 52 patients (15 men and 37 women) with a mean age of 51.94 ± 10.08 years, and the RP-ILD group comprised 21 patients (7 men and 14 women) with a mean age of 45.90 ± 14.61 years. The WBC count ($p = 0.007$), aspartate transaminase concentration ($p = 0.045$), alanine transaminase concentration ($p = 0.039$), and LDH concentration ($p = 0.019$) were significantly higher in the RP-ILD group than in the non-RP-ILD group, whereas the lymphocyte count ($p < 0.001$), albumin concentration ($p = 0.005$), and PNI ($p < 0.001$) were significantly lower in the RP-ILD group than in the non-RP-ILD group. Age, sex, and other laboratory data were not significantly different between the two groups ($p > 0.05$). Glucocorticoids were used in both non-RP-ILD and RP-ILD groups. In the non-RP-ILD group, 45(86.54%) patients received pulse steroid therapy, and in the RP-ILD group, 20 (95.24%) patients received pulse steroid therapy. Both groups used calcineurin inhibitors, 61.54% and 71.43% in each. Table 5 shows the additional parameters compared between the two groups.

10.3389/fimmu.2023.1209282

TABLE 2 Comparison between the PNI and clinical manifestations in patients with anti-MDA5$^+$ DM.

Clinical manifestations	*N (%)*		PNI	
			Mean ± SD	*p*
Oedema	No	43(60.56)	38.16 ± 5.60	0.014*
	Yes	28(39.44)	34.86 ± 5.05	
RP-ILD	No	50(70.42)	38.52 ± 5.03	< 0.001***
	Yes	21(29.58)	32.89 ± 4.90	
Myopathy	No	20(29.85)	39.02 ± 5.60	
	Yes	47(70.15)	36.17 ± 5.48	0.058
Fever	No	39(56.52)	37.92 ± 5.01	
	Yes	30(43.48)	34.86 ± 5.58	0.019*
Raynaud's phenomenon	No	61((88.41)	36.29 ± 5.33	
	Yes	8(11.59)	38.92 ± 6.14	0.201
Sunny rash	No	22(30.99)	36.36 ± 5.10	
	Yes	49(69.01)	37.08 ± 5.83	0.619
Heliotrope rash	No	58(81.69)	36.84 ± 5.27	
	Yes	13(18.31)	36.91 ± 7.10	0.968
Gottron rash	No	42(59.15)	38.06 ± 5.27	
	Yes	29(40.85)	35.11 ± 5.67	0.028*
Dry mouth and eyes	No	44(62.86)	36.20 ± 5.92	
	Yes	26(37.14)	38.14 ± 4.90	0.164
Mouth ulcers	No	58(81.69)	36.61 ± 5.75	
	Yes	13(18.31)	37.95 ± 4.86	0.437

Values are presented as mean ± standard deviation (SD), inter-with t test was used. * $p < 0.05$; *** $p < 0.001$.

ROC analysis

In the ROC analysis, the WBC count predicted RP-ILD with an area under the curve (AUC) of 0.703 (95% CI, 0.551–0.855; sensitivity, 61.9%; specificity, 90.4%; $p = 0.007$), and the cutoff value was 6.93×10^9/L. The LDH concentration predicted RP-ILD with an AUC of 0.677 (95% CI, 0.539–0.814; sensitivity, 52.4%; specificity, 82.7%; $p = 0.019$), and the cutoff value was 365.62 U/L. The AUC for the WBC count combined with the LDH concentration to predict RP-ILD was 0.772 (95% CI, 0.640–0.904; sensitivity, 66.7%; specificity, 92.3%; $p < 0.001$), which was higher than that of either the WBC count or LDH concentration alone for RP-ILD (Figure 4).

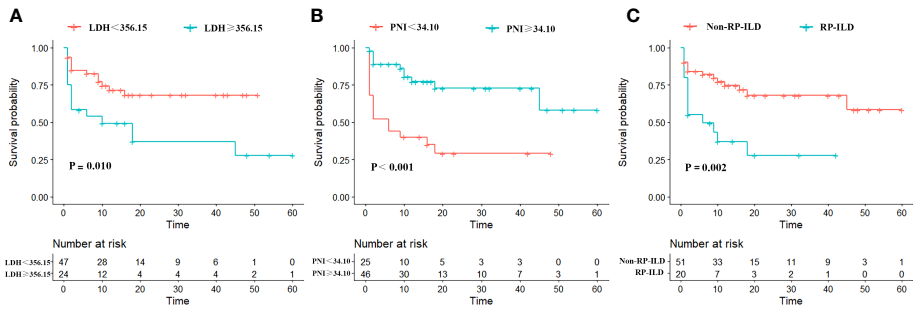

FIGURE 2
Kaplan–Meier survival curves for overall survival of patients with anti-MDA5$^+$ DM, stratified by **(A)** Low/high LDH; **(B)** Low/high PNI; **(C)** Non-RP-ILD/with RP-ILD.

TABLE 3 Mortality in high LDH group and low LDH group at 1, 3, and 5 years.

Parameter	N	1 year		3 years		5 years	
		N	%	N	%	N	%
LDH < 356.15 U/L	49	37	24.49	36	26.53	36	26.53
LDH ≥ 356.15 U/L	22	10	54.55	8	63.64	7	68.18
P		0.028*		0.005**		0.004**	

* p < 0.05; ** p < 0.01.

Binary logistic regression analysis

A logistic regression analysis was applied to identify independent risk factors for MDA5$^+$ DM combined with RP-ILD (Table 6). In deviation with MDA5$^+$ DM patients, the age and sex adjusted multivariate analyses showed that the WBC count (OR 1.54, 95% CI: 1.12 - 2.13, $p = 0.009$) and elevated LDH (OR 8.68, 95% CI: 1.28 - 58.83, $p = 0.027$) were independent risk factors for RP-ILD (Figure 5). Interestingly, the lymphocyte (OR, 0.11; 95% CI, 0.01 - 0.81; $p = 0.03$) was an independent protective factor for MDA5$^+$ DM combined with RP-ILD (Figure 5).

Discussion

In recent years, numerous studies have been conducted to identify markers that can predict the diagnosis and prognosis of secondary ILD with anti-MDA5$^+$ DM in the preclinical stage. However, no ideal results have been obtained. Evidence has shown that the LDH concentration and PNI are related to the diagnosis and prognosis of various inflammatory diseases. Gómez et al. (23) found that in patients with influenza A-associated pneumonia, the LDH concentration was higher in patients who did than did not require mechanical ventilation, suggesting that the LDH concentration is related to the severity of pneumonia. Liu et al. (24) confirmed that an increased LDH concentration was related to the increased mortality of patients with community-acquired pneumonia. Ding et al. (25) found that patients' preoperative LDH concentration was a predictive value for postoperative pneumonia, and the incidence of postoperative pneumonia was significantly higher in patients with a preoperative LDH concentration of >250 U/L. In addition, the serum LDH concentration is a commonly used inflammatory index in clinical

TABLE 4 Mortality of patients with anti-MDA5$^+$ DM based on Cox regression analysis.

Parameter	Univariable		Multivariable	
	HR (95% *CI*)	*p*	HR (95% *CI*)	*p*
Gender(male/female)	1.26(0.54 - 2.98)	0.592		
Age(years)	1.00(0.97 - 1.04)	0.714		
Course of disease (months)	0.99(0.97 - 1.01)	0.277		
WBC ($\times 10^9$/L)	1.07(0.95 - 1.20)	0.274		
Lymphocyte ($\times 10^9$/L)	0.44(0.19 - 0.99)	0.047*	1.36(0.52 - 3.60)	0.533
ESR (mm/h)	1.00(0.98 - 1.02)	0.770		
CRP (mg/L)	0.99(0.97 - 1.02)	0.583		
LDH > 356.15 U/L	2.49(1.18 - 5.26)	0.017*	2.42(1.05 - 5.60)	0.039*
AST (U/L)	1.002(1.000 - 1.005)	0.111	0.997(0.992 - 1.002)	0.189
ALT (U/L)	1.008(1.001 - 1.015)	0.022*	1.01(0.99 - 1.02)	0.143
Albumin (g/L)	0.87(0.80 - 0.95)	0.002**	0.95(0.83 - 1.08)	0.418
PNI > 34.10	0.23(0.10 - 0.51)	< 0.001***	0.27(0.08 - 0.94)	0.039*
Anti-RO52$^+$	2.30(0.80 - 6.65)	0.124		
Glucocorticoids	–	–		
Pulse steroid therapy	25.93(0.25 - 2708.96)	0.17		
Calcineurin inhibitors	1.44(0.61 - 3.40)	0.402		
Mycophenolate mofetil	0.45(0 - 62.41)	0.402		

Continuous variables were converted to dichotomous variables using the ROC-derived cutoffs. The value of LDH was dichotomized into high and low groups using a cut-off point of 356.15; The value of PNI was dichotomized into high and low groups using a cut-off point of 34.10. * p < 0.05; ** p < 0.01; *** p < 0.001.

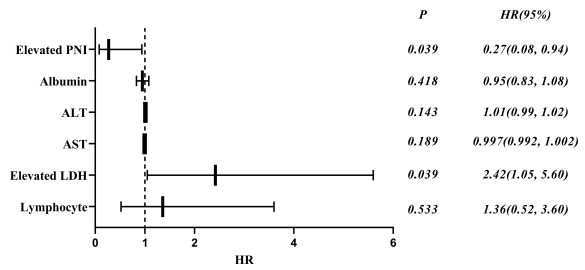

FIGURE 3
Forest plot of multivariate COX analysis of prognostic factors in patients with anti-MDA5$^+$ DM.

practice. Moreover, varying degrees of the systemic inflammatory response are associated with the active period of connective tissue disease; thus, the LDH concentration can also be used to evaluate the activity of such diseases (26). Previous studies have proven that the PNI is associated with CTD. Some researchers have proven that the PNI is associated with the disease activity of systemic lupus erythematosus (27, 28). According to some studies, a low PNI could increase the risk of rheumatoid arthritis complicated with severe infection (29), and also be used for the diagnosis and evaluation of adult-onset Still's disease (30). However, few studies have confirmed the relationship between the PNI, LDH concentration, and anti-MDA5$^+$ DM with RP-ILD. Therefore, the present study was performed as a preliminary investigation of this relationship.

LDH is a stable cytoplasmic enzyme that is present in all cells. Cell membrane permeability increases with cell damage or death, resulting in the release of LDH (31). Macrophages such as liver Kupffer cells can be activated, leading to the injury of liver and then the elevated levels of ALT and AST (3). In addition, in our study, AST not only predicted poor prognosis in MDA5 positive DM patients, but also predicted the occurrence of RP-ILD with predictive values of 58.35 U/L (sensitivity, 67.9%; specificity, 69.8%; 95% CI = 0.536 – 0.795; P = 0.019) and 71.27 U/L (sensitivity, 47.6%; specificity, 82.7%; 95% CI = 0.506 – 0.794; P = 0.046), respectively (Supplementary Figures 1, 2). Therefore, extracellular LDH may be used as an indicator of cell damage or death of various causes (32). In our study, the LDH concentration in patients who had anti-MDA5$^+$ DM with RP-ILD was higher than that in the control group. The LDH concentration was also found to predict RP-ILD, which is similar to the results reported by So (5) and Lian et al. (33). These findings suggest that the LDH concentration may be a predictive marker of the severity of ILD. In the present study, the alanine aminotransferase, aspartate aminotransferase, and LDH concentrations were significantly higher in patients with than without RP-ILD. The specific mechanism of LDH involvement in pulmonary fibrosis is still unknown, but studies have shown that LDH is a marker enzyme of macrophages, and its activity can be used as an indicator of macrophage activation (31). Recent studies have confirmed that activated macrophages were involved in the occurrence and

TABLE 5 Comparison of laboratory parameters between non-RP-ILD and RP-ILD groups.

Parameter	Non-RP-ILD	RP-ILD	*p*
Gender (male/female)	37/15	14/7	0.705
Age (years)	51.94 ± 10.08	45.90 ± 14.61	0.094
Course of disease (months)	6.00 (2.25, 24.00)	2.00 (1.00, 14.00)	0.029*
WBC (× 10^9/L)	4.86 (3.61, 6.33)	7.07 (3.92, 8.63)	0.007**
Lymphocyte (× 10^9/L)	1.27 (0.83, 1.74)	0.69 (0.52, 1.14)	< 0.001***
ESR (mm/h)	33.00 (20.75, 44.50)	28.00 (19.00, 46.00)	0.830
CRP (mg/L)	2.88 (1.09, 8.49)	4.74 (1.15, 9.60)	0.485
AST (U/L)	49.00 (33.25, 70.54)	70.54 (42.20, 103.00)	0.045*
ALT (U/L)	46.00 (23.50, 55.88)	55.52 (35.00, 97.00)	0.039*
Albumin (g/L)	32.56 ± 4.50	29.10 ± 4.79	0.005**
LDH (U/L)	323.47 (251.95, 360.49)	365.90 (311.74, 438.30)	0.019*
PNI	38.52 ± 5.03	32.89 ± 4.90	< 0.001***
Anti-RO52$^+$	37 (74.0%)	17 (81.0%)	0.454
Treatment of MDA5$^+$ DM (n, %)			
Glucocorticoids	52(100%)	21(100%)	
Pulse steroid therapy	45(86.54%)	20(95.24%)	
Calcineurin inhibitors	32(61.54%)	15(71.43%)	
Mycophenolate mofetil	4(7.69%)	0	
Immunoglobulin	11(21.15%)	3(14.29%)	

Values are presented as mean ± standard deviation (SD) or median and interquartile range (IQR), Mann-Whitney U test, inter-with t test and x^2 test were used. * $p < 0.05$; ** $p < 0.01$; *** $p < 0.001$.

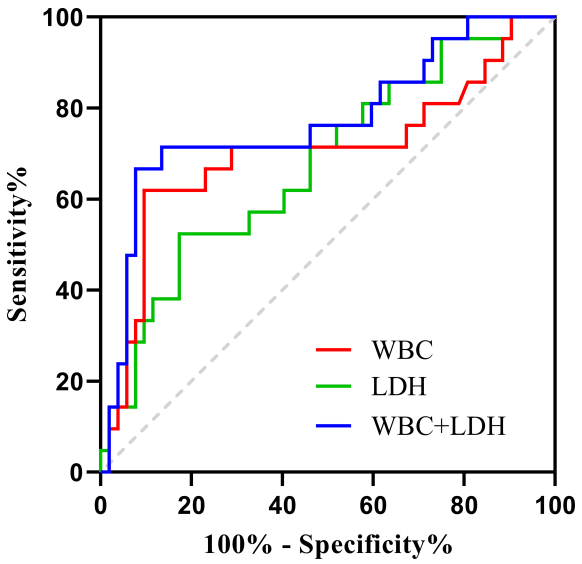

FIGURE 4
ROC curves for WBC count, LDH concentration, and WBC count combined with LDH concentration for predicting MDA5$^+$ DM combined with RP-ILD.

development of pulmonary fibrosis in various ways, such as by causing neutrophils activation and triggering the formation of neutrophil extracellular traps, which in turn contribute to the development of ILD in patients with IIM (34–36). Seto (36) found that anti-MDA5 promotes the formation of neutrophil extracellular traps, which induce epithelial cell injury and the release of inflammatory cytokines. It is also speculated that LDH may bind to macrophage receptors, activate macrophages, and

TABLE 6 Logistic regression analysis of risk factors for MDA5$^+$ DM combined with RP-ILD.

Parameter	Univariable		Multivariable	
	OR (95% *CI*)	*p*	OR (95% *CI*)	*p*
Gender(male/female)	0.81(0.27 - 2.41)	0.706		
Age(years)	0.96(0.91 - 1.00)	0.054		
Course of disease (months)	0.99(0.97 - 1.02)	0.739		
WBC ($\times 10^9$/L)	1.25(1.03 - 1.52)	0.023*	1.54(1.12 - 2.13)	0.009**
Lymphocyte ($\times 10^9$/L)	0.13(0.04 - 0.50)	0.003**	0.11(0.01 - 0.81)	0.03*
ESR (mm/h)	1.00(0.96 - 1.03)	0.800		
CRP (mg/L)	0.99(0.97 - 1.03)	0.872		
LDH > 356.15 U/L	5.26(1.72 - 16.07)	0.004**	8.68 (1.28 - 58.83)	0.027*
AST > 71.27 U/L	3.82(1.27 - 11.47)	0.017*	1.18(0.20 - 6.83)	0.853
ALT > 27.75 U/L	8.89(1.10 - 72.08)	0.041*	3.30(0.28 - 39.62)	0.346
Albumin > 30.9 g/L	0.22(0.07 - 0.66)	0.007**	2.03(0.16 - 25.90)	0.586
PNI > 34.10	0.09(0.03 - 0.29)	< 0.001***	0.20(0.02 - 2.38)	0.205
Anti - RO52$^+$	1.61(0.46 - 5.62)	0.457		
Glucocorticoids	–	–		
Pulse steroid therapy	3.11(0.36 - 26.99)	0.303		
Calcineurin inhibitors	1.56(0.52 - 4.69)	0.426		
Mycophenolate mofetil	–	–		

Continuous variables were converted to dichotomous variables using the ROC-derived cutoffs. The value of LDH, AST, ALT, albumin and PNI was dichotomized into high and low groups using a cut-off point of 356.15 U/L, 71.27 U/L, 27.75 U/L and 30.90g/L.
* $p < 0.05$; ** $p < 0.01$, ***$p<0.001$.

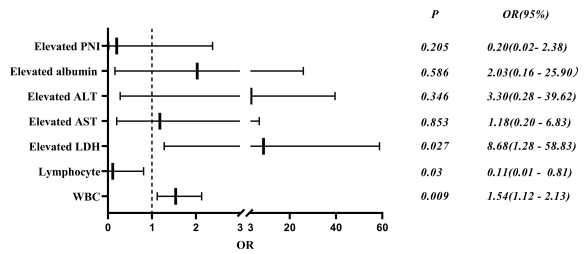

FIGURE 5
Risk factors of RP-ILD in patients with anti-MDA5$^+$ DM.

produce a variety of proinflammatory cytokines, including interleukins 2, 6, 8, and 12 and TNF-α. These inflammatory cytokines can stimulate the activation of neutrophils, leading to the exacerbation of pulmonary fibrosis (37, 38).

Serum LDH is a classic marker reflecting the progression of ILD (39). The concentration of LDH could indicate the disease activity and severity of idiopathic pulmonary fibrosis. Moreover, a high LDH concentration is always associated with severe pulmonary fibrosis and lung injury (40). In previous study, an LDH concentration of >300 U/L was an independent predictor of RP-ILD (5). In the present study, however, the cutoff value of LDH for prediction of RP-ILD was 365.62 U/L, and LDH was an independent predictor of RP-ILD. Factors such as the sample size and analysis methods may be the reasons for this difference. Therefore, more studies are needed to further determine the optimal LDH threshold for predicting RP-ILD in patients with anti-MDA5$^+$ DM. Furthermore, the WBC count in the RP-ILD group was significantly higher than that in the non-RP-ILD group, and it had a predictive effect on RP-ILD. Infection has been considered one of the causes of acute exacerbation of idiopathic pulmonary fibrosis, and it is also a nonspecific inflammatory marker of infection (41). Our study showed that the combination of the LDH concentration and WBC count had a better predictive effect on RP-ILD than either the LDH concentration or WBC count alone.

The mortality rate of patients with anti-MDA5$^+$ DM in our study (39.4%) was similar to that of Japanese patients (36%–41%) but higher than that of European patients (27.3%) (42). The incidence of RP-ILD is high in patients with anti-MDA5$^+$ DM, and RP-ILD is always associated with a lower survival rate (43). Chen et al. (9) reported that 78.9% of patients with anti-MDA5$^+$ DM developed RP-ILD. And another study showed that 85.7% of patients with MDA5$^+$ DM died of RP-ILD (44). Among patients with anti-MDA5$^+$ DM, the survival rate was significantly lower in those with RP-ILD than without RP-ILD, and their risk of death was increased by 9.7 times (5). The survival rate of patients with RP-ILD in our study was significantly lower than that of patients without RP-ILD, and RP-ILD was the most important predictor of an adverse prognosis (P = 0.002),this is similar to the results reported by Li (45). Moreover, patients with anti-MDA5$^+$ had the highest mortality rate (85.71%) within the first year of onset, so early and effective treatment is essential for patients with concurrent RP-ILD and anti-MDA5$^+$. Previous studies have shown that the LDH concentration is an indicator of a poor prognosis for patients with anti-MDA5$^+$ DM (46), and the present study showed that the LDH concentration in the non-survival group was significantly higher than that in the survival group. LDH was an independent prognostic indicator in patients with anti-MDA5$^+$ DM, consistent with the study by Niu et al. (12). In our study, we found an association between the LDH concentration and RP-ILD, indicating that a high LDH concentration could contribute to increased mortality in patients with anti-MDA5$^+$ DM.

PNI was initially proposed by Onodera et al. (47) and used to predict the postoperative prognosis of gastric cancer. In addition to the prognosis of gastric cancer, the PNI is also associated with short-term postoperative complications and long-term adverse prognoses of lymphoma, lung malignant tumor, colorectal cancer, and cardiovascular disease (48–51). In our study, PNI in the survival group was significantly higher than that in the non-survival group, and it was associated with a good prognosis of patients. Additionally, PNI in the RP-ILD group was significantly lower than that in the non-RP-ILD group. Wang et al. (52) reported that the serum albumin level and total peripheral blood lymphocyte count were closely related to the inflammatory response. Studies have shown that RNA helicase encoded by MDA5 is involved in the innate immune defense mechanism during viral infection; thus, it is considered that viral infection may play an important role in the pathogenesis of anti-MDA5$^+$ DM with RP-ILD, leading to the consumption of peripheral blood lymphocytes (53). In addition, studies have shown that among patients with anti-MDA5$^+$ DM, the peripheral CD4$^+$ and CD8$^+$ T-cell counts in those with RP-ILD are significantly lower than in those with chronic ILD, indicating that lymphocytes play an important role in the disease progression (54). Moreover, previous researchers have speculated that the activation of inflammation also lead to a decrease in the lymphocyte count, and the decreased peripheral blood lymphocyte count may be caused by migration of these cells to the lung to participate in the local immune response (55). Advanced malnutrition may lead to deficiencies of essential vitamins and amino acids, which will further inhibit cellular or humoral immunity; this will in turn lead to significant reductions in the number and function of B cells and T cells, resulting in a decrease in the lymphocyte count (56). More studies are needed to elucidate the precise role of lymphocytes in anti-MDA5$^+$ DM patients.

Albumin can inhibit endothelial cell apoptosis, prevent the generation of oxygen radicals, and reduce platelet aggregation; thus, it is a potential protective factor for human health (57). When systemic inflammation occurs, numerous inflammatory cytokines could be produced, which may inhibit the synthesis of albumin in the liver and thus reduce the albumin content; moreover, inflammation can also promote catabolism of albumin. Therefore, the exacerbation of MDA5$^+$ DM-associated ILD may be related to a decrease in albumin, weakening of albumin protection, and activation of fibroblasts (28, 58). PNI is a comprehensive indicator of the body's immune function and nutritional status. As one of its significant advantages, it is readily available and can be efficiently calculated from routinely measured serum albumin and lymphocytes. In this study, the PNI had a more significant clinical

effect in evaluating the prognosis of anti-MDA5$^+$ DM than did either the lymphocyte count or albumin concentration alone.

In this study, the detection rate of anti-Ro52 antibody in patients who had anti-MDA5$^+$ DM was 75%, but the antibody level was not related to the prognosis. The predictive value of anti-Ro52 antibody combined with anti-MDA5 on RP-ILD and the prognosis of patients with DM require further confirmation by clinic studies. The prognosis of anti-MDA5$^+$ DM with RP-ILD is not ideal, and most deaths occur in the first 6 months (59). Therefore, for patients with anti-MDA5$^+$, treatment should be started before the development of respiratory symptoms or lung function damage. Immunosuppressive therapy should be administered in a timely manner, especially when serum markers such as LDH are elevated (39). These measures many help to significantly improve the survival of patients (60).

This study had several limitations. First, this was a retrospective study in which incomplete data collection may have led to systematic errors. Second, the sample size of this study was relatively small; future prospective, multicenter, population-based cohort studies with larger samples are needed. Third, all patients in this study were Chinese Han population, and the predictive effect on other races needs to be further validated. Fourth, although we confirmed the LDH cutoff values for prediction of RP-ILD, further studies are needed to demonstrate the dynamics of the LDH concentration during the progression of RP-ILD.

Conclusion

The LDH and PNI were independent prognostic factors in patients with MDA5$^+$ DM, with LDH being associated with increased mortality and PNI with decreased mortality. This study also showed that among patients with MDA5$^+$ DM, the WBC count and LDH concentration were significantly higher in RP-ILD patients than without RP-ILD. The WBC count and LDH concentration were independent and important risk factors for RP-ILD, and they also had some predictive value; Patients with MDA5$^+$ DM can benefit from measurement of the LDH concentration and PNI, which are inexpensive and simple parameters that can be used for diagnosis as well as prediction of the extent of lung involvement and prognosis.

Data availability statement

The original contributions presented in the study are included in the article/Supplementary Materials, further inquiries can be directed to the corresponding author/s.

Ethics statement

The studies involving humans were approved by Ethics Committee of Shandong Provincial Hospital, Shandong First Medical University. The studies were conducted in accordance with the local legislation and institutional requirements. The participants provided their written informed consent to participate in this study. Written informed consent was obtained from the individual(s) for the publication of any potentially identifiable images or data included in this article.

Author contributions

ML conducted the data collection and completed the data analysis, interpretation and writing of the manuscript. XZ conducted the data collection and completed the data analysis. BL and YZ and XL conducted the data collection. ZM and QY conceived the research plan and participated in the revision of the final manuscript. All authors were involved in reading and reviewing the manuscript. All authors contributed to the article and approved the submitted version.

Funding

This work was supported by the National Natural Science Foundation of China (Youth fund project, Grant NO.82201994) and the Natural Science Foundation of Shandong Province (General Program, Grant NO. ZR2022MH016 and Youth fund project, Grant NO. ZR2021QH043).

Conflict of interest

The authors declare that the research was conducted in the absence of any commercial or financial relationships that could be construed as a potential conflict of interest.

Publisher's note

Supplementary material

The Supplementary Material for this article can be found online at: https://www.frontiersin.org/articles/10.3389/fimmu.2023.1209282/full#supplementary-material

SUPPLEMENTARY FIGURE 1
ROC curves for AST count for predicting the poor prognosis of MDA5$^+$ DM.

SUPPLEMENTARY FIGURE 2
ROC curves for AST count for predicting MDA5$^+$ DM combined with RP-ILD.

References

1. Lundberg IE, Fujimoto M, Vencovsky J, Aggarwal R, Holmqvist M, Christopher-Stine L, et al. Idiopathic inflammatory myopathies. *Nat Rev Dis Primers* (2021) 7(1):86. doi: 10.1038/s41572-021-00321-x

2. Gono T, Masui K, Nishina N, Kawaguchi Y, Kawakami A, Ikeda K, et al. Risk prediction modeling based on a combination of initial serum biomarker levels in polymyositis/dermatomyositis-associated interstitial lung disease. *Arthritis Rheumatol* (2021) 73(4):677–86. doi: 10.1002/art.41566

3. Zhu D, Qiao J, Tang S, Pan Y, Li S, Yang C, et al. Elevated carcinoembryonic antigen predicts rapidly progressive interstitial lung disease in clinically amyopathic dermatomyositis. *Rheumatol (Oxford)* (2021) 60(8):3896–903. doi: 10.1093/rheumatology/keaa819

4. Xu L, You H, Wang L, Lv C, Yuan F, Li J, et al. Identification of three different phenotypes in anti-MDA5 antibody-positive dermatomyositis patients: implications for rapidly progressive interstitial lung disease prediction. *Arthritis Rheumatol* (2022) 75(4):609–619. doi: 10.1002/art.42308

5. So J, So H, Wong VT, Ho R, Wu TY, Wong PC, et al. Predictors of rapidly progressive interstitial lung disease and mortality in patients with autoantibodies against melanoma differentiation-associated protein 5 dermatomyositis. *Rheumatol (Oxford)* (2022) 61(11):4437–44. doi: 10.1093/rheumatology/keac094

6. Fiorentino D, Chung L, Zwerner J, Rosen A, Casciola-Rosen L. The mucocutaneous and systemic phenotype of dermatomyositis patients with antibodies to MDA5 (CADM-140): a retrospective study. *J Am Acad Dermatol* (2011) 65(1):25–34. doi: 10.1016/j.jaad.2010.09.016

7. Sato S, Kuwana M, Fujita T, Suzuki Y. Anti-CADM-140/MDA5 autoantibody titer correlates with disease activity and predicts disease outcome in patients with dermatomyositis and rapidly progressive interstitial lung disease. *Mod Rheumatol* (2013) 23(3):496–502. doi: 10.1007/s10165-012-0663-4

8. Hall JC, Casciola-Rosen L, Samedy LA, Werner J, Owoyemi K, Danoff SK, et al. Anti-melanoma differentiation-associated protein 5-associated dermatomyositis: expanding the clinical spectrum. *Arthritis Care Res (Hoboken)* (2013) 65(8):1307–15. doi: 10.1002/acr.21992

9. Chen F, Wang D, Shu X, Nakashima R, Wang G. Anti-MDA5 antibody is associated with A/SIP and decreased T cells in peripheral blood and predicts poor prognosis of ILD in Chinese patients with dermatomyositis. *Rheumatol Int* (2012) 32(12):3909–15. doi: 10.1007/s00296-011-2323-y

10. Gono T, Sato S, Kawaguchi Y, Kuwana M, Hanaoka M, Katsumata Y, et al. Anti-MDA5 antibody, ferritin and IL-18 are useful for the evaluation of response to treatment in interstitial lung disease with anti-MDA5 antibody-positive dermatomyositis. *Rheumatol (Oxford)* (2012) 51(9):1563–70. doi: 10.1093/rheumatology/kes102

11. Kiely PD, Chua F. Interstitial lung disease in inflammatory myopathies: clinical phenotypes and prognosis. *Curr Rheumatol Rep* (2013) 15(9):359. doi: 10.1007/s11926-013-0359-6

12. Niu Q, Zhao LQ, Ma WL, Xiong L, Wang XR, He XL, et al. A new predictive model for the prognosis of MDA5(+) DM-ILD. *Front Med (Lausanne)* (2022) 9:908365. doi: 10.3389/fmed.2022.908365

13. Li M, Yan S, Dong R, Xiang W, Ma Z, Yang Q. Elevated platelet-to-lymphocyte ratio and neutrophil-to-lymphocyte ratio in patients with polymyositis/dermatomyositis: a retrospective study. *Clin Rheumatol* (2023) 42(6):1615–1624. doi: 10.1007/s10067-023-06542-7

14. Ye S, Chen XX, Lu XY, Wu MF, Deng Y, Huang WQ, et al. Adult clinically amyopathic dermatomyositis with rapid progressive interstitial lung disease: a retrospective cohort study. *Clin Rheumatol* (2007) 26(10):1647–54. doi: 10.1007/s10067-007-0562-9

15. Li T, Guo L, Chen Z, Gu L, Sun F, Tan X, et al. Pirfenidone in patients with rapidly progressive interstitial lung disease associated with clinically amyopathic dermatomyositis. *Sci Rep* (2016) 6:33226. doi: 10.1038/srep33226

16. Romero-Bueno F, Diaz Del Campo P, Trallero-Araguás E, Ruiz-Rodríguez JC, Castellvi I, Rodriguez-Nieto MJ, et al. Recommendations for the treatment of anti-melanoma differentiation-associated gene 5-positive dermatomyositis-associated rapidly progressive interstitial lung disease. *Semin Arthritis Rheum* (2020) 50(4):776–90. doi: 10.1016/j.semarthrit.2020.03.007

17. Bohan A, Peter JB. Polymyositis and dermatomyositis (first of two parts). *N Engl J Med* (1975) 292(7):344–7. doi: 10.1056/nejm197502132920706

18. Bohan A, Peter JB. Polymyositis and dermatomyositis (second of two parts). *N Engl J Med* (1975) 292(8):403–7. doi: 10.1056/nejm197502202920807

19. Uslu AU, Küçük A, Şahin A, Ugan Y, Yılmaz R, Güngör T, et al. Two new inflammatory markers associated with Disease Activity Score-28 in patients with rheumatoid arthritis: neutrophil-lymphocyte ratio and platelet-lymphocyte ratio. *Int J Rheum Dis* (2015) 18(7):731–5. doi: 10.1111/1756-185x.12582

20. Alexandrakis MG, Passam FH, Moschandrea IA, Christophoridou AV, Pappa CA, Coulocheri SA, et al. Levels of serum cytokines and acute phase proteins in patients with essential and cancer-related thrombocytosis. *Am J Clin Oncol* (2003) 26(2):135–40. doi: 10.1097/00000421-200304000-00007

21. Ohsugi Y. Recent advances in immunopathophysiology of interleukin-6: an innovative therapeutic drug, tocilizumab (recombinant humanized anti-human interleukin-6 receptor antibody), unveils the mysterious etiology of immune-mediated inflammatory diseases. *Biol Pharm Bull* (2007) 30(11):2001–6. doi: 10.1248/bpb.30.2001

22. Travis WD, Costabel U, Hansell DM, King TE Jr., Lynch DA, Nicholson AG, et al. An official American Thoracic Society/European Respiratory Society statement: Update of the international multidisciplinary classification of the idiopathic interstitial pneumonias. *Am J Respir Crit Care Med* (2013) 188(6):733–48. doi: 10.1164/rccm.201308-1483ST

23. Gómez-Gómez A, Magaña-Aquino M, Bernal-Silva S, Araujo-Meléndez J, Comas-García A, Alonso-Zúñiga E, et al. Risk factors for severe influenza A-related pneumonia in adult cohort, Mexico, 2013-14. *Emerg Infect Dis* (2014) 20(9):1554–8. doi: 10.3201/eid2009.140115

24. Liu JL, Xu F, Zhou H, Wu XJ, Shi LX, Lu RQ, et al. Expanded CURB-65: a new score system predicts severity of community-acquired pneumonia with superior efficiency. *Sci Rep* (2016) 6:22911. doi: 10.1038/srep22911

25. Ding CY, Peng L, Lin YX, Yu LH, Wang DL, Kang DZ. Elevated lactate dehydrogenase level predicts postoperative pneumonia in patients with aneurysmal subarachnoid hemorrhage. *World Neurosurg* (2019) 129:e821–e30. doi: 10.1016/j.wneu.2019.06.041

26. Gudmann NS, Hirata S, Karsdal MA, Kubo S, Bay-Jensen AC, Tanaka Y. Increased remodelling of interstitial collagens and basement membrane is suppressed by treatment in patients with rheumatoid arthritis: serological evaluation of a one-year prospective study of 149 Japanese patients. *Clin Exp Rheumatol* (2018) 36(3):462–70.

27. Correa-Rodríguez M, Pocovi-Gerardino G, Callejas-Rubio JL, Fernández RR, Martín-Amada M, Cruz-Caparros MG, et al. The prognostic nutritional index and nutritional risk index are associated with disease activity in patients with systemic lupus erythematosus. *Nutrients* (2019) 11(3):638. doi: 10.3390/nu11030638

28. Ahn SS, Jung SM, Song JJ, Park YB, Lee SW. Prognostic nutritional index is correlated with disease activity in patients with systemic lupus erythematosus. *Lupus* (2018) 27(10):1697–705. doi: 10.1177/0961203318787058

29. Isoda K, Tsuji S, Harada Y, Yoshimura M, Nakabayashi A, Sato M, et al. Potential of the prognostic nutritional index to determine the risk factor for severe infection in elderly patients with rheumatoid arthritis. *Mod Rheumatol* (2023) 33(1):88–95. doi: 10.1093/mr/roac001

30. Kim JW, Jung JY, Suh CH, Kim HA. Systemic immune-inflammation index combined with ferritin can serve as a reliable assessment score for adult-onset Still's disease. *Clin Rheumatol* (2021) 40(2):661–8. doi: 10.1007/s10067-020-05266-2

31. Xu X, Huang Q, Mao Y, Cui Z, Li Y, Huang Y, et al. Immunomodulatory effects of Bacillus subtilis (natto) B4 spores on murine macrophages. *Microbiol Immunol* (2012) 56(12):817–24. doi: 10.1111/j.1348-0421.2012.00508.x

32. Drent M, Cobben NA, Henderson RF, Wouters EF, van Dieijen-Visser M. Usefulness of lactate dehydrogenase and its isoenzymes as indicators of lung damage or inflammation. *Eur Respir J* (1996) 9(8):1736–42. doi: 10.1183/09031936.96.09081736

33. Lian X, Zou J, Guo Q, Chen S, Lu L, Wang R, et al. Mortality risk prediction in amyopathic dermatomyositis associated with interstitial lung disease: The FLAIR model. *Chest* (2020) 158(4):1535–45. doi: 10.1016/j.chest.2020.04.057

34. Khawaja AA, Chong DLW, Sahota J, Mikolasch TA, Pericleous C, Ripoll VM, et al. Identification of a novel HIF-1α-α(M)β(2) integrin-NET axis in fibrotic interstitial lung disease. *Front Immunol* (2020) 11:2190. doi: 10.3389/fimmu.2020.02190

35. Zhang S, Jia X, Zhang Q, Zhang L, Yang J, Hu C, et al. Neutrophil extracellular traps activate lung fibroblast to induce polymyositis-related interstitial lung diseases via TLR9-miR-7-Smad2 pathway. *J Cell Mol Med* (2020) 24(2):1658–69. doi: 10.1111/jcmm.14858

36. Seto N, Torres-Ruiz JJ, Carmona-Rivera C, Pinal-Fernandez I, Pak K, Purmalek MM, et al. Neutrophil dysregulation is pathogenic in idiopathic inflammatory myopathies. *JCI Insight* (2020) 5(3):134189. doi: 10.1172/jci.insight.134189

37. Sontheimer RD. Would a new name hasten the acceptance of amyopathic dermatomyositis (dermatomyositis siné myositis) as a distinctive subset within the idiopathic inflammatory dermatomyopathies spectrum of clinical illness? *J Am Acad Dermatol* (2002) 46(4):626–36. doi: 10.1067/mjd.2002.120621

38. Kawasumi H, Gono T, Kawaguchi Y, Kaneko H, Katsumata Y, Hanaoka M, et al. IL-6, IL-8, and IL-10 are associated with hyperferritinemia in rapidly progressive interstitial lung disease with polymyositis/dermatomyositis. *BioMed Res Int* (2014) 2014:815245. doi: 10.1155/2014/815245

39. Liu T, Li W, Zhang Z, Jiang T, Fei Y, Huang J, et al. Neutrophil-to-lymphocyte ratio is a predictive marker for anti-MDA5 positive dermatomyositis. *BMC Pulm Med* (2022) 22(1):316. doi: 10.1186/s12890-022-02106-8

40. van Krugten M, Cobben NA, Lamers RJ, van Dieijen-Visser MP, Wagenaar SS, Wouters EF, et al. Serum LDH: a marker of disease activity and its response to therapy in idiopathic pulmonary fibrosis. *Neth J Med* (1996) 48(6):220–3. doi: 10.1016/0300-2977(95)00074-7

41. Cao M, Sheng J, Qiu X, Wang D, Wang D, Wang Y, et al. Acute exacerbations of fibrosing interstitial lung disease associated with connective tissue diseases: a population-based study. *BMC Pulm Med* (2019) 19(1):215. doi: 10.1186/s12890-019-0960-1

42. Allenbach Y, Uzunhan Y, Toquet S, Leroux G, Gallay L, Marquet A, et al. Different phenotypes in dermatomyositis associated with anti-MDA5 antibody: Study of 121 cases. *Neurology* (2020) 95(1):e70–e8. doi: 10.1212/wnl.0000000000009727

43. Debray MP, Borie R, Revel MP, Naccache JM, Khalil A, Toper C, et al. Interstitial lung disease in anti-synthetase syndrome: initial and follow-up CT findings. *Eur J Radiol* (2015) 84(3):516–23. doi: 10.1016/j.ejrad.2014.11.026

44. Chen Z, Cao M, Plana MN, Liang J, Cai H, Kuwana M, et al. Utility of anti-melanoma differentiation-associated gene 5 antibody measurement in identifying patients with dermatomyositis and a high risk for developing rapidly progressive interstitial lung disease: a review of the literature and a meta-analysis. *Arthritis Care Res (Hoboken)* (2013) 65(8):1316–24. doi: 10.1002/acr.21985

45. Li Y, Li Y, Wu J, Miao M, Gao X, Cai W, et al. Predictors of poor outcome of anti-MDA5-associated rapidly progressive interstitial lung disease in a Chinese cohort with dermatomyositis. *J Immunol Res* (2020) 2020:2024869. doi: 10.1155/2020/2024869

46. Yoshifuji H. Biomarkers and autoantibodies of interstitial lung disease with idiopathic inflammatory myopathies. *Clin Med Insights Circ Respir Pulm Med* (2015) 9 (Suppl 1):141–6. doi: 10.4137/ccrpm.S36748

47. Onodera T, Goseki N, Kosaki G. [Prognostic nutritional index in gastrointestinal surgery of malnourished cancer patients]. *Nihon Geka Gakkai Zasshi* (1984) 85(9):1001–5.

48. Luan C, Wang F, Wei N, Chen B. Prognostic nutritional index and the prognosis of diffuse large b-cell lymphoma: a meta-analysis. *Cancer Cell Int* (2020) 20:455. doi: 10.1186/s12935-020-01535-x

49. Wang Z, Wang Y, Zhang X, Zhang T. Pretreatment prognostic nutritional index as a prognostic factor in lung cancer: Review and meta-analysis. *Clin Chim Acta* (2018) 486:303–10. doi: 10.1016/j.cca.2018.08.030

50. Wang Z, Zhao L, He S. Prognostic nutritional index and the risk of mortality in patients with hypertrophic cardiomyopathy. *Int J Cardiol* (2021) 331:152–7. doi: 10.1016/j.ijcard.2021.01.023

51. Song A, Eo W, Lee S. Comparison of selected inflammation-based prognostic markers in relapsed or refractory metastatic colorectal cancer patients. *World J Gastroenterol* (2015) 21(43):12410–20. doi: 10.3748/wjg.v21.i43.12410

52. Wang DS, Luo HY, Qiu MZ, Wang ZQ, Zhang DS, Wang FH, et al. Comparison of the prognostic values of various inflammation based factors in patients with pancreatic cancer. *Med Oncol* (2012) 29(5):3092–100. doi: 10.1007/s12032-012-0226-8

53. Sato S, Hoshino K, Satoh T, Fujita T, Kawakami Y, Fujita T, et al. RNA helicase encoded by melanoma differentiation-associated gene 5 is a major autoantigen in patients with clinically amyopathic dermatomyositis: Association with rapidly progressive interstitial lung disease. *Arthritis Rheum* (2009) 60(7):2193–200. doi: 10.1002/art.24621

54. Zuo Y, Ye L, Chen F, Shen Y, Lu X, Wang G, et al. Different multivariable risk factors for rapid progressive interstitial lung disease in anti-MDA5 positive dermatomyositis and anti-synthetase syndrome. *Front Immunol* (2022) 13:845988. doi: 10.3389/fimmu.2022.845988

55. Huang W, Ren F, Luo L, Zhou J, Huang D, Pan Z, et al. The characteristics of lymphocytes in patients positive for anti-MDA5 antibodies in interstitial lung disease. *Rheumatol (Oxford)* (2020) 59(12):3886–91. doi: 10.1093/rheumatology/keaa266

56. Shirakabe A, Hata N, Kobayashi N, Okazaki H, Matsushita M, Shibata Y, et al. The prognostic impact of malnutrition in patients with severely decompensated acute heart failure, as assessed using the Prognostic Nutritional Index (PNI) and Controlling Nutritional Status (CONUT) score. *Heart Vessels* (2018) 33(2):134–44. doi: 10.1007/s00380-017-1034-z

57. Don BR, Kaysen G. Serum albumin: relationship to inflammation and nutrition. *Semin Dial* (2004) 17(6):432–7. doi: 10.1111/j.0894-0959.2004.17603.x

58. Bai Z, Shen G, Dong L. Analysis of risk factors of interstitial lung disease and mortality rates in Chinese patients with idiopathic inflammatory myopathy. *Int J Rheum Dis* (2021) 24(6):815–27. doi: 10.1111/1756-185x.14128

59. Xu A, Ye Y, Fu Q, Lian X, Chen S, Guo Q, et al. Prognostic values of anti-Ro52 antibodies in anti-MDA5-positive clinically amyopathic dermatomyositis associated with interstitial lung disease. *Rheumatol (Oxford)* (2021) 60(7):3343–51. doi: 10.1093/rheumatology/keaa786

60. Matsuda KM, Yoshizaki A, Kuzumi A, Fukasawa T, Ebata S, Yoshizaki-Ogawa A, et al. Combined immunosuppressive therapy provides favorable prognosis and increased risk of cytomegalovirus reactivation in anti-melanoma differentiation-associated gene 5 antibody-positive dermatomyositis. *J Dermatol* (2020) 47(5):483–9. doi: 10.1111/1346-8138.15274

frontiers | Frontiers in Immunology

TYPE Original Research
PUBLISHED 27 November 2023
DOI 10.3389/fimmu.2023.1237209

OPEN ACCESS

EDITED BY
Francesca Wanda Rossi,
University of Naples Federico II, Italy

REVIEWED BY
Yasuhiro Shimojima,
Shinshu University, Japan
Pravin Hissaria,
Royal Adelaide Hospital, Australia

*CORRESPONDENCE
Zhankui Wang
wzksdzhy@163.com
Yanfeng Hou
yfhou1016@163.com

RECEIVED 09 June 2023
ACCEPTED 13 November 2023
PUBLISHED 27 November 2023

CITATION
Ji Q, Pan W, Zhang D, Hou Y and Wang Z (2023) Comparison of characteristics and anti-MDA5 antibody distribution and effect between clinically amyopathic dermatomyositis and classic dermatomyositis: a retrospective case-control study.
Front. Immunol. 14:1237209.
doi: 10.3389/fimmu.2023.1237209

Comparison of characteristics and anti-MDA5 antibody distribution and effect between clinically amyopathic dermatomyositis and classic dermatomyositis: a retrospective case-control study

Qiang Ji[1,2,3], Wenping Pan[1,2], Di Zhang[4], Yanfeng Hou[1,2]* and Zhankui Wang[1,2,4]*

[1]Department of Rheumatology and Autoimmunology, The First Affiliated Hospital of Shandong First Medical University, Shandong Provincial Qianfoshan Hospital, Shandong Key Laboratory of Rheumatic Disease and Translational Medicine, Jinan, Shandong, China, [2]Shandong medicine and Health Key Laboratory of Rheumatism, Jinan, Shandong, China, [3]First Clinical Medical College, Shandong University of Traditional Chinese Medicine, Jinan, Shandong, China, [4]Affiliated Hospital of Shandong University of Traditional Chinese Medicine, Jinan, Shandong, China

Background: Clinically amyopathic dermatomyositis (CADM) is a distinct subtype of dermatomyositis (DM) characterized by typical DM cutaneous findings but with minimal or no evidence of myositis. It possesses unique features different from classic DM (CDM). Anti-melanoma differentiation-associated gene 5 (MDA5) antibodies were found in CADM and are thought to increase the risk of rapidly progressive interstitial lung disease (RP-ILD) and are present in both CADM and CDM patients, affecting their condition and prognosis. Nevertheless, no large-sample studies have compared all aspects concerning patients with CADM and those with CDM. This study aimed to investigate differences in clinical characteristics and risk factors for mortality between CADM and CDM and to clarify the distribution and impact of anti-MDA5 antibodies in patients with these conditions.

Methods: A retrospective case-control study included 330 patients and collected and analyzed their clinical data from The First Affiliated Hospital of Shandong First Medical University and Shandong Provincial Hospital of Traditional Chinese Medicine between January 2015 and July 2022; all patients were followed up to evaluate changes in their condition and prognosis. Several new cohorts were designed around anti-MDA5 antibodies to explore their distribution and impact in CADM and CDM.

Results: We found CADM to be associated with higher rates of mortality, 1-year mortality, interstitial lung disease (ILD), and RP-ILD than CDM. In CADM, RP-ILD, anti-MDA5 antibodies, and high ferritin and lactate dehydrogenase (LDH) levels were identified as independent risk factors for death. In CDM, the neutrophil-to-lymphocyte ratio, anti-MDA5 antibodies, and high ferritin levels were shown to be independent risk factors for death, whereas mechanic's hand was considered a

protective factor against it. Anti-MDA5 antibody-positive patients did not exhibit any significant difference based on whether they belonged to the CADM or CDM groups. When no anti-MDA5 antibody-positive patients participated, the ferritin levels and rates of RP-ILD and ILD were still higher in CADM than in CDM; however, such differences decreased, whereas the LDH levels, rates of mortality, and 1-year mortality did not differ. Anti-MDA5 antibody-positive patients consistently showed higher LDH and ferritin levels, lower lymphocyte levels, higher probability of RP-ILD and ILD, and worse prognosis than anti-MDA5 antibody-negative patients, irrespective of whether the patients had DM, CADM, or CDM.

Conclusion: Patients with CADM exhibit relatively worse symptoms, serological findings, and prognosis than those with CDM. Furthermore, patients with CADM and those with CDM have commonalities and differences in risk factors for death. Moreover, CADM may necessitate earlier and more aggressive treatment strategies than CDM. Anti-MDA5 antibodies occur at a high level in patients with CADM, not only affecting the symptoms and prognosis of DM but also having a non-negligible impact on the differences between CADM and CDM. Hence, screening for anti-MDA5 antibodies in patients with CADM and CDM is extremely essential.

KEYWORDS

clinically amyopathic dermatomyositis, classic dermatomyositis, anti-MDA5 antibodies, rapidly progressive interstitial lung disease, risk factors for death

1 Introduction

Idiopathic inflammatory myopathy is a heterogeneous group of diseases characterized by inflammation affecting the skeletal muscles and extramuscular organs, particularly the skin and lungs (1, 2). The most common clinical subtypes of idiopathic inflammatory myopathy in adults are polymyositis and dermatomyositis (DM) (3, 4). First proposed by Euwer and Sontheimer as a subcategory of idiopathic inflammatory myopathy (5), amyopathic dermatomyositis is characterized by the hallmark cutaneous manifestations of DM and the absence of any clinical or laboratory evidence of muscle disease for ≥6 months (6). Clinically amyopathic dermatomyositis (CADM) can be divided into amyopathic DM and hypomyopathic DM (7). Hypomyopathic DM is defined as the presence of cutaneous lesions consistent with DM and in the absence of overt muscle weakness despite laboratory, electrophysiological, and radiologic evidence of muscle disease. Although, the absence of clinically evident muscle diseases in CADM may differentiate it from classic dermatomyositis (CDM), distinguishing the cutaneous manifestations of ADM from those of CDM has not been possible to date.

Dermatomyositis damages not only the skin and muscles but also other organs. Interstitial lung disease (ILD), malignancy, and myocardial involvement are its relatively common extramuscular findings. Of them, ILD is considered a common severe complication, with a reported prevalence of 5–65% (8, 9). The disease course and severity of ILD are highly heterogeneous (10), wherein some patients with mild ILD respond markedly to treatment without exacerbation, whereas others are at a risk of developing rapidly progressive ILD (RP-ILD), which is often insensitive to treatment and has a poor prognosis (11, 12).

Myositis-specific antibodies are present in 50–70% of all DM patients and are associated with distinct clinical features (13). Moreover, Incorporating them into myositis diagnostic algorithms could better define the clinical phenotype, prognosis, and treatment response of patient subgroups. Anti-melanoma differentiation-associated gene 5 (MDA5) antibodies were originally identified in patients with CADM who had predominantly prolonged skin lesions without accompanying muscle weakness and were at risk of progressing to acute RP-ILD (14). Previous reports have indicated that, depending on the cohort (14–22), 23–100% of anti-MDA5 antibody-positive patients develop CADM and have shown that anti-MDA5 antibody-associated ILD rapidly progresses and has a poor prognosis (23).

Several recent studies on DM have focused on the characteristics and poor prognosis of patients with anti-MDA5 antibodies in the CADM cohort. Nonetheless, since CADM was first defined, no large-sample studies have compared all aspects of patients with CADM and those with CDM. Bowerman et al. (24) conducted a retrospective cohort study involving 201 patients with adult-onset DM. However, their main research focus was on the prevalence of tumors in patients with ADM and CDM and on the factors affecting these tumors. The clinical manifestations, serological manifestations, specific autoantibody types, prognosis,

and distribution of patients with anti-MDA5 antibody-associated DM differ between CADM and CDM. Accordingly, the present retrospective study collected and analyzed the clinical data of inpatients with CADM and those with CDM from The First Affiliated Hospital of Shandong First Medical University and Shandong Provincial Hospital of Traditional Chinese Medicine between January 2015 and July 2022. All patients were followed up to evaluate changes in their condition and prognosis. Several new cohorts were designed around anti-MDA5 antibodies to explore the distribution and impact of anti-MDA5 antibodies in patients with CADM and CDM and to clarify differences in clinical, treatment-related, and prognostic features between patients with CADM and those with CDM. As far as we know, this is the only cohort study that includes more than 300 patients for comparison between CADM and CDM.

2 Materials and methods

2.1 Study participants

The study participants were patients diagnosed with DM at The First Affiliated Hospital of Shandong First Medical University and Shandong Provincial Hospital of Traditional Chinese Medicine (The hospitals are located at No. 16766 Jingshi Road and No. 42 Wenhua West Road, Lixia District, Jinan City, Shandong Province, China) between January 2015 and July 2022. Patients whose main condition treated or investigated during hospitalization was not DM were excluded from the analysis. This study was conducted in accordance with the principles embodied in the Declaration of Helsinki and was approved by the Human Research Ethics Boards of The First Affiliated Hospital of Shandong First Medical University (approval no.: YXLL-KY-2020-025) and Shandong Provincial Hospital of Traditional Chinese Medicine (approval no.: 2021-027-KY). Informed consent was obtained from all donors prior to their inclusion in the study, and all patient data were anonymized.

2.2 Data collection

Clinical data collected included demographics, clinical characteristics, and laboratory results. In our cohorts, lymphocyte subset analyses were conducted on 270 patients on their first visit. Although some patients had not previously received glucocorticoid therapy, numerous ones received this therapy at other hospitals for a short period, which might have fluctuated the predictive accuracy of the lymphocyte subsets. The levels of tumor markers, including carcinoembryonic antigen (CEA), alpha-fetoprotein, carbohydrate antigen (CA) 19-9, CA125, CA153, CA724, CA50, and CA242, neuron-specific enolase (NSE), CYFRA21, and squamous cell carcinoma antigen of the 270 patients were measured. Out of 330 patients, 74 underwent pulmonary function tests. We recorded the results of the pulmonary function tests, including the forced vital capacity, forced expiratory volume in 1 s, and diffusing capacity of the lungs for carbon monoxide. Myositis autoantibody and all routine tests were performed on all the patients in our cohorts during their first visit. Serum antinuclear antibody profiles and myositis-specific antibodies were detected by a third-party testing company (EUROIMMUN Medical Laboratory Diagnostics Stock Company, China) according to the manufacturer's instructions (Euroimmun, Germany). The tested antigens were Mi-2α, Mi-2β, TIF1γ, MDA5, NXP2, SAE1, Ku, PM-Scl100, PMScl75, Jo-1, SRP, PL-7, PL-12, EJ, OJ, Ro-52, cN-1A, Ha, Ks and ZO. The cut-offs values for the results were 0–5 (negative), 6-10 (borderline), 11–25 (+) and 26-50 (++), strong positive (+++). Because both the anti-Mi-2α and Mi-2β antigens target two closely related isoforms of the same protein, they were considered together as anti-Mi-2. In this study antibody positivity was defined by a blot intensity of ≥25. We excluded the weakly positive specific autoantibodies in patients who had multiple positive autoantibodies. Moreover, the values for these antibodies might change during follow-up, wherein a patients with double positive antibody values might show single positive values on later testing. Additionally, the neutrophil-to-lymphocyte ratio (NLR) and platelet-to-lymphocyte ratio (PLR) were determined. In our cohorts, the follow-up start point was the patient's first visit, and the follow-up end point was April 30, 2023 or the time patient's death.

2.3 Diagnostic criteria

We diagnosed DM according to the Bohan and Peter criteria and based on the 239th European Neuromuscular Centre international workshop guidelines (25, 26). We categorized ILD into RP-ILD or chronic ILD according to its clinical manifestations. Additionally, RP-ILD was defined as the presence of two or more of the following within 3 months: (i) exacerbation of dyspnea; (ii) an increase in parenchymal abnormalities on high-resolution computed tomography; and (iii) either a decrease of >10% in vital capacity or a decrease of >1.33 kPa in arterial oxygen tension (PaO_2). Chronic ILD was defined as a slowly of the progressive ILD exhibiting gradual deterioration over 3 months (27).

2.4 Cohort design

The cohorts were established based on the anti-MDA5 antibodies to clarify differences in clinical, treatment-related, and prognostic features between patients with CADM and those with CDM along with investigating the distribution and impact of anti-MDA5 antibody-associated DM in patients with CADM and those with CDM. The DM cohort was established to elucidate the differences between patients with CADM (CADM group) and those with CDM (CDM group). The DM-MDA5 cohort was established to evaluate the differences between anti-MDA5 antibody-positive patients (MDA5+ group) and anti-MDA5 antibody-negative patients (MDA5– group). The CADM cohort was established to explore the differences between patients with anti-MDA5 antibody-positive CADM (CADM-MDA5+ group) and those with anti-MDA5 antibody-negative CADM (CADM-MDA5– group). The CDM cohort was established to elucidate the

differences between anti-MDA5 antibody-positive patients with CDM (CDM-MDA5+ group) and anti-MDA5 antibody-negative patients with CDM (CDM-MDA5− group). The DM-MDA5+ cohort was established to assess the differences between anti-MDA5 antibody-positive patients with CADM (CADM-MDA5+ group) and anti-MDA5 antibody-positive patients with CDM (CDM-MDA5+ group). The DM-MDA5- cohort was established to examine the differences between anti-MDA5 antibody-negative patients with CADM (CADM-MDA5− group) and anti-MDA5 antibody-negative patients with CDM (CDM-MDA5− group).

2.5 Statistical analysis

Qualitative data are presented as numbers and percentages, whereas quantitative data are expressed as means and standard deviations or as medians and interquartile ranges, depending on the skewness of data. Regarding group comparisons of various data types, we used the χ^2 test to examine categorical data, while the two-sample *t*-test or Mann–Whitney *U* test was used to analyze continuous data. We determined the optimal cut-off value for death by receiver operating characteristic curve analysis and transformed each continuous parameter into a categorical variable. We built multivariable Cox proportional hazards models to identify the independent prognostic risk factors and to calculate their hazard ratios (HRs), 95% confidence intervals (CIs), and β regression coefficients. The independent risk factors for death in CADM and CDM were evaluated using backward stepwise selection with Cox regression. As for time-event analysis, the cumulative survival rates during the follow-up were calculated using the Kaplan–Meier method, and the different groups were compared using the log-rank test. Statistical significance was set at a two-tailed *P*-value of <0.05. All statistical analyses were performed using SPSS software version 26 (IBM Corp., Armonk, NY, USA).

3 Results

3.1 Clinical characteristics of all patients

The demographic data, clinical manifestations, and laboratory test results of the 330 enrolled patients with DM at the time of diagnosis are summarized in Table 1. The mean patient age at the time of diagnosis was 54.40 ± 12.02 years (range: 15–81 years), and the median duration of symptoms prior to diagnosis was 3 months. Of the enrolled patients, 230 (69.7%) were women. Furthermore, 135 (40.9%) and 195 (59.1%) out of 330 patients had CADM and CDM, respectively. Overall, 243 (73.6%) patients developed ILD, whereas 29 (8.8%) exhibited an RP pattern. The most common skin lesions were Gottron's sign and heliotrope rash, and a malignancy was detected in 25 (7.6%) patients. Myositis autoantibody tests were performed on 313 (94.8%) patients at their first admission, and 265 (84.7%) patients tested positive (including 69 [26.0%] with anti-MDA5 antibodies). All patients received glucocorticoid therapy; however, 31 (9.4%) received pulse-dose therapy. Additionally, 231 (70.0%) were treated with immunosuppressants such as cyclosporine A, tacrolimus, cyclophosphamide, azathioprine, methotrexate, and mycophenolate mofetil. Among the patients, 57 (17.3%) were found to have died owing to exacerbations of ILD or infection at follow-up, whereas 44 (13.3%) died within 1 year. The mortality and 1-year mortality rates were 44.9% and 40.6%, respectively, in anti-MDA5 antibody-positive patients.

3.2 Comparison of clinical characteristics between patients with CADM and those with CDM

We compared the clinical characteristics of the two groups of patients, and the comparison results are shown in Table 1. Patients with CADM had higher rates of death (25.9% vs. 11.3%, *P*=0.001), 1-year mortality (20.0% vs. 8.7%, *P*=0.003), ILD (89.6% vs. 62.6%, *P*<0.001), RP-ILD (17.0% vs. 3.1%, *P*<0.001), cough or dyspnea (85.2% vs. 57.4%, *P*<0.001), Gottron's sign (77.8% vs. 65.6%, *P*=0.026), cardiac involvement (29.6% vs. 16.4%, *P*=0.004), pleural effusion (17.8% vs. 8.7%, *P*=0.014), hoarseness (14.8% vs. 4.1%, *P*=0.001), and numbness in the extremities (10.4% vs. 3.1%, *P*=0.006) than patients with CDM. Furthermore, patients with CADM exhibited lower rates of the V sign (28.9% vs. 40.0%, *P*=0.038), shawl sign (13.3% vs. 23.6%, *P*=0.021), and dysphagia (3.7% vs. 14.4%, *P*=0.002) than patients with CDM. The two groups showed similar rates for clinical symptoms such as mechanic's hand, heliotrope rash, V sign, Holster sign, arthritis/arthralgia, Raynaud's phenomenon, gastroesophageal reflux, dry eyes, dry mouth, pleural effusion, pericardial effusion, fatigue, and tumors.

With respect to serological indices, the lymphocyte levels in the CADM group were significantly lower than those in the CDM group (0.81 vs. 1.38 $\times10^9$/L, *P*<0.001). The NLR (7.14 vs. 3.46, *P*<0.001), PLR (265.79 vs. 172.06, *P*<0.001), and neutrophil (6.30 vs. 5.19$\times10^9$/L, *P*=0.012), lactate dehydrogenase (LDH) (307.00 vs. 275.80 U/L, *P*=0.004), ferritin (361.30 vs. 239.03 ng/mL, *P*<0.001), and C-reactive protein (CRP) levels (8.45 vs. 4.10 mg/L, *P*=0.002) in the CADM group were significantly higher than those in the CDM group.

In our cohorts, lymphocyte subset analyses were conducted on a total of 270 patients at their first visit (Supplementary Table 1). The CD3+ (502.00 vs. 882.65 cells/mm^3, *P*<0.001), CD3+CD4+ (324.48 vs. 670.45 cells/mm^3, *P*<0.001), CD3+CD8+ (162.69 vs. 229.60 cells/mm^3, *P*=0.048), and CD16+CD56+ (89.00 vs. 125.30 cells/mm^3, *P*=0.002) cell counts in the CADM group were significantly lower than those in the CDM group. Tumor marker levels were also measured in these 270 patients (Supplementary Table 2). the serum CEA (3.30 vs. 2.06 ng/mL, *P*<0.001), CA724 (2.43 vs. 1.82 U/mL, *P*=0.015), NSE (17.11 vs. 13.02 ng/mL, *P*<0.001), CYFRA21 (4.82 vs. 3.18 ng/mL, *P*<0.001), and CA242 (6.50 vs. 4.10 U/mL, *P*=0.024) levels in the CADM group were significantly higher than those in the CDM group. The differences in lymphocyte subsets and tumor marker levels between the CADM and CDM groups are shown in Figure 1.

The distribution of myositis-specific autoantibodies in patients with CADM and those with CDM is shown in Table 2. Patients with CDM had higher levels of negative myositis-specific autoantibodies (20.9% vs. 7.6%, *P*=0.001) and anti-NXP2 antibodies

10.3389/fimmu.2023.1237209

TABLE 1 Clinical differences between clinically amyopathic dermatomyositis and classic dermatomyositis.

	DM cohort (*N*=330)	CADM (*N*=135)	CDM (*N*=195)	*P*-value
Age at diagnosis, mean ± SD, years	54.40 ± 12.02	55.05 ± 11.82	53.94 ± 12.16	0.411
Disease duration at diagnosis, median (IQR), months	3.00 (1.00, 7.00)	3.00 (2.00, 7.00)	3.00 (1.00, 7.00)	0.543
Male/female	100/230 (1:2.30)	45/90 (1:2.00)	55/140 (1:2.55)	0.319
Death, *n* (%)	57 (17.3)	35 (25.9)	22 (11.3)	0.001
Died within 1 year, *n* (%)	44 (13.3)	27 (20.0)	17 (8.7)	0.003
RP-ILD, *n* (%)	29 (8.8)	23 (17.0)	6 (3.1)	<0.001
ILD, *n* (%)	243 (73.6)	121 (89.6)	122 (62.6)	<0.001
Fever, *n* (%)	101 (30.6)	41 (30.4)	60 (30.8)	0.938
Cough or dyspnea, *n* (%)	227 (68.8)	115 (85.2)	112 (57.4)	<0.001
Mechanic's hand, *n* (%)	104 (31.5)	37 (27.4)	67 (34.4)	0.181
Heliotrope rash, *n* (%)	143 (43.3)	55 (40.7)	88 (45.1)	0.429
Gottron's sign, *n* (%)	233 (70.6)	105 (77.8)	128 (65.6)	0.017
V sign, *n* (%)	117 (35.5)	39 (28.9)	78 (40.0)	0.038
Shawl sign, *n* (%)	64 (19.4)	18 (13.3)	46 (23.6)	0.021
Holster sign, *n* (%)	38 (11.5)	13 (9.6)	25 (12.8)	0.372
Arthritis/arthralgia, *n* (%)	137 (41.5)	49 (36.3)	88 (45.1)	0.109
Raynaud's phenomenon, *n* (%)	34 (10.3)	14 (10.4)	20 (10.3)	0.973
Dysphagia, *n* (%)	33 (10.0)	5 (3.7)	28 (14.4)	0.002
Gastroesophageal reflux, *n* (%)	15 (4.5)	6 (4.4)	9 (4.6)	0.942
Dry eyes, *n* (%)	25 (7.6)	11 (8.1)	14 (7.2)	0.744
Dry mouth, *n* (%)	56 (17.0)	27 (20.0)	29 (14.9)	0.222
Cardiac involvement, *n* (%)	72 (21.8)	40 (29.6)	32 (16.4)	0.004
Pleural effusion, *n* (%)	41 (12.4)	24 (17.8)	17 (8.7)	0.014
Pericardial effusion, *n* (%)	32 (9.7)	16 (11.9)	16 (8.2)	0.271
Fatigue, *n* (%)	98 (29.7)	39 (28.9)	59 (30.3)	0.789
Hoarseness, *n* (%)	28 (8.5)	20 (14.8)	8 (4.1)	0.001
Tumor, *n* (%)	25 (7.6)	9 (6.7)	16 (8.2)	0.604
Numbness in the extremities	20 (6.1)	14 (10.4)	6 (3.1)	0.006
Anti-MDA5 antibodies, *n* (%)	69 (21.1)	49 (37.4)	20 (11.0)	<0.001
LYM, median (IQR), $\times10^9$/L	1.12 (0.72, 1.57)	0.81 (0.61, 1.10)	1.38 (1.00, 1.91)	<0.001
WBC count, median (IQR), $\times10^9$/L	7.56 (5.57, 10.25)	7.64 (5.74, 10.55)	6.98 (4.94, 10.39)	0.373
NEUT, median (IQR), $\times10^9$/L	5.45 (3.8, 7.95)	6.30 (4.32, 8.39)	5.19 (3.30, 8.06)	0.012
NLR, median (IQR)	4.48 (2.84, 8.33)	7.14 (4.40, 12.05)	3.46 (2.42, 5.65)	<0.001
PLT, median (IQR), $\times10^9$/L	226.50 (177.00, 293.25)	227.00 (165.25, 297.75)	236.00 (186.25, 289.75)	0.711
PLR, median (IQR)	199.52 (132.99, 304.62)	265.79 (205.63, 379.25)	172.06 (115.59,276.07)	<0.001
LDH, median (IQR), U/L	284.50 (207.75, 393.00)	307.00 (221.25, 429.50)	275.80 (208.75, 364.00)	0.004
α-HBDH, median (IQR), U/L	206.00 (142.75, 301.50)	199.50 (154.25, 283.50)	243.00 (170.25, 350.00)	0.677
Serum ferritin, median (IQR), ng/mL	258.00 (134.55, 620.75)	361.30 (159.30, 885.82)	239.03 (123.10, 550.80)	<0.001

(Continued)

TABLE 1 Continued

	DM cohort (*N*=330)	CADM (*N*=135)	CDM (*N*=195)	*P*-value
CRP, median (IQR), mg/L	6.20 (3.19, 20.60)	8.45 (3.30, 27.00)	4.10 (3.12, 14.08)	0.002
ESR, median (IQR), mm/h	24.00 (14.00, 44.25)	26.5 (16.00, 43.25)	23 (14.00, 41.50)	0.111
Procalcitonin, median (IQR), mg/L	0.05 (0.04, 0.13)	0.05 (0.04, 0.12)	0.05 (0.04, 0.08)	0.268
D-dimer, median (IQR), mg/L	0.60 (0.29, 1.29)	0.56 (0.30, 1.26)	0.69 (0.28, 1.31)	0.582
LYM ≤785×10^6/L, *n* (%)	102 (30.9)	67 (49.6)	35 (17.9)	<0.001
NLR ≥6.83, *n* (%)	110 (33.3)	72 (53.3)	38 (19.5)	<0.001
LDH ≥354.50 U/L, *n* (%)	112 (33.9)	58 (4.3)	54 (27.7)	0.004
Serum ferritin ≥649.95 ng/mL, *n* (%)	78 (23.6)	48 (35.6)	30 (15.4)	<0.001

ILD, interstitial lung disease; RP-ILD, rapidly progressive interstitial lung disease; LYM, lymphocyte; WBC, white blood cell; NEUT, neutrophil; NLR, NEUT-to-LYM ratio; PLT, platelet; PLR, PLT-to-LYM ratio; LDH, lactate dehydrogenase; α-HBDH, α-hydroxybutyrate dehydrogenase; CRP, C-reactive protein; ESR, erythrocyte sedimentation rate; IQR, interquartile range; CADM, clinically amyopathic dermatomyositis; CDM, classic dermatomyositis.

(7.7% vs. 1.5%, *P*=0.029) than those with CADM. However, the CADM group exhibited higher levels of anti-MDA5 antibodies (37.4% vs. 11.0%, *P*<0.001) than the CDM group.

Out of 330 patients, 74 underwent pulmonary function tests. The forced vital capacity, forced expiratory volume in 1 s, and diffusing capacity of the lungs for carbon monoxide were lower in the CADM group than those in the CDM group, albeit without statistically significant differences. Nevertheless, because some patients with dyspnea were unable to undergo pulmonary function tests, we believe that the recorded pulmonary function test results were not representative of the true level in patients with DM. A comparison of pulmonary function test results for each cohort is presented in Supplementary Table 3.

3.3 Risk factors independently associated with prognosis in patients with CADM and those with CDM

We determined the optimal cut-off value for death by receiver operating characteristic curve analysis and transformed each continuous parameter into a categorical variable. The optimal cut-off points for NLR, LDH, ferritin, and lymphocytes were 6.83 (area under the curve [AUC], 0.861; sensitivity, 88.7%; specificity, 78.0%), 354.50 U/L (AUC, 0.907; sensitivity, 94.7%; specificity, 78.4%), 649.95 ng/mL (AUC, 0.898; sensitivity, 78.9%; specificity, 87.5%), and 785.00×10^6/L (AUC, 0.853; sensitivity, 77.2%; specificity, 80.2%), respectively (Figure 2).

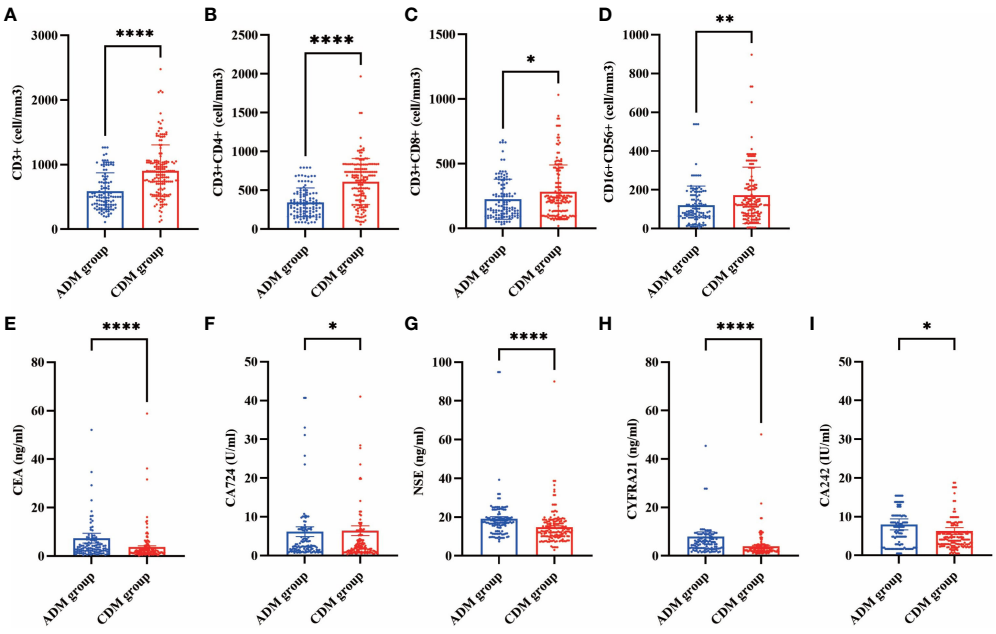

FIGURE 1
Differences in lymphocyte subsets (**A**, CD3+ **B**, CD3+CD4+ **C**, CD3+CD8+ **D**, CD16+CD56+) and tumor markers (**E**, CEA **F**, CA724 **G**, NSE **H**, CYFRA21 **I**, CA242) levels between the CADM and CDM groups. (*, P≤ 0.05 **, P≤ 0.01 ****, P≤ 0.0001).

10.3389/fimmu.2023.1237209

TABLE 2 Comparison of myositis-specific autoantibodies between clinically amyopathic dermatomyositis (CADM) and classic dermatomyositis (CDM).

Myositis-specific autoantibodies	CADM group (*N*=131)	CDM group (*N*=182)	*P*-value
Negative	10 (7.6%)	38 (20.9%)	0.001
Anti-JO-1	21 (16.0%)	45 (24.7%)	0.063
Anti-PL-7	14 (10.7%)	10 (5.5%)	0.089
Anti-PL-12	9 (6.9%)	3 (1.6%)	0.038
Anti-HA	1 (0.8%)	0 (0%)	0.419
Anti-EJ	10 (7.6%)	14 (7.7%)	0.985
Anti-OJ	1 (0.8%)	0 (0%)	0.419
Anti-Mi-2	3 (2.3%)	10 (5.5%)	0.265
Anti-MDA5	49 (37.4%)	20 (11.0%)	<0.001
Anti-NXP2	2 (1.5%)	14 (7.7%)	0.029
Anti-TIF-1γ	8 (6.1%)	22 (12.1%)	0.076
Anti-SAE1	3 (2.3%)	2 (1.1%)	0.710
Anti-SPR	0 (0%)	4 (2.2%)	0.143

The independent risk factors for death in CADM and CDM were evaluated using backward stepwise selection with Cox regression. Multivariate Cox analysis revealed that RP-ILD (HR, 1.938; 95% CI, 0.934–4.020; *P*=0.076), anti-MDA5 antibodies (HR, 2.247; 95% CI, 1.077–4.688; *P*=0.031), ferritin levels ≥649.95 ng/mL (HR, 3.324; 95% CI, 1.253–8.817; *P*=0.016), and LDH levels ≥354.5 U/L (HR, 4.963; 95% CI, 1.311–18.78; *P*=0.018) were independent risk factors for death in CADM (Figure 3), whereas NLR ≥6.83 (HR, 7.807; 95% CI, 2.431–25.074; *P*=0.001), anti-MDA5 antibodies (HR, 3.223; 95% CI, 1.167–8.899; *P*=0.024), and ferritin levels ≥649.95 ng/mL (HR, 13.357; 95% CI, 3.957–45.086; *P*<0.001) were independent risk factors for death in CDM. Notably, mechanic's hand was considered a protective factor against death in CDM (HR, 0.212; 95% CI, 0.049–0.928; *P*=0.039) (Figure 4).

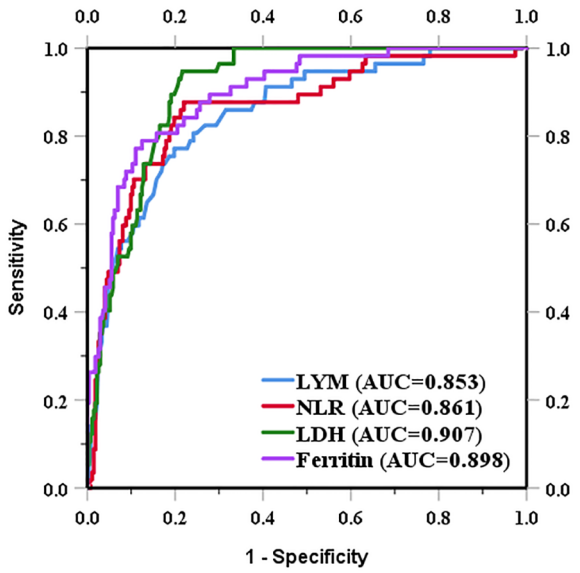

FIGURE 2
Prognostic value of the NLR and the levels of LDH, ferritin, and lymphocytes in DM.

3.4 Clinical treatment and treatment response

The responses to clinical therapy and treatment in the 330 patients are detailed in Table 3. During treatment, intravenous immunoglobulin (IVIG) was administered to 27.9% of patients, whereas biological agents were used in 6.1% of patients. Patients with CADM had significantly lower rates of only using oral corticosteroid (3.7% vs. 14.9%, *P*=0.001) and higher rates of cyclosporine A use (16.3% vs. 6.2%, *P*=0.003), corticosteroid (IV and/or oral) + cyclosporine A or tacrolimus + cyclophosphamide use (16.3% vs. 8.2%, *P*=0.024), corticosteroid pulse-dose therapy (15.6% vs. 5.2%, *P*=0.001), IVIG use (40.7% vs. 19.0%, *P*<0.001), and biological agent use (9.6% vs. 3.6%, *P*=0.024) than patients with CDM. With respect to ILD's response to treatment, patients with CADM showed a higher rate of worsening (44.3% vs. 24.4%, *P*=0.001) and a lower rate of improvement (13.9% vs. 35.6%, *P*<0.001) than patients with CDM.

3.5 Impact of anti-MDA5 antibodies on CADM and CDM

The positivity rates for anti-MDA5 antibodies in patients with CADM and those with CDM were 37.4% and 11.0%, respectively. Clinical characteristics and serological indices were compared between patients with CADM and those with CDM who tested positive for anti-MDA5 antibodies to explore the differences in anti-MDA5 antibodies between CADM and CDM. We found that only the incidence of the V sign was significantly lower in the CADM-MDA5+ group than in the CDM-MDA5+ group (*P*=0.032). However, the differences in the remaining characteristics were not statistically significant.

Differences between CADM and CDM in patients who tested negative for anti-MDA5 antibodies were also analyzed. After

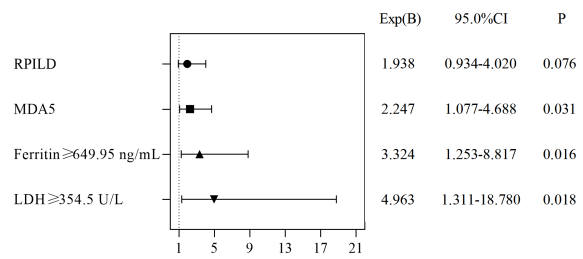

FIGURE 3
Risk factors for mortality in patients with CADM.

10.3389/fimmu.2023.1237209

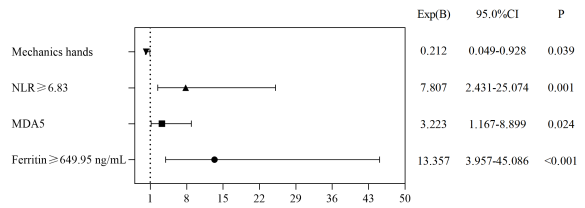

FIGURE 4
Risk factors for mortality in patients with CDM.

excluding MDA5 patients, the rates of RP-ILD (P=0.005), ILD (P<0.001), cough or dyspnea (P=0.001), cardiac involvement (P=0.029), the numbness in the extremities (P=0.028), the NLR (P=0.001), PLR (P=0.001), and the levels of ferritin (P=0.003), CRP (P=0.025), NSE (P=0.002), and CYFRA21 (P<0.001) in the CADM-MDA5− group were still higher than those in the CDM-MDA5− group. Furthermore, the rates of the shawl sign (P=0.025) and dysphagia (P=0.028) and the levels of lymphocytes (P=0.001) in the CADM-MDA5− group were still lower than those in the CDM-MDA5− group. Notably, the differences in RP-ILD, cough or dyspnea, cardiac involvement, NLR, ferritin levels, and lymphocyte levels between the two groups decreased. Furthermore, the differences in the rates of mortality, 1-year mortality, Gottron's sign, V sign, pleural effusion, hoarseness and in the levels of LDH, CEA, CA724, and CA242 were no longer statistically significant. Clearly, when anti-MDA5 antibodies were involved, some symptoms and serological indicators differed across CADM and CDM, becoming substantial, or even changing from "nothing" to "something."

Differences in the clinical characteristics and serological indices were also examined between anti-MDA5 antibody-positive and anti-MDA5 antibody-negative patients with DM, those with CADM, and those with CDM to evaluate the impact of anti-MDA5 antibodies on patients with DM. Whether in DM, CADM, or CDM, anti-MDA5 antibody-positive patients had consistently significantly higher rates of mortality, 1-year mortality, RP-ILD, ILD, fever, cough or dyspnea, heliotrope rashes, higher PLR, and higher levels of LDH, ferritin, and CEA than anti-MDA5 antibody-negative patients. Conversely, the disease duration at diagnosis and lymphocyte levels were consistently significantly lower than those in anti-MDA5-negative patients. However, anti-MDA5 antibody-positive patients had consistently significantly lower lymphocyte levels and disease duration at diagnosis. Variables with P<0.05 in the above differential analysis are shown in Table 4.

3.6 Clinical characteristics of dead patients

For all patients, the median follow-up duration was 28.5 months (range: 1–100 months). The median survival period among patients with CADM was significantly shorter than that among patients with CDM (20.00 vs. 35.00 months, respectively, P<0.001). Overall, patients with CADM had a significantly lower survival rate (P<0.001, Figure 5A) and 1-year survival rate (P=0.003, Figure 5B) than those with CDM. A total of 57 (17.3%) patients were found to have died owing to exacerbations of ILD or infection at follow-up, whereas 44 (13.3%) died within 1 year. In order to explore the clinical differences between patients who died in the CADM and CDM groups, we further compared the clinical data of the 57 patients who died in Table 5. Out of the 57 deceased patients (average age: 57.81 years), 54 (94.7%) had ILD, 23 (40.4%) had RP-ILD, and 31 (54.4%) had anti-MDA5 antibodies. The rates of anti-MDA5 antibodies (P=0.030), ILD (P=0.025), RP-ILD (P=0.032), cough or dyspnea (P=0.009), and the levels of CRP (P=0.004) and neutrophils (P=0.023) in dead patients with CADM were significantly higher than those in dead patients with CDM. Conversely, the rates of Holster sign (P=0.023) and dysphagia in dead patients with CDM were significantly higher than those in dead patients with CADM. Notably, all patients who died in the CADM group had cough or dyspnea, but none had dysphagia. In terms of serological indices, serum ferritin and LDH levels were significantly increased, and lymphocyte levels were significantly decreased; nevertheless, no significant differences between dead CADM patients and dead CDM patients were observed. Eighteen dead patients had serum ferritin levels >2000 ng/mL; of them, 12 belonged to the CADM group, whereas 13 were accompanied by anti-MDA5 antibodies.

TABLE 3 Treatment and clinical course in the entire cohort.

Characteristic	CADM	CDM	P-value
Initial treatment			
CS (oral only)	5 (3.7%)	29 (14.9%)	0.001
CS (IV + oral only)	28 (20.7%)	37 (19.0%)	0.692
CS (IV and/or oral) + CsA	22 (16.3%)	12 (6.2%)	0.003
CS (IV and/or oral) + Tac	29 (21.5%)	26 (13.3%)	0.051
CS (IV and/or oral) + CY (oral and/or IV)	6 (4.4%)	16 (8.2%)	0.178
CS (IV and/or oral) + AZA	2 (1.5%)	5 (2.6%)	0.778
CS (IV and/or oral) + MTX	1 (0.7%)	9 (4.6%)	0.091
CS (IV and/or oral) + MMF	22 (16.3%)	44 (22.6%)	0.162
CS (IV and/or oral) + CsA or Tac + CY (oral and/or IV)	22 (16.3%)	16 (8.2%)	0.024
CS pulse-dose	21 (15.6%)	10 (5.2%)	0.001
IVIG	55 (40.7%)	37 (19.0%)	<0.001
JAK inhibitors	7 (5.2%)	7 (3.6%)	0.480
Biological agents	13 (9.6%)	7 (3.6%)	0.024
ILD response to treatment			
Worsening	54 (44.3%)	33 (24.4%)	0.001
Stability	45 (36.9%)	41 (30.4%)	0.269
Improved	17 13.9%)	48 (35.6%)	<0.001
Unknown	6 (4.9%)	13 (9.6%)	0.149

CS, corticosteroid; CsA, cyclosporine A; Tac, tacrolimus; CY, cyclophosphamide; IV, intravenous; IVIG, intravenous immunoglobulin; AZA, azathioprine; MTX, methotrexate; MMF, mycophenolate mofetil; CS pulse-dose, 0.5–1.0 g per day for 1–5 days; CADM, clinically amyopathic dermatomyositis; CDM, classic dermatomyositis.

10.3389/fimmu.2023.1237209

TABLE 4 *P*-value after the analysis of each cohort.

	P-value (CADM vs. CDM)	*P*-value (CADM-MDA5+ vs. CDM-MDA5+)	*P*-value (CADM-MDA5- vs. CDM-MDA5-)	*P*-value (MDA5+ vs. MDA5-)	*P*-value (CADM-MDA5+ vs. CADM-MDA5-)	*P*-value (CDM-MDA5+ vs. CDM-MDA5-)
Disease duration at diagnosis	0.543	0.157	0.198	<0.001^{-}	<0.001^{-}	0.001^{-}
Death	0.001^{+}	0.599	0.152	<0.001^{+}	<0.001^{+}	<0.001^{+}
Died within 1 year	0.003^{+}	0.950	0.374	<0.001^{+}	<0.001^{+}	<0.001^{+}
RP-ILD	<0.001^{+}	0.550	0.005^{+}	<0.001^{+}	0.002^{+}	<0.001^{+}
ILD	<0.001^{+}	0.412	<0.001^{+}	<0.001^{+}	0.013^{+}	0.028^{+}
Fever	0.938	0.588	0.445	0.006^{+}	0.027^{+}	0.056
Cough or dyspnea	<0.001^{+}	0.282	0.001^{+}	<0.001^{+}	0.006^{+}	0.029^{+}
Mechanic's hand	0.181	0.200	0.656	0.022^{-}	0.038^{-}	0.608
Heliotrope rash	0.429	0.364	0.237	0.011^{+}	0.033^{+}	0.051
Gottron's sign	0.017^{+}	0.534	0.102	0.115	0.516	0.453
V sign	0.038^{-}	0.032^{-}	0.058	0.054	0.132	0.014^{+}
Shawl sign	0.021^{-}	0.988	0.025^{-}	0.783	0.378	0.998
Holster sign	0.372	0.534	0.084	0.014^{+}	0.028^{+}	0.098
Raynaud's phenomenon	0.973	1.000	0.520	0.034^{-}	0.110	0.137
Dysphagia	0.002^{-}	0.128	0.028^{-}	0.218	0.727	1.000
Cardiac involvement	0.004^{+}	0.491	0.029^{+}	0.001^{+}	0.113	0.068
Pleural effusion	0.014^{-}	0.135	0.556	0.001^{+}	0.005^{+}	1.000
Pericardial effusion	0.271	0.534	0.493	0.001^{+}	0.096	0.004^{+}
Fatigue	0.789	0.119	0.875	0.036^{+}	0.341	0.013^{+}
Hoarseness	0.001^{+}	0.233	0.732	<0.001^{+}	<0.001+	0.061
Tumor	0.604	0.290	0.671	0.044^{-}	0.026^{-}	0.829
Numbness in the extremities	0.006^{+}	0.822	0.028^{+}	0.301	0.934	1.000
LYM	<0.001^{-}	0.588	0.001^{-}	0.001^{-}	<0.001^{-}	<0.001^{-}
NLR	<0.001^{+}	0.116	0.001^{+}	0.001^{+}	0.109	0.010^{+}
PLR	<0.001^{+}	0.390	0.001^{+}	0.001^{+}	0.022^{+}	0.001^{+}
LDH	0.004^{+}	0.552	0.184	0.001^{+}	0.002^{+}	0.023^{+}
Serum ferritin	<0.001^{+}	0.341	0.003^{+}	0.001^{+}	<0.001^{+}	0.002^{+}
CRP	0.002^{+}	0.084	0.025^{+}	0.205	0.498	0.726
ESR	0.111	0.900	0.326	0.026+	0.210	0.180
D-dimer	0.582	0.969	0.045^{-}	0.013^{+}	0.001^{+}	0.524
LYM ≤785×10^{6}/L	<0.001^{+}	0.523	<0.001^{+}	<0.001^{+}	0.016^{+}	<0.001^{+}

(Continued)

10.3389/fimmu.2023.1237209

TABLE 4 Continued

	P-value (CADM vs. CDM)	*P*-value (CADM-MDA5+ vs. CDM-MDA5+)	*P*-value (CADM-MDA5- vs. CDM-MDA5-)	*P*-value (MDA5+ vs. MDA5-)	*P*-value (CADM-MDA5+ vs. CADM-MDA5-)	*P*-value (CDM-MDA5+ vs. CDM-MDA5-)
NLR ≥6.83	<0.001^{+}	0.309	<0.001^{+}	<0.001^{+}	0.081	0.001^{+}
LDH ≥354.50 U/L	0.004^{+}	0.309	0.398	<0.001^{+}	<0.001^{+}	0.029^{+}
Serum ferritin ≥649.95 ng/mL	<0.001^{+}	0.147	0.058	<0.001^{+}	<0.001^{+}	0.003^{+}
CEA	<0.001^{+}	0.209	0.082	<0.001^{+}	<0.001^{+}	0.001^{+}
CA125	0.765	0.902	0.339	0.046^{+}	0.045^{+}	0.325
CA153	0.061	0.485	0.255	0.001^{+}	0.086	0.012^{+}
CA724	0.016^{+}	0.737	0.134	0.004^{+}	0.072	0.231
NSE	<0.001^{+}	0.290	0.002^{+}	<0.001^{+}	0.065	0.150
CYFRA21	<0.001^{+}	0.082	<0.001^{+}	0.002^{+}	0.104	0.385
CA50	0.054	0.516	0.027^{+}	0.782	0.221	0.935
CA242	0.024^{+}	0.289	0.292	0.017^{+}	0.236	0.305

$^{-}$, the former is lower than the latter; $^{+}$, the former is higher than the latter.
ILD, interstitial lung disease; RP-ILD, rapidly progressive interstitial lung disease; LYM, lymphocyte; NLR, NEUT-to-LYM ratio; PLR, PLT-to-LYM ratio; LDH, lactate dehydrogenase; CRP, C-reactive protein; ESR, erythrocyte sedimentation rate; CADM, clinically amyopathic dermatomyositis; CDM, classic dermatomyositis.

The mortality rate and 1-year mortality rate of the 29 patients with RP-ILD were 79.3% and 72.4%, respectively, of whom 23 (79.3%) belonged to the CADM group. One case was negative for any specific autoantibody, two cases were combined with an anti-PL-7 antibody, two cases were combined with an anti-PL-12 antibody, one case was combined with an anti-EJ antibody, one case was combined with an anti-OJ antibody, two cases were combined with an anti-Mi-2 antibody, one case was combined with an anti-TIF1-γ antibody, and 19 (65.5%) cases were combined with an anti-MDA5 antibodies. A total of 17 (89.5%) RP-ILD patients with anti-MDA5 antibodies died. These results indicate that patients with DM accompanied by RP-ILD had an very high mortality rate within the first year after disease diagnosis and that patients with anti-MDA5 antibodies and/or those belonging to the CADM group require urgent attention with respect to the development of RP-ILD.

Only two out of the six surviving patients with RP-ILD had combined anti-MDA5 antibodies. Surviving patients with RP-ILD had a mean LDH level of 583.67 U/L, ferritin level of 1090.62 ng/mL, and lymphocyte level of 776.67×10^6/L on admission. Additionally, the deceased patients had a mean LDH level of 777.83 U/L, ferritin level of 2063.03 ng/mL, and lymphocyte level of 511.87×10^6/L. Fortunately, all surviving patients were diagnosed with DM using autoantibody tests within 1 week of presentation to our department. Although these patients later developed RP-ILD, their condition improved after treatment with glucocorticoids, immunosuppressants, IVIG, and anti-infection agents, and they have survived to date. For patients with RP-ILD, we believe that relatively optimistic LDH, ferritin, and lymphocyte levels may indicate a good prognosis and that early screening for anti-MDA5 antibodies is necessary.

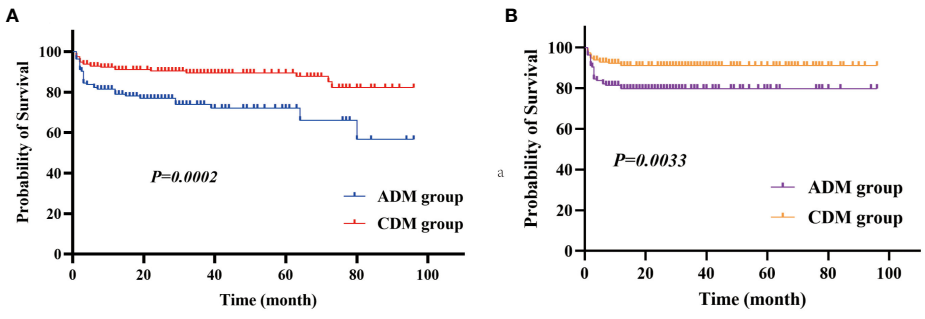

FIGURE 5
(A) Survival rate and **(B)** 1-year survival rate in the CADM and CDM groups.

TABLE 5 Data of the 57 deceased patients.

	Dead patients (*N*=57)	Dead patients with CADM (*N*=35)	Dead patients with CDM (*N*=22)	*P*-value
Age at diagnosis, mean ± SD, years	57.81 ± 12.80	57.26 ± 12.40	58.68 ± 13.67	0.686
Male/female	26/31 (1:1.19)	16/19 (1:1.19)	10/12 (1:1.20)	0.985
Died within 1 year, *n* (%)	44 (77.2)	27 (77.1)	17 (77.3)	0.991
Anti-MDA5 antibodies, *n* (%)	31 (54.4)	23 (65.7)	8 (36.4)	0.030
ILD, *n* (%)	54 (94.7)	35 (100.0)	19 (86.4)	0.025
RP-ILD, *n* (%)	23 (40.4)	18 (51.4)	5 (22.7)	0.032
Cough or dyspnea, *n* (%)	53 (93.0)	35 (100.0)	18 (81.8)	0.009
Holster sign, *n* (%)	8 (14.0)	2 (5.7)	6 (27.3)	0.023
Dysphagia, *n* (%)	7 (12.3)	0 (0.0)	7 (31.8)	0.001
LYM, median (IQR), $\times10^9$/L	0.65 (0.45, 0.77)	0.54 (0.45, 0.71)	0.71 (0.45, 1.06)	0.268
LDH, median (IQR), U/L	528.00 (391.50, 707.00)	481.00 (384.00, 699.70)	544.00 (409.35, 818.75)	0.372
Serum ferritin, median (IQR), ng/mL	1154.00 (700.18, 2257.95)	1281.00 (705.45, 2500.00)	1104.50 (530.75, 1756.17)	0.342
CRP, median (IQR), mg/L	18.60 (7.17, 43.00)	30.40 (9.11, 68.80)	8.26 (3.78, 20.48)	0.004
NEUT, median (IQR), $\times10^9$/L	7.24 (5.31, 10.72)	8.31 (6.87, 10.79)	5.66 (3.83, 9.30)	0.023

ILD, interstitial lung disease; RP-ILD, rapidly progressive interstitial lung disease; LYM, lymphocyte; LDH, lactate dehydrogenase; CRP, C-reactive protein; NEUT, neutrophil; SD, standard deviation; IQR, interquartile range; CADM, clinically amyopathic dermatomyositis; CDM, classic dermatomyositis.

4 Discussion

This study reveals the following: (i) CADM was associated with a higher frequency of ILD and RP-ILD and a worse prognosis than CDM. (ii) Patients with anti-MDA5 antibodies and/or CADM required urgent attention to detect the development of RP-ILD. (iii) Patients with CDM were likely to have anti-NXP2 antibodies and negative myositis-specific autoantibodies, whereas those with CADM were likely to have anti-MDA5 antibodies. (iv) The presence of RP-ILD and high LDH levels were risk factors for death in CADM, but not in CDM. Mechanic's hand was a protective factor against death in patients with CDM, but not in patients with CADM. Positive results for anti-MDA5 antibodies and high ferritin levels were risk factors for CADM and CDM. (v) Anti-MDA5 antibody-positive patients did not differ significantly, depending on whether they had CADM or CDM. (vi) When no anti-MDA5 antibody-positive patients participated, RP-ILD rates, ILD rates, and ferritin levels in patients with CADM were still higher than those in patients with CDM; whereas the mortality rates, 1-year mortality rates, and LDH levels did not differ significantly. (vii) Among patients with DM, CADM, or CDM, anti-MDA5 antibody-positive patients consistently had higher ILD and RP-ILD rates, LDH levels, lower lymphocyte levels, and worse prognoses than those who were negative for anti-MDA5 antibodies. (viii) Screening for anti-MDA5 antibodies should be the first step when suspecting the presence of CADM or CDM.

Of the 330 DM samples collected, CADM accounted for 40.9%, which was higher than that reported in previous studies (28, 29). In the comparison between CADM and CDM, we found that patients with CADM showed significantly higher anti-MDA5 antibody levels and significantly higher ILD, RP-ILD, mortality, and 1-year mortality rates than those with CDM, which were similar to the findings of a previous study (30). Additionally, we found that RP-ILD patients had anti-MDA5 antibodies and a very high probability of mortality within 1 year; furthermore, most of them had CADM. Therefore, we believe that patients with anti-MDA5 antibodies and/or CADM require urgent attention to monitor the development of RP-ILD. Surviving RP-ILD patients exhibited a significantly lower severity of anti-MDA5 antibodies and serological levels than deceased RP-ILD patients. Therefore, for patients with RP-ILD, we believe that relatively optimistic LDH, ferritin, and lymphocyte levels may indicate a good prognosis, and early screening for anti-MDA5 antibodies is necessary. Similarly, Xu et al. (31) believed that in addition to anti-MDA5 antibodies, ulcerations, serum ferritin, and lymphocyte count may aid in predicting the occurrence of RP-ILD in patients with CADM.

In our study, patients with CDM had higher rates of negative myositis-specific autoantibodies and anti-NXP2 antibodies than those with CADM, and patients with CADM had higher rates of anti-MDA5 antibodies than those with CDM. Anti-MDA5 antibodies (36.3%) were the most common specific autoantibodies in CADM, followed by anti-Jo-1, anti-PL-7, anti-EJ, and anti-PL-12, which is similar to that observed in the CADM-ILD cohort reported by Wu et al. (32).

Lymphocyte subsets in DM are thought to be reflected with ILD and disease activity to some extent (33, 34). Tumor marker levels can be used to evaluate the disease severity of DM. Additionally, CEA can be used as a noninvasive diagnostic biomarker for patients

with DM-RP-ILD (35). The counts of CD3+, CD3+CD4+, CD3+CD8+, and CD16+CD56+ cells in CADM were significantly lower than those in CDM, and the levels of CEA, CA724, NSE, CYFRA21, and CA242 in CADM were significantly higher than those in CDM. Because there were insufficient data regarding the measured lymphocyte subsets and tumor marker levels of the patients, we were unable to include these two items into the prognostic risk factor prediction models of CADM and CDM. Future studies are needed to explore the impact of lymphocyte subsets and tumor marker levels on the prognosis of CADM and CDM. The prevalence of tumor events in this study was 7.6%, which is at the lower end of previously reported values (24, 36–38). During the follow-up of all patients, the probability of tumor events occurring in the CADM and CDM groups was similar to that previously reported (11, 24). At the two-year time node, Bowerman et al. (24) reported that CDM had significantly more tumor events than CADM; additionally, old age and CDM were considered independent risk factors for tumor events within 2 years of onset. Of the 25 patients with tumor-associated DM in our study, the most common antibody was the anti-TIF-1 gamma antibody (52%), similar to previous studies' findings (39, 40).

The independent risk factors for death in CADM and CDM were evaluated using backward stepwise selection with Cox regression. In the present study, RP-ILD and high LDH levels were risk factors for death in CADM, but not in CDM. Mechanics' hands were a protective factor against death in CDM but not in CADM; however, because of the impact of the sample size on the results, future studies are needed to confirm this. Positive anti-MDA5 antibodies and high ferritin levels are risk factors for CADM and CDM. Lian et al. (41) modeled a mortality risk score for CADM-associated ILD, identifying a ferritin level of 636 ng/mL and an LDH level of 355 U/L as the optimal clinical thresholds, similar to our results. Gan et al. (42) believed that a higher anti-MDA5 antibody titer indicated an increased likelihood of RP-ILD. Xu et al. (31) concluded that anti-MDA5 antibodies, elevated CRP levels, and decreased lymphocyte counts were independent risk factors for RP-ILD. These results further support the importance of LDH, serum ferritin, RP-ILD, anti-MDA5 antibodies, and lymphocyte levels in predicting poor outcomes.

In our study, all patients received corticosteroids during treatment. More patients with CADM received corticosteroid pulse-dose therapy, IVIG, and biological agents during treatment than those with CDM, whereas more patients with CDM maintained or even improved their condition with oral corticosteroids alone than those with CADM. In terms of the response of ILD to treatment, the presence of CADM worsened it more than that of CDM. A systematic review (43) of the treatment of MDA5-antibody-positive CADM complicated with ILD concluded that initiating combined immunosuppressive therapy early in the disease course is generally beneficial, mainly in terms of reduced morbidity and mortality. A systematic review (44) of 153 CADM cases suggested that IVIG treatment led to improvement or remission in most patients. A systematic review (45) of CADM treatment reported that most patients required more than one treatment owing to refractoriness or side effects, and IVIG was the most successful treatment. A retrospective study (46) found that IVIG is effective in the treatment of refractory cutaneous DM, enables reduction or withdrawal of immunosuppressive drugs in almost 80% of patients. Oral glucocorticoids is the first-line treatment for CDM; however, there is no consensus regarding its dosing or the addition of immunosuppressants in steroid-resistant disease. For severe CADM, the first-line therapy is antimalarials; however, it usually requires the addition of second-line cytotoxic agents. In severely refractory cases, IVIG and/or systemic calcineurin inhibitors may be employed. For severely refractory patients, IVIG and/or systemic calcineurin inhibitors are often used for treatment (47). In conclusion, DM presents a major therapeutic challenge, largely owing to our incomplete understanding of its pathogenesis and the heterogeneity of the disease itself. Randomized controlled trials are needed to determine the effects of treatment in patients with CADM. Furthermore, IVIG is the most successful treatment option for DM.

We analyzed the distribution and effects of anti-MDA5 antibodies in each group. We obtained the following findings: (i) Anti-MDA5 antibodies were prominently present in CADM. (ii) Anti-MDA5 antibody-positive patients did not show significant differences based on whether they belonged to the CADM or CDM group. (iii) When no anti-MDA5 antibody-positive patients participated, the RP-ILD rates, ILD rates, and ferritin levels in CADM were still higher than those in CDM; nonetheless, the differences decreased, whereas the mortality rates, 1-year mortality rates, and LDH levels were no longer different. (iv) Anti-MDA5 antibody-positive patients consistently exhibited higher LDH and ferritin levels, lower lymphocyte levels, higher probability of RP-ILD and ILD occurrence, and worse prognosis than anti-MDA5 antibody-negative patients, irrespective of DM, CADM, or CDM. These results indicate that anti-MDA5 antibodies not only affect the symptoms and prognosis of patients with DM but also have a non-negligible impact on the differences between CADM and CDM.

As far as we know, this is the only cohort study that enrolled more than 300 patients to compare CADM with CDM and to evaluate the distribution and impact of anti-MDA5 antibodies in these two subtypes. Nonetheless, our study still has some limitations. First, it had a retrospective design and had a sample size that was not sufficiently large. Second, myositis-specific antibody titers were not measured, and the significance of disease activity and prognosis need to be determined. Third, some patients with ILD were severely ill and unable to undergo pulmonary function tests. Fourth, the majority of our patients did not undergo pulmonary function tests owing to poor compliance or physicians' omission. Fifth, since this is a clinical retrospective study, we only compared the medication use and prognosis of patients with CADM and those with CDM; accordingly, the comparison results are general and disordered. Despite these limitations, our study revealed differences in the clinical characteristics, antibody distribution, prognosis, and risk factors for mortality between CADM and CDM. Furthermore, it focused

on the distribution and influence of anti-MDA5 antibodies in these two subtypes, Which may make clinicians view anti-MDA5 antibodies in a new light.

Data availability statement

The original contributions presented in the study are included in the article/Supplementary Material. Further inquiries can be directed to the corresponding author.

Ethics statement

The studies involving humans were approved by the Human Research Ethics Boards of The First Affiliated Hospital of Shandong First Medical University and Shandong Provincial Hospital of Traditional Chinese Medicine. The studies were conducted in accordance with the local legislation and institutional requirements. Written informed consent for participation was not required from the participants or the participants' legal guardians/next of kin in accordance with the national legislation and institutional requirements. The animal studies were approved by the Human Research Ethics Boards of The First Affiliated Hospital of Shandong First Medical University and Shandong Provincial Hospital of Traditional Chinese Medicine. The studies were conducted in accordance with the local legislation and institutional requirements. Written informed consent was obtained from the owners for the participation of their animals in this study.

Author contributions

QJ and DZ contributed to the collection and analysis of data. QJ, WP, YH, and ZW approved the manuscript. All authors contributed to the article and approved the submitted version.

Funding

The author(s) declare financial support was received for the research, authorship, and/or publication of this article. The Bethune Medical Science Research Fund (grant no. TY017AN), the Shandong Province Traditional Chinese Medicine Science and Technology Development Plan Project (grant no. 2019-0129), Special Fund for Flow Cytometry Lymphocyte Subgroups of Shandong Provincial Medical Association (YXH2022ZX03223) and Open Project of Shandong Key Laboratory of Rheumatic Disease and Translational medicine (QYKFKT2023-7) funded our work.

Acknowledgments

The authors thank the participants of the study.

Conflict of interest

The authors declare that the research was conducted in the absence of any commercial or financial relationships that could be construed as a potential conflict of interest.

Publisher's note

Supplementary material

The Supplementary Material for this article can be found online at: https://www.frontiersin.org/articles/10.3389/fimmu.2023.1237209/full#supplementary-material

References

1. Plotz PH, Rider LG, Targoff IN, Raben N, O'Hanlon TP, Miller FW, et al. Myositis: immunologic contributions to understanding cause, pathogenesis, and therapy. *Ann Intern Med* (1995) 122:715–24. doi: 10.7326/0003-4819-122-9-199505010-00010

2. Barsotti S, Dastmalchi M, Notarnicola A, Leclaire V, Dani L, Gheorghe K, et al. Performance of the new EULAR/ACR classification criteria for idiopathic inflammatory myopathies (IIM) in a large monocentric IIM cohort. *Semin Arthritis Rheum* (2020) 50:492–7. doi: 10.1016/j.semarthrit.2019.12.001

3. Dalakas MC. Inflammatory muscle diseases. *N Engl J Med* (2015) 372:1734–47. doi: 10.1056/NEJMra1402225

4. Lilleker JB, Vencovsky J, Wang G, Wedderburn LR, Diederichsen LP, Schmidt J, et al. The EuroMyositis registry: an international collaborative tool to facilitate myositis research. *Ann Rheum Dis* (2018) 77:30–9. doi: 10.1136/annrheumdis-2017-211868

5. Euwer RL, Sontheimer RD. Amyopathic dermatomyositis (dermatomyositis siné myositis). Presentation of six new cases and review of the literature. *J Am Acad Dermatol* (1991) 24:959–66. doi: 10.1016/0190-9622(91)70153-S

6. Bottai M, Tjärnlund A, Santoni G, Werth VP, Pilkington C, de Visser M, et al. EULAR/ACR classification criteria for adult and juvenile idiopathic inflammatory myopathies and their major subgroups: a methodology report. *RMD Open* (2017) 3:e000507. doi: 10.1136/rmdopen-2017-000507

7. Sontheimer RD. Would a new name hasten the acceptance of amyopathic dermatomyositis (dermatomyositis siné myositis) as a distinctive subset within the idiopathic inflammatory dermatomyopathies spectrum of clinical illness? *J Am Acad Dermatol* (2002) 46:626–36. doi: 10.1067/mjd.2002.120621

8. Fathi M, Lundberg IE. Interstitial lung disease in polymyositis and dermatomyositis. *Curr Opin Rheumatol* (2005) 17:701–6. doi: 10.1097/01.bor.0000179949.65895.53

9. Sakamoto N, Ishimoto H, Nakashima S, Yura H, Miyamura T, Okuno D, et al. Clinical features of anti-MDA5 antibody-positive rapidly progressive interstitial lung disease without signs of dermatomyositis. *Intern Med* (2019) 58:837–41. doi: 10.2169/internalmedicine.1516-18

10. Fathi M, Lundberg IE, Tornling G. Pulmonary complications of polymyositis and dermatomyositis. *Semin Respir Crit Care Med* (2007) 28:451–8. doi: 10.1055/s-2007-985666

11. Sato S, Kuwana M. Clinically amyopathic dermatomyositis. *Curr Opin Rheumatol* (2010) 22:639–43. doi: 10.1097/BOR.0b013e32833f1987

12. Selva-O'Callaghan A, Pinal-Fernandez I, Trallero-Araguás E, Milisenda JC, Grau-Junyent JM, Mammen AL. Classification and management of adult inflammatory myopathies. *Lancet Neurol* (2018) 17:816–28. doi: 10.1016/S1474-4422(18)30254-0

13. Gunawardena H, Betteridge ZE, McHugh NJ. Myositis-specific autoantibodies: their clinical and pathogenic significance in disease expression. *Rheumatol (Oxf Engl)* (2009) 48:607–12. doi: 10.1093/rheumatology/kep078

14. Sato S, Hirakata M, Kuwana M, Suwa A, Inada S, Mimori T, et al. Autoantibodies to a 140-kd polypeptide, CADM-140, in Japanese patients with clinically amyopathic dermatomyositis. *Arthritis Rheum* (2005) 52:1571–6. doi: 10.1002/art.21023

15. Li Y, Li Y, Wu J, Miao M, Gao X, Cai W, et al. Predictors of poor outcome of anti-MDA5-associated rapidly progressive interstitial lung disease in a Chinese cohort with dermatomyositis. *J Immunol Res* (2020) 2020:2024869. doi: 10.1155/2020/2024869

16. Borges IBP, Silva MG, Shinjo SK. Prevalence and reactivity of anti-melanoma differentiation-associated gene 5 (anti-MDA-5) autoantibody in Brazilian patients with dermatomyositis. *Bras Dermatol* (2018) 93:517–23. doi: 10.1590/abd1806-4841.20186803

17. Labrador-Horrillo M, Martinez MA, Selva-O'Callaghan A, Trallero-Araguas E, Balada E, Vilardell-Tarres M, et al. Anti-MDA5 antibodies in a large Mediterranean population of adults with dermatomyositis. *J Immunol Res* (2014) 2014:290797. doi: 10.1155/2014/290797

18. Chen Z, Cao M, Plana MN, Liang J, Cai H, Kuwana M, et al. Utility of anti-melanoma differentiation-associated gene 5 antibody measurement in identifying patients with dermatomyositis and a high risk for developing rapidly progressive interstitial lung disease: a review of the literature and a meta-analysis. *Arthritis Care Res* (2013) 65:1316–24. doi: 10.1002/acr.21985

19. Cao H, Pan M, Kang Y, Xia Q, Li X, Zhao X, et al. Clinical manifestations of dermatomyositis and clinically amyopathic dermatomyositis patients with positive expression of anti-melanoma differentiation-associated gene 5 antibody. *Arthritis Care Res* (2012) 64:1602–10. doi: 10.1002/acr.21728

20. Hamaguchi Y, Kuwana M, Hoshino K, Hasegawa M, Kaji K, Matsushita T, et al. Clinical correlations with dermatomyositis-specific autoantibodies in adult Japanese patients with dermatomyositis: a multicenter cross-sectional study. *Arch Dermatol* (2011) 147:391–8. doi: 10.1001/archdermatol.2011.52

21. Gono T, Kawaguchi Y, Satoh T, Kuwana M, Katsumata Y, Takagi K, et al. Clinical manifestation and prognostic factor in anti-melanoma differentiation-associated gene 5 antibody-associated interstitial lung disease as a complication of dermatomyositis. *Rheumatol (Oxf Engl)* (2010) 49:1713–9. doi: 10.1093/rheumatology/keq149

22. Fujikawa K, Kawakami A, Kaji K, Fujimoto M, Kawashiri S, Iwamoto N, et al. Association of distinct clinical subsets with myositis-specific autoantibodies towards anti-155/140-kDa polypeptides, anti-140-kDa polypeptides, and anti-aminoacyl tRNA synthetases in Japanese patients with dermatomyositis: a single-centre, cross-sectional study. *Scand J Rheumatol* (2009) 38:263–7. doi: 10.1080/03009740802687455

23. Yoshida N, Okamoto M, Kaieda S, Fujimoto K, Ebata T, Tajiri M, et al. Association of anti-aminoacyl-transfer RNA synthetase antibody and anti-melanoma differentiation-associated gene 5 antibody with the therapeutic response of polymyositis/dermatomyositis-associated interstitial lung disease. *Respir Investig* (2017) 55:24–32. doi: 10.1016/j.resinv.2016.08.007

24. Bowerman K, Pearson DR, Okawa J, Werth VP. Malignancy in dermatomyositis: A retrospective study of 201 patients seen at the University of Pennsylvania. *J Am Acad Dermatol* (2020) 83:117–22. doi: 10.1016/j.jaad.2020.02.061

25. Mammen AL, Allenbach Y, Stenzel W, Benveniste OENMC 239th Workshop Study Group. 239th ENMC International Workshop: classification of dermatomyositis, Amsterdam, the Netherlands, 14-16 December 2018. *Neuromuscul Disord* (2020) 30:70–92. doi: 10.1016/j.nmd.2019.10.005

26. Bohan A, Peter JB. Polymyositis and dermatomyositis (first of two parts). *N Engl J Med* (1975) 292:344–7. doi: 10.1056/NEJM197502132920706

27. Won Huh J, Soon Kim D, Keun Lee C, Yoo B, Bum Seo J, Kitaichi M, et al. Two distinct clinical types of interstitial lung disease associated with polymyositis-dermatomyositis. *Respir Med* (2007) 101:1761–9. doi: 10.1016/j.rmed.2007.02.017

28. Bendewald MJ, Wetter DA, Li X, Davis MD. Incidence of dermatomyositis and clinically amyopathic dermatomyositis: a population-based study in Olmsted County, Minnesota. *Arch Dermatol* (2010) 146:26–30. doi: 10.1001/archdermatol.2009.328

29. el-Azhary RA, Pakzad SY. Amyopathic dermatomyositis: retrospective review of 37 cases. *J Am Acad Dermatol* (2002) 46:560–5. doi: 10.1067/mjd.2002.120620

30. Mukae H, Ishimoto H, Sakamoto N, Hara S, Kakugawa T, Nakayama S, et al. Clinical differences between interstitial lung disease associated with clinically amyopathic dermatomyositis and classic dermatomyositis. *Chest* (2009) 136:1341–7. doi: 10.1378/chest.08-2740

31. Xu Y, Yang CS, Li YJ, Liu XD, Wang JN, Zhao Q, et al. Predictive factors of rapidly progressive-interstitial lung disease in patients with clinically amyopathic dermatomyositis. *Clin Rheumatol* (2016) 35:113–6. doi: 10.1007/s10067-015-3139-z

32. Wu T, Zhou H, Xu S, Deng Z, Zhang Y, Ding Q. Clinical and HRCT features of amyopathic dermatomyositis associated with interstitial lung disease: A retrospective study of 128 patients with connective tissue disease-related interstitial lung disease. *Am J Med Sci* (2023) 365:429–36. doi: 10.1016/j.amjms.2022.12.001

33. Wang DX, Lu X, Zu N, Lin B, Wang LY, Shu XM, et al. Clinical significance of peripheral blood lymphocyte subsets in patients with polymyositis and dermatomyositis. *Clin Rheumatol* (2012) 31:1691–7. doi: 10.1007/s10067-012-2075-4

34. Sasaki H, Takamura A, Kawahata K, Takashima T, Imai K, Morio T, et al. Peripheral blood lymphocyte subset repertoires are biased and reflect clinical features in patients with dermatomyositis. *Scand J Rheumatol* (2019) 48:225–9. doi: 10.1080/03009742.2018.1530371

35. Wang Q, Gao C, Zhang C, Yao M, Liang W, Sun W, et al. Tumor markers are associated with rapidly progressive interstitial lung disease in adult-dermatomyositis. *Clin Rheumatol* (2022) 41:1731–9. doi: 10.1007/s10067-022-06089-z

36. Gerami P, Schope JM, McDonald L, Walling HW, Sontheimer RD. A systematic review of adult-onset clinically amyopathic dermatomyositis (dermatomyositis sine myositis): a missing link within the spectrum of the idiopathic inflammatory myopathies. *J Am Acad Dermatol* (2006) 54:597–613. doi: 10.1016/j.jaad.2005.10.041

37. Klein RQ, Teal V, Taylor L, Troxel AB, Werth VP. Number, characteristics, and classification of patients with dermatomyositis seen by dermatology and rheumatology departments at a large tertiary medical center. *J Am Acad Dermatol* (2007) 57:937–43. doi: 10.1016/j.jaad.2007.08.024

38. Fardet L, Dupuy A, Gain M, Kettaneh A, Chérin P, Bachelez H, et al. Factors associated with underlying Malignancy in a retrospective cohort of 121 patients with dermatomyositis. *Medicine* (2009) 88:91–7. doi: 10.1097/MD.0b013e31819da352

39. Chinoy H, Fertig N, Oddis CV, Ollier WE, Cooper RG. The diagnostic utility of myositis autoantibody testing for predicting the risk of cancer-associated myositis. *Ann Rheum Dis* (2007) 66:1345–9. doi: 10.1136/ard.2006.068502

40. Fiorentino DF, Chung LS, Christopher-Stine L, Zaba L, Li S, Mammen AL, et al. Most patients with cancer-associated dermatomyositis have antibodies to nuclear matrix protein NXP-2 or transcription intermediary factor 1γ. *Arthritis Rheum* (2013) 65:2954–62. doi: 10.1002/art.38093

41. Lian X, Zou J, Guo Q, Chen S, Lu L, Wang R, et al. Mortality risk prediction in amyopathic dermatomyositis associated with interstitial lung disease: the FLAIR model. *Chest* (2020) 158:1535–45. doi: 10.1016/j.chest.2020.04.057

42. Gan YZ, Zhang LH, Ma L, Sun F, Li YH, An Y, et al. Risk factors of interstitial lung diseases in clinically amyopathic dermatomyositis. *Chin Med J (Engl)* (2020) 133:644–9. doi: 10.1097/CM9.0000000000000691

43. McPherson M, Economidou S, Liampas A, Zis P, Parperis K. Management of MDA-5 antibody positive clinically amyopathic dermatomyositis associated interstitial lung disease: A systematic review. *Semin Arthritis Rheum* (2022) 53:151959. doi: 10.1016/j.semarthrit.2022.151959

44. Galimberti F, Li Y, Fernandez AP. Clinically amyopathic dermatomyositis: clinical features, response to medications and Malignancy-associated risk factors in a specific tertiary-care-centre cohort. *Br J Dermatol* (2016) 174:158–64. doi: 10.1111/bjd.14227

45. Callander J, Robson Y, Ingram J, Piguet V. Treatment of clinically amyopathic dermatomyositis in adults: a systematic review. *Br J Dermatol* (2018) 179:1248–55. doi: 10.1111/bjd.14726

46. Galimberti F, Kooistra L, Li Y, Chatterjee S, Fernandez AP. Intravenous immunoglobulin is an effective treatment for refractory cutaneous dermatomyositis. *Clin Exp Dermatol* (2018) 43:906–12. doi: 10.1111/ced.13607

47. Chen KL, Zeidi M, Werth VP. Recent advances in pharmacological treatments of adult dermatomyositis. *Curr Rheumatol Rep* (2019) 21:53. doi: 10.1007/s11926-019-0850-9

frontiers | Frontiers in Immunology

TYPE Original Research
PUBLISHED 29 January 2024
DOI 10.3389/fimmu.2024.1273358

OPEN ACCESS

EDITED BY
Francesca Wanda Rossi,
University of Naples Federico II, Italy

REVIEWED BY
Daniele Sola,
University of Eastern Piedmont, Italy
Silvia Martina Ferrari,
University of Pisa, Italy

*CORRESPONDENCE
Dide Wu
wudd7@mail.sysu.edu.cn
Yanbing Li
liyb@mail.sysu.edu.cn

†These authors have contributed equally to this work and share first authorship

RECEIVED 06 August 2023
ACCEPTED 12 January 2024
PUBLISHED 29 January 2024

CITATION
Xian W, Liu B, Li J, Yang Y, Hong S, Xiao H, Wu D and Li Y (2024) Graves' disease and systemic lupus erythematosus: a Mendelian randomization study.
Front. Immunol. 15:1273358.
doi: 10.3389/fimmu.2024.1273358

Graves' disease and systemic lupus erythematosus: a Mendelian randomization study

Wei Xian[1,2†], Boyuan Liu[1†], Jinjian Li[1†], Yuxin Yang[3], Shubin Hong[1], Haipeng Xiao[1], Dide Wu[1*] and Yanbing Li[1*]

[1]Department of Endocrinology, The First Affiliated Hospital of Sun Yat-sen University, Guangzhou, Guangdong, China, [2]Department of Pediatric Allergy, Immunology & Rheumatology, Guangzhou Women and Children's Medical Center, Guangzhou, Guangdong, China, [3]Zhongshan School of Medicine, Sun Yat Sen University, Guangzhou, Guangdong, China

Introduction: Previous observational studies have established a correlation between Graves' disease(GD) and systemic lupus erythematosus(SLE). However, whether a causal relationship exists between these two diseases remains unknown.We utilized Mendelian randomization to infer the causal association between GD and SLE.

Methods: This study employed GWAS summary statistics of GD and SLE in individuals of Asian descent. The random effect inverse variance weighted (IVW) method was utilized to aggregate the causal effect estimates of all SNPs. Cochran's Q values were computed to evaluate the heterogeneity among instrumental variables. Sensitivity analyses such as MR-Egger method, median weighting method, leave-one-out method, and MR-PRESSO method were used to test whether there was horizontal pleiotropy of instrumental variables.

Results: Our study found genetically predicted GD may increase risk of SLE (OR=1.17, 95% CI 0.99-1.40, p=0.069). Additionally, genetically predicted SLE elevated the risk of developing GD by 15% (OR=1.15, 95% CI 1.05-1.27, p= 0.004). After correcting for possible horizontal pleiotropy by excluding outlier SNPs, the results suggested that GD increased the risk of SLE (OR=1.27, 95% CI 1.09-1.48, p =0.018), while SLE also increased the risk of developing GD (OR=1.13, 95% CI 1.05-1.22, p =0.003).

Conclusion: The findings of the study indicate that there may be a correlation between GD and SLE, with each potentially increasing the risk of the other. These results have important implications for the screening and treatment of patients with co-morbidities in clinical settings, as well as for further research into the molecular mechanisms underlying the relationship between GD and SLE.

KEYWORDS

Graves' disease, systemic lupus erythematosus, GWAS, causal relationship, Mendelian randomization

1 Introduction

Graves' disease(GD) is an autoimmune disease and is the most common cause of hyperthyroidism (1). Its global incidence ranges from 20 to 50 cases per 100,000 individuals, with a prevalence of approximately 1% to 1.5% (2, 3). Graves' disease is an autoimmune disorder that primarily affects specific organs and is susceptible to comorbidities with other autoimmune conditions, including systemic lupus erythematosus (SLE), rheumatoid arthritis, type 1 diabetes, and Addison's disease (4). According to a comprehensive case series report, a notable proportion of patients diagnosed with GD were found to have an additional autoimmune condition, such as SLE, rheumatoid arthritis, multiple sclerosis, celiac disease, type 1 diabetes, sarcoidosis, and Sjogren's syndrome, with a prevalence of 16.7%. Furthermore, 1.5% of patients with GD were observed to have three concurrent autoimmune diseases (4).

SLE is an autoimmune disease characterized by a diverse clinical presentation that may affect one or multiple organs, including the skin, kidneys, joints, and nervous system (5). A multicenter cohort study conducted in China revealed that individuals with GD exhibited a greater susceptibility to developing SLE compared to healthy controls (6). Previous observational studies have indicated a strong correlation between GD and SLE. However, observational studies inevitably have some shortcomings that bias the inference of causality between GD and SLE.

Mendelian randomization (MR) is an analytical approach that utilizes genetic variation as an instrumental variable to draw inferences regarding the causal relationships between variable risk factors that impact population health and target outcome factors (7). The theoretical basis for Mendelian randomization is founded on Mendel's laws of inheritance, which dictate that allele pairs segregate and are randomly distributed to offspring during gamete formation (8). The process is similar to that of a clinical randomized controlled trial, where eligible genetic variants are used as instrumental variables for subsequent causality analysis (9). Our study aims to investigate the causal relationship between GD and SLE using bidirectional Mendelian randomization based on GWAS summary data from Asian populations.

2 Methods and materials

2.1 Data sources

In this study, we extracted SNPs for GD in Asian populations from Biobank Japan (BBJ), the largest non-European population-based biobank, which contains aggregated GWAS data for approximately 200,000 individuals of Asian origin (10). BBJ has compiled GWAS data for approximately 200,000 individuals of Asian origin and has identified 47 target diseases based on their prevalence, mortality rates, and clinical significance in the Japanese population. Patients with these diseases were enrolled and followed up at 66 hospitals in 12 Japanese medical institutions between 2003 and 2018 (10). Patients who did not belong to the Asian population or had undergone bone marrow transplantation were excluded from the study. The target diseases were diagnosed by physicians at the respective partner medical institutions, relying on their observations. The corresponding medical institutions collected both DNA and serum samples from the patients (10, 11).We accessed the summary GWAS data for GD from the Japanese ENcyclopedia of GEnetic associations by Riken (JENGER; http://jenger.riken.jp/en/) and the Medical Research Council Integrative Epidemiology Open GWAS database at the University of Bristol (MRCIEU; https://gwas.mrcieu.ac.uk/).

We obtained SNP information related to SLE in Asian populations from the GWAS published by Wang et al. in 2021, which included 4222 cases and 8431 controls from Han Chinese populations in Hong Kong, Guangzhou and Central China (12). This data was utilized to investigate the causal relationship between GD and SLE in Asian populations. The cases and controls were collected by the University of Hong Kong, Hong Kong Island West Hospital Network, and Guangzhou Women's and Children's Medical Center, with informed consent being obtained from all participants (12). We accessed the summary GWAS data for SLE from the GWAS catalog (https://www.ebi.ac.uk/gwas/) under data number GCST90011866.

2.2 Instrumental variables

Genetic variation as an instrumental variable in Mendelian randomization studies needs to satisfy three basic assumptions: i) genetic variation needs to be strongly correlated with exposure factors; ii) genetic variation must not be correlated with confounding factors; and iii) there is no independent causal pathway between genetic variation and outcome except through exposure (7, 13, 14).

SNPs that were strongly correlated with exposure factors were screened as instrumental variables from publicly available GWAS database using genomic significant level ($p<5\times10^{-8}$) as the threshold (15). To avoid weak instrumental variable bias, the F-statistic of each instrumental variable SNP was calculated in this study to assess the strength of association between SNPs and exposure factors (16). SNPs with F-statistic <10 were considered as weak instrumental variables and were excluded (16). To ensure independence between instrumental variables, we clumped the selected SNPs based on the 1000 genomes reference panel with a clumping window of 10,000 kb and an r^2 threshold of 0.01 (8, 17).

When specific target SNPs were absent in the outcome GWAS dataset, SNPs with high LD with the target SNPs in the exposure dataset were selected as proxy SNPs from the outcome GWAS dataset in this study. To ensure a strong correlation between the proxy SNPs and the target SNPs, a threshold of $r^2 = 0.8$ was set, and the proxy SNPs were subsequently used in place of the target SNPs for subsequent analysis (8).

Palindromic SNPs refer to SNPs with A/T or G/C alleles. In this study, we excluded palindromic SNPs with effect allele frequency between 0.3 and 0.7 to ensure that the reference strand where the palindromic SNP is located can be inferred (8).

2.3 Statistical analysis

In this study, the causal association between GD and SLE was analyzed using the random-effects inverse variance weighted (IVW) method, which can return causal estimates corrected for heterogeneity among instrumental variables (18). Satisfaction of the second and third assumptions needs evaluation of horizontal pleiotropy (8). MR-Egger regression, median weighting, MR-PRESSO, and leave-one-out methods were operated to assess horizontal pleiotropy (8, 19, 20). MR-Egger method can be used to detect and adjust for the presence of horizontal pleiotropy, and intercept of MR-Egger regression can indicate whether horizontal pleiotropy is present (21). Cochran's Q value was calculated to assess the heterogeneity of the causal effects among genetic variants (22). The weighted median method is able to provide a consistent estimate of the causal effect when only 50% of instrumental variables are valid (23). Mendelian Randomization Pleiotropy RESidual Sum and Outlier (MR-PRESSO) is a method for testing and identifying outliers and correcting horizontal pleiotropy (20). The leave-one-out analysis is used to test whether a particular SNP or a group of SNPs has a significant influence on the causal effect estimate and to assess the robustness of the results (8). Estimates of causal effects were reflected using the odds ratio (OR) and 95% confidence interval (CI). The main statistical analyses were performed using R software (version 4.2.1) and the R language packages TwoSampleMR (version 0.5.6), ieugwasr (version 0.1.5). Flow chart of this study is shown in Figure 1.

3 Results

Thirteen SNPs significantly related to GD were extracted from the results of BBJ. Thirty-nine SNPs significantly related to SLE were obtained from summary data of Wang et al. After clumping and removing palindromic SNPs with effect allele frequency between 0.3 and 0.7, 12 SNPs were eligible to analyze causal effect of GD on SLE, and 36 SNPs were eligible to analyze causal effect of SLE on GD. Details of SNPs associated with GD and SLE were shown in Supplementary Tables 1–4 (24).

As shown in Table 1, GD slightly increased the risk of SLE as an exposure factor (OR=1.17, 95% CI 0.99-1.40, p =0.069). Moreover, the median weighting analysis showed a more significant causal relationship (OR=1.27, 95% CI 1.12-1.44, p <0.001). The MR-Egger intercept did not indicate significant horizontal pleiotropy bias (p =0.410). Cochran's Q value revealed heterogeneity among the causal effects derived from different GD instrumental variables (p <0.001). The forest plots, scatter plots, and funnel plots suggested that there was heterogeneity between the effect estimates of instrumental variables for GD on SLE. In sensitivity analysis, the leave-one-out method indicated that removing GD-related SNPs one by one did not significantly alter the causal effect (Figure 2).

As shown in Table 2, SLE increased the risk of GD when GD was the outcome. SLE raised the risk of developing GD by 15% (OR=1.15, 95% CI 1.05-1.27, p =0.004). The weighted median analysis showed a consistent causal effect (OR=1.09, 95% CI 1.01-1.19, p =0.038). The MR-Egger intercept was not significant

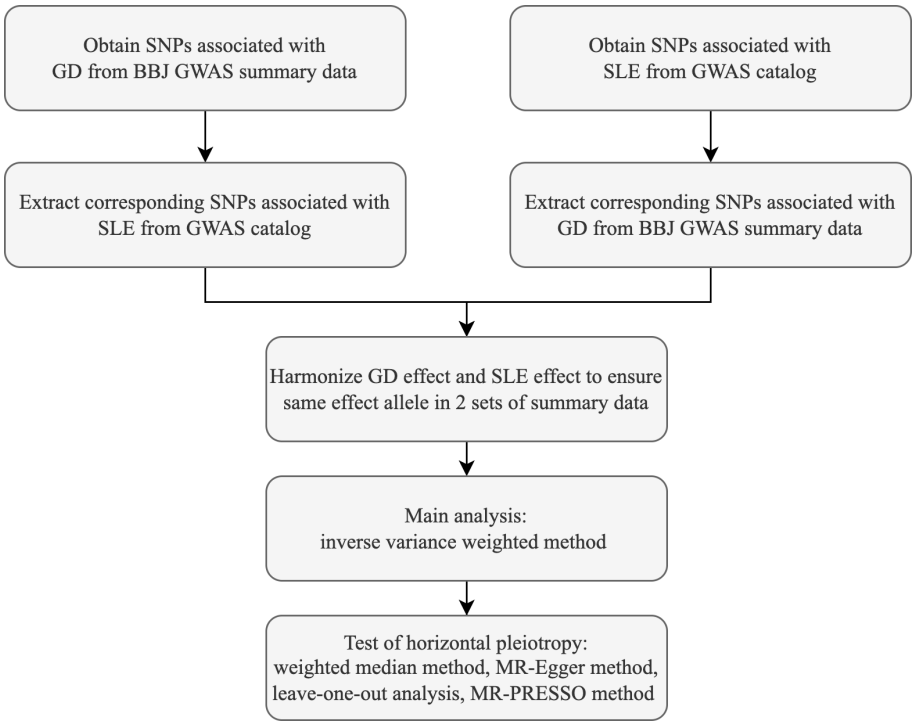

FIGURE 1
Flow chart of the 2-sample mendelian randomization study.

10.3389/fimmu.2024.1273358

TABLE 1 Mendelian randomization estimates of genetically predicted Graves' disease on systemic lupus erythematosus.

Outcome	Method	OR	95% CI	p	Cochran's Q (p)	Intercept (p)
SLE	IVW	1.17	0.99-1.40	0.069	80.50(<0.001)	
	MR-Egger	1.49	0.84-2.61	0.200		-0.07(0.410)
	WM	1.27	1.12-1.44	<0.001		

(p =0.510), and there was heterogeneity among the causal effect estimates derived from different SLE instrumental variables (p <0.001).The forest plot and scatter plot indicated that SNPs rs13213165 and rs244689 had more prominent effects. In sensitivity analysis, the leave-one-out method indicated that removing the SNPs associated with SLE with prominent effects one by one did not significantly change the overall causal effect (Figure 3).

The MR-PRESSO overall test and outlier test suggested that there might be outlier SNPs influencing the causal effect estimates between GD and SLE (Table 3). After correcting for possible horizontal pleiotropy by excluding outlier SNPs, the effect of GD on SLE (Distortion p =0.303) and the causal effect of SLE on GD (Distortion p =0.517) were not significantly different from those before correction (Table 3). The corrected results suggested that GD increased the risk of SLE (OR=1.27, 95% CI 1.09-1.48, p =0.018), while SLE also increased the risk of developing GD (OR=1.13, 95% CI 1.05-1.22, p =0.003).

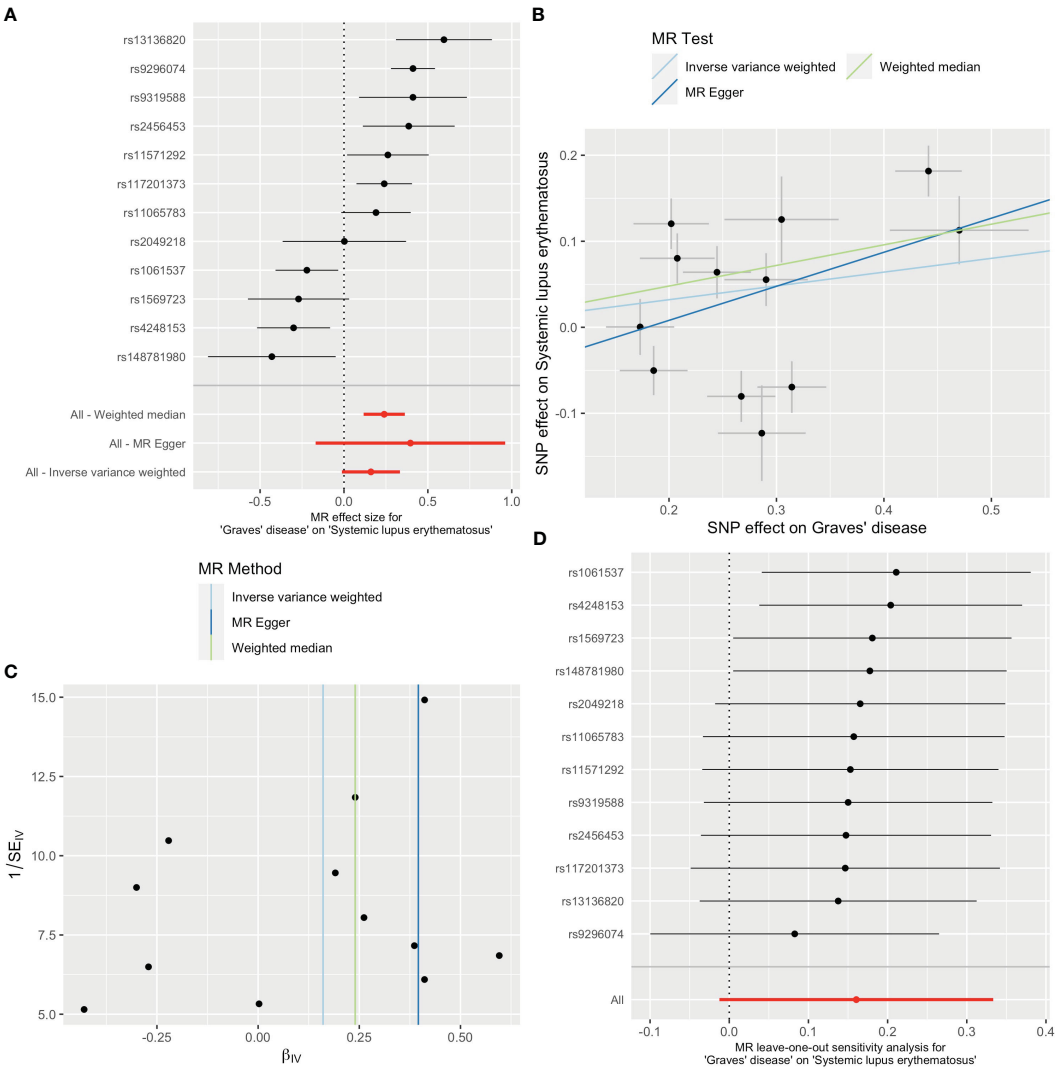

FIGURE 2
Plots of causal estimates of genetically predicted Graves' disease on systemic lupus erythematosus. **(A)** The forest plot. **(B)** The scatter plot. **(C)** The funnel plot. **(D)** The leave-one-out plot.

10.3389/fimmu.2024.1273358

TABLE 2 Mendelian randomization estimates of genetically predicted systemic lupus erythematosus on Graves' disease.

Exposure	Method	OR	95% CI	p	Cochran's Q (p)	Intercept (p)
SLE	IVW	1.15	1.05-1.27	0.004	119.71(<0.001)	
	MR-Egger	1.05	0.79-1.40	0.745		0.03(0.510)
	WM	1.09	1.01-1.19	0.038		

4 Discussion

In this study, we identified a bidirectional causal association between genetically predicted GD and SLE. Prior epidemiological investigations have indicated the co-occurrence of GD and SLE in certain patients, and a multicenter cohort study has reported a higher risk of SLE in individuals with GD compared to those without GD (6). Patients with SLE may exhibit clinical indications of thyroid dysfunction and comorbidity with GD (4, 25). The causal association between GD and SLE found in our study further confirms these previous epidemiological findings.

The development of SLE and GD may be influenced by mutations in HLA genes. A meta-analysis conducted recently revealed that mutations in HLA-DR3 and HLA-DR15 significantly increased the likelihood of developing SLE, thereby indicating the potential role of the HLA-DRB1 gene as a susceptibility gene for SLE (26). A study by Zawadzka-Starczewska et al. also found that HLA-DRB1 gene mutations were associated with the risk of developing GD (27). The

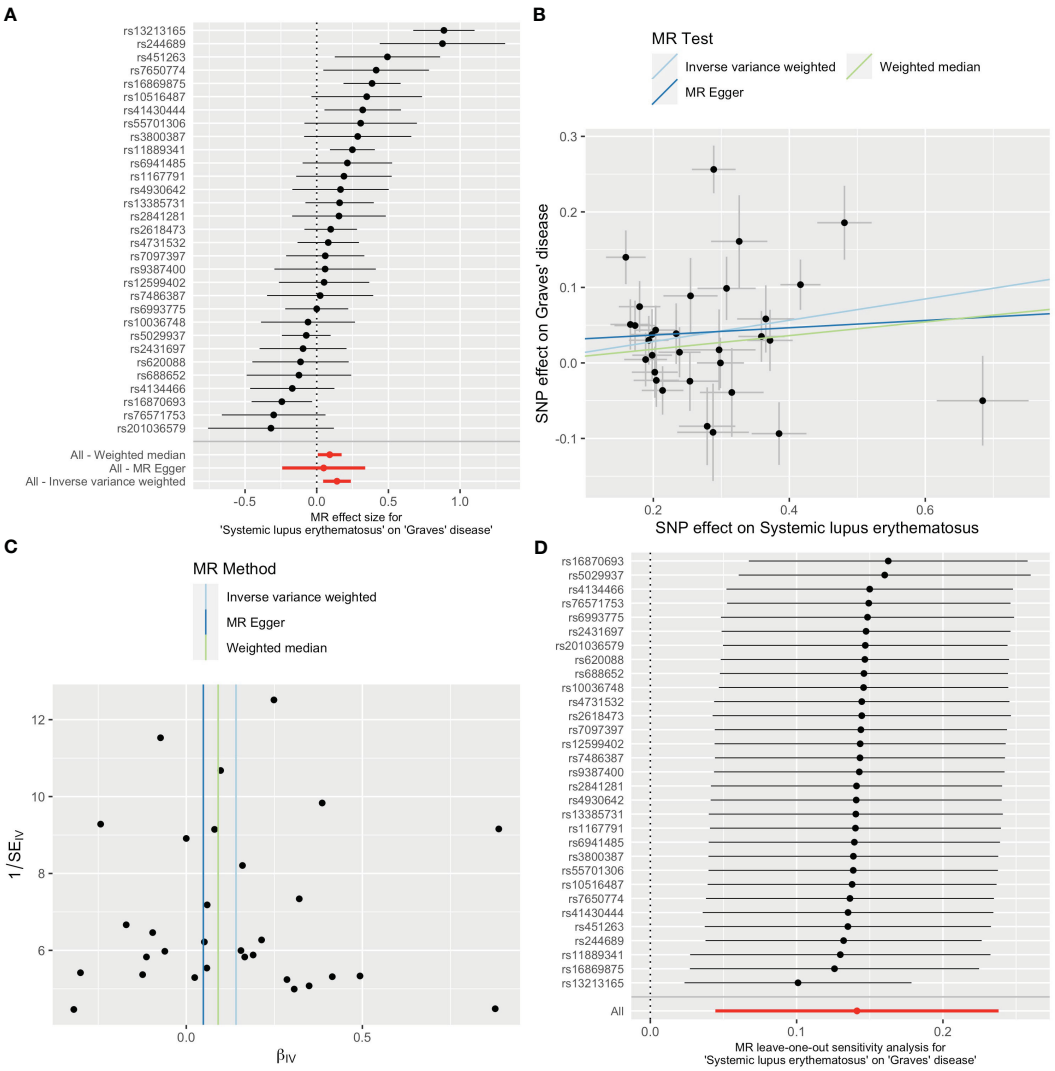

FIGURE 3
Plots of causal estimates of genetically predicted systemic lupus erythematosus on Graves' disease. **(A)** The forest plot. **(B)** The scatter plot. **(C)** The funnel plot. **(D)** The leave-one-out plot.

TABLE 3 MR-PRESSO results of the causal relationship between genetically predicted Graves' disease and systemic lupus erythematosus.

Exposure	Outcome	Global p	Outliers	Original OR (95%CI)	Original p	Corrected OR (95%CI)	Corrected p
GD	SLE	<0.001	4	1.17(0.99-1.39)	0.096	1.27(1.09-1.48)	0.018
SLE	GD	<0.001	2	1.15(1.05-1.27)	0.007	1.13(1.05-1.22)	0.003

presence of mutated HLA genes can result in alterations to the HLA complex on antigen-presenting cells, thereby influencing the interaction between B and T cells. This situation can lead to the dysregulation of self-reactive B cells and the production of autoantibodies, which may serve as mediators of the causal effect of SLE on GD.

In addition to HLA genes, non-HLA genes may also play an important role in the interaction between SLE and GD. Cytotoxic T-lymphocyte-associated protein 4 (CTLA-4) is a protein receptor that functions as an immune checkpoint to downregulate immune responses by binding to ligands CD80 and CD86 on the surface of antigen-presenting cells, thereby regulating T-cell activation and proliferation (28). Mutations in the CTLA-4 gene have been associated with both SLE and GD. A meta-analysis indicated that CTLA-4 gene polymorphisms in Asian populations were associated with the risk of developing SLE (29). A study by Lee et al. found that multiple single nucleotide polymorphisms of CTLA-4 were associated with GD and autoimmune thyroid diseases such as Hashimoto's thyroiditis (30). Mutations in the CTLA-4 gene may lead to a deficiency in regulatory T-cell downregulation of immune responses, resulting in T-cell hyperactivation and thus triggering autoimmune diseases. They may also play a mediating role in the relationship between GD and SLE.

The PTPN22 gene is another common genetic susceptibility locus for GD and SLE. A meta-analysis conducted by Hu et al. suggested that the SNP rs2476601 mutation in the PTPN gene was linked to an elevated risk of developing SLE in European and American populations (31). Further studies suggested that downregulation of PTPN22 mRNA expression levels was associated with higher SLE activity and more severe lupus nephritis (32). A study conducted by Ichimura et al. found a higher susceptibility to GD in a Japanese population with mutations in the PTPN22 gene (33). The presence of polymorphisms in the PTPN22 gene may affect the functions of T, B, and myeloid cells, as well as regulate their cytokine secretion, potentially influencing the onset of SLE. These genetic variations may play a role in the development of autoimmune disorders, including SLE and GD, and may be implicated in the causal relationship between them (34).

Both SLE and GD are characterized by immune regulation abnormalities, which may be closely associated with type I interferon (IFN-I) (35). Type I interferons, including IFN-α, IFN-β, IFN-ϵ, IFN-κ, etc., are cytokines that play crucial roles in inflammation, immune regulation, tumor cell recognition, and T-cell responses. In the context of autoimmune diseases, IFN-I can contribute to the development and progression of SLE by promoting antigen presentation and lymphocyte responses, as well as inducing chemokine expression. They can also promote cell activation and enhance responsiveness to inflammatory factors (36). IFN-I enhances B cell activation, differentiation, proliferation and antibody production, and may induce the expression of thyroid-stimulating hormone receptors. Thus, it may have an impact on the development of GD (37). Several type I interferon-related genes, including STAT4, IRF5, IFIH1, and PLZF, have been found in previous studies to be associated with both GD and SLE (38).

Furthermore, aside from aberrant immune regulation, SLE and GD may share a common pathogenesis with regards to autoantibodies that result in tissue damage. A meta-analysis conducted by Pan et al. indicated that levels of thyroid peroxidase antibodies (TPOAb) and thyroglobulin antibodies (TgAb) were considerably higher in SLE patients compared to the non-affected population, implying a correlation between SLE and autoimmune thyroid disease (39). This is consistent with the causal association results of our study. A study conducted by Lanzolla et al. indicated that the presence of antinuclear antibodies was observed in around 80% of patients diagnosed with GD. This finding suggested that GD may potentially influence the development of SLE through the autoantibody pathway (40). Furthermore, a shared immunological pathway in the development of SLE and GD is suggested by the overlapping presence of specific chemokines and cytokines. Recent researches have highlighted that the interaction between CXCL10 and CXCR3 in the T helper 1 immune response is pivotal in the etiology of both GD and SLE (41, 42). Moreover, it was reported that elevated levels of IL-37 was positively correlated with the concentration of TRAb and the severity of SLE, proposing that IL-37 could play a significant role in the co-occurrence of GD and SLE (43).

In addition, environmental factors may play a role in triggering or exacerbating immune disorders in GD and SLE. A previous study conducted by Parks et al. found that air pollution and dust exposure may elevate the risk of SLE through epigenetic alterations, increased oxidative stress, and increased secretion of systemic inflammatory factors (44). Similarly, a study by Kim et al. in a Korean cohort proposed a potential association between air pollution and aberrant thyroid function in the general populace (45). Changes in the composition of the microbiota are linked to impaired intestinal barrier function and dysregulation of the mucosal immune system, which may be connected to the development of GD and SLE (46, 47). Smoking may also have an impact on the development of SLE and GD through epigenetic and systemic inflammatory responses (48, 49). Infection with some viruses such as EBV and CMV is also associated with the risk of developing SLE and GD (49, 50). The postulated potential mechanism is that EBV persists in B cells and is activated from time to time, possibly by stimulating TRAb-producing B cells to promote TRAb production in

patients with GD (49). On the other hand, both lysed and latent EBV proteins elicit strong T- and B-cell responses and the EBV virus itself induces a series of changes in the body's immune system, which may induce systemic lupus erythematosus (51).

Our study has the following strengths. First, it builds on a large body of previous epidemiological evidence suggesting a co-morbid relationship between GD and SLE. It is the first to explore the causal relationship between GD and SLE at the genetic level using the Mendelian randomization method and to determine the direction of the causal effect. Second, it uses the results of large-scale GWAS studies for analysis and provides a high level of evidence. Third, it extracts GWAS summary data from an Asian population, which has a genetic background similar to ours.

The limitations of this study include following aspects. First, it only analyzes data from the genetic background of Asian populations, and its applicability to European, American and African populations still needs further validation. Second, it does not further analyze the molecular mechanisms of GD and SLE, so more studies are still needed to explore the molecular mechanisms in the causal effects of GD and SLE. This would help to better select targets for screening and treatment.

5 Conclusion

Genetically predicted GD increases the risk of developing SLE, and vice versa. The results of our study provide a new basis for screening and treatment of co-morbidities in clinical practice. Patients with GD who have a longer duration or new non-specific symptoms should be screened for SLE to facilitate timely diagnosis and treatment and avoid delay or exacerbation of the disease. At the same time, it is also necessary to monitor thyroid function during the diagnosis and treatment of SLE, so as to adjust the treatment plan accordingly and ensure the quality of life of patients.

Data availability statement

The original contributions presented in the study are included in the article/Supplementary Material. Further inquiries can be directed to the corresponding authors.

Ethics statement

Ethical approval was not required for the study involving humans in accordance with the local legislation and institutional requirements. Written informed consent to participate in this study was not required from the participants or the participants' legal guardians/next of kin in accordance with the national legislation and the institutional requirements.

Author contributions

WX: Conceptualization, Formal analysis, Methodology, Software, Validation, Visualization, Writing – original draft, Writing – review & editing, Data curation. BL: Conceptualization, Writing – original draft, Writing – review & editing, Data curation, Formal analysis, Methodology, Software, Validation, Visualization. JL: Conceptualization, Formal analysis, Methodology, Validation, Writing – original draft, Writing – review & editing. YY: Validation, Visualization, Writing – original draft. SH: Formal analysis, Methodology, Validation, Visualization, Writing – original draft. HX: Data curation, Supervision, Validation, Visualization, Writing – original draft. DW: Conceptualization, Formal analysis, Funding acquisition, Methodology, Supervision, Validation, Writing – original draft, Writing – review & editing. YL: Conceptualization, Investigation, Project administration, Supervision, Writing – original draft, Writing – review & editing.

Funding

The author(s) declare financial support was received for the research, authorship, and/or publication of this article. This work was supported by 2022 Thyroid Young Doctors Research Program (BJHPA-2022-JZHXZHQNYJ-LCH-07) and National Natural Science Foundation of China (No. 82072956).

Conflict of interest

The authors declare that the research was conducted in the absence of any commercial or financial relationships that could be construed as a potential conflict of interest.

Publisher's note

Supplementary material

The Supplementary Material for this article can be found online at: https://www.frontiersin.org/articles/10.3389/fimmu.2024.1273358/full#supplementary-material

References

1. Smith TJ, Hegedüs L. Graves' Disease. *N Engl J Med* (2016) 375(16):1552–65. doi: 10.1056/NEJMra1510030

2. Zimmermann MB, Boelaert K. Iodine deficiency and thyroid disorders. *Lancet Diabetes Endocrinol* (2015) 3(4):286–95. doi: 10.1016/s2213-8587(14)70225-6

3. Davies TF, Andersen S, Latif R, Nagayama Y, Barbesino G, Brito M, et al. Graves' disease. *Nat Rev Dis Primers* (2020) 6(1):52. doi: 10.1038/s41572-020-0184-y

4. Ferrari SM, Fallahi P, Ruffilli I, Elia G, Ragusa F, Benvenga S, et al. The association of other autoimmune diseases in patients with Graves' disease (with or without ophthalmopathy): Review of the literature and report of a large series. *Autoimmun Rev* (2019) 18(3):287–92. doi: 10.1016/j.autrev.2018.10.001

5. Durcan L, O'Dwyer T, Petri M. Management strategies and future directions for systemic lupus erythematosus in adults. *Lancet* (2019) 393(10188):2332–43. doi: 10.1016/s0140-6736(19)30237-5

6. Lee C, Chen SF, Yang YC, Hsu CY, Shen YC. Association between Graves' disease and risk of incident systemic lupus erythematosus: A nationwide population-based cohort study. *Int J Rheum Dis* (2021) 24(2):240–5. doi: 10.1111/1756-185x.14027

7. Davies NM, Holmes MV, Davey Smith G. Reading Mendelian randomisation studies: a guide, glossary, and checklist for clinicians. *Bmj* (2018) 362:k601. doi: 10.1136/bmj.k601

8. Hemani G, Zheng J, Elsworth B, Wade KH, Haberland V, Baird D, et al. The MR-Base platform supports systematic causal inference across the human phenome. *Elife* (2018) 7:e34408. doi: 10.7554/eLife.34408

9. Zhao SS, Mackie SL, Zheng J. Why clinicians should know about Mendelian randomization. *Rheumatol (Oxford)* (2021) 60(4):1577–9. doi: 10.1093/rheumatology/keab007

10. Nagai A, Hirata M, Kamatani Y, Muto K, Matsuda K, Kiyohara Y, et al. Overview of the BioBank Japan Project: Study design and profile. *J Epidemiol* (2017) 27(3s):S2–s8. doi: 10.1016/j.je.2016.12.005

11. Ishigaki K, Akiyama M, Kanai M, Takahashi A, Kawakami E, Sugishita H, et al. Large-scale genome-wide association study in a Japanese population identifies novel susceptibility loci across different diseases. *Nat Genet* (2020) 52(7):669–79. doi: 10.1038/s41588-020-0640-3

12. Wang YF, Zhang Y, Lin Z, Zhang H, Wang TY, Cao Y, et al. Identification of 38 novel loci for systemic lupus erythematosus and genetic heterogeneity between ancestral groups. *Nat Commun* (2021) 12(1):772. doi: 10.1038/s41467-021-21049-y

13. Burgess S, Thompson SG. Interpreting findings from Mendelian randomization using the MR-Egger method. *Eur J Epidemiol* (2017) 32(5):377–89. doi: 10.1007/s10654-017-0255-x

14. Emdin CA, Khera AV, Kathiresan S. Mendelian randomization. *Jama* (2017) 318 (19):1925–6. doi: 10.1001/jama.2017.17219

15. Lawlor DA, Harbord RM, Sterne JA, Timpson N, Davey Smith G. Mendelian randomization: using genes as instruments for making causal inferences in epidemiology. *Stat Med* (2008) 27(8):1133–63. doi: 10.1002/sim.3034

16. Burgess S, Thompson SG. Avoiding bias from weak instruments in Mendelian randomization studies. *Int J Epidemiol* (2011) 40(3):755–64. doi: 10.1093/ije/dyr036

17. Auton A, Brooks LD, Durbin RM, Garrison EP, Kang HM, Korbel JO, et al. A global reference for human genetic variation. *Nature* (2015) 526(7571):68–74. doi: 10.1038/nature15393

18. Burgess S, Small DS, Thompson SG. A review of instrumental variable estimators for Mendelian randomization. *Stat Methods Med Res* (2017) 26(5):2333–55. doi: 10.1177/0962280215597579

19. Hemani G, Bowden J, Davey Smith G. Evaluating the potential role of pleiotropy in Mendelian randomization studies. *Hum Mol Genet* (2018) 27(R2):R195–r208. doi: 10.1093/hmg/ddy163

20. Verbanck M, Chen CY, Neale B, Do R. Detection of widespread horizontal pleiotropy in causal relationships inferred from Mendelian randomization between complex traits and diseases. *Nat Genet* (2018) 50(5):693–8. doi: 10.1038/s41588-018-0099-7

21. Bowden J, Davey Smith G, Burgess S. Mendelian randomization with invalid instruments: effect estimation and bias detection through Egger regression. *Int J Epidemiol* (2015) 44(2):512–25. doi: 10.1093/ije/dyv080

22. Bowden J, Del Greco MF, Minelli C, Zhao Q, Lawlor DA, Sheehan NA, et al. Improving the accuracy of two-sample summary-data Mendelian randomization: moving beyond the NOME assumption. *Int J Epidemiol* (2019) 48(3):728–42. doi: 10.1093/ije/dyy258

23. Bowden J, Davey Smith G, Haycock PC, Burgess S. Consistent estimation in Mendelian randomization with some invalid instruments using a weighted median estimator. *Genet Epidemiol* (2016) 40(4):304–14. doi: 10.1002/gepi.21965

24. Xian W, Liu B, Li J, Yang Y, Hong S, Xiao H, et al. Supplementary materials for Graves' disease and systemic lupus erythematosus: a Mendelian randomization. *figshare* (2023). doi: 10.6084/m9.figshare.23500653.v1

25. Liu YC, Lin WY, Tsai MC, Fu LS. Systemic lupus erythematosus and thyroid disease - Experience in a single medical center in Taiwan. *J Microbiol Immunol Infect* (2019) 52(3):480–6. doi: 10.1016/j.jmii.2016.11.008

26. Xue K, Niu WQ, Cui Y. Association of HLA-DR3 and HLA-DR15 polymorphisms with risk of systemic lupus erythematosus. *Chin Med J (Engl)* (2018) 131(23):2844–51. doi: 10.4103/0366-6999.246058

27. Zawadzka-Starczewska K, Tymoniuk B, Stasiak B, Lewiński A, Stasiak M. Actual associations between HLA haplotype and Graves' Disease development. *J Clin Med* (2022) 11(9):2492. doi: 10.3390/jcm11092492

28. Syn NL, Teng MWL, Mok TSK, Soo RA. *De-novo* and acquired resistance to immune checkpoint targeting. *Lancet Oncol* (2017) 18(12):e731–e41. doi: 10.1016/s1470-2045(17)30607-1

29. Zhai JX, Zou LW, Zhang ZX, Fan WJ, Wang HY, Liu T, et al. CTLA-4 polymorphisms and systemic lupus erythematosus (SLE): a meta-analysis. *Mol Biol Rep* (2013) 40(9):5213–23. doi: 10.1007/s11033-012-2125-7

30. Lee HJ, Li CW, Hammerstad SS, Stefan M, Tomer Y. Immunogenetics of autoimmune thyroid diseases: A comprehensive review. *J Autoimmun* (2015) 64:82–90. doi: 10.1016/j.jaut.2015.07.009

31. Hu LY, Cheng Z, Zhang B, Yin Q, Zhu XW, Zhao PP, et al. Associations between PTPN22 and TLR9 polymorphisms and systemic lupus erythematosus: a comprehensive meta-analysis. *Arch Dermatol Res* (2017) 309(6):461–77. doi: 10.1007/s00403-017-1745-0

32. Román-Fernández IV, MaChado-Contreras JR, Muñoz-Valle JF, Cruz A, Salazar-Camarena DC, Palafox-Sánchez CA. Altered PTPN22 and IL10 mRNA expression is associated with disease activity and renal involvement in systemic lupus erythematosus. *Diagnostics (Basel)* (2022) 12(11):.2859. doi: 10.3390/diagnostics12112859

33. Ichimura M, Kaku H, Fukutani T, Koga H, Mukai T, Miyake I, et al. Associations of protein tyrosine phosphatase nonreceptor 22 (PTPN22) gene polymorphisms with susceptibility to Graves' disease in a Japanese population. *Thyroid* (2008) 18(6):625–30. doi: 10.1089/thy.2007.0353

34. Tizaoui K, Terrazzino S, Cargnin S, Lee KH, Gauckler P, Li H, et al. The role of PTPN22 in the pathogenesis of autoimmune diseases: A comprehensive review. *Semin Arthritis Rheum* (2021) 51(3):513–22. doi: 10.1016/j.semarthrit.2021.03.004

35. Pan L, Lu MP, Wang JH, Xu M, Yang SR. Immunological pathogenesis and treatment of systemic lupus erythematosus. *World J Pediatr* (2020) 16(1):19–30. doi: 10.1007/s12519-019-00229-3

36. Ivashkiv LB, Donlin LT. Regulation of type I interferon responses. *Nat Rev Immunol* (2014) 14(1):36–49. doi: 10.1038/nri3581

37. Crow MK. Pathogenesis of systemic lupus erythematosus: risks, mechanisms and therapeutic targets. *Ann Rheum Dis* (2023) 82(8):999-1014. doi: 10.1136/ard-2022-223741

38. Chen S, Pu W, Guo S, Jin L, He D, Wang J. Genome-wide DNA methylation profiles reveal common epigenetic patterns of interferon-related genes in multiple autoimmune diseases. *Front Genet* (2019) 10:223. doi: 10.3389/fgene.2019.00223

39. Pan XF, Gu JQ, Shan ZY. Patients with systemic lupus erythematosus have higher prevalence of thyroid autoantibodies: a systematic review and meta-analysis. *PloS One* (2015) 10(4):e0123291. doi: 10.1371/journal.pone.0123291

40. Lanzolla G, Puccinelli L, Giudetti M, Comi S, Menconi F, Maglionico MN, et al. Anti-nuclear autoantibodies in Graves' disease and Graves' orbitopathy. *J Endocrinol Invest* (2023) 46(2):337–44. doi: 10.1007/s40618-022-01906-3

41. Antonelli A, Ferrari SM, Giuggioli D, Ferrannini E, Ferri C, Fallahi P. Chemokine (C-X-C motif) ligand (CXCL)10 in autoimmune diseases. *Autoimmun Rev* (2014) 13(3):272–80. doi: 10.1016/j.autrev.2013.10.010

42. Antonelli A, Fallahi P, Elia G, Ragusa F, Paparo SR, Ruffilli I, et al. Graves' disease: Clinical manifestations, immune pathogenesis (cytokines and chemokines) and therapy. *Best Pract Res Clin Endocrinol Metab* (2020) 34(1):101388. doi: 10.1016/j.beem.2020.101388

43. Xu WD, Zhao Y, Liu Y. Insights into IL-37, the role in autoimmune diseases. *Autoimmun Rev* (2015) 14(12):1170–5. doi: 10.1016/j.autrev.2015.08.006

44. Parks CG, de Souza Espindola Santos A, Barbhaiya M, Costenbader KH. Understanding the role of environmental factors in the development of systemic lupus erythematosus. *Best Pract Res Clin Rheumatol* (2017) 31(3):306–20. doi: 10.1016/j.berh.2017.09.005

45. Kim HJ, Kwon H, Yun JM, Cho B, Park JH. Association between exposure to ambient air pollution and thyroid function in Korean adults. *J Clin Endocrinol Metab* (2020) 105(8):dgaa338. doi: 10.1210/clinem/dgaa338

46. Khan MF, Wang H. Environmental exposures and autoimmune diseases: contribution of gut microbiome. *Front Immunol* (2019) 10:3094. doi: 10.3389/fimmu.2019.03094

47. Biscarini F, Masetti G, Muller I, Verhasselt HL, Covelli D, Colucci G, et al. Gut microbiome associated with Graves disease and Graves orbitopathy: the INDIGO multicenter European study. *J Clin Endocrinol Metab* (2023) 108(8):2065–77. doi: 10.1210/clinem/dgad030

48. Barbhaiya M, Costenbader KH. Environmental exposures and the development of systemic lupus erythematosus. *Curr Opin Rheumatol* (2016) 28(5):497–505. doi: 10.1097/bor.0000000000000318

49. Antonelli A, Ferrari SM, Ragusa F, Elia G, Paparo SR, Ruffilli I, et al. Graves' disease: Epidemiology, genetic and environmental risk factors and viruses. *Best Pract Res Clin Endocrinol Metab* (2020) 34(1):101387. doi: 10.1016/j.beem.2020.101387

50. Mak A, Tay SH. Environmental factors, toxicants and systemic lupus erythematosus. *Int J Mol Sci* (2014) 15(9):16043–56. doi: 10.3390/ijms150916043

51. Quaglia M, Merlotti G, De Andrea M, Borgogna C, Cantaluppi V. Viral infections and systemic lupus erythematosus: new players in an old story. *Viruses* (2021) 13(2):277. doi: 10.3390/v13020277

frontiers | Frontiers in Immunology

TYPE Original Research
PUBLISHED 29 January 2024
DOI 10.3389/fimmu.2024.1273559

OPEN ACCESS

EDITED BY
Francesca Wanda Rossi,
University of Naples Federico II, Italy

REVIEWED BY
Gianluca Moroncini,
Marche Polytechnic University, Italy
Swati Bhattacharyya,
University of Michigan, United States

*CORRESPONDENCE
Cheng Zhao
zhaochenggx@163.com
Xiaoning Zhong
xnzhong101@sina.com

RECEIVED 06 August 2023
ACCEPTED 12 January 2024
PUBLISHED 29 January 2024

CITATION
Zheng L, Wu Q, Chen S, Wen J, Dong F, Meng N, Zeng W, Zhao C and Zhong X (2024) Development and validation of a new diagnostic prediction model of ENHO and NOX4 for early diagnosis of systemic sclerosis.
Front. Immunol. 15:1273559.
doi: 10.3389/fimmu.2024.1273559

Development and validation of a new diagnostic prediction model of ENHO and NOX4 for early diagnosis of systemic sclerosis

Leting Zheng[1], Qiulin Wu[2], Shuyuan Chen[1], Jing Wen[1], Fei Dong[1], Ningqin Meng[1], Wen Zeng[1], Cheng Zhao[1*] and Xiaoning Zhong[3*]

[1]Department of Rheumatology and Clinical Immunology, The First Affiliated Hospital of Guangxi Medical University, Nanning, China, [2]Department of General Surgery, The Second Affiliated Hospital of Guangxi Medical University, Nanning, China, [3]Department of Respiratory and Critical Care Medicine, the First Affiliated Hospital of Guangxi Medical University, Nanning, China

Objective: Systemic sclerosis (SSc) is a chronic autoimmune disease characterized by fibrosis. The challenge of early diagnosis, along with the lack of effective treatments for fibrosis, contribute to poor therapeutic outcomes and high mortality of SSc. Therefore, there is an urgent need to identify suitable biomarkers for early diagnosis of SSc.

Methods: Three skin gene expression datasets of SSc patients and healthy controls were downloaded from Gene Expression Omnibus (GEO) database (GSE130955, GSE58095, and GSE181549). GSE130955 (48 early diffuse cutaneous SSc and 33 controls) were utilized to screen differentially expressed genes (DEGs) between SSc and normal skin samples. Least absolute shrinkage and selection operator (LASSO) regression and support vector machine recursive feature elimination (SVM-RFE) were performed to identify diagnostic genes and construct a diagnostic prediction model. The results were further validated in GSE58095 (61 SSc and 36 controls) and GSE181549 (113 SSc and 44 controls) datasets. Receiver operating characteristic (ROC) curves were applied for assessing the level of diagnostic ability. Reverse transcription-quantitative polymerase chain reaction (RT-qPCR) was used to verify the diagnostic genes in skin tissues of out cohort (10 SSc and 5 controls). Immune infiltration analysis were performed using CIBERSORT algorithm.

Results: A total of 200 DEGs were identified between SSc and normal skin samples. Functional enrichment analysis revealed that these DEGs may be involved in the pathogenesis of SSc, such as extracellular matrix remodeling, cell-cell interactions, and metabolism. Subsequently, two critical genes (ENHO and NOX4) were identified by LASSO and SVM-RFE. ENHO was found down-regulated while NOX4 was up-regulated in skin of SSc patients and their expression levels were validated by above three datasets and our cohort. Notably, these differential expressions were more pronounced in patients with diffuse cutaneous SSc than in those with limited cutaneous SSc. Next, we developed a novel diagnostic model for SSc using ENHO and NOX4, which

demonstrated strong predictive power in above three cohorts and in our own cohort. Furthermore, immune infiltration analysis revealed dysregulated levels of various immune cell subtypes within early SSc skin specimens, and a negative correlation was observed between the levels of ENHO and Macrophages M1 and M2, while a positive correlation was observed between the levels of NOX4 and Macrophages M1 and M2.

Conclusion: This study identified ENHO and NOX4 as novel biomarkers that can be serve as a diagnostic prediction model for early detection of SSc and play a potential role in the pathogenesis of the disease.

KEYWORDS

systemic sclerosis, prediction model, machine learning, ENHO, NOX4, macrophage

Introduction

Systemic sclerosis (SSc) is a chronic connective tissue disease characterized by the fibrosis of skin and visceral organ affecting various internal organs such as the lungs, hearts, gastrointestinal tract and kidneys. Subset of SSc includes diffuse cutaneous SSc (dcSSc) and limited cutaneous SSc (lcSSc) (1). The global prevalence of SSc ranges from approximately 5 to 50 cases per 100,000 individuals (2). Despite its relatively low prevalence, due to no effective treatment available, SSc exhibits the highest mortality rate among all connective tissue diseases, with a five-year survival rate of 74.9%, which plummets to 40% in patients with concurrent visceral involvement, with pulmonary hypertension and pulmonary fibrosis being the main causes of death (3, 4). The pathogenesis of SSc remains unknown, however, potential mechanisms include immune dysregulation, vasculopathy and excessive production and deposition of extracellular matrix (5). Notably, immune dysregulation and inflammation serve as the initiating and central factor in early stage of SSc (6–9). Abnormal activation of various immune cells, such as dendritic cells, macrophages, T and B lymphocytes, along with the secretion of diverse cytokines and autoantibodies contribute to the over-activation of fibroblasts. This process leads to increased synthesis of extracellular matrix and subsequent fibrosis of skin and visceral organs. Since fibrosis is largely untreatable, it is mandatory to start the treatment before fibrosis develops.

Different from advanced SSc, which mainly presents fibrosis, early SSc is characterized by inflammation and is considered to be the window of opportunity for effective treatment of SSc (10). For example, of the 7 patients treated with mycophenolate mofetil, all 4 patients with improved skin were in the inflammatory subgroup, and those identified as fibroproliferative subgroup before treatment did not have improvement (11). Meanwhile, four of the five dcSSc patients who had an improvement with abatacept treatment were in the inflammatory subgroup at the baseline (12). Whether patients can be treated in time before collagen deposition occurs, the key is early diagnosis of SSc. However, the diagnosis of early SSc remains a challenge for doctors (13). SSc has broad clinical heterogeneity, ranging from a milder subset to a more rapidly extensive fibrosis of skin and visceral organs. Additionally, most of the typical signs and symptoms are absent in early stage SSc. The American Rheumatism Association(ARA) preliminary criteria (1980) for SSc were ill-suited to identify an early SSc and the limited subset (14). The new 2013 ACR/EULAR classification criteria for SSc presents a higher specificity and sensitivity compared to the 1980 ARA criteria, however, those with a higher risk of developing SSc, characterized by Raynaud's phenomenon(RP), puffy fingers, specific autoantibodies, and/or capillaroscopic specific abnormalities, could not achieve a score sufficient to be classified as SSc (15, 16). Therefore, even new 2013 ACR/EULAR classification criteria may lead to a possible late recognition of SSc. Most SSc patients present with RP as the initial symptom, however, RP is widely diffuse in the population, and 90% of cases are idiopathic (17, 18). Moreover, RP is not exclusive to SSc, as it is also seen in other connective tissue diseases (19). In addition, early identification and diagnosis of SSc are also important for drug clinical trials, which can help select appropriate SSc patients for therapeutic clinical trials and improve the efficacy of trials. Whereas the optimal design of clinical trials to test new therapeutics for SSc has suffered from difficulties in patient selection (20). Therefore, the need for early diagnosis of SSc is largely unmet.

Transcriptomics investigations entail the comprehensive profiling of all transcripts within a tissue or cell, thereby unveiling alterations in gene expression specific to certain disease states. By employing high-throughput sequencing technologies such as RNA-seq, researchers can acquire gene expression data spanning the entire genome and conduct differential gene expression analyses to pinpoint disease-associated markers (21, 22). These differentially expressed genes offer valuable insights into disease mechanisms and hold potential as diagnostic and therapeutic targets. Given the escalating magnitude of bioinformatics data, the integration of machine learning and artificial intelligence has gained increasing prominence in the identification of disease biomarkers (23, 24).

These methodologies possess the capacity to effectively handle vast amounts of genomic data and unveil. intricate patterns and associations. Notably, machine learning algorithms have been employed to construct prediction models that leverage genomic data and clinical features, thereby aiding in disease diagnosis and treatment decision-making (25). Recent investigations have utilized machine learning techniques to identify novel biomarkers for various diseases including SSc. However, the application of machine learning methods to construct diagnostic prediction models specific to SSc is currently rarely reported (26, 27). Furthermore, in the context of SSc, the immune microenvironment undergoes abnormal changes in immune cells, inflammatory cytokines, autoantibodies and extracellular matrix components, ultimately fostering fibrosis and organ damage (28). Consequently, it is imperative to explore the pivotal genes implicated in immune infiltration for the treatment of SSc.

In this study, we initially screened differentially expressed genes (DEGs) of skin samples from early dcSSc patients through analysis of GSE130955 dataset. Subsequently, we employed LASSO regression analysis and the machine learning SVM approach to identify diagnostic genes and construct a diagnostic prediction model. Importantly, we successfully developed a novel diagnostic model, which demonstrated strong predictive power in screening SSc in GSE130955, GSE58095, GSE181549 datasets and our cohort. Furthermore, we validated the differential expression of diagnosis genes in above three cohorts and our cohort. Lastly, we conducted an analysis to explore the potential association between the critical genes and the immune microenvironment of SSc.

Materials and methods

Data acquisition and processing

To access the necessary data, we utilized the GEO database maintained by the National Center for Biotechnology Information (NCBI), which offers an open data access platform containing high-throughput sequencing gene expression profiling data. Specifically, we obtained three distinct SSc skin tissue gene expression data from GEO datasets, namely GSE130955, GSE58095, and GSE181549, which were subsequently downloaded for further analysis. GSE130955 encompassed a cohort of 48 early diffuse SSc samples and 33 normal samples, while GSE58095 consisted of 61 SSc samples (dcSSc=43, lcSSc=18) and 36 normal samples, and GSE181549 comprised 113 SSc samples (dcSSc=70, lcSSc=43) and 44 normal samples. In this study, the GSE130955 cohort was utilized as the training cohort, while the GSE58095 and GSE181549 cohorts were employed for the validation purposes.

Data processing and differentially expressed genes screening

Data processing and screening for DEGs were conducted using the limma package in the R programming language. This involved correcting background errors, normalizing arrays, and performing differential expression analysis on a total of 48 SSc skin samples and 33 normal skin samples in GSE130955. The cutoff values for DEGs were set as having a log fold change (FC) greater than 1 and an adjusted false discovery rate P lower than 0.05.

Functional enrichment analysis

Utilizing the clusterProfiler software package allowed for the completion of both the Gene Ontology (GO) analysis and the Kyoto Encyclopedia of Genes and Genomes (KEGG) pathway enrichment investigations. This was carried out in order to ascertain the possible activities and pathways in which DEGs are engaged. The outcomes of the study were presented using the visualization module of clusterProfiler since it was the most effective way to do so. In order to carry out disease ontology (DO) enrichment analysis on DEGs, the "clusterProfiler" and DOSE packages found in R were put to use. For the purpose of these studies, a significance level of P 0.05 was used to serve as the cut-off parameter. When comparing the SSc group to the control group, gene set enrichment analysis, also known as GSEA, was employed in order to ascertain which functional terms were more significant than others. We used the "c2.cp.kegg.v7.0.symbols.gmt" file that was found in the Molecular Signatures Database (MSigDB) as the gene set that served as our reference.

Candidate diagnostic biomarkers

Various machine learning methodologies were explored to identify relevant prognostic markers and generate disease progression forecasts. In the realm of regression analysis, the LASSO approach, which employs regularization to enhance prediction accuracy by reducing the number of exercises in the training set, was employed. The LASSO regression analysis was conducted using the "glmnet" package in R. Additionally, the support vector machine (SVM), a widely recognized supervised machine learning method applicable to both classification and regression tasks, was utilized. To avoid overfitting and ensure accurate results, an RFE approach was employed to select the most suitable genes from the meta-data cohort. Consequently, support vector machine recursive feature elimination (SVM-RFE) was utilized to identify the optimal features for discriminating between different groups. To further validate the expression levels of potential genes, we employed the datasets GSE58095 and GSE181549. The study was expanded to include the overlapping genes that were found as a consequence of employing each of these methodologies simultaneously. In addition, using the predict function that can be found in the glm package of the R programming language, a diagnostic model that was developed using two marker genes was completed. This model was based on the results of the analysis. After that, predictions were created by applying this model to the various types of samples that were contained inside the GSE130955 dataset. In a manner that was comparable to the illustration that came before it, ROC curves were applied for assessing the level of diagnostic ability offered by the novel diagnostic model.

CIBERSORT-based immune infiltration analysis

The utilization of immune cell deconvolution, a technique based on gene expression profiling, offers a promising alternative to flow cytometry for quantifying immune cells in bulk tissues. Notably, in comparison to flow cytometry, the deconvolution method provides additional details of biological processes and enables retrospective analysis of previous RNA sequencing data available in GEO repositories. Therefore, In this study, the CIBERSORT deconvolution was utilized to quantify the infiltration of 22 immune cells in 48 early SSc skin samples and 33 normal skin samples in GSE130955, facilitating a comparative assessment. To visually represent the distribution of immune cell proportions in each sample, boxplots were generated. The green color denotes the proportion of immune cells in normal samples, while the red color represents the proportion in SSc samples. Furthermore, a nortest analysis, specifically an analysis of variance test, was conducted to evaluate the conformity of the data to a normal distribution. The data were subjected to the t-test method to assess the statistical significance of the results, following confirmation of adherence to a normal distribution. The outcomes of this analysis are presented in the uppermost section of the figure. For correlation analysis and visualization of the 22 distinct immune cell types infiltrating the tissue, the "corrplot" tool in R was employed. Both tasks were executed within the R environment. To depict variations in immune cell infiltration between the SSc and control samples, violin plots were generated using the "vioplot" package in R. These disparities were observed upon comparing the SSc skin samples with the control skin samples.

Patients and healthy controls

The forearm skin tissue biopsies were obtained from 10 individuals newly diagnosed with dcSSc in accordance with the 2013 criteria established by the American College of Rheumatology (ACR)/European League of Rheumatology (EULAR), including 7 females and 3 males, with a average age of 54.3 ± 9.9 years. Those patients were admitted to the Department of Rheumatology and clinical Immunology at the First Affiliated Hospital of Guangxi Medical University between 2021 and 2023. As a control group, forearm skin tissue biopsies were obtained from 5 individuals of matching age and sex who had undergone internal fixation of forearm fractures for nail removal, including 3 females and 2 males, with a average age of 48 ± 9.03 years. The research protocol adhered to ethical guidelines and was approved by the Ethics Committee of the First Affiliated Hospital of Guangxi Medical University. All participants provided informed consent in writing.

Real-time quantitative polymerase chain reaction

Isolation of total RNA was achieved using TRIzol Reagent (Invitrogen, Carlsbad, CA, USA). Subsequently, complementary DNA synthesis was performed using the PrimeScriptTM RT Master Mix kit (TaKaRa BIO, Shiga, Japan).Gene expression analysis was conducted using the SYBR Green PCR Kit (TaKaRa) in conjunction with the ABI Prism 7900HT sequence detector. The 2 Ct approach was employed for data analysis, with the GAPDH gene serving as a reference control. Biological replicates were conducted three times. The primer sequences used in our study are listed below: human ENHO forward 5'-CCATTCTCGCTCTGCCGAC-3', reverse 5'-CAAGCTGGCTAGACTCTGGG'; human NOX4 forward 5'-TGAATCAGATGATGGTCTACACTTG-3', reverse 5'-AGTGGTCCAAA GGCTTAACATTCC-3'.

Statistical analysis

All data were processed using R language (version 4.0.2) and statistical analyses were performed using corresponding R package. The unpaired, two-tailed Student's t-test was employed to assess group differences. Receiver operating characteristic (ROC) analysis was utilized to evaluate the diagnostic relevance of essential genes in SSc samples. Differences were deemed to be significant whenever p was found to be less than 0.05.

Results

Identification of DEGs in SSc

In this study, a retrospective analysis was conducted on a dataset (GSE130955) comprising a total of 48 early dcSSc skin samples and 33 normal skin samples. The samples were categorized into SSc and normalgroups, and a comparative analysis was performed. Differential expression analysis was carried out using the limma tool, resulting in the identification of 200 DEGs. Among these DEGs, 163 genes were upregulated, while 37 genes were downregulated (Figures 1A, B). Correlation analysis was performed on 56 DEGs with a log fold change (FC) greater than 1.5, as depicted in Figure 1C.

Functional correlation analysis

To investigate the potential functional roles of 200 DEGs in SSc, a functional correlation analysis was conducted. GO analysis revealed that the 200 DEGs were primarily enriched in processes such as receptor-mediated endocytosis, humoral immune response, extracellular matrix organization, endoplasmic reticulum lumen, collagen-containing extracellular matrix, extracellular structure organization, collagen trimer, extracellular matrix structural constituent, antigen binding and glycosaminoglycan binding (Figure 2A). Additionally, KEGG analysis indicated that the 200 DEGs were predominantly associated with ECM-receptor interaction, focal adhesion, phagosome, protein digestion and absorption, malaria and amoebiasis (Figure 2B). DO enrichment analyses revealed that 200 DEGs were mainly related to lung disease, kidney disease, urinary system disease, obesity,

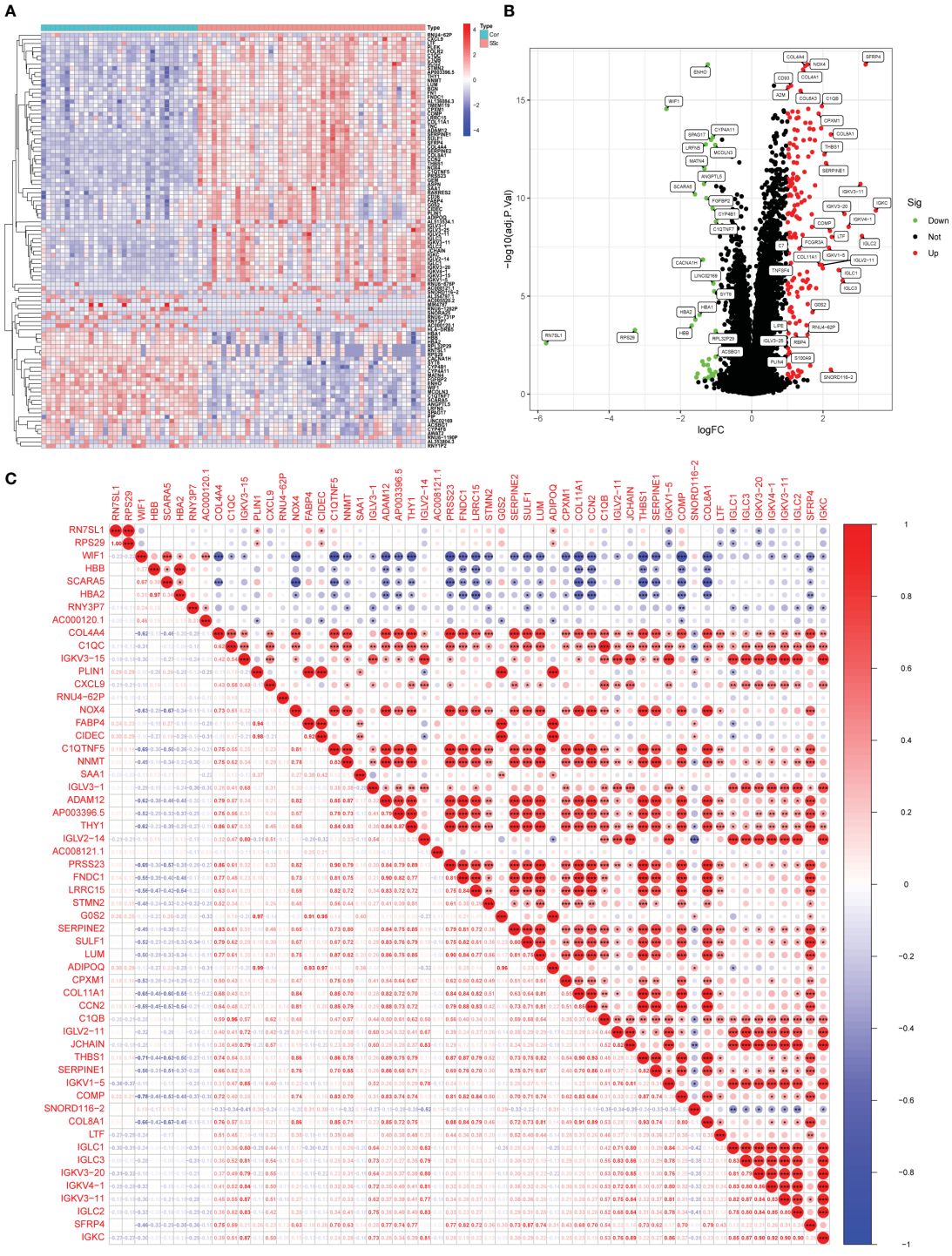

FIGURE 1
Identification of d DEGs between SSc skin specimens and normal skin specimens. **(A, B)** The expressing pattern of 200 DEGs were shown in Heat map and volcano plot. **(C)** The correlation analysis of 56 DEGs with log FC >1.5. *<0.05, **<0.01, ***<0.001..

overnutrition and nutrition disease (Figure 2C). Subsequently, GSEA assays were conducted to further investigate the enriched pathways in the SSc group. The results demonstrated that the enriched pathways mainly involved chemokine signaling, cytokine-cytokine receptor interaction, ECM receptor interaction, focal adhesion, and natural killer cell-mediated cytotoxicity (Figure 2D).

Identification and validation of diagnostic feature biomarkers

Moving forward, the study aimed to identify and validate diagnostic feature biomarkers. Two separate algorithms were employed for this purpose. Firstly, the DEGs were narrowed down

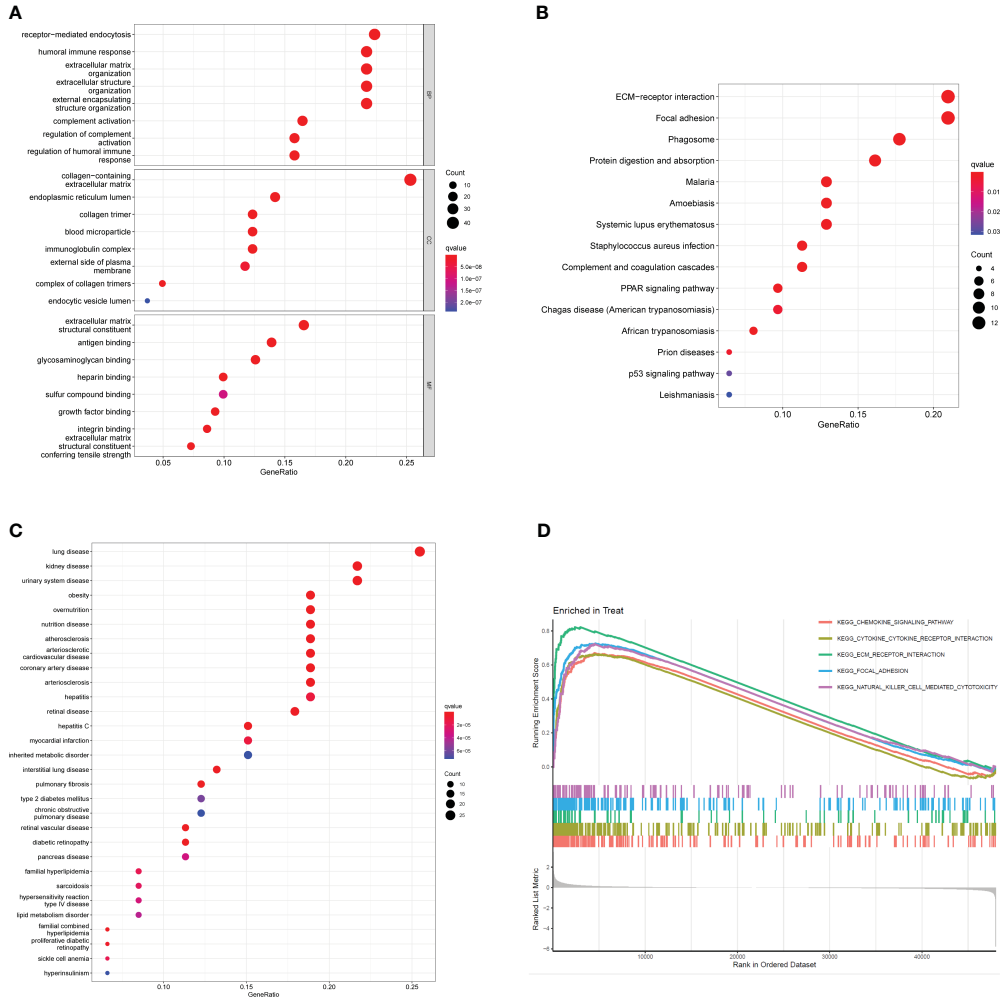

FIGURE 2
Functional analysis based on 200 DEGs. **(A)** Significantly enriched GO terms of DEGs. **(B)** Significant KEGG pathway terms of DEGs. **(C)** Disease ontology enrichment analysis of 200 DEGs between SSc skin specimens and control skin specimens. **(D)** Enrichment analyses via GSEA.

using the LASSO regression method, resulting in the identification of 19 potential diagnostic biomarkers for SSc (Figure 3A). The association between these 19 genes was analyzed and presented in Figure 3B. Additionally, the Support Vector Machine Recursive Feature Elimination (SVM-RFE) methodology was applied, leading to the recognition of a subset of two features that were shared by the DEGs (Figure 3C). Ultimately, the two overlapping features, namely ENHO and NOX4, were selected as the final diagnostic biomarkers (Figure 3D). Furthermore, the expression and diagnostic value of ENHO and NOX4 were analyzed in the GSE130955, GSE58095 and GSE181549 datasets. ENHO expression levels were found to be significantly decreased in SSc specimens compared to normal specimens. Notably, ENHO demonstrated a strong predictive ability in distinguishing SSc specimens from normal specimens in various datasets, including GSE130955 (Figure 4A), GSE58095 (Figure 4B), GSE181549 (Figure 4C) and our own cohorts (Figure 4D). Similarly, we observed that NOX4 expression was markedly increased in SSc samples compared to normal samples. Furthermore, NOX4 exhibited a strong predictive ability in discriminating SSc samples from normal samples in GSE130955 (Figure 4A), GSE58095 (Figure 4B), GSE181549 (Figure 4C) and our own cohorts (Figure 4D). Next, we conducted a comparative analysis of ENHO and NOX4 expression levels in the skin of dcSSc and lcSSc subgroups, utilizing data obtained from the GSE58095 and GSE181549 datasets. In the smaller dataset GSE58095 (43 dcSSc *vs* 18 lcSSc), no difference in ENHO expression was observed between two subgroups. However, in the relatively larger dataset GSE181549 (70 dcSSc *vs* 43 lcSSc), a significant decrease in ENHO expression was evident in dcSSc when compared to lcSSc (Figure 5A). Conversely, the expression of NOX4 was significantly higher in the skin of dcSSc patients in both datasets, as opposed to lcSSc patients (Figure 5B). Subsequently, a diagnostic model was developed utilizing ENHO and NOX4. The diagnostic value of this novel model was further validated in multiple datasets, including GSE130955 (Figure 6A), GSE58095 (Figure 6B), GSE181549 (Figure 6C) and our won cohort (Figure 6D), with all AUC>0.7.

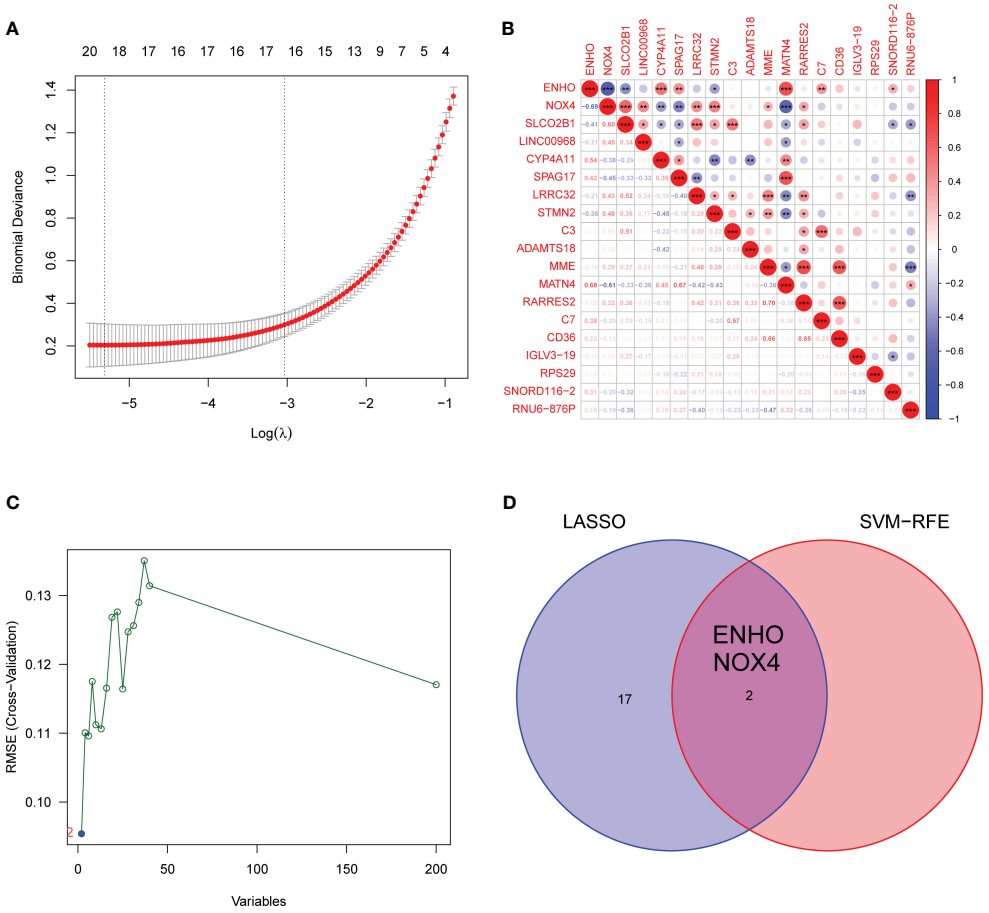

FIGURE 3
Identification of diagnostic genes for SSc diagnosis. **(A)** LASSO model. **(B)** The correlation analysis of 19 diagnostic genes by LASSO. *<0.05, **<0.01, ***<0.001. **(C)** A plot of biomarkers selection via SVM-RFE methods. **(D)** Venn diagram demonstrating two diagnostic markers (ENHO and NOX4) shared by LASSO and SVM-RFE methods.

Association between ENHO and NOX4 and CIBERSORT-based immune cells

Figure 7A presents a comprehensive visualization of the 22 immune cell subtypes based on CIBERSORT deconvolution that infiltrated in early dcSSc skin specimens and normal skin specimens. Furthermore, we investigated the potential correlations among different immune cell subtypes, as depicted in Figure 7B. Significantly, our findings revealed dysregulated levels of various immune cell subtypes within SSc skin specimens. Noteworthy alterations were observed in Monocytes, Macrophages M1, and Macrophages M2, which displayed substantial increases in the skin of individuals with early dcSSc. Conversely, naïve CD4 T cells, resting CD4 memory T cells, resting Dendritic cells, and resting Mast cells exhibited marked reductions in early dcSSc skin when compared to control samples. Furthermore, there was a tendency towards increased levels of naive B cells and plasma cells in SSc, although statistical significance was not observed (Figure 7C). Moreover, we conducted an analysis to explore the association between ENHO and NOX4 expression levels and CIBERSORT-based immune cells. Importantly, our results demonstrated a positive correlation between ENHO levels and resting Mast cells, resting Dendritic cells, resting CD4 memory T cells, and naïve CD4 T cells. Conversely, ENHO levels were found to be negatively associated with activated NK cells, naïve B cells, Monocytes, gamma delta T cells, Macrophages M2, and Macrophages M1 (Figure 8 and Figure 9A). Furthermore, our investigation revealed a positive correlation between NOX4 levels and Macrophages M1, Macrophages M2, gamma delta T cells, Monocytes, activated NK cells, and memory B cells. Conversely, NOX4 levels were found to be negatively associated with naïve CD4 T cells, resting Mast cells, and resting Dendritic cells (Figure 10 and Figure 9B).

Discussion

The therapeutic management of SSc has been challenging, primarily attributed to the complex pathogenesis and delayed detection of the disease. In its initial stages, SSc is characterized by inflammatory processes in affected tissues, which gradually subside as the disease advances, leading to the development of fibrosis in advanced SSc cases (29). Considering the irreversible nature of fibrosis and the promising outcomes observed in several

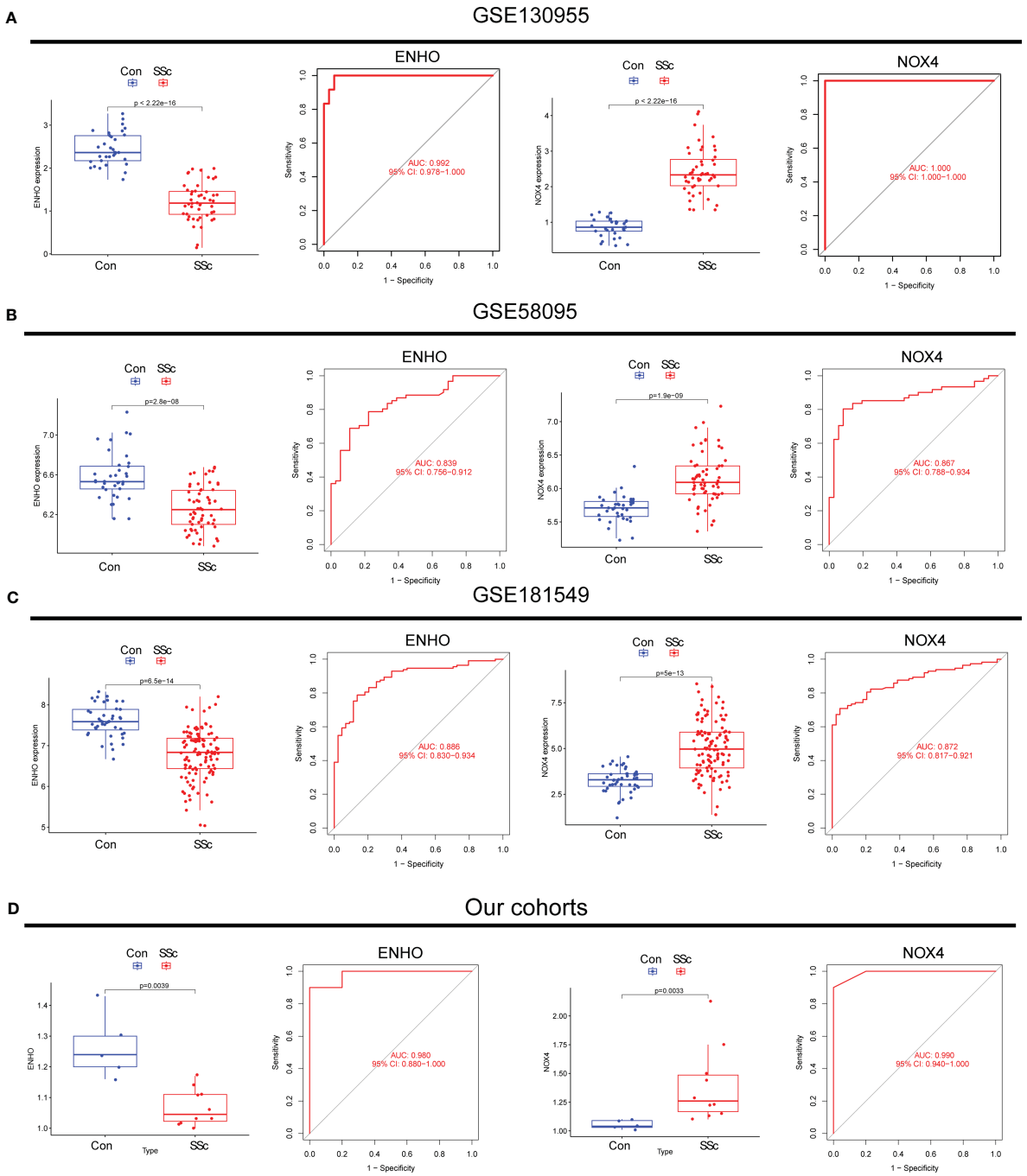

FIGURE 4
The expression pattern of ENHO and NOX4 and their diagnostic for SSc from **(A)** GSE130955, **(B)** GSE58095, **(C)** GSE181549 datasets and **(D)** our cohorts.

clinical trials where patients with improved skin conditions were predominantly in the inflammatory phase, the identification and early diagnosis of SSc assume paramount importance in the effective management of the disease. Timely recognition enables healthcare practitioners to promptly implement treatment strategies, impede disease progression, attenuate tissue fibrosis, and minimize the risk of organ damage. Notably, recent investigations employing skin transcriptome analysis have unveiled significant profiles of innate and adaptive immune cells in the early stages of SSc (30). Consequently, the identification of specific biomarkers associated with infiltrated immune cells holds promise as a potential method for the early diagnosis of SSc. Further research is warranted to elucidate the precise mechanisms underlying these immune cell infiltrations and to explore their potential as diagnostic markers in the context of SSc.

In this study, we conducted an analysis of the GSE130955 datasets and identified 200 DEGs between SSc skin specimens and normal skin specimens. GO assays were performed to

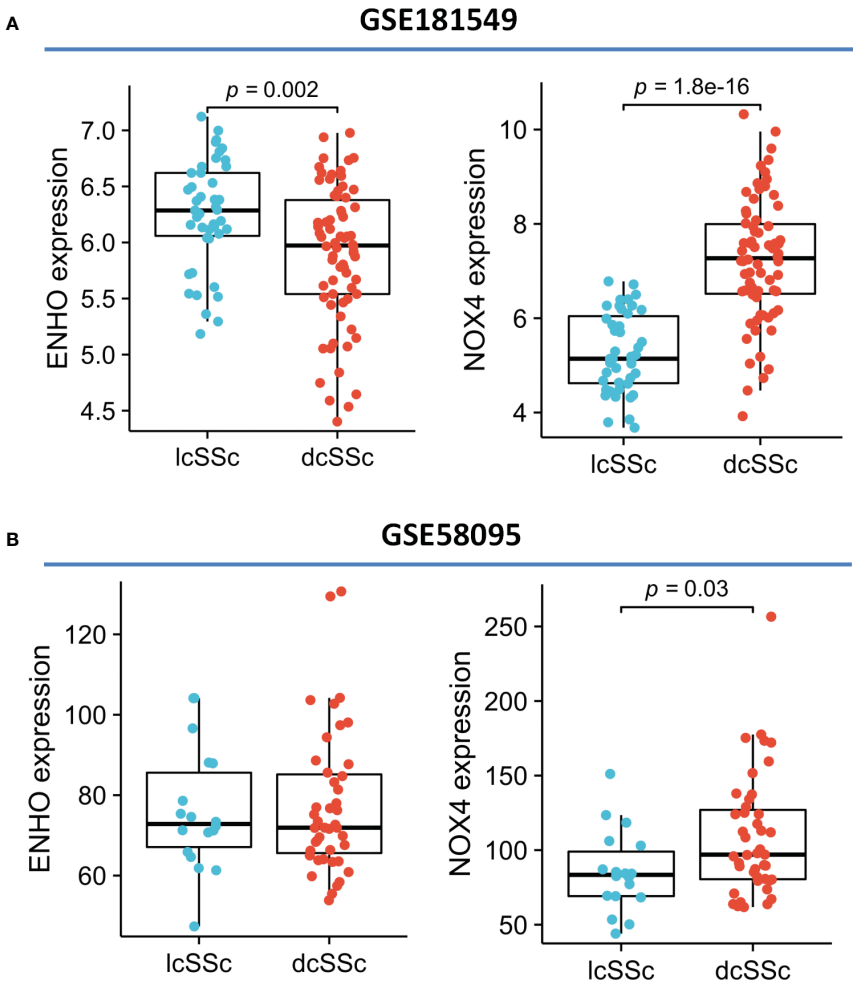

FIGURE 5
The expression of ENHO and NOX4 in skin specimens of dcSSc and lcSSc from **(A)** GSE181549 and **(B)** GSE58095.

investigate the functional relevance of these DEGs, revealing their close association with humoral immune response and ECM organization and functions. These findings align with the pathological characteristics of SSc, which is characterized by excessive deposition of ECM leading to fibrosis in the skin and internal organs. SSc patients also exhibit humoral immune dysfunction, including B cell activation, increased plasma cells, and overproduction of pathogenic autoantibodies. Notably, some SSc patients have shown positive responses to B cell-depleting therapy (31–33). Furthermore, the GO assays demonstrated a strong correlation between the DEGs and integrin binding to the ECM, which was consistent with the results obtained from the KEGG pathway assays. The KEGG pathway analysis revealed that the DEGs primarily participate in ECM-receptor interaction and focal adhesion. Integrins, known as cell adhesion receptors, play a crucial role in mediating cell attachment to the ECM. Importantly, integrins also activate transforming growth factor-beta (TGF-β) and exert significant effects on the fibrotic process (34, 35). Based on the above findings, the 200 DEGs identified in this study are likely to play crucial roles in the pathogenesis of SSc, encompassing immune dysregulation, extracellular matrix remodeling, cell-cell interactions, as well as metabolism and parasitic infections. Further investigation is warranted to elucidate the specific functions of these genes and their contributions to the underlying mechanisms of the disease.

Furthermore, we employed LASSO and SVM techniques to identify two key genes, namely ENHO and NOX4. ENHO, known as an energy homeostasis-associated gene, is expressed in various tissues including the brain, heart, liver, pancreas, and blood vessels. The transcript of the ENHO gene encodes a secreted protein called adropin (36, 37). Previous studies have reported that ENHO can upregulate the expression of endothelial nitric oxide synthase (eNOS), enhance the release of nitric oxide (NO), improve endothelial cell function, and facilitate neovascularization, thereby exerting a protective effect on the cardiovascular system. Treatment of endothelial cells with adropin has been shown to promote proliferation, migration, and capillary tubule formation, while reducing permeability and tumor necrosis factor-α-induced apoptosis. It has been demonstrated that adropin administration can enhance blood perfusion and increase capillary density in a murine model of hind limb ischemia (38). Notably, reduced levels of adropin in the bloodstream have been associated with endothelial

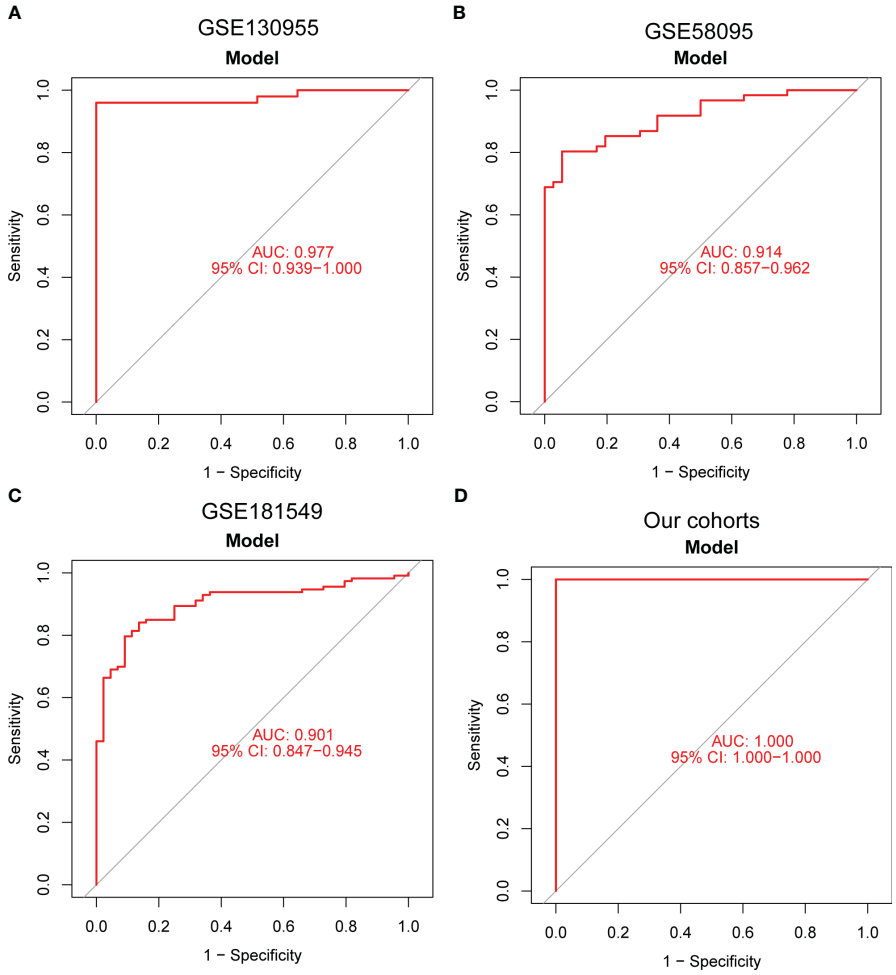

FIGURE 6
A new diagnostic model was developed using ENHO and NOX4, and its diagnostic value was demonstrated in **(A)** GSE130955, **(B)** GSE58095, **(C)** GSE181549 datasets and **(D)** our cohorts.

dysfunction (39, 40). Additionally, it has been reported that mutations in ENHO or adropin deficiency can lead to increased expression of vascular endothelial growth factor (VEGF), thereby promoting the proliferation of endothelial cells in both vascular and inflammatory contexts, ultimately triggering MPO-ANCA-associated lung injury (41). Endothelial cell dysfunction and vasculopathy are recognized as characteristic pathological features of SSc, contributing to the development of Raynaud's phenomenon and ultimately resulting in vascular occlusion and diminished capillary bed. In our investigation, we observed a decrease in ENHO expression in SSc skin tissues, suggesting a potential involvement of ENHO in the pathogenesis of endothelial cell dysfunction and vasculopathy in SSc. Notably, the decreased expression of ENHO in dcSSc skin tissue is more pronounced than that in lcSSc, suggesting that ENHO may be associated with the skin severity of SSc. Furthermore, Servet et al. reported a decrease in ENHO expression specifically in SSc patients with lung involvement compared to those without, while no significant difference in ENHO mRNA expression was observed in peripheral blood mononuclear cells (PBMCs) of SSc patients compared to normal controls (42). These findings and our results suggest that ENHO acts primarily in the tissue lesions of SSc rather than in the peripheral blood. This highlights the need for further investigation into the precise role of ENHO in the context of SSc.

NOX4, a gene encoding the enzyme NADPH oxidase 4, is highly expressed in fibroblasts, microvascular endothelial cells, lung epithelial cells, kidney and smooth muscle cells (43). Studies have shown that NOX4 were upregulated in SSc dermal fibroblasts. NOX4 plays a crucial role in the generation of intracellular reactive oxygen species (ROS), NOX4-stimulated ROS production may be involved in the development of tissue fibrosis, abnormalities of endothelial and vascular, and even the generation of autoantibodies. Reduction or abrogation of NOX4 decreased ROS production and expression of type I collagen and α-smooth muscle actin in SSc fibroblasts (43–46). Moreover, TGF-β, a well-recognized profibrotic cytokine, has been demonstrated to promote the expression of NOX4 in dermal and pulmonary fibroblasts. Deletion of Nox4 abolished TGF-β1-induced fibrosis in the skin and lung tissues of mice (47). Our results further confirmed that NOX4 expression was significantly increased in

10.3389/fimmu.2024.1273559

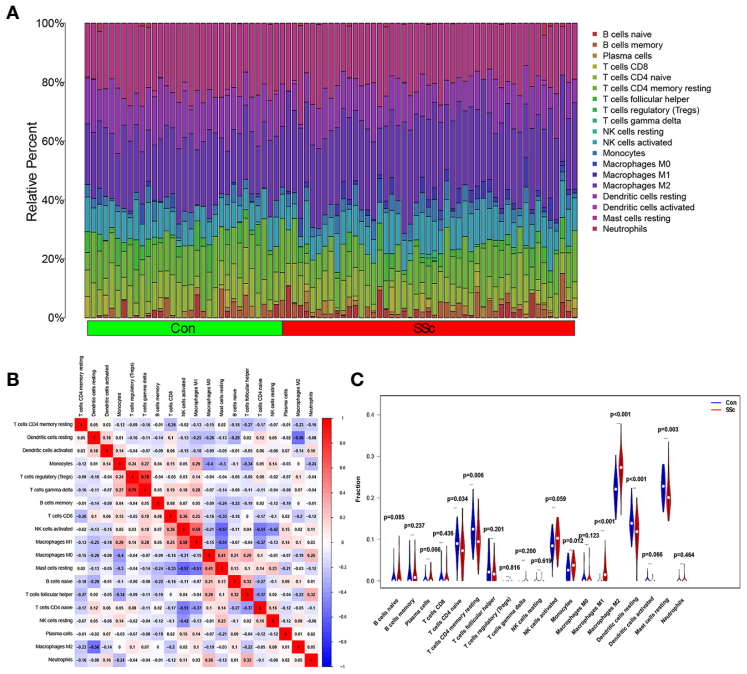

FIGURE 7
An investigation on the expressions of immune cells and the relationships between them in SSc skin specimens and normal skin specimens was carried out using data from GSE130955. **(A)** Heatmap of 22 immune cells among 48 SSc and 33 normal skin specimens. **(B)** In order to conduct an analysis of the matrix consisting of 22 different types of immune cells, the Pearson correlation coefficient was used. **(C)** The dissimilarity in the composition of immune cells between SSc skin specimens and normal skin specimens.

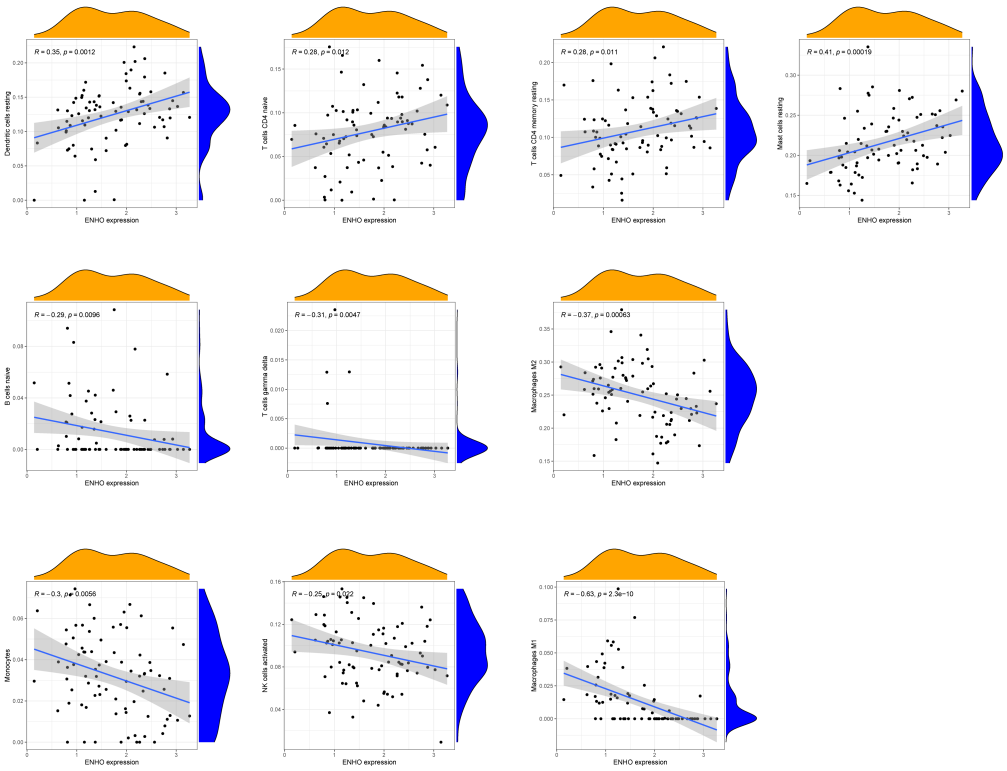

FIGURE 8
Pearson correlation analysis between NOX4 and immune cells.

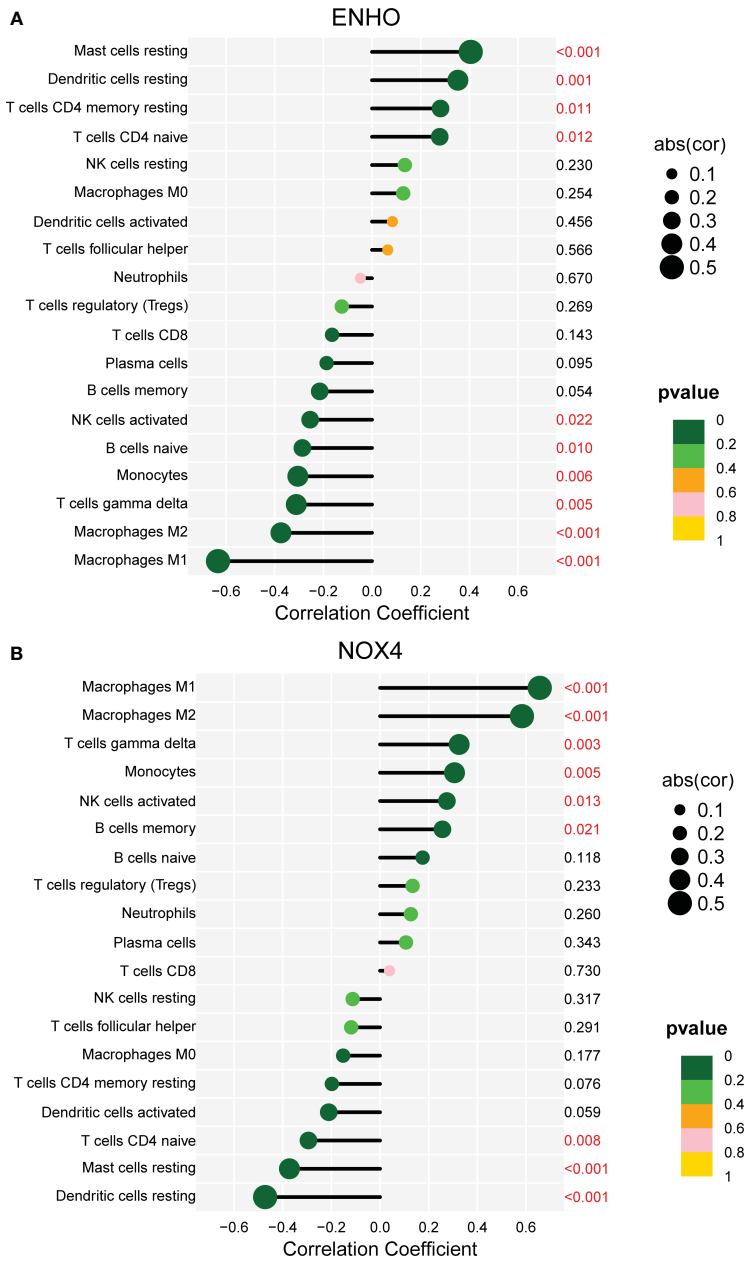

FIGURE 9
Correlation between ENHO and NOX4, and infiltrating immune cells in SSc skin specimens.

SSc skin specimens, especially in patients with dcSSc, suggesting that NOX4 may contribute to the progression of skin lesions in SSc. Taken together, these findings suggest that NOX4 may represent a promising therapeutic target for SSc.

Building upon these observations, we have developed a novel diagnostic prediction model utilizing ENHO and NOX4, and its diagnostic predictive efficacy has been further validated in multiple datasets (GSE130955, GSE58095, GSE181549) as well as our own cohort. This finding, based on the novel diagnostic prediction model incorporating ENHO and NOX4, has demonstrated its predictive power across various datasets and our cohort, indicating its role in early detection and prediction of SSc risk. Lafyatis et al. previously developed a four-gene biomarker for predicting skin disease in dcSSc, including two TGFβ-regulated genes (cartilage oligomeric matrix protein, COMP and thrombospondin-1, THS1) and two interferon(IFN)-regulated genes(interferon-induced 44, IFI44 and sialoadhesin, SIG1). However, it is important to note that their approach differs from our study. They utilized RT-PCR to measure the expression levels of known TGFβ and IFN-regulated genes, and subsequently correlated these levels with the modified Rodnan skin score (MRSS) using multiple regression analyses to achieve the best-fit models. The four-gene predictor serve as an objective surrogate outcome measure, complementing the skin score evaluations in dcSSc (48).

The immune microenvironment plays a crucial role in the etiology and progression of SSc. A comprehensive understanding

10.3389/fimmu.2024.1273559

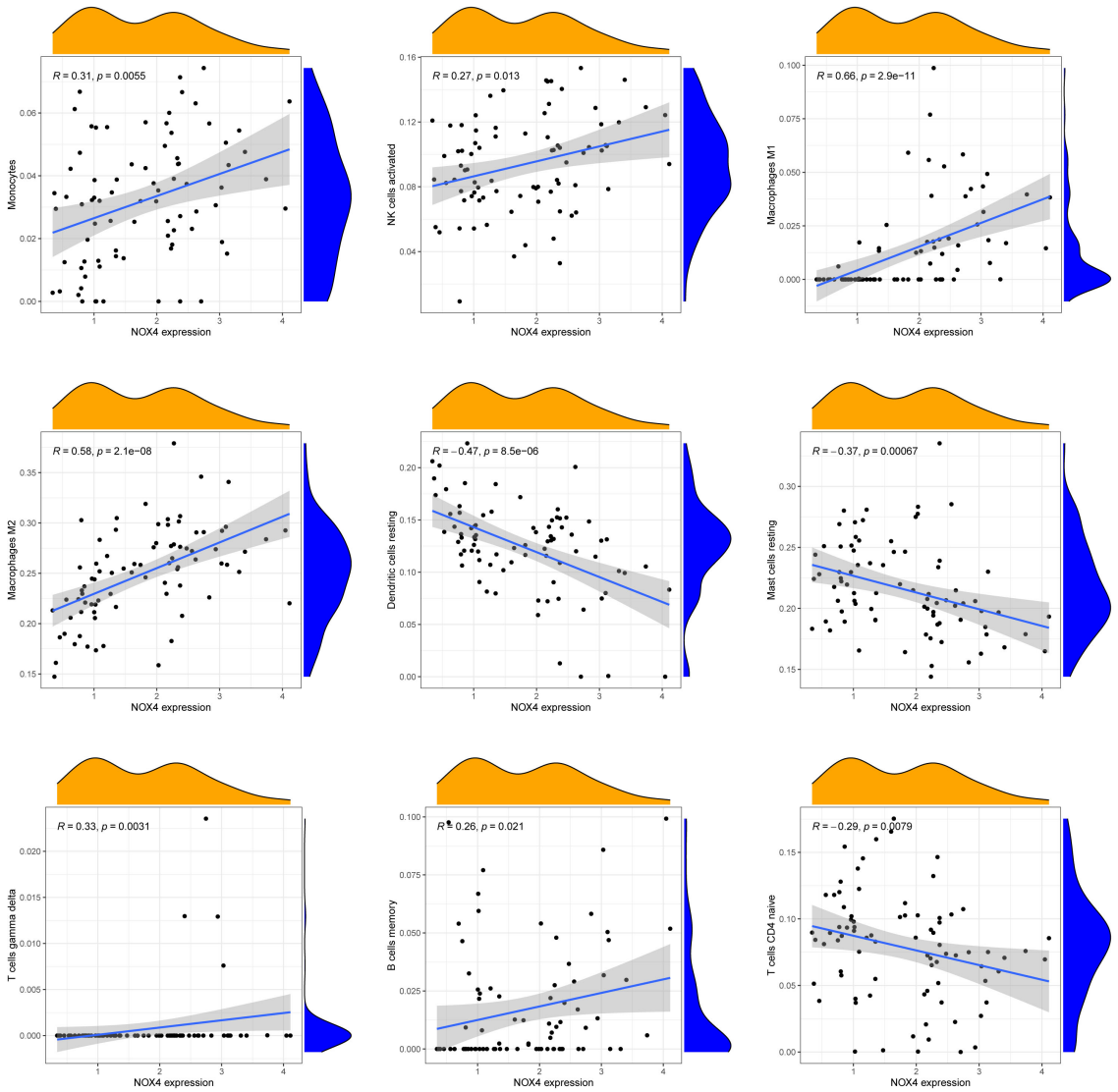

FIGURE 10
Pearson correlation analysis between ENHO and immune cells.

of the interplay between the immune microenvironment and SSc can provide valuable insights into the disease's pathogenesis and facilitate the development of therapeutic interventions. Our analysis of immune infiltration using CIBERSORT deconvolution revealed an elevated presence of Macrophages M1 and Macrophages M2 in the skin of early dcSSc patients, which aligns with previous research findings (49, 50). Macrophages exhibit remarkable plasticity and can undergo distinct forms of polarized activation, traditionally classified as M1 (classically activated) and M2 (alternatively activated) macrophages. M1 macrophages contribute to inflammatory processes that are detrimental to overall health and can lead to tissue damage, suggesting their potential involvement in the early stage of SSc. Conversely, M2 macrophages release profibrotic factors such as TGF-β and contribute to the development of fibrosis in the later stages of the disease (51, 52). Interestingly, we observed a negative correlation between the levels of ENHO and Macrophages M1 and M2, while the levels of NOX4 showed a positive association with Macrophages M1 and M2. The latest findings have demonstrated that adropin promotes M2 polarization of lung macrophages and mitigate the severity of pancreatitis-associated lung injury (53). Adropin deficiency has been shown to result in increased infiltration of M1 macrophages in colon and mesentery tissues, leading to the development of colitis. Additionally, an imbalance of M2 to M1 macrophage polarization was observed in colon and mesentery of Enho-/- mice (54). These studies indicate the potential of ENHO to regulate macrophage polarization, although its role in SSc macrophages remains unexplored. Notably, pulmonary macrophages from individuals with asbestosis-induced pulmonary fibrosis exhibit elevated expression of NOX4, which contributes to apoptosis resistance in monocyte-derived macrophages and the progression of pulmonary fibrosis (55). Furthermore, NOX4 has been implicated in the regulation of macrophage polarization through various mechanisms (56, 57). However, the role of

NOX4 in SSc macrophages has yet to be investigated. Our findings suggest that ENHO and NOX4 may potentially promote the progression of SSc by exerting negative and positive regulatory effects on Macrophages M1 and M2, respectively. Further researches are necessary to fully elucidate these mechanisms.

Conclusion

Following LASSO and SVM analysis, we have successfully identified two pivotal genes, ENHO and NOX4, that play a crucial role in the pathogenesis and progression of SSc. To validate our findings, we conducted extensive analyses on multiple datasets as well as our own SSc cohorts. As a result, we have developed a novel diagnostic model utilizing ENHO and NOX4 as biomarkers, which exhibits promising clinical utility in terms of early diagnosis and disease risk prediction. Notably, ENHO and NOX4 have been found to be associated with immune cell activation and fibroblast activity. Moreover, our study suggests that ENHO and NOX4 may contribute to the advancement of SSc by exerting negative and positive regulatory effects on macrophages M1 and M2, respectively. In conclusion, this study provides valuable insights into the potential clinical significance of ENHO and NOX4 in early diagnosis and risk prediction of SSc. However, further clinical investigation is warranted to evaluate the efficacy and feasibility of implementing this model in real-world clinical settings.

Data availability statement

The datasets presented in this study can be found in online repositories. The names of the repository/repositories and accession number(s) can be found in the article.

Ethics statement

The studies involving humans were approved by the Ethics Committee of the First Affiliated Hospital of Guangxi Medical University. The studies were conducted in accordance with the local legislation and institutional requirements. The participants provided their written informed consent to participate in this study.

Author contributions

LZ: Methodology, Investigation, Writing – original draft. QW: Investigation, Visualization, Writing – review & editing. SC: Validation, Formal analysis, Writing – review & editing. JW: Validation, Writing – review & editing. FD: Formal analysis, Writing – review & editing. NM: Data curation, Writing – review & editing. WZ: Project administration, Writing – review & editing. CZ: Writing – review & editing. XZ: Conceptualization, Writing – review & editing.

Funding

The author(s) declare financial support was received for the research, authorship, and/or publication of this article. This work was supported by the National Natural Science Foundation of China (82360326, LZ), the Joint Project on Regional High-Incidence Diseases Research of Guangxi Natural Science Foundation (2023GXNSFAA026302, LZ), Guangxi Natural Science Foundation (2018GXNSFAA281257, CZ) and the Scientific Research Project of Guangxi Health Commission (S2021103, LZ).

Conflict of interest

The authors declare that the research was conducted in the absence of any commercial or financial relationships that could be construed as a potential conflict of interest.

Publisher's note

References

1. Volkmann ER, Andréasson K, Smith V. Systemic sclerosis. *Lancet* (2023) 401 (10373):304–18. doi: 10.1016/S0140-6736(22)01692-0

2. Meier FM, Frommer KW, Dinser R, Walker UA, Czirjak L, Denton CP, et al. Update on the profile of the EUSTAR cohort: an analysis of the EULAR Scleroderma Trials and Research group database. *Ann Rheum Dis* (2012) 71(8):1355–60. doi: 10.1136/annrheumdis-2011-200742

3. Bournia VK, Fragoulis GE, Mitrou P, Mathioudakis K, Tsolakidis A, Konstantonis G, et al. All-cause mortality in systemic rheumatic diseases under treatment compared with the general population, 2015-2019. *RMD Open* (2021) 7(3):e001694. doi: 10.1136/rmdopen-2021-001694

4. Perelas A, Silver RM, Arrossi AV, Highland KB. Systemic sclerosis-associated interstitial lung disease. *Lancet Respir Med* (2020) 8(3):304–20. doi: 10.1016/S2213-2600(19)30480-1

5. Jerjen R, Nikpour M, Krieg T, Denton CP, Saracino AM. Systemic sclerosis in adults. Part I: Clinical features and pathogenesis. *J Am Acad Dermatol* (2022) 87 (5):937–54. doi: 10.1016/j.jaad.2021.10.065

6. Jin W, Zheng Y, Zhu P. T cell abnormalities in systemic sclerosis. *Autoimmun Rev* (2022) 21(11):103185. doi: 10.1016/j.autrev.2022.103185

7. Beesley CF, Goldman NR, Taher TE, Denton CP, Abraham DJ, Mageed RA, et al. Dysregulated B cell function and disease pathogenesis in systemic sclerosis. *Front Immunol* (2023) 13:999008. doi: 10.3389/fimmu.2022.999008

8. Ah Kioon MD, Tripodo C, Fernandez D, Kirou KA, Spiera RF, Crow MK, et al. Plasmacytoid dendritic cells promote systemic sclerosis with a key role for TLR8. *Sci Transl Med* (2018) 10(423):eaam8458. doi: 10.1126/scitranslmed.aam8458

9. Lescoat A, Lecureur V, Varga J. Contribution of monocytes and macrophages to the pathogenesis of systemic sclerosis: recent insights and therapeutic implications. *Curr Opin Rheumatol* (2021) 33(6):463–70. doi: 10.1097/BOR.0000000000000835

10. Sakkas LI, Simopoulou T, Katsiari C, Bogdanos D, Chikanza IC. Early systemic sclerosis-opportunities for treatment. *Clin Rheumatol* (2015) 34(8):1327–31. doi: 10.1007/s10067-015-2902-5

11. Hinchcliff M, Huang CC, Wood TA, Matthew Mahoney J, Martyanov V, Bhattacharyya S, et al. Molecular signatures in skin associated with clinical improvement during mycophenolate treatment in systemic sclerosis. *J Invest Dermatol* (2013) 133(8):1979–89. doi: 10.1038/jid.2013.130

12. Chakravarty EF, Martyanov V, Fiorentino D, et al. Gene expression changes reflect clinical response in a placebo-controlled randomized trial of abatacept in patients with diffuse cutaneous systemic sclerosis. *Arthritis Res Ther* (2015) 17 (1):159. doi: 10.1186/s13075-015-0669-3

13. Lepri G, Bellando Randone S, Matucci Cerinic M, Guiducci S. Early diagnosis of systemic sclerosis, where do we stand today? *Expert Rev Clin Immunol* (2022) 18(1):1–3. doi: 10.1080/1744666X.2022.2015327

14. Preliminary criteria for the classification of systemic sclerosis (scleroderma). Subcommittee for scleroderma criteria of the American Rheumatism Association Diagnostic and Therapeutic Criteria Committee. *Arthritis Rheum* (1980) 23(5):581–90. doi: 10.1002/art.1780230510

15. van den Hoogen F, Khanna D, Fransen J, Johnson SR, Baron M, Tyndall A, et al. 2013 classification criteria for systemic sclerosis: an American college of rheumatology/European league against rheumatism collaborative initiative. *Ann Rheum Dis* (2013) 72 (11):1747–55. doi: 10.1136/annrheumdis-2013-204424

16. Bellando Randone S, Del Galdo F, Lepri G, Minier T, Huscher D, Furst D, et al. Progression of patients with Raynaud's phenomenon to Systemic Sclerosis classified according to the 2013 ACR/EULAR criteria: five year analysis of the EUSTAR multicentre prospective study for Very Early Diagnosis Of Systemic Sclerosis (VEDOSS). *Lancet Rheumatol* (2021) 3:e834–43. doi: 10.1016/S2665-9913(21)00244-7

17. Haque A, Hughes M. Raynaud's phenomenon. *Clin Med (Lond).* (2020) 20 (6):580–7. doi: 10.7861/clinmed.2020-0754

18. Maundrell A, Proudman SM.). Epidemiology of Raynaud's phenomenon. In: Wigley F, Herrick A, Flavahan N, editors. *Raynaud's phenomenon*. New York, NY: Springer (2015). doi: 10.1007/978-1-4939-1526-2_3

19. Caccavo D, Del Porto F, Garzia P, Mitterhofer AP, Galluzzo S, Rigon A, et al. Raynaud's phenomenon and antiphospholipid antibodies in systemic lupus erythematosus: is there an association? *Ann Rheum Dis* (2003) 62(10):1003–5. doi: 10.1136/ard.62.10.1003

20. Lafyatis R, Valenzi E. Assessment of disease outcome measures in systemic sclerosis. *Nat Rev Rheumatol* (2022) 18(9):527–41. doi: 10.1038/s41584-022-00803-6

21. Stark R, Grzelak M, Hadfield J. RNA sequencing: the teenage years. *Nat Rev Genet* (2019) 20(11):631–56. doi: 10.1038/s41576-019-0150-2

22. Byron SA, Van Keuren-Jensen KR, Engelthaler DM, Carpten JD, Craig DW. Translating RNA sequencing into clinical diagnostics: opportunities and challenges. *Nat Rev Genet* (2016) 17(5):257–71. doi: 10.1038/nrg.2016.10

23. Greener JG, Kandathil SM, Moffat L, Jones DT. A guide to machine learning for biologists. *Nat Rev Mol Cell Biol* (2022) 23(1):40–55. doi: 10.1038/s41580-021-00407-0

24. Deo RC. Machine learning in medicine. *Circulation* (2015) 132(20):1920–30. doi: 10.1161/CIRCULATIONAHA.115.001593

25. Gupta R, Srivastava D, Sahu M, Tiwari S, Ambasta RK, Kumar P. Artificial intelligence to deep learning: machine intelligence approach for drug discovery. *Mol Divers* (2021) 25(3):1315–60. doi: 10.1007/s11030-021-10217-3

26. Bonomi F, Peretti S, Lepri G, Venerito V, Russo E, Bruni C, et al. The use and utility of machine learning in achieving precision medicine in systemic sclerosis: A narrative review. *J Pers Med* (2022) 12(8):1198. doi: 10.3390/jpm12081198

27. Keret S, Rimar D, Lansiaux P, Feldman E, Lescoat A, Milman N, et al. Differentially expressed genes in systemic sclerosis: Towards predictive medicine with new molecular tools for clinicians. *Autoimmun Rev* (2023) 22(6):103314. doi: 10.1016/j.autrev.2023.103314

28. Fang D, Chen B, Lescoat A, Khanna D, Mu R. Immune cell dysregulation as a mediator of fibrosis in systemic sclerosis. *Nat Rev Rheumatol* (2022) 18(12):683–93. doi: 10.1038/s41584-022-00864-7

29. Sakkas LI, Chikanza IC, Platsoucas CD. Mechanisms of Disease: the role of immune cells in the pathogenesis of systemic sclerosis. *Nat Clin Pract Rheumatol* (2006) 2(12):679–85. doi: 10.1038/ncprheum0346

30. Skaug B, Khanna D, Swindell WR, Hinchcliff ME, Frech TM, Steen VD, et al. Global skin gene expression analysis of early diffuse cutaneous systemic sclerosis shows a prominent innate and adaptive inflammatory profile. *Ann Rheum Dis* (2020) 79 (3):379–86. doi: 10.1136/annrheumdis-2019-215894

31. Agarbati S, Benfaremo D, Viola N, Paolini C, Svegliati Baroni S, et al. Increased expression of the ectoenzyme CD38 in peripheral blood plasmablasts and plasma cells of patients with systemic sclerosis. *Front Immunol* (2022) 13:1072462. doi: 10.3389/fimmu.2022.1072462

32. Streicher K, Sridhar S, Kuziora M, Morehouse CA, Higgs BW, Sebastian Y, et al. Baseline plasma cell gene signature predicts improvement in systemic sclerosis skin scores following treatment with inebilizumab (MEDI-551) and correlates with disease activity in systemic lupus erythematosus and chronic obstructive pulmonary disease. *Arthritis Rheumatol* (2018) 70(12):2087–95. doi: 10.1002/art.40656

33. Moroncini G, Svegliati Baroni S, Gabrielli A. Agonistic antibodies in systemic sclerosis. *Immunol Lett* (2018) 195:83–7. doi: 10.1016/j.imlet.2017.10.007

34. Munger JS, Huang X, Kawakatsu H, Griffiths MJ, Dalton SL, Wu J, et al. The integrin alpha v beta 6 binds and activates latent TGF beta 1: a mechanism for regulating pulmonary inflammation and fibrosis. *Cell* (1999) 96(3):319–28. doi: 10.1016/s0092-8674(00)80545-0

35. Gerber EE, Gallo EM, Fontana SC, Davis EC, Wigley FM, Huso DL, et al. Integrin-modulating therapy prevents fibrosis and autoimmunity in mouse models of scleroderma. *Nature* (2013) 503(7474):126–30. doi: 10.1038/nature12614

36. Han W, Zhang C, Wang H, Yang M, Guo Y, Li G, et al. Alterations of irisin, adropin, preptin and BDNF concentrations in coronary heart disease patients comorbid with depression. *Ann Transl Med* (2019) 7(14):298. doi: 10.21037/atm.2019.05.77

37. Kumar KG, Trevaskis JL, Lam DD, Sutton GM, Koza RA, Chouljenko VN, et al. Identification of adropin as a secreted factor linking dietary macronutrient intake with energy homeostasis and lipid metabolism. *Cell Metab* (2008) 8(6):468–81. doi: 10.1016/j.cmet.2008.10.011

38. Lovren F, Pan Y, Quan A, Singh KK, Shukla PC, Gupta M, et al. Adropin is a novel regulator of endothelial function. *Circulation* (2010) 122(11 Suppl):S185–92. doi: 10.1161/CIRCULATIONAHA.109.931782

39. Topuz M, Celik A, Aslantas T, Demir AK, Aydin S, Aydin S. Plasma adropin levels predict endothelial dysfunction like flow-mediated dilatation in patients with type 2 diabetes mellitus. *J Investig Med* (2013) 61(8):1161–4. doi: 10.2310/JIM.0000000000000003

40. Oruc CU, Akpinar YE, Dervisoglu E, Amikishiyev S, Salmaslıoglu A, Gurdol F, et al. Low concentrations of adropin are associated with endothelial dysfunction as assessed by flow-mediated dilatation in patients with metabolic syndrome. *Clin Chem Lab Med* (2017) 55(1):139–44. doi: 10.1515/cclm-2016-0329

41. Gao F, Fang J, Chen F, Wang C, Chen S, Zhang S, et al. Enho mutations causing low adropin: A possible pathomechanism of MPO-ANCA associated lung injury. *EBioMedicine* (2016) 9:324–35. doi: 10.1016/j.ebiom.2016.05.036

42. Yolbas S, Kara M, Yilmaz M, Aydin S, Koca SS. Serum adropin level and ENHO gene expression in systemic sclerosis. *Clin Rheumatol* (2016) 35(6):1535–40. doi: 10.1007/s10067-016-3266-1

43. Piera-Velazquez S, Jimenez SA. Oxidative stress induced by reactive oxygen species (ROS) and NADPH oxidase 4 (NOX4) in the pathogenesis of the fibrotic process in systemic sclerosis: A promising therapeutic target. *J Clin Med* (2021) 10 (20):4791. doi: 10.3390/jcm10204791

44. Piera-Velazquez S, Makul A, Jiménez SA. Increased expression of NAPDH oxidase 4 in systemic sclerosis dermal fibroblasts: regulation by transforming growth factor β. *Arthritis Rheumatol* (2015) 67(10):2749–58. doi: 10.1002/art.39242

45. Li K, Wang Q, Bian B, Xu J, Bian H. Exploration and validation of the hub genes involved in hypoxia-induced endothelial-mesenchymal transition of systemic sclerosis. *Clin Exp Rheumatol* (2023) 41(8):1618–31. doi: 10.55563/clinexprheumatol/j7ema8

46. Spadoni T, Svegliati Baroni S, Amico D, Albani L, Moroncini G, Avvedimento EV, et al. A reactive oxygen species-mediated loop maintains increased expression of NADPH oxidases 2 and 4 in skin fibroblasts from patients with systemic sclerosis. *Arthritis Rheumatol* (2015) 67(6):1611–22. doi: 10.1002/art.39084

47. Wermuth PJ, Mendoza FA, Jimenez SA. Abrogation of transforming growth factor-β-induced tissue fibrosis in mice with a global genetic deletion of Nox4. *Lab Invest.* (2019) 99(4):470–82. doi: 10.1038/s41374-018-0161-1

48. Farina G, Lafyatis D, Lemaire R, Lafyatis R. A four-gene biomarker predicts skin disease in patients with diffuse cutaneous systemic sclerosis. *Arthritis Rheumatol* (2010) 62(2):580–8. doi: 10.1002/art.27220

49. Higashi-Kuwata N, Jinnin M, Makino T, Fukushima S, Inoue Y, Muchemwa FC, et al. Characterization of monocyte/macrophage subsets in the skin and peripheral blood derived from patients with systemic sclerosis. *Arthritis Res Ther* (2010) 12(4): R128. doi: 10.1186/ar3066

50. Higashi-Kuwata N, Makino T, Inoue Y, Takeya M, Ihn H. Alternatively activated macrophages (M2 macrophages) in the skin of patient with localized scleroderma. *Exp Dermatol* (2009) 18(8):727–9. doi: 10.1111/j.1600-0625.2008.00828.x

51. Al-Adwi Y, Westra J, van Goor H, Burgess JK, Denton CP, Mulder DJ. Macrophages as determinants and regulators of fibrosis in systemic sclerosis. *Rheumatol (Oxford).* (2023) 62(2):535–45. doi: 10.1093/rheumatology/keac410

52. Bhandari R, Ball MS, Martyanov V, Popovich D, Schaafsma E, Han S, et al. Profibrotic activation of human macrophages in systemic sclerosis. *Arthritis Rheumatol* (2020) 72(7):1160–9. doi: 10.1002/art.41243

53. Ding F, Liu G, Gao F, Zheng Z, Hong Y, Chen Y, et al. Adropin attenuates pancreatitis-associated lung injury through PPARγ phosphorylation-related macrophage polarization. *Int J Mol Med* (2023) 52(4):95. doi: 10.3892/ijmm.2023.5298

54. Liu Q, Zhang S, Liu G, Zhou H, Guo Y, Gao F, et al. Adropin deficiency worsens TNBS-induced colitis. *Int Immunopharmacol* (2023) 124(Pt A):110891. doi: 10.1016/j.intimp.2023.110891

55. Larson-Casey JL, Gu L, Kang J, Dhyani A, Carter AB. NOX4 regulates macrophage apoptosis resistance to induce fibrotic progression. *J Biol Chem* (2021) 297(1):100810. doi: 10.1016/j.jbc.2021.100810

56. Helfinger V, Palfi K, Weigert A, Schröder K. The NADPH oxidase nox4 controls macrophage polarization in an NFκB-dependent manner. *Oxid Med Cell Longev* (2019) 2019:3264858. doi: 10.1155/2019/3264858

57. He C, Larson-Casey JL, Davis D, Hanumanthu VS, Longhini ALF, Thannickal VJ, et al. NOX4 modulates macrophage phenotype and mitochondrial biogenesis in asbestosis. *JCI Insight* (2019) 4(16):e126551. doi: 10.1172/jci.insight.126551

frontiers | Frontiers in Immunology

TYPE Original Research
PUBLISHED 01 February 2024
DOI 10.3389/fimmu.2024.1286973

OPEN ACCESS

EDITED BY
Francesca Wanda Rossi,
University of Naples Federico II, Italy

REVIEWED BY
Zhengping Huang,
Guangdong Second Provincial General Hospital, China
José Jiram Torres-Ruiz,
National Institute of Medical Sciences and Nutrition Salvador Zubirán, Mexico
Frédéric Coutant,
Universitéde Lyon, France

*CORRESPONDENCE
Wenfeng Tan
tanwenfeng2005@126.com

RECEIVED 01 September 2023
ACCEPTED 19 January 2024
PUBLISHED 01 February 2024

CITATION
Wang L, Lv C, You H, Xu L, Yuan F, Li J, Wu M, Zhou S, Da Z, Qian J, Wei H, Yan W, Zhou L, Wang Y, Yin S, Zhou D, Wu J, Lu Y, Su D, Liu Z, Liu L, Ma L, Xu X, Zang Y, Liu H, Ren T, Liu J, Wang F, Zhang M and Tan W (2024) Rapidly progressive interstitial lung disease risk prediction in anti-MDA5 positive dermatomyositis: the CROSS model. *Front. Immunol.* 15:1286973. doi: 10.3389/fimmu.2024.1286973

Rapidly progressive interstitial lung disease risk prediction in anti-MDA5 positive dermatomyositis: the CROSS model

Lei Wang[1], Chengyin Lv[1], Hanxiao You[1], Lingxiao Xu[1], Fenghong Yuan[2], Ju Li[3], Min Wu[4], Shiliang Zhou[4], Zhanyun Da[5], Jie Qian[5], Hua Wei[6], Wei Yan[6], Lei Zhou[7], Yan Wang[7], Songlou Yin[8], Dongmei Zhou[8], Jian Wu[9], Yan Lu[10], Dinglei Su[11], Zhichun Liu[12], Lin Liu[13], Longxin Ma[14], Xiaoyan Xu[15], Yinshan Zang[16], Huijie Liu[17], Tianli Ren[18], Jin Liu[19], Fang Wang[20], Miaojia Zhang[1] and Wenfeng Tan[1]*

[1]Division of Rheumatology, The First Affiliated Hospital of Nanjing Medical University, Nanjing, Jiangsu, China, [2]Division of Rheumatology, Wuxi People's Hospital, Wuxi, Jiangsu, China, [3]Division of Rheumatology, Huai'an First People's Hospital, Huai'an, Jiangsu, China, [4]Division of Rheumatology, The First People's Hospital of Changzhou, Changzhou, Jiangsu, China, [5]Division of Rheumatology, Affiliated Hospital of Nantong University, Nantong, Jiangsu, China, [6]Division of Rheumatology, Northern Jiangsu People's Hospital, Yangzhou, Jiangsu, China, [7]Division of Rheumatology, Changzhou No.2 People's Hospital, Changzhou, Jiangsu, China, [8]Division of Rheumatology, Affiliated Hospital of Xuzhou Medical University, Xuzhou, Jiangsu, China, [9]Division of Rheumatology, The First Affiliated Hospital of Soochow University, Suzhou, Jiangsu, China, [10]Division of Rheumatology, Jiangsu Province Hospital of Chinese Medicine, Nanjing, Jiangsu, China, [11]Division of Rheumatology, Nanjing First Hospital, Nanjing, Jiangsu, China, [12]Division of Rheumatology, The Second Affiliated Hospital of Soochow University, Suzhou, Jiangsu, China, [13]Division of Rheumatology, Xuzhou Central Hospital, Xuzhou, Jiangsu, China, [14]Division of Rheumatology, Yancheng No.1 People's Hospital, Yancheng, Jiangsu, China, [15]Division of Rheumatology, Zhongda Hospital Southeast University, Nanjing, Jiangsu, China, [16]Division of Rheumatology, The Affiliated Suqian First People's Hospital of Nanjing Medical University, Suqian, Jiangsu, China, [17]Division of Rheumatology, The First People's Hospital of Lianyungang, Lianyungang, Jiangsu, China, [18]Division of Rheumatology, Wuxi No.2 People's Hospital, Wuxi, Jiangsu, China, [19]Research Institute of Clinical Medicine, The First Affiliated Hospital of Nanjing Medical University, Nanjing, Jiangsu, China, [20]Division of Cardiology, The First Affiliated Hospital of Nanjing Medical University, Nanjing, Jiangsu, China

Background: The prognosis of anti-melanoma differentiation-associated gene 5 positive dermatomyositis (anti-MDA5$^+$DM) is poor and heterogeneous. Rapidly progressive interstitial lung disease (RP-ILD) is these patients' leading cause of death. We sought to develop prediction models for RP-ILD risk in anti-MDA5$^+$DM patients.

Methods: Patients with anti-MDA5$^+$DM were enrolled in two cohorts: 170 patients from the southern region of Jiangsu province (discovery cohort) and 85 patients from the northern region of Jiangsu province (validation cohort). Cox proportional hazards models were used to identify risk factors of RP-ILD. RP-ILD risk prediction models were developed and validated by testing every independent prognostic risk factor derived from the Cox model.

Results: There are no significant differences in baseline clinical parameters and prognosis between discovery and validation cohorts. Among all 255 anti-

MDA5$^+$DM patients, with a median follow-up of 12 months, the incidence of RP-ILD was 36.86%. Using the discovery cohort, four variables were included in the final risk prediction model for RP-ILD: C-reactive protein (CRP) levels, anti-Ro52 antibody positivity, short disease duration, and male sex. A point scoring system was used to classify anti-MDA5$^+$DM patients into moderate, high, and very high risk of RP-ILD. After one-year follow-up, the incidence of RP-ILD in the very high risk group was 71.3% and 85.71%, significantly higher than those in the high-risk group (35.19%, 41.69%) and moderate-risk group (9.54%, 6.67%) in both cohorts.

Conclusions: The CROSS model is an easy-to-use prediction classification system for RP-ILD risk in anti-MDA5$^+$DM patients. It has great application prospect in disease management.

KEYWORDS

anti-melanoma differentiation-associated gene 5, dermatomyositis, rapidly progressive interstitial lung disease, predict models, easy-to-use

1 Background

Anti-melanoma differentiation-associated gene 5 positive (anti-MDA5$^+$) dermatomyositis (DM) is a subtype of DM characterized by distinct cutaneous lesions, little or no muscle involvement, and interstitial lung disease (ILD) (1). ILD is the most important clinical feature of anti-MDA5$^+$DM affecting approximately 60–100% of patients; importantly, over 40% (20–75%) of them tend to develop the rapidly progressive ILD phenotype (RP-ILD), especially in the Asian population (2–5). Anti-MDA5$^+$DM patients with RP-ILD are generally resistant to glucocorticoid and immunosuppressant therapy, leading to a 6-month mortality rate as high as 50-70% (6). Risk stratification to predict patients who will develop fatal RP-ILD at the early stage of the disease is very important for discussing patient expectations and supporting therapy decision-making in anti-MDA5$^+$DM patients.

In the past decade, a great effort has been attempted to identify risk factors that predict ILD progression and mortality in anti-MDA5$^+$DM. Old age, skin ulceration, and lack of myositis are suggested as risk factors for RP-ILD (7). Elevated serum CRP, ferritin level, and Krebs von den Lungen-6 (KL-6) levels have been linked to poor outcomes in RP-ILD patients (8, 9). Most recently, forced vital capacity has been validated as a predictor for the survival of ILD in anti-MDA5$^+$DM (10). However, the accuracy of this single risk factor for prognosis estimation is limited by small size, lack of validation, and disease heterogeneity, hindering them from being genuinely applied in the clinic.

Recently, a clinical prediction model of FLAIR score that combines five clinical items, including ferritin, lactate dehydrogenase, anti-MDA5 antibody, CT imaging score, and RP-ILD, has been developed (11). The FLAIR risk score model could help to predict survival in amyopathic DM with ILD. However, the availability of certain items, such as the HRCT scoring system and anti-MDA5 antibody titers, limited the FLAIR model from being quickly adopted in daily clinical practice (12–14).

The current study aims to establish a simple-to-use risk prediction model for RP-ILD based on easily available clinical variables. Using a discovery cohort and an independent validation cohort, we identified and validated that the CROSS model is a readily available risk classification system for predicting RP-ILD in anti-MDA5$^+$DM patients.

Abbreviations: MDA5, Melanoma Differentiation-associated Gene 5; DM, Dermatomyositis; RP-ILD, Rapidly Progressive Interstitial Lung Disease; CRP, C-reactive Protein; KL-6, Krebs von den Lungen-6; ENMC, European NeuroMusclar Center; ALT, Alanine Transaminase; AST, Aspartate Aminotransferase; LDH, Lactic Dehydrogenase; CK, Creatine Kinase; ESR, Erythrocyte Sedimentation Rate; SF, Serum Ferritin; ANA, Anti-nuclear Antibodies; FVC, Forced Vital Capacity; DLCO, Diffusion Capacity for Carbon Monoxide of the Lung; HRCT, High-resolution CT; EDC, Electronic Data Capture; ROC, Receiver Operating Characteristic; AUC, The Area Under the Curve; COVID-19, Coronavirus Disease 2019; HR, Hazard Ratio.

2 Methods

2.1 Study cohort and participants

Our cohort study was registered (ClinicalTrials.gov NCT04747652). Adult patients with DM meeting the European NeuroMusclar Center (ENMC) criteria or Sontheimer criteria were recruited into the cohort after excluding other autoimmune diseases or other causes of ILD (15, 16). Consecutive anti-MDA5$^+$DM collected from ten tertiary hospitals in southern Jiangsu province from March 2019 to March 2021 were included in the discovery cohort. To externally verify the derived prediction model, 85 eligible

consecutive anti-MDA5$^+$DM patients were recruited into the validation cohort from eight tertiary hospitals in the northern region of Jiangsu province between March 2019 and March 2021 (Figure 1).

All clinical data were collected at baseline (initially diagnosed as DM), to death or the last follow-up visit. Clinical parameters of all subjects include the demographic information (including age at onset, gender, disease duration (defined as from disease onset to the cohort enrollment), initial symptoms associated with the disease), clinical manifestation (including muscle weakness, rash, periungual erythema, arthritis, mechanic's hand, skin ulcer, and interstitial lung disease) and laboratory indicators (including alanine transaminase [ALT], aspartate aminotransferase [AST], lactic dehydrogenase [LDH], creatine kinase [CK], erythrocyte sedimentation rate [ESR], C-reactive protein [CRP], serum ferritin [SF], autoantibodies [including MDA5, ANA and Ro-52]). CT scans were obtained at 1- to 3-month intervals. Two expert thoracic radiologists re-reviewed all available HRCT imaging from baseline to death or the last follow-up visit.

The definition of RP-ILD was according to the descriptions in previous literature with some modifications (17, 18). Briefly, RP-ILD was defined as the presence of any of the following four conditions within one month after the onset of respiratory symptoms: 1) acute and progressive worsening of dyspnea requiring hospitalization or supplementary oxygen; 2) lung function including forced vital capacity (FVC) decreases by more than 10%, or diffusion capacity for carbon monoxide of the Lung (DLCO) falls over 15% with the decreased FVC; 3) high-resolution CT (HRCT) of the chest demonstrates that the extent of interstitial abnormalities increased more than 20%; 4) arterial blood gas analysis suggests respiratory failure or the oxygen partial pressure reduction is more significant than 10mmHg.

2.2 Statistical strategy and modeling

Medical records were reviewed retrospectively to collect clinical, laboratory, and imaging data, and all data were collected using an Electronic Data Capture (EDC) System explicitly designed for the cohort. If a patient developed RP-ILD during follow-up, it will be recorded as an endpoint event for poor outcomes.

In data processing, some continuous variables were transformed into dichotomies. Patients' median age and disease duration at baseline were used as the cutoff value to distinguish elderly patients and short course of disease. The abnormal thresholds of laboratory indicators used the upper end of their normal reference range. Anti-MDA5 antibodies were tested by immunoblot testing (Euroimmun, Lubeck, Germany) in the same central laboratory for all subjects, and the high titer positivity is defined as +++. ANA is detected using the indirect immunofluorescence assay, and a titre greater than 1:40 is considered positive.

SPSS 23.0, GraphPad Prism 8.4.2, and R version 3.6.3 were used in the statistical analysis. Differences between the different groups (whether an RP-ILD and death endpoint event occurred in the discovery cohort) were calculated with the Mann-Whitney U test and Pearson's chi-square test in measurement and categorical data, respectively. $P < 0.05$ was considered statistically significant, and all statistical tests were two-tailed probability tests.

A discovery cohort was used to develop a prediction model of RP-ILD in anti-MDA5$^+$DM patients. All transformed dichotomous variables were tested by univariate Cox analysis to screen whether it is a related factor to the occurrence of RP-ILD. Some continuous variables were dichotomized based on the median, including age, course of the disease (short disease duration is defined as ≤ 3 months after anti-MDA5$^+$DM onset), follow-up time, etc. In contrast, other continuous variables were dichotomized based on the upper limit of 95% confidence interval of clinical tests, including ALT, AST, LDH, CK, ESR, CRP and SF. Univariate and multivariable Cox analyses were then performed to identify the independent risk factors for developing RP-ILD in anti-MDA5$^+$DM patients. Variables with $p < 0.2$ in the univariate analysis were included in the multivariable Cox analysis as the covariates. To identify independent prognostic risk factors and calculate their weightiness, β regression coefficient and integer estimation were used to form an integral model for predicting the occurrence of RP-ILD.

Time-dependent receiver operating characteristic (ROC) curve analysis was used to determine whether the two score models were

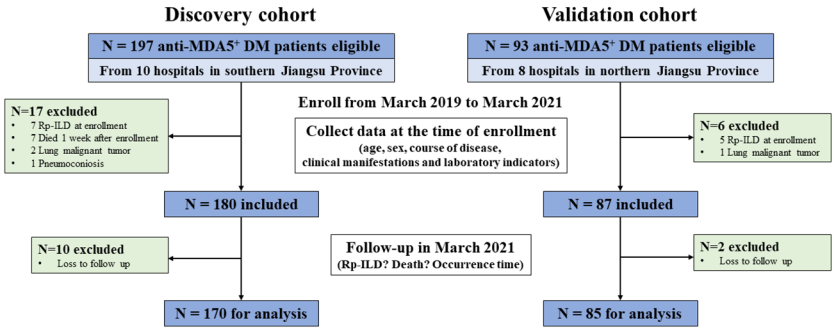

FIGURE 1
Flow chart of study enrollment. Patients who were diagnosed with dermatomyositis and had positive serum anti-MDA5 antibodies were included in this study. Among them, patients who presented with RP-ILD at enrollment and died within one week of enrollment, as well as those with lung malignant tumor, pneumoconiosis, and loss to follow-up were excluded. Anti-MDA5$^+$DM, anti-melanoma differentiation-associated gene 5 positive dermatomyositis; RP-ILD, rapidly progressive interstitial lung disease.

the optimal clinical significance threshold. Kaplan-Meier method was used to calculate the cumulative poor prognosis rates during follow-up, and the logarithmic rank test was used to compare different risk groups. Finally, the incidence of RP-ILD and mortality at 3 months, 6 months, and 1 year in anti-MDA5$^+$DM patients with varying levels of risk was accurately measured and demonstrated. The above verification methods are carried out in the external validation cohort to verify the prediction models' reliability further.

3 Results

3.1 Baseline characteristics of anti-MDA5$^+$DM patients in the discovery and validation cohort

Table 1 shows the baseline characteristics of the discovery and validation cohorts. Patients in the discovery and validation cohorts do not show marked differences at baseline. As one group, anti-MDA5$^+$DM patients are predominantly women (69.8%) with a median age of 53.0 (47.0-63.0) years old. The median follow-up time is 10.0 (3.0-14.0) and 12.0 (3.0-14.0) months in the discovery and validation cohorts, respectively. The overall incidence of RP-ILD in anti-MDA5$^+$DM patients was 36.86% (94/255), and the mortality was 24.71% (63/255).

3.2 Development of the CROSS model to predict the risk of RP-ILD

After univariate Cox analysis, variables with $p < 0.2$ were included in the multivariable Cox analysis as the covariates, including male sex, short disease duration, abnormal laboratory parameters (including AST, LDH, CK, CRP, and SF), anti-Ro52 antibody positivity and high titer positivity of anti-MDA5 antibody defined as +++.

After COX regression, four risk factors were finally determined as the independent risk factors for the development of RP-ILD, including CRP abnormal (defined as exceed the upper limit of the normal detection range), anti-Ro52 antibody positivity, male sex, and short disease duration (Figure 2). We then selected these four independent risk factors to create a new RP-ILD risk prediction model of the CROSS score (CRP abnormal, anti-Ro52 antibody, sex [male sex], and short disease duration). These four variables were weighted according to the ratio of the β coefficient. When calculating the CROSS score, anti-Ro52 positivity and short disease duration scored 2 points, respectively, and abnormal CRP and male sex scored one point. The Alignment Diagram also shows the weighted relationship between these four predictors and the occurrence of RP-ILD, and the concordance index reached 0.825 (Supplementary Figure 1).

Based on the CROSS score with a range from 0 to 6, anti-MDA5$^+$DM patients were classified as moderate risk (CROSS score = 0-2), high risk (CROSS score = 3-4), and very high risk (CROSS score = 5-6) for developing of RP-ILD, respectively (Table 2).

3.3 Efficiency validation of the CROSS model

To verify the accuracy of the predictive model, the CROSS score was calculated in both cohorts as the internal validation and external validation datasets, respectively. Compared with patients without RP-ILD, the CROSS score at baseline was significantly higher in anti-MDA5$^+$DM patients with RP-ILD in both cohorts (Supplementary Figure 2). Then, time-dependent ROC curves were performed to evaluate the forecast effects of the CROSS model. The area under the curve (AUC) of the CROSS model in both cohorts are more than 0.8 at each time point within one year, which indicates excellent differentiation efficiency of the CROSS model (Supplementary Figure 3).

Next, Kaplan-Meier analysis was used to assess whether the percentage of adverse events in patients at different risk levels differed significantly over time. The proportion of anti-MDA5$^+$DM patients developing RP-ILD over time increases considerably as the risk level assessed based on the CROSS model increases in both cohorts ($p< 0.0001$). In the discovery cohort, the 1-year non-RP-ILD survival rate of the moderate-, high-, and very high-risk groups were 90.46%, 64.81%, and 28.7%, respectively (Figure 3A). In the validation cohort, the 1-year non-RP-ILD survival rate of the moderate-, high-, and very high-risk groups were 93.33%, 58.31%, and 14.29%, respectively ($p< 0.0001$) (Figure 3B). At the same time, we further analyzed the time-dependent mortality of these three groups of anti-MDA5$^+$DM patients. The prognostic grouping based on the CROSS model also has an excellent predictive effect on the risk of death ($p=0.0003$ in the discovery cohort and $p< 0.0001$ in the validation cohort). The one-year survival rates of very high-risk patients were 54.28% and 30.86%, significantly lower than those in moderate- and high-risk patients (Figures 3C, D).

3.4 Incidence rate of poor prognosis in various risk grades evaluated by the models

At last, we calculated the rates of RP-ILD in anti-MDA5$^+$DM patients with moderate, high, and very high-risk stratification at different time points. As the risk level rises, the incidence rate of RP-ILD based on the CROSS model was gradually raised in both cohorts. Of note, the incidence rate of RP-ILD in very high-risk patients is over 70%, high-risk patients are around 25%-50%, and less than 15% in moderate-risk patients (Figure 4).

4 Discussion

RP-ILD is a common and potentially fatal complication of anti-MDA5$^+$DM. Risk stratification to predict patients who will develop fatal RP-ILD at the early stage of the disease is very important for discussing patient expectations and supporting therapy decision-making in anti-MDA5$^+$DM patients. Based on the current largest

10.3389/fimmu.2024.1286973

TABLE 1 Comparison of clinical manifestations and laboratory features between discovery and validation cohorts at baseline.

Parameters	Total (n=255)	Discovery Cohort (n=170)	Validation Cohort (n=85)	p value
General information				
Gender, male sex, No. (%)	77 (30.2%)	54 (31.8%)	23 (27.1%)	0.440
Age, median (Q1-Q3), years	53.0 (47.0-63.0)	53.0 (46.8-62.0)	53.0 (47.0-64.0)	0.568
Disease durations, median (Q1-Q3), months	3.0 (1.0-5.0)	3.0 (1.0-5.0)	3.0 (1.0-5.0)	0.482
Follow-up periods, median (Q1-Q3), months	12.0 (3.0-14.0)	10.0 (3.0-14.0)	12.0 (3.0-14.0)	0.165
Clinical manifestations				
Muscle weakness, No. (%)	117 (45.9%)	81 (47.7%)	36 (42.4%)	0.424
Rash, No. (%)	238 (93.3%)	162 (95.3%)	76 (89.4%)	0.076
Gottron's sign, No. (%)	170 (66.7%)	113 (66.5%)	57 (67.1%)	0.925
Heliotrope rash, No. (%)	147 (57.7%)	104 (61.2%)	43 (50.6%)	0.107
V sign, No. (%)	92 (36.1%)	59 (34.7%)	33 (38.8%)	0.519
Shawl sign, No. (%)	59 (23.1%)	43 (25.3%)	16 (18.8%)	0.248
Periungual erythema, No. (%)	55 (21.6%)	36 (21.2%)	19 (22.4%)	0.830
Arthritis, No. (%)	92 (36.1%)	64 (37.7%)	28 (32.9%)	0.461
Mechanic's hand, No. (%)	70 (27.5%)	41 (24.1%)	29 (34.1%)	0.092
Skin ulcer, No. (%)	36 (14.1%)	24 (14.1%)	12 (14.1%)	1.000
Laboratory features				
ALT, median (Q1-Q3), units/L	46 (28.5-85.0)	46.1 (28.8-79.1)	46 (28-95.4)	0.961
AST, median (Q1-Q3), units/L	52 (33.1-83)	53 (34-82.9)	50 (30–83)	0.429
LDH, median (Q1-Q3), units/L	340 (256–430)	340 (267-423.5)	337 (224-490.25)	0.895
CK, median (Q1-Q3), units/L	61.5 (36-144.3)	64 (36.5-141)	57 (34-163.5)	0.996
ESR, median (Q1-Q3), mm/H	37.1 (23–56)	39 (23-56.8)	37 (21–56)	0.741
CRP, median (Q1-Q3), mg/L	5.8 (3.1-12.3)	6.1 (3.1-14.5)	4.6 (2-10.8)	0.063
SF, median (Q1-Q3), ng/mL	869.5 (340.8-1500)	869.5 (323.8-1642.3)	886.3 (390.6-1500)	0.917
ANA, positive, No. (%)	131 (51.4%)	83 (48.8%)	48 (56.5%)	0.249
Anti-Ro52 antibody, positive, No. (%)	164 (64.3%)	114 (67.1%)	50 (58.8%)	0.196
Anti-MDA5 antibody, No. (%)				0.456
Low titer, +	76 (29.8%)	54 (31.8%)	22 (25.9%)	
Moderate titer, ++	46 (18.0%)	32 (18.8%)	14 (16.5%)	
High titer, +++	133 (52.2%)	84 (49.4%)	49 (57.7%)	
Prognosis				
RP-ILD, No. (%)	94 (36.9%)	60 (35.3%)	34 (40.0%)	0.463
3-months incidence rate	85/244 (34.8%)	51/160 (31.9%)	34/84 (40.5%)	0.180
6-months incidence rate	92/235 (39.2%)	58/151 (38.4%)	34/84 (40.5%)	0.756
12-months incidence rate	94/205 (45.9%)	60/122 (49.2%)	34/83 (41.0%)	0.246
Mortality, No. (%)	63 (24.7%)	42 (24.7%)	21 (24.7%)	1.000
3-months mortality	44/240 (18.3%)	25/157 (15.9%)	19/83 (22.9%)	0.185

(Continued)

TABLE 1 Continued

Parameters	Total (n=255)	Discovery Cohort (n=170)	Validation Cohort (n=85)	p value
6-months mortality	54/224 (24.1%)	33/144 (22.9%)	21/80 (26.3%)	0.576
12-months mortality	62/197 (31.5%)	41/118 (34.8%)	21/79 (26.68%)	0.227

*Data are presented as median (1st quartile [Q1]-3rd quartile [Q3]) or case number (percentage). Mann-Whitney U and Pearson's Chi-square test were used to analysis. RP-ILD, rapidly progressive interstitial lung disease; ALT, alanine transaminase; AST, aspartate aminotransferase; LDH, lactic dehydrogenase; CK, creatine kinase; ESR, erythrocyte sedimentation rate; CRP, C-reactive protein; SF, serum ferritin; ANA, anti-nuclear antibodies; MDA5, anti-melanoma differentiation-associated gene 5.

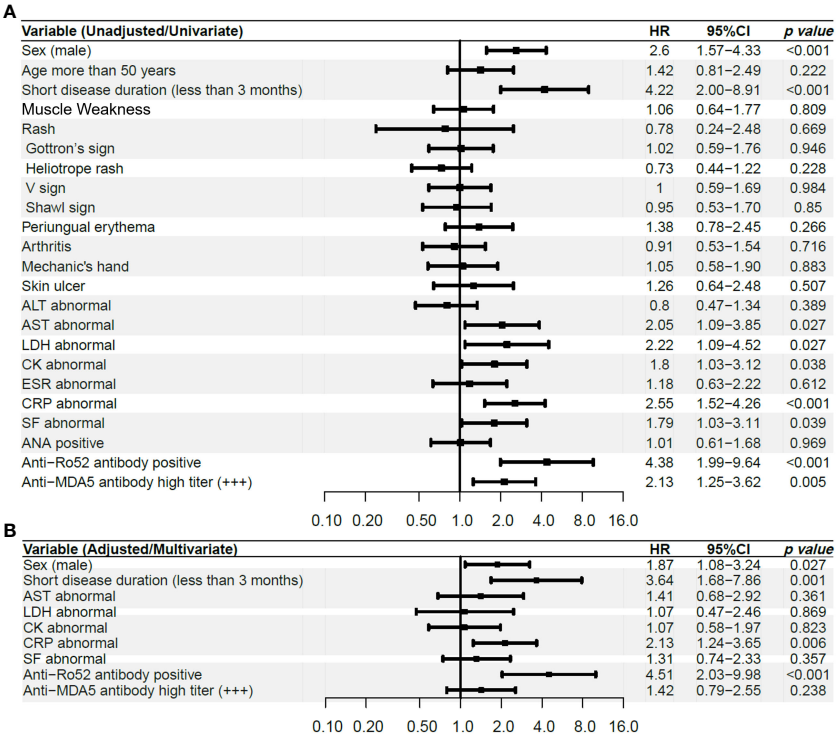

FIGURE 2
Univariate and Multivariate COX analysis of RP-ILD influenced by baseline manifestations in the discovery cohort **(A)** Univariate COX analysis, **(B)** Multivariate COX analysis. ALT, alanine transaminase; AST, aspartate aminotransferase; LDH, lactic dehydrogenase; CK= creatine kinase; ESR, erythrocyte sedimentation rate; CRP, C-reactive protein; SF, serum ferritin; ANA, anti-nuclear antibodies; MDA5, anti-melanoma differentiation-associated gene 5; RP-ILD, rapidly progressive interstitial lung disease; HR, Hazard ratio.

reported anti-MDA5$^+$DM cohort containing 255 consecutive anti-MDA5$^+$DM patients, we developed and validated a CROSS model that successfully predicts RP-ILD and mortality risk.

There are three essential differences between the FLAIR model (11) mentioned in introduction and our own. First, all patients included in our cohort are anti-MDA5$^+$DM patients. Second, unlike the FLAIR model for predicting death risk, the CROSS model represents the first prognostic tool for RP-ILD in anti-MDA5$^+$DM patients. RP-ILD is linked to high mortality. Given that only about 1/3 of anti-MDA5$^+$DM may develop RP-ILD after disease onset in our cohort and the previous report, early recognition of patients with high RP-ILD risk is particularly important in halting disease progression and improving prognosis in anti-MDA5$^+$DM. Third, the inconvenience of obtaining HRCT scoring and anti-MDA5 titers data limits the FLAIR model's widespread adoption in daily clinical practice (12–14). To overcome these limitations, we developed a simpler prognostic model.

TABLE 2 CROSS prognostic score system in discovery cohort.

Parameters	β coefficient	Score
CRP abnormal	0.754	1
Anti-Ro52 positivity	1.505	2
Sex (male sex)	0.624	1
Short disease duration (less than 3 months)	1.291	2

†To predict the risk of RP-ILD, CROSS model: score 0-2, moderate risk; score 3-4, high risk; score 5-6 very high risk. CRP, C-reactive protein; AST, aspartate aminotransferase; RP-ILD, rapidly progressive interstitial lung disease; HR, Hazard ratio.

We compared 26 clinical or laboratory parameters from 255 patients (94 RP-ILD and 161 non-RP-ILD; 192 survivors and 63 non-survivors). Amongst all parameters investigated, we found four parameters to be independent risk factors for RP-ILD in the discovery cohort. We then developed and externally validated a

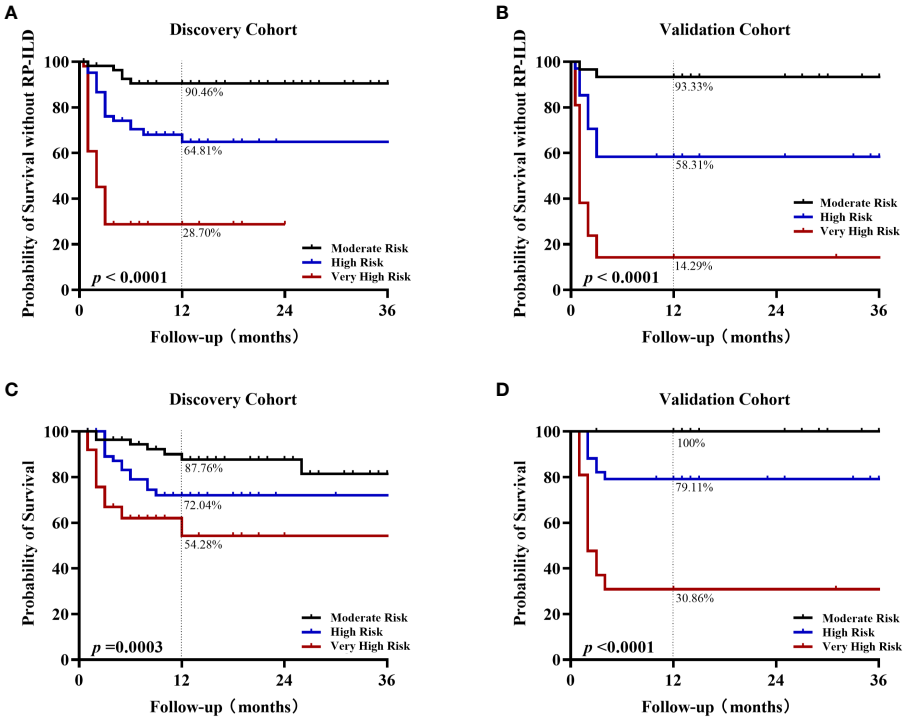

FIGURE 3
Kaplan-Meier analysis of different risk grades in survival rate and RP-ILD-free survival rate Kaplan-Meier non-RPILD survival curves for the different risk stratification groups according to the CROSS model in the discovery cohort **(A)** or validation cohort **(B)**. Kaplan-Meier survival curves in the discovery cohort **(C)** or validation cohort **(D)**.

CROSS (CRP, anti-Ro52 antibody, short disease duration, Sex[male sex]) for predicting RP-ILD risk in two different anti-MDA5$^+$DM cohorts. The CROSS model is an easy-to-use risk prediction system based on commonly used and easily obtained variables in the clinical setting. In both discovery and validation cohorts, very high-risk patients had significantly higher RP-ILD rates than moderate- and high-risk patients. Interestingly, the risk of death in anti-MDA5$^+$DM patients was also well stratified based on the predictive model (Figures 3C, D). However, there was no significant difference in overall mortality among the three groups based on the CROSS model in the validation cohort (Figure 4B).

According to the CROSS model, 51 patients (30.0%) were classified as at very high risk of developing RP-ILD in the discovery cohort, and 76.6% of them eventually developed RP-ILD in the first 6 months. Similar accuracy was confirmed in the validation cohort and achieved 85.7%. Stratifying anti-MDA5$^+$DM into different risk categories allows for closer monitoring of very high-risk patients and guiding management decisions.

In our cohort, 34.84% of anti-MDA5$^+$DM patients will develop RP-ILD during the first 3 months after disease onset. Actually we find significant, time- time-dependent changes in RP-ILD and mortality risk in MDA5+ DM patients in our cohort. More than 90% RP-ILD and 84% mortality occurs in the first 6-months after disease onset. Notably, the first 3-months is a particularly high-risk period, with 50% RP-ILD and 46% death occurring. We proposed the first 6-months, especially the first 3-months, is a risk window for the poor outcome in anti-MDA5+ DM patients (19). We recommend calculating the CROSS score initially after the patient is diagnosed with anti-MDA5$^+$DM. Then, the CROSS risk classification system can be used sequentially, particularly in the first 3~6 months.

Among the variables in the CROSS model, the increased CRP levels imply high disease activity and hyperinflammatory state in anti-MDA5$^+$DM. We previously identified 3 distinct phenotypes with significantly different prognoses in patients with anti-MDA5$^+$DM. The most prominent feature in anti-MDA5$^+$DM with RP-ILD is the high inflammatory status (20), supporting CRP played an important role in the CROSS score. CRP is a dynamic index. Besides its association with an inflammatory state, CRP levels are also linked to potential infection, which might warn differential diagnosis during disease progression. Based on the requirement of simplification of the clinical model, all quantitative parameters were qualified based on whether they were abnormal, which may even weaken the impact of CRP in predicting the prognosis of anti-MDA5$^+$DM patients.

In our CROSS model, anti-Ro52 is a strong prognostic factor for RP-ILD. Anti-Ro52 is the most common autoantibody detected in polymyositis and the anti-synthetase syndrome. Previous studies have reported that anti-Ro52 antibodies significantly correlated with ILD in DM, juvenile myositis, primary Sjögren syndrome, and connective tissue diseases, suggesting anti-Ro52 is an intended risk factor for ILD (21–25). Consistent with our findings, recent studies have found that the coexistence of anti-MDA5 and anti-Ro52 correlates with an increased frequency of RP-ILD and poor prognosis in anti-MDA5 DM patients (25). Thus, the presence of

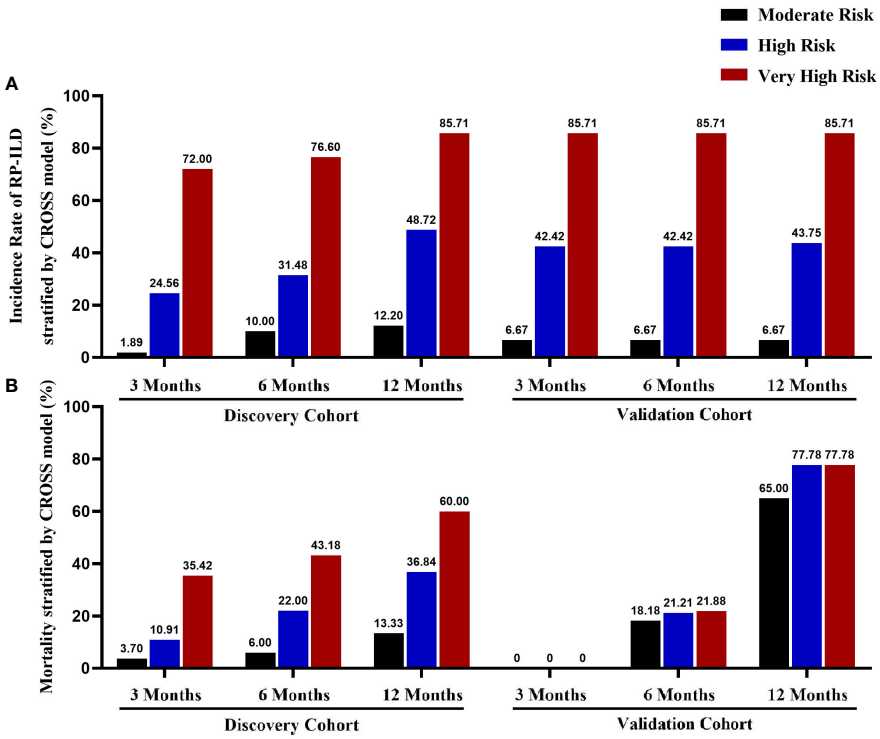

FIGURE 4
The incidence rate of RP-ILD and mortality according to the CROSS model Comparison of 3-months, 6-months, and 1-year incidence rates of RP-ILD **(A)** and mortality **(B)** in the discovery and validation cohorts with different risk stratification.

anti-Ro52 might help to distinguish a subgroup of anti-MDA5$^+$DM patients with more aggressive phenotypes.

There are limitations to this study. First, all data are obtained from a multicenter retrospective study, and missing data could not be avoided, which might be a bias of the analysis. Second, FVC, DLCO values, and hypoxemia have been reported as risk factors for RP-ILD and poor prognosis in patients with anti-MDA5$^+$DM (7). Approximately36.9% of patients develop RP-ILD during the follow-up period in our cohort, and most patients have no markedly respiratory symptoms at the beginning of disease onset. Our goal is to create an easy-to-use prediction model that could be applied at the initial visit of a patient with anti-MDA5 DM. Therefore, we did not include lung function and arterial blood gas in our risk classification system. Third, the treatment regimen was not analyzed in the current study, especially lacking the relationship between changes in CROSS score over time with treatment response. Fourth, the worldwide coronavirus disease 2019 (COVID-19) pandemic indicated a similar cytokine storm in anti-MDA5$^+$DM with RP-ILD. CROSS score did not take into account blood cytokine profiles with clinical outcomes. Given that the development and validation of the CROSS model were conducted with patients from various hospitals in Jiangsu Province, China, its applicability to populations in other regions or ethnic groups beyond Asians has yet to be established. This necessitates additional validation to confirm its effectiveness in diverse settings. Despite its limitations, based on the most significant reported study populations, our CROSS score provides a simple and accurate model for predicting RP-ILD onset and mortality risk in anti-MDA5$^+$DM patients. Further prospective studies are needed to validate its accuracy in risk prediction further, facilitating the truly clinical decision-making support in anti-MDA5$^+$DM patients.

Recently, Jacqueline So et al. also revealed a FLAW model that based on fever, LDH, age, and white cell count maybe useful to predict the risk of RP-ILD in anti-MDA5$^+$DM patients (26). Similar to our CROSS model, FLAW provide a simple pragmatic model for predicting RP-ILD. Although the variables are different, both these two models showed good predictive effects. Future prospective studies are needed to compare the clinical application value of these two models. Using the largest reported cohort, we developed and validated a prediction model for RP-ILD risk in anti-MDA5$^+$DM patients. The strength of this model is the use of clinical variables that could be easily obtained during the routine clinic visit. This simple predictive model could aid in the early detection of anti-MDA5$^+$DM patients without RP-ILD at poor prognosis risk, guiding treatment and improving outcomes.

5 Conclusions

The CROSS model could help to identify anti-MDA5$^+$DM patient who are at high risk of RP-ILD. It provides a simple and easy-used mothed to early warning and early detection of anti-

MDA5$^+$DM patients with poor outcomes in in daily clinical practice.

Data availability statement

The raw data supporting the conclusions of this article will be made available by the authors, without undue reservation.

Ethics statement

The studies involving humans were approved by the ethical committee of the First Affiliated Hospital of Nanjing Medical University: 2020-SR-265. The studies were conducted in accordance with the local legislation and institutional requirements. The participants provided their written informed consent to participate in this study. Written informed consent was obtained from the individual(s) for the publication of any potentially identifiable images or data included in this article.

Author contributions

LW: Conceptualization, Data curation, Investigation, Writing – original draft, Formal Analysis, Methodology, Project administration, Software, Visualization. CL: Conceptualization, Supervision, Validation, Writing – review & editing. HY: Writing – review & editing, Data curation, Supervision, Validation. LX: Data curation, Writing – review & editing, Supervision, Validation. FY: Writing – review & editing, Investigation. JLi: Investigation, Writing – review & editing. MW: Investigation, Writing – review & editing. SZ: Investigation, Writing – review & editing. ZD: Investigation, Writing – review & editing. JQ: Investigation, Writing – review & editing. HW: Investigation, Writing – review & editing. WY: Investigation, Writing – review & editing. LZ: Investigation, Writing – review & editing. YW: Investigation, Writing – review & editing. SY: Investigation, Writing – review & editing. DZ: Investigation, Writing – review & editing. JW: Investigation, Writing – review & editing. YL: Investigation, Writing – review & editing. DS: Investigation, Writing – review & editing. ZL: Investigation, Writing – review & editing. LL: Investigation, Writing – review & editing. LM: Investigation, Writing – review & editing. XX: Investigation, Writing – review & editing. YZ: Investigation, Writing – review & editing. HL: Investigation, Writing – review & editing. TR: Investigation, Writing – review & editing. JLiu: Writing – review & editing, Data curation. FW: Writing – review & editing, Funding acquisition. MZ: Writing – review & editing, Data curation. WT: Data curation, Conceptualization, Funding acquisition, Investigation, Supervision, Writing – original draft.

Funding

The author(s) declare financial support was received for the research, authorship, and/or publication of this article. This work was supported by the National Natural Science Foundation of China (NSFC) [grant numbers: 81971532, 81971533].

Acknowledgments

We thank all authors for their continuous and excellent support with patient data collection, data analysis, statistical analysis, and valuable suggestions for the article.

Conflict of interest

The authors declare that the research was conducted in the absence of any commercial or financial relationships that could be construed as a potential conflict of interest.

Publisher's note

Supplementary material

The Supplementary Material for this article can be found online at: https://www.frontiersin.org/articles/10.3389/fimmu.2024.1286973/full#supplementary-material

SUPPLEMENTARY FIGURE 1
A nomogram predicting RP-ILD risk of anti-MDA5$^+$DM patients Each variable's value was given a score on the point scale axis. A total score could be calculated by adding every single score, and by projecting the complete score to the lower full-point scale, we could estimate the probability of RP-ILD.

SUPPLEMENTARY FIGURE 2
Differences in CROSS scores in anti-MDA5$^+$DM patients The violin diagram shows the difference in CROSS scores between patients who progressed to RP-ILD and those who did not in both discovery **(A)** and validation cohort **(B)**.

SUPPLEMENTARY FIGURE 3
AUC value of time-dependent ROC curve in CROSS model The area under the curve (AUC) value of the time-dependent ROC curve shows that the CROSS model has excellent differentiation efficiency in both cohorts within different time points.

References

1. Kurtzman DJB, Vleugels RA. Anti-melanoma differentiation-associated gene 5 (MDA5) dermatomyositis: A concise review with an emphasis on distinctive clinical features. *J Am Acad Dermatol* (2018) 78(4):776–85. doi: 10.1016/j.jaad.2017.12.010

2. Koga T, Fujikawa K, Horai Y, Okada A, Kawashiri SY, Iwamoto N, et al. The diagnostic utility of anti-melanoma differentiation-associated gene 5 antibody testing for predicting the prognosis of Japanese patients with DM. *Rheumatol (Oxford)* (2012) 51(7):1278–84. doi: 10.1093/rheumatology/ker518

3. Moghadam-Kia S, Oddis CV, Sato S, Kuwana M, Aggarwal R. Antimelanoma differentiation-associated gene 5 antibody: expanding the clinical spectrum in north american patients with dermatomyositis. *J Rheumatol* (2017) 44(3):319–25. doi: 10.3899/jrheum.160682

4. Allenbach Y, Uzunhan Y, Toquet S, Leroux G, Gallay L, Marquet A, et al. Different phenotypes in dermatomyositis associated with anti-MDA5 antibody: Study of 121 cases. *Neurology* (2020) 95(1):e70–8. doi: 10.1212/WNL.0000000000009727

5. Fujimoto M, Watanabe R, Ishitsuka Y, Okiyama N. Recent advances in dermatomyositis-specific autoantibodies. *Curr Opin Rheumatol* (2016) 28(6):636–44. doi: 10.1097/BOR.0000000000000329

6. Wu W, Guo L, Fu Y, Wang K, Zhang D, Xu W, et al. Interstitial lung disease in anti-MDA5 positive dermatomyositis. *Clin Rev Allergy Immunol* (2021) 60(2):293–304. doi: 10.1007/s12016-020-08822-5

7. Motegi SI, Sekiguchi A, Toki S, Kishi C, Endo Y, Yasuda M, et al. Clinical features and poor prognostic factors of anti-melanoma differentiation-associated gene 5 antibody-positive dermatomyositis with rapid progressive interstitial lung disease. *Eur J Dermatol* (2019) 29(5):511–7. doi: 10.1684/ejd.2019.3634

8. Gono T, Masui K, Nishina N, Kawaguchi Y, Kawakami A, Ikeda K, et al. Risk prediction modeling based on a combination of initial serum biomarker levels in polymyositis/dermatomyositis-associated interstitial lung disease. *Arthritis Rheumatol* (2021) 73(4):677–86. doi: 10.1002/art.41566

9. Zhu Y, Wang L, Sun Y, Wang J, Lv C, You H, et al. Serum Krebs von den Lungen-6 concentrations reflect severity of anti-melanoma differentiation-associated protein 5 antibody positive dermatomyositis associated interstitial lung disease. *Clin Exp Rheumatol* (2022) 40(2):292–7. doi: 10.55563/clinexprheumatol/zmn18h

10. Wu W, Xu W, Sun W, Zhang D, Zhao J, Luo Q, et al. Forced vital capacity predicts the survival of interstitial lung disease in anti-MDA5 positive dermatomyositis: a multi-centre cohort study. *Rheumatology* (2022) 61(1):230–9.

11. Lian X, Zou J, Guo Q, Chen S, Lu L, Wang R, et al. Mortality risk prediction in amyopathic dermatomyositis associated with interstitial lung disease: the FLAIR model. *Chest* (2020) 158(4):1535–45. doi: 10.1016/j.chest.2020.04.057

12. Baker MC, Chung L, Fiorentino DF. A mortality risk score model for clinically amyopathic dermatomyositis-associated interstitial lung disease: will it have the necessary "FLAIR" to improve clinical outcomes? *Chest* (2020) 158(4):1307–9. doi: 10.1016/j.chest.2020.06.001

13. Waki D, Nishimura K. Impact of the combined immunosuppressive therapy on different mortality score groups in amyopathic dermatomyositis-associated interstitial lung disease and the problem of sample splitting. *Chest* (2021) 159(2):882–3. doi: 10.1016/j.chest.2020.07.099

14. Wang M, Fan C. Mortality risk prediction in amyopathic dermatomyositis associated with interstitial lung disease: perhaps some potential details to consider. *Chest* (2021) 159(4):1686–7. doi: 10.1016/j.chest.2020.10.096

15. Hoogendijk JE, Amato AA, Lecky BR, Choy EH, Lundberg IE, Rose MR, et al. 119th ENMC international workshop: trial design in adult idiopathic inflammatory myopathies, with the exception of inclusion body myositis, 10-12 October 2003, Naarden, The Netherlands. *Neuromuscul Disord* (2004) 14(5):337–45. doi: 10.1016/j.nmd.2004.02.006

16. Euwer R, Sontheimer R. Dermatologic aspects of myositis. *Curr Opin Rheumatol* (1994) 6(6):583–9. doi: 10.1097/00002281-199411000-00006

17. Sato S, Hirakata M, Kuwana M, Suwa A, Inada S, Mimori T, et al. Autoantibodies to a 140-kd polypeptide, CADM-140, in Japanese patients with clinically amyopathic dermatomyositis. *Arthritis Rheum* (2005) 52(5):1571–6. doi: 10.1002/art.21023

18. Abe Y, Kusaoi M, Tada K, Yamaji K, Tamura N. Successful treatment of anti-MDA5 antibody-positive refractory interstitial lung disease with plasma exchange therapy. *Rheumatol (Oxford)* (2020) 59(4):767–71. doi: 10.1093/rheumatology/kez357

19. You H, Wang L, Wang J, Lv C, Xu L, Yuan F, et al. Time-dependent changes in RPILD and mortality risk in anti-MDA5+ DM patients: a cohort study of 272 cases in China. *Rheumatol (Oxford)* (2023) 62(3):1216–26. doi: 10.1093/rheumatology/keac450

20. Xu L, You H, Wang L, Lv C, Yuan F, Li J, et al. Identification of three different phenotypes in anti-MDA5 antibody-positive dermatomyositis patients: implications for rapidly progressive interstitial lung disease prediction. *Arthritis Rheumatol* (2022).

21. Xing X, Li A, Li C. Anti-Ro52 antibody is an independent risk factor for interstitial lung disease in dermatomyositis. *Respir Med* (2020) 172:106134.

22. Vojinovic T, Cavazzana I, Ceruti P, Fredi M, Modina D, Berlendis M, et al. Predictive features and clinical presentation of interstitial lung disease in inflammatory myositis. *Clin Rev Allergy Immunol* (2021) 60(1):87–94.

23. Sabbagh S, Pinal-Fernandez I, Kishi T, Targoff IN, Miller FW, Rider LG, et al. Anti-Ro52 autoantibodies are associated with interstitial lung disease and more severe disease in patients with juvenile myositis. *Ann Rheum Dis* (2019) 78(7):988–95.

24. Buvry C, Cassagnes L, Tekath M, Artigues M, Pereira B, Rieu V, et al. Anti-Ro52 antibodies are a risk factor for interstitial lung disease in primary Sjogren syndrome. *Respir Med* (2020) 163:105895.

25. Xu A, Ye Y, Fu Q, Lian X, Chen S, Guo Q, et al. Prognostic values of anti-Ro52 antibodies in anti-MDA5-positive clinically amyopathic dermatomyositis associated with interstitial lung disease. *Rheumatol (Oxford)* (2021) 60(7):3343–51.

26. So J, So H, Wong V, Ho R, Wu T, Wong P, et al. Predictors of rapidly progressive interstitial lung disease and mortality in patients with autoantibodies against melanoma differentiation-associated protein 5 dermatomyositis. *Rheumatol (Oxford)* (2022) 61(11):4437–44. doi: 10.1093/rheumatology/keac094

frontiers | Frontiers in Immunology

TYPE Original Research
PUBLISHED 13 February 2024
DOI 10.3389/fimmu.2024.1321507

OPEN ACCESS

EDITED BY
Francesca Wanda Rossi,
University of Naples Federico II, Italy

REVIEWED BY
Filippo Fagni,
University of Erlangen
Nuremberg, Germany
Marc Hilhorst,
Academic Medical Center, Netherlands
Paul Hoover,
Harvard Medical School, United States

*CORRESPONDENCE
Zhen Cheng
chengzhen33@hotmail.com
Haitao Zhang
htzhang163@163.com

RECEIVED 14 October 2023
ACCEPTED 29 January 2024
PUBLISHED 13 February 2024

CITATION
Wang J, Lou W, Zhu M, Tu Y, Chen D, Qiu D, Xu F, Liang D, Cheng Z and Zhang H (2024) Prediction of treatment response in lupus nephritis using density of tubulointerstitial macrophage infiltration.
Front. Immunol. 15:1321507.
doi: 10.3389/fimmu.2024.1321507

Prediction of treatment response in lupus nephritis using density of tubulointerstitial macrophage infiltration

Jingjing Wang[1], Wenyuan Lou[1], Mengyue Zhu[2], Yuanmao Tu[1], Duqun Chen[1], Dandan Qiu[1], Feng Xu[1], Dandan Liang[1], Zhen Cheng[1*] and Haitao Zhang[1*]

[1]National Clinical Research Center for Kidney Diseases, Jinling Hospital, Affiliated Hospital of Medical School, Nanjing University, Nanjing, China, [2]Northern Jiangsu People's Hospital, Yangzhou University, Yangzhou, China

Background: Lupus nephritis (LN) is a common disease with diverse clinical and pathological manifestations. A major challenge in the management of LN is the inability to predict its treatment response at an early stage. The objective of this study was to determine whether the density of tubulointerstitial macrophage infiltration can be used to predict treatment response in LN and whether its addition to clinicopathological data at the time of biopsy would improve risk prediction.

Methods: In this retrospective cohort study, 430 patients with LN in our hospital from January 2010 to December 2017 were included. We used immunohistochemistry to show macrophage and lymphocyte infiltration in their biopsy specimens, followed by quantification of the infiltration density. The outcome was the treatment response, defined as complete or partial remission at 12 months of immunosuppression.

Results: The infiltration of $CD68^+$ macrophages in the interstitium increased in patients with LN. High levels of $CD68^+$ macrophage infiltration in the interstitium were associated with a low probability of treatment response in the adjusted analysis, and verse vice. The density of $CD68^+$ macrophage infiltration in the interstitium alone predicted the response to immunosuppression (area under the curve [AUC], 0.70; 95% CI, 0.63 to 0.76). The addition of $CD68^+$cells/interstitial field to the pathological and clinical data at biopsy in the prediction model resulted in an increased AUC of 0.78 (95% CI, 0.73 to 0.84).

Conclusion: The density of tubulointerstitial macrophage infiltration is an independent predictor for treatment response in LN. Adding tubulointerstitial macrophage infiltration density to clinicopathological data at the time of biopsy significantly improves risk prediction of treatment response in LN patients.

KEYWORDS

lupus nephritis, macrophage infiltration, treatment response, predictor, predictive models

Introduction

Lupus nephritis (LN) is a common and important manifestation of systemic lupus erythematosus (SLE). About 60% of patients with SLE experience renal involvement, and 10% to 20% progress to end-stage kidney disease (ESKD) (1, 2). Chronic kidney disease (CKD) and ESKD caused by LN are the leading causes of mortality among patients with SLE. Although the precise pathogenesis of LN is not very clear at present, it is widely believed that immune and autoimmune activation plays an important role. Pathologically, LN is characterized by immune complex deposition and inflammation in glomeruli and the tubulointerstitium (3). Therefore, glucocorticoid steroids combined with other immunosuppressants are recommended to treat LN. With the rapid progress in the treatment of LN, several new immunosuppression strategies that target different pathways in the pathogenesis of LN have recently emerged (4). Despite these advancements, a subset of patients remains unresponsive to current therapeutic interventions.

It has been desired that a physician can predict the treatment response of patients with LN based on the biopsy. Unfortunately, there is a lack of good biomarkers that predict the response to treatment. Previous studies have shown that hypertension, serum creatinine (SCr), chronicity index score (CIs), and other indicators can serve as predictors of treatment response (5–8). However, the prognostic value of the conventional clinicopathological features remains low. Immune cells, including T lymphocytes, B lymphocytes, and macrophages, play roles in the pathogenesis of LN. The density of the immune cell infiltration, especially macrophages, correlates with the severity of renal histologic lesions and the level of SCr at biopsy (9, 10). Previous studies have demonstrated that an increased number of macrophages is associated with impaired kidney function. After activation, macrophages can secrete proinflammatory cytokines and activate other immune cells (9, 11). Additionally, macrophages exhibit compromised phagocytic activity and a diminished ability to eliminate apoptotic cells, resulting in the excessive generation of autoantibodies in LN patients.

Based on the above studies, macrophages have been suggested to be closely associated with LN. Therapeutic interventions targeting macrophage function in LN patients have been explored, and ongoing studies are investigating the potential benefits of macrophage depletion (12, 13). Nevertheless, it is not known whether the density of macrophage infiltration can serve as a predictor for treatment response in LN. Therefore, we aimed to determine whether the extent of macrophage infiltration in kidney can predict the response to immunosuppression in LN patients.

Methods

Patients

This retrospective cohort study was conducted with the approval of the Institutional Review Board of Nanjing Jinling Hospital (2021NZKY-021-01). A total of 1,297 patients with biopsy-proven LN in the hospital from January 2010 to December 2017 were screened for the cohort. Their renal biopsy samples were assessed following the classification criteria established by the International Society of Nephrology/Renal Pathology Society (ISN/RPS) (14). The patients who met at least four of the criteria for SLE in the 1997 revised American College of Rheumatology classification were selected for the cohort. Baseline and follow-up data of the LN patients were obtained from the database of the National Clinical Research Center of Kidney Diseases, Jinling Hospital.

All the patients received regular immunosuppressive therapy for one year. Patients with incomplete information of $CD4^+$, $CD8^+$ lymphocytes, and $CD68^+$ macrophages in kidney tissue and follow-up records were excluded (Figure 1). Ultimately, a total of 430 patients were enrolled in the study.

Treatment response and definition

Baseline data collection and follow-up visits were conducted by research personnel. Data on demographic characteristics, clinicopathological features, treatment modalities, and treatment response were obtained. Anti-nuclear antibodies (ANA) and anti-double stranded DNA antibodies (anti-dsDNA) were described as positive or negative. The estimated glomerular filtration rate (eGFR) was calculated by the Chronic Kidney Disease Epidemiology Collaboration (CKD-EPI) (15). Disease activity was scored according to the Systemic Lupus Erythematous Disease Activity Index (SLEDAI). Treatment response included complete remission (urinary protein quantitation (UPRO) < 0.4 g/24 hours and normal SCr) and partial remission (≥ 50% reduction in proteinuria and UPRO < 3.5 g/24 hours, serum albumin (ALB) level ≥ 30 g/L, and normal or ≤ 25% increase in SCr level from baseline) at 12 months.

Histopathology and macrophage infiltration in renal tissue

All renal biopsy specimens were obtained by percutaneous needle biopsy and were routinely examined by light microscopy, immunofluorescence, and electron microscopy. Two experienced pathologists independently examined the kidney biopsy specimens. They had access to the patient's clinical information, including vital

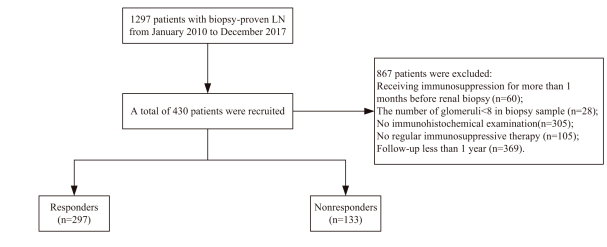

FIGURE 1
Flowchart of the study.

signs, blood test results, urinalysis results, and clinical diagnoses. Pathological parameters such as activity index score (AIs) and chronicity index score (CIs) were evaluated as described previously (16).

Infiltrating macrophages and lymphocytes in renal tissue were identified using immunohistochemical staining. Paraffin-embedded tissue sections (2 μm) were incubated with the following primary antibodies: mouse anti-human CD68 mAb (M0876; DAKO, Glostrup, Denmark), rabbit antihuman CD3 antibody (SP7; LEICA), rabbit antihuman CD4 antibody (NCL-L-368; LEICA) and rabbit antihuman CD8 (NCL-L-295). The slides were then incubated with the secondary antibody and visualized using a LEICA System Kit and counterstained with hematoxylin. The stained sections were scanned with a Digital Pathology Slide Scanner (Leica, Wetzlar, Germany). Positive-stained cells were automatically counted in all nonglobally sclerotic glomeruli at 400 magnifications using Aperio eSlide Manager (Leica)(Figure 2).

Statistical analyses

The density of glomerular and tubulointerstitial infiltration between the response and nonresponse groups was compared using the Mann–Whitney test and the Spearman correlation between the density of glomerular and tubulointerstitial infiltration and clinicopathologic variables was calculated. In addition, logistic regression analyses were used to examine the association between different levels of glomerular and tubulointerstitial infiltration and the treatment response, with and without adjustment for gender, age, UPRO, SCr, C4, LN duration, hypertension, repeat biopsy, AIs, CIs, and ISN/RPS classification. Then all patients included in this study were randomly categorized into a training cohort or validation cohort in a 3:1 ratio. Three prediction models were used: a univariable model with the level of infiltration in glomeruli or tubulointerstitium separately; a model with $CD4^+$ cells/interstitial field, $CD8^+$ cells/interstitial field, and $CD68^+$ cells/interstitial field together; and a model using combinations of the level of infiltration in glomerulus or tubulointerstitium, other pathological and clinical data. We also used stepwise regression with forward selection and backward elimination to obtain the model that minimizes the Alkaike information criterion (AIC). Performance of three logistic regression models in predicting the treatment response in both the training set and the validation set was reported and the predictive accuracy of these models was assessed by discrimination as measured by AUC.

Data analysis was performed using RStudio version 2023.03.0, an integrated development environment for R version 4.2.3 (R Core Team, Vienna, Austria). The difference was considered statistically significant as a two-sided P-value < 0.05.

Results

Characteristics of patients

Included in this study were 430 biopsy-proven LN patients, with the female gender predominating (84.65%) and a mean age of 30.31 ± 11.14 years (Table 1). The median SCr level at presentation was 0.83 (0.63–1.31) mg/dl. The median UPRO was 3.10 (1.72-5.58) g/24h. The median C3 and C4 levels were 0.41 (0.10-1.28) g/L and 0.08 (0.04-0.12) g/L, respectively. Most patients in our study had proliferative LN, of which 209 patients (48.60%) had pure proliferative LN (n = 35 for class III and n = 174 for class IV), 167 patients (38.83%) mixed proliferative LN (n = 44 for class III + V and n = 123 for class IV + V), 2 (0.47%) lupus podocytopathy, 5 (1.16%) class II LN, and 47 (10.93%) membranous LN. At the time of biopsy, the median AIs and CIs were evaluated by modified NIH activity and chronicity index of 7.00 (4.00-9.00) and 2.00 (1.00-3.00), respectively. The induction therapy was based on the histological lesions shown by renal biopsy. All the patients received treatment with corticosteroids without contraindications. Additionally, 126 (29.30%) received multi-target therapy, of which 120 cases of mycophenolate mofetil (MMF) combined with tacrolimus and 6 MMF combined with cyclosporine.

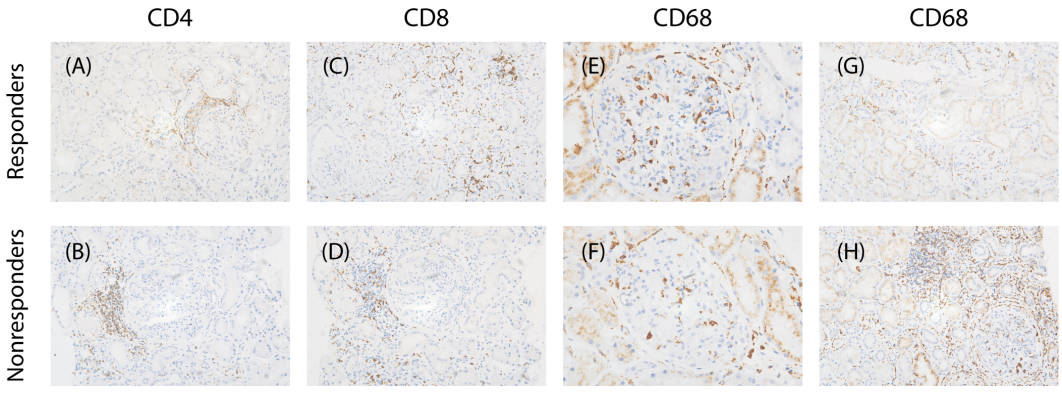

FIGURE 2
Characteristics of infiltrating cells in two groups. **(A, B)** Representative images of immunostaining for CD4 of tubulointerstitial (×200), **(C, D)** immunostaining for CD8 of tubulointerstitial(×200), **(E, F)** immunostaining for CD68 of glomerular (×400), **(G,H)** immunostaining for CD68 of tubulointerstitial(×200).

10.3389/fimmu.2024.1321507

TABLE 1 Baseline clinical characteristics of patients with lupus nephritis.

	Overall n=430	Responders n=297	Nonresponders n=133	P-value
Female gender,n (%)	364 (84.65%)	268 (90.24%)	96 (72.18%)	<0.001
Age (years)	30.31 ± 11.14	30.67 ± 11.18	29.50 ± 11.06	0.315
SLE duration (months)	6.00 (1.00-40.50)	6.00 (1.00-36.00)	12.00 (1.00-48.00)	0.015
LN duration (months)	2.00 (0.67-23.50)	1.00 (0.67-12.00)	4.00 (1.00-36.00)	0.018
SLEDAI (2K)	14.37 ± 5.28	14.80 ± 5.37	13.43 ± 4.96	0.013
Co-morbidities				
Hypertension, n (%)	136 (31.63%)	77 (25.93%)	59 (44.36%)	<0.001
Diabetes, n (%)	40 (9.30%)	27 (9.09%)	13 (9.77%)	0.822
SS, n (%)	9 (2.09%)	5 (1.68%)	4 (3.01%)	0.468
Extrarenal organ-system involvement, n (%)				
Cutaneous involvement	223 (51.86%)	158 (53.20%)	65 (48.87%)	0.407
Serositis	58 (13.49%)	36 (12.12%)	22 (16.54%)	0.215
Arthritis	200 (46.51%)	135 (45.45%)	65 (48.87%)	0.511
Neurological disorder	18 (4.19%)	12 (4.04%)	6 (4.51%)	0.822
Haematologic disorder	320 (74.42%)	217 (73.06%)	103 (77.44%)	0.336
Cardiac involvement	11 (2.56%)	4 (1.35%)	7 (5.26%)	0.017
Gastrointestinal involvement	47 (10.93%)	29 (9.76%)	18 (13.53%)	0.247
Laboratory parameters				
WBC (*10^9)	5.60 (4.23-8.30)	5.60 (4.30-8.40)	5.70 (4.20-8.20)	0.839
PLT (*10^12)	183.15 ± 79.43	183.63 ± 76.09	182.09 ± 86.74	0.853
Hb (g/L)	101.91 ± 20.13	103.00 ± 18.85	99.50 ± 22.61	0.096
ALB(g/L)	28.60 ± 5.87	28.82 ± 5.84	28.10 ± 5.93	0.240
BUN(mg/dl)	23.15 (15.43-38.45)	21.90 (14.90-33.10)	28.85 (17.70-55.80)	<0.001
SCr (mg/dl)	0.83 (0.63-1.31)	0.76 (0.62-1.04)	1.20 (0.70-2.25)	<0.001
UA (μmol/L)	400.50 (320.00-504.50)	379.00 (307.00-481.00)	439.00 (348.00-563.00)	<0.001
eGFR(mL/min per 1.73 m2)	96.44 (56.47-121.76)	103.55 (73.42-122.25)	64.98 (32.15-115.16)	<0.001
UPRO (g/24h)	3.10 (1.72-5.58)	3.30 (1.72-5.40)	2.95 (1.74-6.25)	0.962
Positive ANA, n (%)	414 (96.28%)	291 (97.98%)	123 (92.48%)	0.005
Positive anti-dsDNA, n (%)	245 (56.98%)	178 (59.93%)	67 (50.38%)	0.064
C3(g/L)	0.41 (0.10-1.28)	0.40 (0.10-1.28)	0.44 (0.10-1.23)	0.037
C4(g/L)	0.08 (0.04-0.12)	0.08 (0.04-0.10)	0.10 (0.06-0.15)	<0.001
C1q(U/ml)	25.29 (10.36-56.90) (n=381)	26.08 (10.79-62.08) (n=263)	21.70 (7.85-50.06) (n=118)	0.193
$CD3^+$ cell counts (/μL)	790.50 (548.50-1082.75)	801.00 (566.00-1088.00)	749.00 (529.00-1053.00)	0.365
$CD4^+$ cell counts (/μL)	303.50 (214.00-459.75)	312.00 (223.00-472.00)	259.00 (192.00-417.00)	0.006
$CD8^+$ cell counts (/μL)	404.50 (265.00-585.75)	395.00 (262.00-554.00)	421.00 (274.00-611.00)	0.537
$CD20^+$ cell counts (/μL)	163.50 (81.75-279.00) (n=400)	181.50 (98.00-308.25) (n=278)	119.00 (71.25-239.00) (n=122)	<0.001
Treatment				0.436

(Continued)

TABLE 1 Continued

	Overall n=430	Responders n=297	Nonresponders n=133	P-value
Pred+MMF+CNIs	126 (29.30%)	90 (30.30%)	36 (27.07%)	
Pred+CYC	112 (26.05%)	71 (23.91%)	41 (30.83%)	
Pred+MMF	74 (17.21%)	54 (18.18%)	20 (15.04%)	
Pred+CNIs	66 (15.35%)	45 (15.15%)	21 (15.79%)	
Pred only	18 (4.19%)	10 (3.37%)	8 (6.02%)	
Pred+TW	16 (3.72%)	14 (4.71%)	2 (1.50%)	
Pred+RTX	7 (1.63%)	4 (1.35%)	3 (2.26%)	
Pred+AZA	6 (1.40%)	5 (1.68%)	1 (0.75%)	
Pred+AHSCT	5 (1.16%)	4 (1.35%)	1 (0.75%)	

SLE, systemic lupus erythematous; LN, lupus nephritis; SLEDAI, Systemic Lupus Erythematous Disease Activity; SS, Sjogren's syndrome; WBC, white blood cell; PLT, blood platelet; Hb, hemoglobin; ALB, albumin; SCr, serum creatinine; UA, blood uric acid; eGFR, the estimated glomerular filtration rate; UPRO, urinary protein quantitation; C3, complement 3; C4, complement 4; ANA, anti-nuclear; anti-dsDNA, anti-double stranded DNA antibodies; Pred, prednisone; MMF, Mycophenolate Mofetil; CNIs, Calcineurin Inhibitors; CYC, Cyclophosphamide; TW, Triptergium wilfordii; RTX, Rituximab; AZA, Azathioprine; AHSCT, Autologous hematopoietic stem cell transplantation.

There were 112 (26.05%) cyclophosphamide (CYC), 74 (17.21%) MMF, 66 (15.35%) calcineurin inhibitors (including 60 tacrolimus and 6 cyclosporine), 16 (3.72%) Triptergium wilfordii (TW), 7 (1.63%) rituximab (RTX), 6 (1.40%) azathioprine (AZA), and 5 (1.16%) autologous hematopoietic stem cell transplantation (AHSCT), respectively. 18 (4.19%) patients were treated with corticosteroids alone (Table 1).

Clinicopathologic features in patients with or without response to treatment

Our analysis encompassed four patients who underwent repeat renal biopsies. The characteristics of the patients at the time of kidney biopsy were stratified by response to immunosuppression and are presented in Tables 1, 2.

TABLE 2 Renal pathological features in the patients of lupus nephritis.

	Overall N=430	Responders n=297	Nonresponders n=133	P-value
Repeat biopsy	4 (0.93%)	4 (3.01%)	0 (0.00%)	0.009
Glomerular number	30.34 ± 11.80	31.33 ± 12.01	28.14 ± 11.05	0.009
ISN/RPS classification, n (%)				0.952
LP	2 (0.47%)	2 (0.67%)	0 (0.00%)	
Class II	5 (1.16%)	3 (1.01%)	2 (1.50%)	
Class III	35 (8.14%)	26 (8.75%)	9 (6.77%)	
Class III+V	44 (10.23%)	30 (10.10%)	14 (10.53%)	
Class IV	174 (40.47%)	119 (40.07%)	55 (41.35%)	
Class IV+V	123 (28.60%)	85 (28.62%)	38 (28.57%)	
Class V	47 (10.93%)	32 (10.77%)	15 (11.28%)	
AIs	7.00 (4.00-9.00)	7.00 (4.00-9.00)	6.00 (4.00-10.00)	0.788
CIs	2.00 (1.00-3.00)	1.00 (0.00-3.00)	2.00 (1.00-4.00)	<0.001
$CD4^+$cells/interstitial field	92.00 (48.00-168.00)	76.00 (40.00-140.00)	144.00 (72.00-208.00)	<0.001
$CD8^+$cells/interstitial field	96.00 (48.00-167.00)	76.00 (40.00-144.00)	148.00 (72.00-204.00)	<0.001
$CD68^+$cells/glomerulus	9.80 (3.70-21.30)	11.00 (4.30-22.40)	7.40 (3.00-17.00)	0.011
$CD68^+$cells/interstitial field	332.00 (184.00-504.00)	276.00 (168.00-452.00)	468.00 (280.00-636.00)	<0.001

LP, Lupus podocytopathy; AIs, activity index score; CIs, activity index score.

10.3389/fimmu.2024.1321507

There were 69.07% of patients (n = 297) in the response group and the rest patients (n = 133) in the nonresponse group. The proportion of women in the response group was significantly higher than in the nonresponse group ($P < 0.01$). Patients in the response group were more likely to have higher SLEDAI scores ($P = 0.013$). However, patients in the nonresponse group were more likely to have comorbid hypertension, a longer course of SLE and LN, and a higher frequency of cardiac involvement ($P < 0.05$). Regarding laboratory parameters, patients in the response group were more likely to have better renal function, fewer immunological indexes, and more numbers of lymphocyte subsets than the nonresponse group ($P < 0.05$). There were no significant differences in age, diabetes, SS, induction therapy, and baseline level of leukocyte counts, platelets (PLT), hemoglobin (Hb), ALB, UPRO, Anti-Complement 1q antibodies (anti-C1q), $CD3^+$ cell counts (CD3), and $CD8^+$ cell counts (CD8) between the two groups ($P > 0.05$).

Histologically, there was no significant difference in pathological classification between the two groups. The patients in the nonresponse group had higher CIs compared with those in the response group ($P < 0.05$). Most importantly, the level of inflammatory infiltration including $CD4^+$, $CD8^+$ T cells, and $CD68^+$ macrophages in tubulointerstitium was significantly higher in the nonresponse group. However, infiltrated $CD68^+$ macrophages in glomeruli were increased in the response group.

Correlations between cellular infiltration and clinicopathological parameters

We estimated the levels of $CD4^+$, $CD8^+$ lymphocytes, and $CD68^+$ macrophages in glomeruli and tubulointerstitium in 430 patients with LN. As shown in Figure 3, Table 3, infiltrated $CD4^+$, $CD8^+$ lymphocytes, and $CD68^+$ macrophages in tubulointerstitium were increased in patients with proliferative LN compared with those with pure SLE ISN/RPS class V. The number of $CD68^+$ macrophages in glomeruli was also increased in patients with proliferative LN, but the statistical difference was not significant.

The density of infiltrated $CD68^+$ macrophages in glomeruli correlated with age, SLEDAI, SLE duration, LN duration, PLT, Hb, blood urea nitrogen (BUN), UA, C3, C4, CD3, CD8, AIs, and CIs, with the highest Spearman correlation coefficients (r) being 0.41. The density of tubulointerstitial infiltration, including $CD4^+$ cells, $CD8^+$ cells, and $CD68^+$ cells, positively correlated with BUN, SCr, and CIs, and negatively correlated with Hb and eGFR. The absolute values of r ranged from 0.31 to 0.51 (Figure 4, Table 4).

Association between cell infiltration and response to treatment in patients with LN

The logistic regression analyses indicated that the tertile groups with more infiltration had a lower probability of responding to

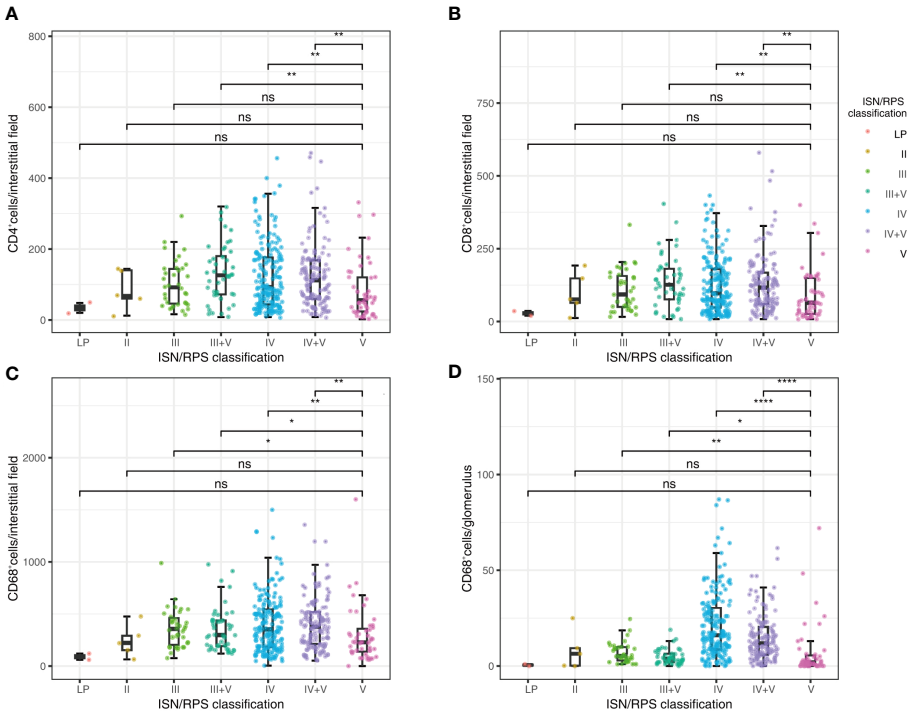

FIGURE 3
Correlations between ISN/RPS classification in LN with $CD4^+$ lymphocyte infiltration in tubulointerstitium **(A)**, $CD8^+$ lymphocyte infiltration in tubulointerstitium **(B)**, $CD68^+$ macrophage infiltration in tubulointerstitium **(C)**, and $CD68^+$ macrophage infiltration in glomeruli **(D)**. *P < 0.05, **P < 0.01, ***P < 0.001, ****P < 0.0001. Boxplot: boxplot medians (center lines), interquartile ranges (box ranges), whisker ranges; LP, lupus podocytopathy. ns, not significant.

10.3389/fimmu.2024.1321507

TABLE 3 The inflammatory cell infiltration in different ISN/RPS classifications of lupus nephritis.

	$CD4^+$cells /interstitial field	$CD8^+$cells /interstitial field	$CD68^+$cells /glomerulus	$CD68^+$cells /interstitial field
LP (n = 2)	34.00 (27.00-41.00)	28.00 (24.00-32.00)	0.50 (0.25-0.75)	90.00 (75.00-105.00)
Class II (n = 5)	68.00 (60.00-140.00)	76.00 (64.00-148.00)	6.40 (0.20-9.30)	220.00 (152.00-292.00)
Class III (n = 35)	92.00 (46.00-144.00)	92.00 (50.00-156.00)	5.30 (2.90-9.85)	356.00 (202.00-460.00)
Class III+V (n = 44)	126.00 (72.00-180.00)	126.00 (76.00-181.00)	3.70 (2.00-6.45)	298.00 (191.00-438.00)
Class IV (n = 174)	92.00 (44.00-176.00)	96.00 (48.00-180.00)	16.00 (8.67-30.27)	350.00 (184.00-544.00)
Class IV+V (n = 123)	112.00 (60.00-168.00)	116.00 (60.00-168.00)	11.70 (5.90-20.45)	376.00 (210.00-516.00)
Class V (n = 47)	56.00 (24.00-120.00)	64.00 (26.00-148.00)	2.00 (0.35-5.50)	228.00 (138.00-358.00)

LP, Lupus podocytopathy.

treatment in the crude model when they were compared with the groups with fewer $CD4^+$, $CD8^+$, and $CD68^+$ cells infiltrated in the tubulointerstitium. The association between the density of $CD68^+$ cell infiltration in the glomeruli and the treatment response disappeared even without adjustment (Table 5).

After adjusting for gender, age, UPRO, UA, SCr, and C4, the density of interstitium infiltration, expressed as $CD4^+$, $CD8^+$, and $CD68^+$ cells in the tubulointerstitium, remained significantly associated with treatment response, although this association was attenuated. The association between the density of $CD4^+$ and $CD8^+$ cells in the tubulointerstitium and treatment response disappeared after further adjusting for gender, age, UPRO, SCr, C4, LN duration, hypertension, repeat biopsy, AIs, CIs, and ISN/RPS classification. However, the density of $CD68^+$ cells in the tubulointerstitium remained significantly associated with treatment response after further adjustment. Among different level groups, the density of $CD68^+$ cells in the tubulointerstitium was significantly associated with treatment response in a high-level group (452–1600) (adjusted HR, 0.451; 95% CI, 0.231, 0.878) (Table 5).

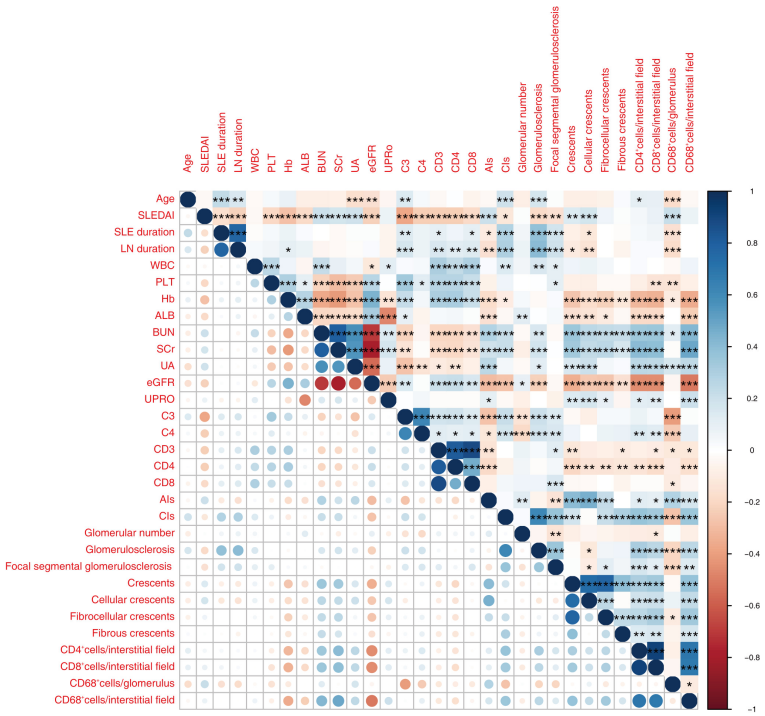

FIGURE 4
The heatmap shows correlations between parameters relevant for LN among the 430 patients enrolled. Only significant p values ($P < 0.05$) are shown. Red and blue colors represent significant negative and positive correlations. Darker color represents stronger correlations. *$P < 0.05$, **$P < 0.01$, ***$P < 0.001$.WBC, white blood cell; PLT, blood platelet; Hb, hemoglobin; ALB, albumin; SCr, serum creatinine; UA, blood uric acid; UPRO, urinary protein quantitation; eGFR, estimated glomerular filtration rate; C3, complement 3; C4, complement 4; CD4, $CD4^+$ cell count; CD8, $CD8^+$ cell count; AIs, activity index score; CIs, chronicity index score; GN, glomerulus number.

TABLE 4 The relationship between inflammatory cell infiltration and clinicopathological factors.

	$CD4^+$cells/ interstitial field		$CD8^+$cells/ interstitial field		$CD68^+$cells/ glomerulus		$CD68^+$cells/ interstitial field	
	r	P	r	P	r	P	r	P
Age	0.1028	0.0330	0.0913	0.0585	-0.1706	0.0004	-0.0324	0.5024
SLE duration	0.0391	0.4190	0.0535	0.2683	-0.1582	0.0010	-0.0096	0.8422
LN duration	0.0300	0.5354	0.0285	0.5560	-0.1724	0.0003	-0.0056	0.9083
SLEDAI (2K)	0.0445	0.3573	0.0835	0.0838	0.2164	<0.0001	0.0752	0.1192
WBC	0.0204	0.6727	-0.0061	0.8990	-0.0288	0.5510	0.0674	0.1628
PLT	-0.0877	0.0692	-0.1400	0.0036	-0.1457	0.0025	-0.0708	0.1429
Hb	-0.3120	<0.0001	-0.3313	<0.0001	-0.1053	0.0290	-0.3528	<0.0001
ALB	-0.1837	0.0001	-0.1871	0.0001	-0.0023	0.9626	-0.2322	<0.0001
BUN	0.3416	<0.0001	0.3535	<0.0001	0.1234	0.0104	0.4251	<0.0001
SCr	0.4015	<0.0001	0.3974	<0.0001	-0.0164	0.7350	0.4874	<0.0001
UA	0.2513	<0.0001	0.2405	<0.0001	0.1669	0.0005	0.2442	<0.0001
eGFR	-0.4514	<0.0001	-0.4543	<0.0001	-0.0486	0.3151	-0.5137	<0.0001
UPRO	0.1114	0.0209	0.1278	0.0080	-0.0067	0.8904	0.2048	<0.0001
C3	0.0763	0.1142	0.0376	0.4365	-0.4057	<0.0001	0.0128	0.7908
C4	0.1481	0.0021	0.1265	0.0087	-0.2462	<0.0001	0.0938	0.0520
CD3	-0.0764	0.1138	-0.0997	0.0389	-0.1137	0.0184	-0.1133	0.0187
CD4	-0.1367	0.0045	-0.1760	0.0002	-0.0943	0.0507	-0.1637	0.0007
CD8	-0.0151	0.7556	-0.0152	0.7530	-0.1078	0.0254	-0.0421	0.3842
AIs	0.1231	0.0106	0.1045	0.0303	0.2845	<0.0001	0.1615	0.0008
CIs	0.3688	<0.0001	0.3377	<0.0001	-0.2759	<0.0001	0.3552	<0.0001

SLE, systemic lupus erythematous; LN, lupus nephritis; SLEDAI, Systemic Lupus Erythematous Disease Activity; WBC, white blood cell; PLT, blood platelet; Hb, hemoglobin; ALB, albumin; SCr, serum creatinine; UA, blood uric acid; eGFR, estimated glomerular filtration rate; UPRO, urinary protein quantitation; C3, complement 3; C4, complement 4; CD4, CD4+ cell count; CD8, CD8+ cell count; AIs, activity index score; CIs, activity index score.

Predicting the response to treatment using the density of $CD4^+$, $CD8^+$ T cells, and $CD68^+$ macrophages in tubulointerstitium

Among the univariable models, inflammatory cell infiltration in tubulointerstitium had good performance in predicting the response to treatment with AUCs of 0.6672, 0.6592, and 0.6973 for $CD4^+$, $CD8^+$, and $CD68^+$ cells, respectively (Table 6).

Multivariable models incorporating infiltrations of all the inflammatory cells in tubulointerstitium, including $CD4^+$, $CD8^+$, and $CD68^+$ cells, did not improve the predictive performance as compared with the single density of $CD68^+$ macrophages in tubulointerstitium. To select a model that is convenient for clinical use, we used stepwise regression to select the variables with a minimized Alkaike information criterion. The final model included eight variables, including sex, SLEDAI, SCr, ANA, C4, CD4, CIs, and the density of $CD68^+$ macrophage in the tubulointerstitium. The model was logit (P)= -0.4844 + 0.6953 (if male) +0.0887*SLEDAI -0.5931*SCr -4.1868*C4 + 1.4451 (if ANA positive) +0.0010*CD4 -0.2040*CIs -0.0017*the density of $CD68^+$ macrophages in tubulointerstitium, where p is the probability of being responsive to treatment. This model produced an AUC of 0.7812 (95% CI, 0.7266 to 0.8358) in the training cohort and 0.7315 (95% CI, 0.6010 to 0.8620) in the validation cohort, respectively (Table 6).

Compared with the model containing $CD68^+$ macrophages only in tubulointerstitium, the final model significantly improved the risk reclassification, and net reclassification improved by 4.5%.

Therefore, our subsequent study was focused on the infiltration of $CD68^+$ macrophages in the tubulointerstitium. The relationship between $CD68^+$ macrophages and response to immunosuppression was further stratified by gender, age, SLEDAI, SCr, UA, eGFR, UPRO, anti-dsDNA, C3, C4, CD4, PLN (proliferative lupus nephritis), AIs, and CIs (Table 7).

Discussion

Our study has indicated that the density of $CD68^+$ macrophage infiltration in the tubulointerstitium can predict the treatment response with high accuracy. Among the inflammatory cells tested, only the density of $CD68^+$ macrophage infiltration in the

TABLE 5 Association between inflammatory cell infiltration and response to treatment in the study.

Exposure	Crude model	Model I	Model II
$CD4^+$cells/interstitial field	0.994 (0.991, 0.996) <0.00001	0.996 (0.994, 0.999) 0.00727	0.997 (0.994, 1.000) 0.06717
Tertile 1 (2 – 56)	1.0	1.0	1.0
Tertile 2(60 - 136)	0.624 (0.350, 1.112) 0.10973	0.746 (0.407, 1.367) 0.34306	0.826 (0.429, 1.590) 0.56695
Tertile 3(140 - 472)	0.244 (0.140, 0.425) <0.00001	0.387 (0.208, 0.721) 0.00276	0.516 (0.260, 1.022) 0.05790
Trend	0.991 (0.988, 0.994) <0.00001	0.994 (0.990, 0.998) 0.00139	0.707 (0.503, 0.994) 0.04640
$CD8^+$cells/interstitial field	0.995 (0.992, 0.997) <0.00001	0.997 (0.994, 0.999) 0.01472	0.998 (0.995, 1.000) 0.08402
Tertile 1(8 - 60)	1.0	1.0	1.0
Tertile 2(64 - 144)	0.713 (0.403, 1.262) 0.24540	0.873 (0.477, 1.597) 0.65879	0.952 (0.501, 1.809) 0.88034
Tertile 3(148 - 580)	0.236 (0.137, 0.406) <0.00001	0.381 (0.207, 0.703) 0.00201	0.514 (0.263, 1.004) 0.05139
Trend	0.991 (0.988, 0.994) <0.00001	0.994 (0.990, 0.997) 0.00065	0.700 (0.499, 0.982) 0.03891
$CD68^+$cells/glomerulus	1.014 (0.999, 1.029) 0.07419	1.009 (0.992, 1.026) 0.31941	0.997 (0.979, 1.016) 0.76542
Tertile 1(0 - 5.5)	1.0	1.0	1.0
Tertile 2(5.6 - 15.8)	1.181 (0.723, 1.929) 0.50721	1.237 (0.714, 2.141) 0.44812	1.075 (0.577, 2.005) 0.81973
Tertile 3(16 - 87)	1.865 (1.120, 3.107) 0.01662	1.857 (1.007, 3.424) 0.04748	1.340 (0.645, 2.785) 0.43285
Trend	1.026 (1.005, 1.047) 0.01431	1.025 (1.000, 1.051) 0.04645	1.157 (0.804, 1.667) 0.43248
$CD68^+$cells/interstitial field	0.997 (0.996, 0.998) <0.00001	0.998 (0.997, 0.999) 0.00041	0.998 (0.997, 0.999) 0.00522
Tertile 1(0.2 - 220)	1.0	1.0	1.0
Tertile 2(224 - 448)	0.637 (0.364, 1.115) 0.11439	0.814 (0.449, 1.477) 0.49837	0.817 (0.436, 1.529) 0.52679
Tertile 3(452 - 1600)	0.264 (0.155, 0.448) <0.00001	0.390 (0.213, 0.715) 0.00232	0.451 (0.231, 0.878) 0.01910
Trend	0.997 (0.996, 0.998) <0.00001	0.998 (0.996, 0.999) 0.00160	0.668 (0.477, 0.935) 0.01864

The crude model is not adjusted.
Adjust model I adjust for gender, age, UPRO, SCr, C4;
Adjust model II adjust for gender, age, UPRO, SCr, C4,LN duration, hypertension, repeat biopsy, AIs, CIs, and ISN/RPS classification.

TABLE 6 Performance of inflammatory cell infiltration, clinical data, or other renal pathological features for predicting response to treatment.

Variables	AUC (95% Confidence Interval)	
	Training Cohort (n=322)	Validation Cohort (n=108)
$CD4^+$cells/interstitial field	0.6672 (0.6004,0.7340)	0.6569 (0.5479,0.7660)
$CD8^+$cells/interstitial field	0.6592 (0.5916,0.7268)	0.6491 (0.5403,0.7579)
$CD68^+$cells/interstitial field	0.6973 (0.6324,0.7622)	0.6061 (0.4882,0.7239)
$CD4^+$cells/interstitial field, $CD8^+$cells/interstitial field and $CD68^+$cells/interstitial field	0.6975 (0.6327,0.7623)	0.6288 (0.5148,0.7427)
$CD68^+$cells/interstitial field, other pathological and clinical data	0.7812 (0.7266,0.8358)	0.7315 (0.6010, 0.8620)

tubulointerstitium at the time of renal biopsy was associated with response in the treatment for one year. The density of $CD68^+$ macrophage infiltration was shown to be a more effective predictor of treatment outcome compared to conventional histological assessment. Furthermore, we have developed a simple prediction model that incorporates clinicopathological variables and $CD68^+$ cell infiltration and has an AUC of 0.78.

In the majority of previous studies, several variables such as SCr, CIs, age, sex, Hb, urine protein-to-creatinine ratio (UPCR) or UPRO, LN duration, ISN/RPS classification, interstitial fibrosis, and tubular atrophy, have been identified as independent risk factors for poor treatment response in LN patients. In this study, eight factors were included in the prediction model, namely SCr, CIs, the density of $CD68^+$ macrophages in the tubulointerstitium, sex, SLEDAI, ANA, C4, and CD4. Notably, the density of $CD68^+$ macrophage infiltration in the tubulointerstitium demonstrated exceptional predictive ability for treatment response, even superior over the established factors such as SCr and CIs. Indeed, it has previously been suggested that urine macrophages could be a promising marker for identifying patients

TABLE 7 Relationship between the density of CD68$^+$ macrophage in tubulointerstitium and response to treatment under different stratification.

Subgroupstratification		Cases	HR (95%CI)	P-value	P for interaction
Gender	male	66	0.998 (0.996, 1.000)	0.0194	0.7779
	female	364	0.997 (0.996, 0.998)	<0.0001	
Age	≤38	334	0.998 (0.997, 0.999)	<0.0001	0.0234
	>38	96	0.994 (0.991, 0.997)	0.0004	
SLEDAI	≤12	317	0.997 (0.996, 0.998)	<0.0001	0.8869
	>12	113	0.997 (0.995, 0.999)	0.0058	
SCr	≤1.2	312	0.999 (0.997, 1.000)	0.0470	0.4323
	>1.2	118	0.998 (0.996, 0.999)	0.0021	
UA	≤380	192	0.998 (0.996, 1.000)	0.0117	0.7326
	>380	238	0.997 (0.996, 0.999)	<0.0001	
eGFR	>60	118	0.997 (0.996, 0.999)	0.0005	0.1434
	≤60	312	0.999 (0.997, 1.000)	0.0831	
UPRO	≤2.5	184	0.997 (0.996, 0.999)	0.0004	0.8852
	>2.5	246	0.997 (0.996, 0.998)	<0.0001	
A-dsDNA	negative	185	0.997 (0.996, 0.999)	0.0001	0.8366
	positive	245	0.997 (0.996, 0.999)	<0.0001	
C3	≤0.46	254	0.997 (0.996, 0.998)	<0.0001	0.9764
	>0.46	176	0.997 (0.996, 0.999)	0.0001	
C4	≤0.09	248	0.998 (0.996, 0.999)	0.0002	0.7275
	>0.09	182	0.997 (0.996, 0.999)	<0.0001	
CD4	≤260	173	0.998 (0.996, 0.999)	0.0001	0.5375
	>260	257	0.997 (0.996, 0.998)	<0.0001	
PLN	NO	54	0.996 (0.993, 1.000)	0.0232	0.5639
	YES	376	0.997 (0.996, 0.998)	<0.0001	
AIs	≤3	66	0.997 (0.994, 1.000)	0.0311	0.8287
	>3	364	0.997 (0.996, 0.998)	<0.0001	
CIs	≤3	361	0.998 (0.997, 0.999)	<0.0001	0.4082
	>3	69	0.997 (0.995, 0.999)	0.0079	

SLEDAI, Systemic Lupus Erythematous Disease Activity; SCr, serum creatinine; UA, blood uric acid; eGFR, estimated glomerular filtration rate; UPRO, urinary protein quantitation; C3, complement 3; C4, complement 4; CD4, CD4+ cell count; LP, Lupus podocytopathy; AIs, activity index score; CIs, activity index score.

with active kidney disease in childhood-onset systemic lupus erythematosus (cSLE) (17). Also, one study showed that the number of CD68$^+$ macrophages in the tubulointerstitium was an independent variable associated with poor renal outcomes in proliferative LN patients with a mean follow-up of 45 months (18).

Previous studies showed that macrophage infiltration density was closely associated with renal function decline in both transplanted kidneys and immunocomplex nephritis. Jan Hinrich Brasen et al. showed that the density of macrophages predicted future renal transplant function and improved the prognostic value of early renal transplant biopsies (19). Consistently, one study showed that tubulointerstitial macrophage infiltration was correlated with renal interstitial fibrosis and significant reduction of eGFR in patients with IgA Nephropathy (IgAN) (20), suggesting that renal tubulointerstitial macrophage infiltration was a potential hallmark of chronic kidney injury. Macrophages were shown to be necessary for the development of immune glomerulonephritis mediated by pathogenic antibodies in mouse models of LN, thus being a potential therapeutic target for LN (12, 21–23). In mouse models of lupus, functional impairment or depletion of macrophages resulted in attenuation of kidney injury (24, 25). Consistently, the reduction of macrophage recruitment to the kidney by disrupting the action of the related chemokines or their receptors also alleviated kidney injury in the lupus mice (26, 27). Similarly, macrophage injection or macrophage infiltration

stimulation in lupus-prone mice aggravated nephritis and kidney damage (28).

At present, there is no panel of biomarkers or modeling approach for LN that exhibits superiority in predicting the response after treatment for one year. Quantification of tubulointerstitial macrophage infiltration is simple and robust, which may help improve the treatment decision for LN patients, particularly those who are at high risk of disease progression. After comparing the predictive performance of various types of inflammatory cell infiltration, we have developed a model combining tubulointerstitial macrophage infiltration and clinicohistological data in the present study. The results of response prediction to immunosuppression were consistent between training and validation cohorts. For simplicity and convenience, the final model uses only eight variables, nevertheless, it still shows good predictive performance. In addition, we conducted internal verification in the Pred+MMF+CNIs, Pred+CYC, Pred+MMF, and Pred+CNIs groups, and the AUC were 0.758, 0.719, 0.747, and 0.722 respectively, and there were no statistical differences between the groups.

This study has several limitations. Firstly, we excluded the patients whose data of $CD4^+$, $CD8^+$ lymphocytes, and $CD68^+$ macrophages in the kidney biopsy sample and follow-up records were lacking, as noted earlier in the Methods. This exclusion might have resulted in both selection bias and confounding bias. Secondly, it was a pity that we did not have the quantitative data about the level of anti-dsDNA antibody, so we were unable to analyze the association between the level of anti-dsDNA antibody and response to treatment. Thirdly, the retrospective nature of this study prevented the collection of data on cumulative immunosuppressive agent dosage. Future prospective studies should be considered analyzing the correlation between cumulative immunosuppressive agent dosage and the level of $CD68^+$ macrophage infiltration. Lastly, this is a single-center study conducted and validated in a Chinese population.

In conclusion, we have identified the density of macrophage infiltration in tubulointerstitium as an independent and robust predictor of response to immunosuppression in patients with LN. Our prediction model that combines the density of $CD68^+$ macrophage in tubulointerstitium with clinicopathologic data can improve early treatment decisions for patients with LN.

Data availability statement

The raw data supporting the conclusions of this article will be made available by the authors, without undue reservation.

Ethics statement

The studies involving humans were approved by Institutional Review Board of Nanjing Jinling Hospital. The studies were conducted in accordance with the local legislation and institutional requirements. Written informed consent for participation was not required from the participants or the participants' legal guardians/next of kin in accordance with the national legislation and institutional requirements.

Author contributions

JW: Data curation, Investigation, Methodology, Writing – original draft, Writing – review & editing, Project administration, Validation. WL: Data curation, Investigation, Writing – original draft. MZ: Data curation, Investigation, Writing – original draft. YT: Data curation, Investigation, Writing – original draft. DC: Data curation, Investigation, Writing – original draft. DQ: Data curation, Investigation, Writing – original draft. FX: Methodology, Writing – original draft. DL: Methodology, Writing – original draft. ZC: Conceptualization, Supervision, Writing – review & editing. HZ: Conceptualization, Supervision, Writing – review & editing.

Funding

The author(s) declare financial support was received for the research, authorship, and/or publication of this article. This work was supported by the National Key Research and Development Project of China (Grant number 2021YFC2501302) and Jinling Hospital (2023LCZLXB049, 2023JCYJYB126, 2022LCZLXJS7).

Acknowledgments

The authors thank Professor Shi Shaolin for his help in revising and polishing the manuscript.

Conflict of interest

The authors declare that the research was conducted in the absence of any commercial or financial relationships that could be construed as a potential conflict of interest.

Publisher's note

References

1. Croca SC, Rodrigues T, Isenberg DA. Assessment of a lupus nephritis cohort over a 30-year period. *Rheumatol (Oxford)* (2011) 50(8):1424–30. doi: 10.1093/rheumatology/ker101

2. Maroz N, Segal MS. Lupus nephritis and end-stage kidney disease. *Am J Med Sci* (2013) 346(4):319–23. doi: 10.1097/MAJ.0b013e31827f4ee3

3. Giannakakis K, Faraggiana T. Histopathology of lupus nephritis. *Clin Rev Allergy Immunol* (2011) 40(3):170–80. doi: 10.1007/s12016-010-8207-1

4. Mok CC, Teng Y, Saxena R, Tanaka Y. Treatment of lupus nephritis: consensus, evidence and perspectives. *Nat Rev Rheumatol* (2023) 19(4):227–38. doi: 10.1038/s41584-023-00925-5

5. Moroni G, Gatto M, Tamborini F, Quaglini S, Radice F, Saccon F, et al. Lack of EULAR/ERA-EDTA response at 1 year predicts poor long-term renal outcome in patients with lupus nephritis. *Ann Rheum Dis* (2020) 79(8):1077–83. doi: 10.1136/annrheumdis-2020-216965

6. Chen YE, Korbet SM, Katz RS, Schwartz MM, Lewis EJ. Value of a complete or partial remission in severe lupus nephritis. *Clin J Am Soc Nephrol* (2008) 3(1):46–53. doi: 10.2215/CJN.03280807

7. Ioannidis JP, Boki KA, Katsorida ME, Drosos AA, Skopouli FN, Boletis JN, et al. Remission, relapse, and re-remission of proliferative lupus nephritis treated with cyclophosphamide. *Kidney Int* (2000) 57(1):258–64. doi: 10.1046/j.1523-1755.2000.00832.x

8. Ichinose K, Kitamura M, Sato S, Eguchi M, Okamoto M, Endo Y, et al. Complete renal response at 12 months after induction therapy is associated with renal relapse-free rate in lupus nephritis: a single-center, retrospective cohort study. *Lupus* (2019) 28(4):501–9. doi: 10.1177/0961203319829827

9. Tucci M, Stucci S, Strippoli S, Silvestris F. Cytokine overproduction, T-cell activation, and defective T-regulatory functions promote nephritis in systemic lupus erythematosus. *J BioMed Biotechnol* (2010) 2010:457146. doi: 10.1155/2010/457146

10. Olmes G, Büttner-Herold M, Ferrazzi F, Distel L, Amann K, Daniel C. CD163+ M2c-like macrophages predominate in renal biopsies from patients with lupus nephritis. *Arthritis Res Ther* (2016) 18:90. doi: 10.1186/s13075-016-0989-y

11. Biermann MH, Veissi S, Maueröder C, Chaurio R, Berens C, Herrmann M, et al. The role of dead cell clearance in the etiology and pathogenesis of systemic lupus erythematosus: dendritic cells as potential targets. *Expert Rev Clin Immunol* (2014) 10(9):1151–64. doi: 10.1586/1744666X.2014.944162

12. Ahamada MM, Jia Y, Wu X. Macrophage polarization and plasticity in systemic lupus erythematosus. *Front Immunol* (2021) 12:734008. doi: 10.3389/fimmu.2021.734008

13. Yoo EJ, Oh KH, Piao H, Kang HJ, Jeong GW, Park H, et al. Macrophage transcription factor TonEBP promotes systemic lupus erythematosus and kidney injury via damage-induced signaling pathways. *Kidney Int* (2023) 104(1):163–80. doi: 10.1016/j.kint.2023.03.030

14. Weening JJ, D'Agati VD, Schwartz MM, Seshan SV, Alpers CE, Appel GB, et al. The classification of glomerulonephritis in systemic lupus erythematosus revisited. *Kidney Int* (2004) 65(2):521–30. doi: 10.1111/j.1523-1755.2004.00443.x

15. Levey AS, Stevens LA, Schmid CH, Zhang YL, Castro AF3, Feldman HI, et al. A new equation to estimate glomerular filtration rate. *Ann Intern Med* (2009) 150(9):604–12. doi: 10.7326/0003-4819-150-9-200905050-00006

16. Bajema IM, Wilhelmus S, Alpers CE, Bruijn JA, Colvin RB, Cook HT, et al. Revision of the International Society of Nephrology/Renal Pathology Society classification for lupus nephritis: clarification of definitions, and modified National Institutes of Health activity and chronicity indices. *Kidney Int* (2018) 93(4):789–96. doi: 10.1016/j.kint.2017.11.023

17. Inthavong H, Vanarsa K, Castillo J, Hicks MJ, Mohan C, Wenderfer SE. Urinary CD163 is a marker of active kidney disease in childhood-onset lupus nephritis. *Rheumatol (Oxford)* (2023) 62(3):1335–42. doi: 10.1093/rheumatology/keac465

18. Chen J, Cui L, Ouyang J, Wang J, Xu W. Clinicopathological significance of tubulointerstitial CD68 macrophages in proliferative lupus nephritis. *Clin Rheumatol* (2022) 41(9):2729–36. doi: 10.1007/s10067-022-06214-y

19. Bräsen JH, Khalifa A, Schmitz J, Dai W, Einecke G, Schwarz A, et al. Macrophage density in early surveillance biopsies predicts future renal transplant function. *Kidney Int* (2017) 92(2):479–89. doi: 10.1016/j.kint.2017.01.029

20. Soares MF, Genitsch V, Chakera A, Smith A, MacEwen C, Bellur SS, et al. Relationship between renal CD68(+) infiltrates and the Oxford Classification of IgA nephropathy. *Histopathology* (2019) 74(4):629–37. doi: 10.1111/his.13768

21. Luan J, Fu J, Chen C, Jiao C, Kong W, Zhang Y, et al. LNA-anti-miR-150 ameliorated kidney injury of lupus nephritis by inhibiting renal fibrosis and macrophage infiltration. *Arthritis Res Ther* (2019) 21(1):276. doi: 10.1186/s13075-019-2044-2

22. Ding T, Yi T, Li Y, Zhang W, Wang X, Liu J, et al. Luteolin attenuates lupus nephritis by regulating macrophage oxidative stress via HIF-1α pathway. *Eur J Pharmacol* (2023) 953:175823. doi: 10.1016/j.ejphar.2023.175823

23. Jing C, Castro-Dopico T, Richoz N, Tuong ZK, Ferdinand JR, Lok L, et al. Macrophage metabolic reprogramming presents a therapeutic target in lupus nephritis. *Proc Natl Acad Sci U.S.A.* (2020) 117(26):15160–71. doi: 10.1073/pnas.2000943117

24. Chalmers SA, Chitu V, Herlitz LC, Sahu R, Stanley ER, Putterman C. Macrophage depletion ameliorates nephritis induced by pathogenic antibodies. *J Autoimmun* (2015) 57:42–52. doi: 10.1016/j.jaut.2014.11.007

25. Zhang W, Zhou Q, Xu W, Cai Y, Yin Z, Gao X, et al. DNA-dependent activator of interferon-regulatory factors (DAI) promotes lupus nephritis by activating the calcium pathway. *J Biol Chem* (2013) 288(19):13534–50. doi: 10.1074/jbc.M113.457218

26. Devarapu SK, Kumar Vr S, Rupanagudi KV, Kulkarni OP, Eulberg D, Klussmann S, et al. Dual blockade of the pro-inflammatory chemokine CCL2 and the homeostatic chemokine CXCL12 is as effective as high dose cyclophosphamide in murine proliferative lupus nephritis. *Clin Immunol* (2016) 169:139–47. doi: 10.1016/j.clim.2016.07.003

27. Liu H, Diao C, Wu C, Xia L, Duan H, Fang F, et al. Anti-macrophage-derived chemokine antibody relieves murine lupus nephritis. *Rheumatol Int* (2011) 31(11):1459–64. doi: 10.1007/s00296-010-1499-x

28. Hu L, Hu J, Chen L, Zhang Y, Wang Q, Yang X. Interleukin-22 from type 3 innate lymphoid cells aggravates lupus nephritis by promoting macrophage infiltration in lupus-prone mice. *Front Immunol* (2021) 12:584414. doi: 10.3389/fimmu.2021.584414

frontiers | Frontiers in Immunology

TYPE Original Research
PUBLISHED 15 April 2024
DOI 10.3389/fimmu.2024.1300457

OPEN ACCESS

EDITED BY
Francesca Wanda Rossi,
University of Naples Federico II, Italy

REVIEWED BY
Kezhen Yang,
Zhejiang University, China
Umesh Kumar,
University of Innsbruck, Austria

*CORRESPONDENCE
Ling Wang
wl.medstat@qq.com
Chen Li
lc.biosta@qq.com

†These authors have contributed equally to this work

RECEIVED 23 September 2023
ACCEPTED 05 April 2024
PUBLISHED 15 April 2024

CITATION
Wang W, Huang M, Ge W, Feng J, Zhang X, Li C and Wang L (2024) Identifying serum metabolite biomarkers for autoimmune diseases: a two-sample mendelian randomization and meta-analysis. *Front. Immunol.* 15:1300457. doi: 10.3389/fimmu.2024.1300457

Identifying serum metabolite biomarkers for autoimmune diseases: a two-sample mendelian randomization and meta-analysis

Wenwen Wang[1†], Manli Huang[1†], Wei Ge[2], Junling Feng[1], Xihua Zhang[3], Chen Li[1*] and Ling Wang[1*]

[1]Department of Health Statistics, School of Preventive Medicine, Ministry of Education Key Lab of Hazard Assessment and Control in Special Operational Environment, Fourth Military Medical University, Xi'an, Shaanxi, China, [2]Department of Field and Disaster Nursing, Fourth Military Medical University, Xi'an, Shaanxi, China, [3]Department of Neurological Intensive Care Rehabilitation, Xi'an International Medical Center Hospital, Xi'an, Shaanxi, China

Background: Extensive evidence suggests a link between alterations in serum metabolite composition and various autoimmune diseases (ADs). Nevertheless, the causal relationship underlying these correlations and their potential utility as dependable biomarkers for early AD detection remain uncertain.

Objective: The objective of this study was to employ a two-sample Mendelian randomization (MR) approach to ascertain the causal relationship between serum metabolites and ADs. Additionally, a meta-analysis incorporating data from diverse samples was conducted to enhance the validation of this causal effect.

Materials and methods: A two-sample MR analysis was performed to investigate the association between 486 human serum metabolites and six prevalent autoimmune diseases: systemic lupus erythematosus (SLE), rheumatoid arthritis (RA), inflammatory bowel disease (IBD), dermatomyositis (DM), type 1 diabetes (T1D), and celiac disease (CeD). The inverse variance weighted (IVW) model was employed as the primary analytical technique for the two-sample MR analysis, aiming to identify blood metabolites linked with autoimmune diseases. Independent outcome samples were utilized for further validation of significant blood metabolites. Additional sensitivity analyses, including heterogeneity test, horizontal pleiotropy test, and retention rate analysis, were conducted. The results from these analyses were subsequently meta-integrated. Finally, metabolic pathway analysis was performed using the KEGG and Small Molecule Pathway Databases (SMPD).

Results: Following the discovery and replication phases, eight metabolites were identified as causally associated with various autoimmune diseases, encompassing five lipid metabolism types: 1-oleoylglycerophosphoethanolamine, 1-arachidonoylglycerophosphoethanolamine, 1-myristoylglycerophosphocholine, arachidonate (20:4 n6), and glycerol. The meta-analysis indicated that three out of these eight metabolites exhibited a protective effect, while the remaining five were designated as pathogenic factors. The robustness of these associations was further confirmed through sensitivity analysis. Moreover, an investigation into

metabolic pathways revealed a significant correlation between galactose metabolism and autoimmune diseases.

Conclusion: This study revealed a causal relationship between lipid metabolites and ADs, providing novel insights into the mechanism of AD development mediated by serum metabolites and possible biomarkers for early diagnosis.

KEYWORDS

autoimmune diseases, biomarkers, Mendelian randomization, meta-analysis, serum metabolites

Introduction

Autoimmune diseases (ADs) arise from a disruption in the immune system's ability to tolerate self-antigens and its subsequent response to these antigens (1). Epidemiological studies have shown a gradual increase in the global prevalence of ADs over the years (2). Individuals with ADs often experience persistent symptoms that significantly impact their quality of life, leading to long-term debilitation, organ dysfunction, reduced work productivity, and substantial medical expenses (3). These challenges not only affect patients but also have a significant impact on the social and economic aspects of society. Despite numerous studies attempting to understand the nature of ADs, their pathogenesis and risk factors remain elusive (4–6). The preclinical phase of AD is characterized by an initial asymptomatic stage of varying duration, followed by non-specific signs and symptoms. Most AD cases have a considerably long prodromal phase with either no symptoms or mild symptoms that can last for several years. Additionally, various inflammatory manifestations may occur and often intensify in the months to years leading up to a clinical diagnosis (7, 8). A promising strategy for preventing ADs could involve addressing adverse lifestyle factors through public health initiatives at the population level, highlighting the importance of effective early screening strategies for ADs.

Controlling inflammation remains a pivotal aspect of ADs therapy, including conditions like RA (9) and SLE (10). A growing body of evidence indicates that immune cell regulatory mechanisms are intricately connected to metabolic pathways, with various subpopulations of immune cells having distinct metabolic requirements that are influenced by disease-specific microenvironments (11–13). For example, effector T cells rely on glycolytic metabolism for their development and function, while regulatory T cells primarily use lipids to generate energy through mitochondrial beta-oxidation, leading to ATP production via oxidative phosphorylation (OXPHOS) (14). Furthermore, inflammatory M1 macrophages predominantly utilize glycolysis, whereas anti-inflammatory M2 macrophages favor beta-oxidation (15). In ADs, the autoinflammatory response is characterized by high energy consumption and involves processes such as adipogenesis, altered glucose metabolism, and glutamine metabolism, resulting in a shift from OXPHOS to glycolysis for energy production. In specific scenarios, such as in RA, hypoxia in the synovial membrane triggers chronic mitochondrial hyperpolarization in T cells, leading to increased glucose metabolism and ATP synthesis (16). Additionally, chronically activated T cells in individuals with SLE and lupus-prone mice exhibit heightened mitochondrial glucose oxidation and hyperpolarization. Individuals with multiple sclerosis (MS) have been found to have elevated plasma levels of acetoacetic acid, acetone, and 3-hydroxybutyric acid, along with altered profiles of circulating lipids and lipoprotein metabolism (17, 18). Additionally, metabolites are compounds that act as intermediates or end products in metabolic pathways. Detecting metabolites in the bloodstream provides a robust method for early disease diagnosis, owing to their accessibility and ease of detection (19). Consequently, understanding the underlying mechanisms linking metabolic changes to AD pathogenesis could lead to the development of new early screening tools and therapeutic interventions (3).

Indeed, while cross-sectional studies have identified associations between blood metabolites and ADs, establishing causality remains a crucial area of investigation. Further research is required to determine if altered metabolite levels are a cause or consequence of ADs. Longitudinal studies incorporating both healthy individuals and those at risk of developing ADs could help elucidate the causal relationships between metabolites and ADs. In addition, interventional studies that examine the effects of lifestyle changes on metabolite levels and disease outcomes may also provide valuable insights into the role of metabolites in ADs. Ultimately, determining the causality of metabolite-AD associations could lead to the identification of novel therapeutic targets and personalized treatment options for individuals with ADs.

The advancement of high-throughput techniques has enabled the simultaneous assessment of a broad range of circulating serum metabolites and genotyping in parallel populations. Genome-wide association studies (GWAS) provide valuable insights into the complex molecular interactions between environmental and

genetic factors in disease pathogenesis. Numerous single nucleotide polymorphisms (SNPs) have shown strong associations with serum metabolites. Mendelian randomization (MR), an epidemiological statistical analysis tool, utilizes genetic variation linked to exposure as an unconfounded instrumental variable to assess the relationship between exposure and clinical disease outcomes (20). GWAS have expanded to include metabolic phenotypes, producing maps of genetically determined metabolites (GDM) (21). Several MR causal analyses have explored the link between blood metabolite levels and disease. For example, Huang et al. used MR to identify key pathogenic metabolites influencing both T2D and more severe COVID-19 phenotypes in obese patients (22). Additionally, a study from *Gu* (23) investigated the causal relationship between osteoarthritis at different sites and blood metabolites. Likewise, *Xiao et al.* discovered 11 metabolites with a significant causal association with anxiety disorders (24). Furthermore, *Angela Ge et al.* conducted an MR analysis to examine the causal relationship between serum metabolite composition and MS (25). However, there is still a lack of in-depth research on large-scale blood metabolites and multiple autoimmune diseases.

Therefore, the main aim of this research was to investigate the potential causal relationships between serum metabolites through a two-sample MR and meta-analysis involving six autoimmune diseases: SLE, RA, IBD, DM, T1D, and CeD.

Materials and methods

Ethics statement and MR design

This research exclusively relied on publicly available GWAS data, and all necessary ethical approvals, participant consents, and permissions from the original GWAS study are readily accessible. No new data were collected for this investigation, rendering any additional ethical approvals unnecessary.

The flow chart outlining the methodology of this study is illustrated in Figure 1. In summary, serum metabolites function as exposure indicators, while ADs represent the outcomes. Rigorous inclusion and exclusion criteria guided the selection of single nucleotide polymorphisms (SNPs) strongly associated with specific serum metabolites as instrumental variables (IVs). The samples included both discovery and validation cohorts, with significant associations identified through various sensitivity analyses. Furthermore, reverse MR analysis was performed to mitigate potential confounding effects of ADs on the pathogenic serum metabolites.

Serum metabolites datasets

The metabolomics GWAS server (http://metabolomics.helmholtz-muenchen.de/gwas/) was utilized to obtain genetic association information for serum metabolites. Shin et al. conducted a study involving a total of 7,824 participants from two European population cohorts (21). This cohort consisted of 1,768 participants from the German KORA F4 study and 6,056 from the UK Twin study. Fasting serum samples were subjected to non-targeted mass spectrometry analysis. Following stringent quality control measures, the researchers successfully identified 486 metabolites (comprising 309 known metabolites and 177 unknown metabolites) that demonstrated a genetic influence on serum metabolites. The 309 known metabolites were systematically categorized into eight distinct biochemical classifications, encompassing lipids, peptides, nucleotides, energy, amino acids, cofactors and vitamins, carbohydrates, and exogenous substances.

Autoimmune disease discovery and validation datasets

During the discovery phase, GWAS summary statistics were obtained from publicly available analyses for each of the six AD

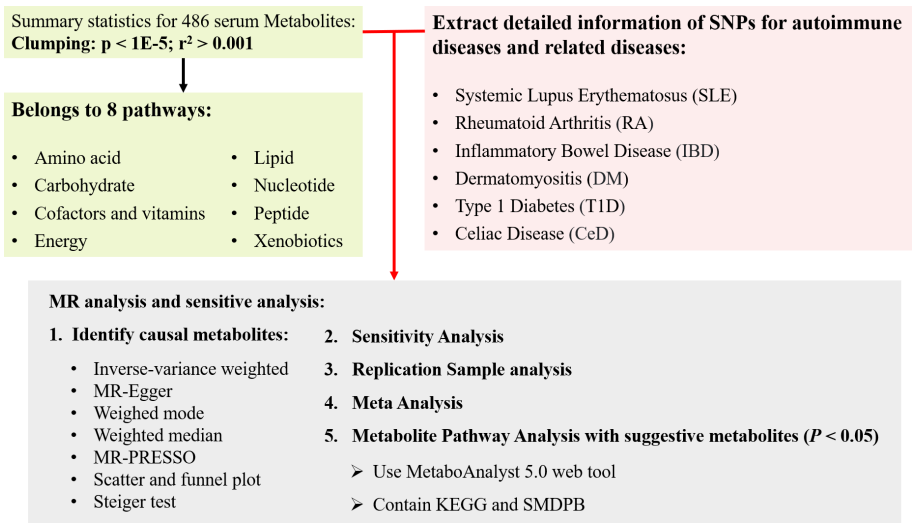

FIGURE 1
The overview of the research workflow.

types and Table 1 provides additional information about the dataset. The GWAS meta-analysis for IBD encompassed 12,882 cases of European ancestry and 21,770 controls (26). Furthermore, for RA, the pooled data included information from 1,605 RA cases and 359,589 controls of European ancestry across 18 studies. In the case of SLE, the pooled measurements were derived from a GWAS meta-analysis involving 1,311 SLE cases and 1,783 controls of European ancestry (27). Additionally, summary statistics for T1D were sourced from the discovery phase of the latest GWAS meta-analysis conducted in Finland, involving 1,238 T1D cases and 183,185 controls of European ancestry. Similarly, pooled measurements of DM) were obtained from the GWAS and included 208 DM cases and 213,145 controls of European ancestry. Finally, a pooled genetic measure for CeD was derived from a GWAS meta-analysis that incorporated data from five different sample groups, comprising 4,533 CeD cases and 10,750 controls (28).

Furthermore, repeated MR analyses were performed on 486 serum metabolites to facilitate validation of the findings in the discovery database. The validated outcome samples for IBD comprised 25,042 case and 25,042 control samples of European ancestry (29). The validation samples for RA were sourced from the UK Biobank, which included 1,401 cases and 359,793 control samples. Similarly, the local replicate samples for SLE consisted of 7,219 and 15,991 control GWAS of European ancestry (30). Moreover, the duplicate samples for T1D and DM were obtained from the FINNGEN database, which included 5,928 and 201 cases and 183,185 and 172,834 control samples. The GWAS meta-analysis of replicated CeD samples involved 12,041 CeD cases and 12,228 controls of European ancestry (31). More specific information about the data used can be found in Supplementary Table 1.

Quality control measures were implemented for SNPs to ensure the validity of the analysis. These measures involved removing non-dual allelic SNPs, SNPs with duplicate rsID or base pair locations, SNPs lacking rsID, SNPs with strand ambiguous alleles, SNPs not present in Phase 3 of the 1000 Genomes Project, SNPs with base pair locations or allele mismatches in Phase 3 of the 1000 Genomes Project, SNPs with interpolated information scores below 0.9, and all SNPs located on the *X* and *Y* chromosomes.

Selection of instrumental variables

In this MR analysis, the selection of IVs was predicated on three fundamental assumptions. SNPs associated with the metabolite at the genome-wide significance threshold $P < 1 \times 10^{-5}$ were chosen as potential IVs. Eligible IVs were further refined through a series of quality control steps. Initially, SNPs with inconsistent alleles (e.g., T/C vs. T/G) between the exposure and outcome samples were excluded. Subsequently, palindromic alleles (A/T or G/C) were also excluded. Thirdly, SNPs within each metabolite were subjected to clumping in order to retain only independent variants. The linkage disequilibrium (LD) threshold for clumping was set at $R^2 < 0.001$ within a 500 kilobase distance, utilizing the European-based 1,000 Genome Projects reference panel for estimation. Finally, the MR pleiotropy residual sum and outlier (MR-PRESSO) test was utilized to detect potential horizontal pleiotropy, addressing it by removing outliers (32). To quantitatively ascertain the strength of the selected SNPs as instruments, the ratio of phenotypic variation explained for each metabolite and *F*-statistics of the instrument were calculated (33):

$$F = \frac{r^2(n-1-k)}{(1-r^2)k}$$

Here, r^2 represents the part of the exposure variance explained by IVs, n is the sample size, and k is the number of IVs. A statistic of. signifies a lack of strong evidence for weak instrument bias (34). In this research, IVs with F -statistics less than 10 were classified as weak IVs and were thus excluded. Finally, a coordinated analysis was performed to compare exposure and outcome SNP alleles, excluding the alleles with intermediate effects ($EAF > 0.42$) of palindromic SNPs or SNPs with incompatible alleles (35).

TABLE 1 Autoimmune diseases GWAS samples used in this study.

Stage	Trait	Consortium	N.case	N.controls	SNPs
Discovery	IBD	IIBDGC	12,882	21,770	12,716,084
	RA	UK Biobank	1,605	359,589	10,079,899
	SLE	IEU	1,311	1,783	489,877
	T1D	NA	9,266	15,574	12,783,129
	DM	FINNGEN	208	213,145	16,380,451
	CeD	NA	4,533	10,750	523,399
Validation	IBD	NA	25,042	25,042	9,619,016
	RA	UK Biobank	1,401	359,793	9,944,222
	SLE	NA	5,201	9,066	7,071,163
	T1D	FINNGEN	2,542	182,573	16,380,230
	DM	FINNGEN	201	172,834	16,380,281
	CeD	IEU	3,796	8,154	231,359

Mendelian randomization analysis

In this MR analysis, several tests were conducted to evaluate the causal relationship between metabolites and AD. These tests included fixed/random effects inverse variance weighting (IVW) tests (36), weighted median (WM) (37), and MR-Egger (38). The IVW method, known for providing the most accurate estimate for valid SNPs, was utilized as the primary analysis to assess the causal relationship between serum metabolites and ADs, with a significance level set at $P< 0.05$. Additionally, complementary analyses such as WM and MR-Egger were performed to enhance the confidence of the estimates and offer advantages under different assumptions. The WM method yields a consistent causal estimate when at least 50% of the weight comes from valid instrumental variables (37). On the other hand, the MR-Egger regression helps to address pleiotropy when all instrumental variables are invalid (30).

Sensitivity analysis

The IVW method provides a robust estimate of the causal effect of exposure when all three IV assumptions are met, and it is considered the most reliable MR method. However, if certain instrumental variables contradict the IV assumptions, the analysis may produce erroneous results. Therefore, the following sensitivity analyses were conducted: 1) *Cochrane's Q* test for IVW and MR-Egger was employed to investigate potential violations of the assumptions due to heterogeneity in the association among individual IVs (36). 2) The intercept estimate of horizontal pleiotropy in MR-Egger was used to assess any independent association of genetic variation with exposure and outcome. 3) Additional MR methods with varying modeling assumptions and strengths were used to enhance the stability and robustness of the results. 4) MR-PRESSO was utilized to identify outliers and correct for horizontal pleiotropy. 5) Individual SNP analysis and leave-one-out (LOO) analysis were employed to evaluate whether individual SNPs influenced the observed associations.

The following principles guided the identification of potentially suitable candidate metabolite IVs associated with ADs: 1) Ensuring amplitude and directional consistency across the results from the four MR analysis methods; 2) Confirming the absence of pleiotropy and heterogeneity; 3) Using LOO analysis to confirm the absence of any influential data points exerting substantial influence on the outcomes.

Genetic correlation and direction validation

The MR results may potentially generate false positives as a result of genetic correlations between traits (39). Throughout the process of IV selection, SNPs associated with ADs were deliberately excluded. Nonetheless, it is crucial to acknowledge that combinations of SNPs that are not significantly correlated with ADs could still contribute to the genetic predisposition for ADs (40). Furthermore, the Steiger test was utilized to ascertain whether reverse causality had an impact on the observed causality. This test evaluates whether the selected SNPs explain the variance in ADs more effectively than the identified metabolites. In cases where the collective SNPs were determined to not pose a genetic risk for ADs in comparison to the metabolites, the results indicated the absence of bias in causal inference (Steiger $P< 0.05$).

Meta-analysis and metabolic pathway analysis

The robustness of the candidate metabolites, identified based on the aforementioned criteria, was thoroughly assessed by replicating the IVW analysis in an additional six AD cohorts. In essence, the initial analysis employed GWAS datasets designated as discovery, while supplementary GWAS datasets were utilized for the replication analysis. A meta-analysis of two MR analyses was conducted to determine the serum metabolites with causal effects on ADs. This meta-analysis employed a random-effects IVW model using the meta package (41).

To identify the final candidates from the additional GWAS data of ADs, significant associations ($P_{IVW}< 0.05$) were evaluated through replication analysis and meta-analysis. MetaboAnalyst 5.0 (https://www.metaboanalyst.ca/) was employed for the metabolic pathway analysis of known metabolites. Two databases, namely the KEGG database and the Small Molecule Pathway Database (SMPDB), were utilized in this study. The significance threshold value for pathway analysis was set at 0.10.

Statistical analysis

The statistical analysis was conducted using R4.2.2 software, and the MR analysis was primarily performed using the TwoSampleMR (42) package. Additionally, error detection rate (false discovery rate; FDR) correction was employed to mitigate false positives in multiple tests. A given metabolite's estimated causal effect was considered statistically significant when it had an FDR< 0.05, it was considered statistically significant. The data and source code can be downloaded from https://github.com/wewen1996/Two-sample-Mendelian-Randomization-and-Meta-Analysis.

Results

Selection of instrumental variables

A total of 486 metabolites were selected, with the number of instrumental variables (IVs) ranging from 3 to 485, and a median of 27 (Supplementary Table 4). These IVs accounted for a variance in their corresponding metabolites ranging from 0.0082% to 188.8405%. The MR-PRESSO global test did not provide any evidence of pleiotropic effects ($P > 0.05$). Importantly, all the minimum F-statistics for the validity test exceeded 10, ranging

10.3389/fimmu.2024.1300457

from 17.64 to 21.00 (Supplementary Table 4). This indicates that weak instrument bias was unlikely to have occurred.

Causal effects of metabolites on autoimmune diseases

To gain a more comprehensive understanding of metabolic changes, this analysis excluded 177 unidentified metabolites and focused on the 309 metabolites with known structures and functions, estimating the causal relationship between these metabolites and six AD phenotypes using the selected IVs.

In the discovery phase, the first one or two serum metabolites most associated with the risk of CeD, DM, IBD, SLE, RA, SLE, and T1D were screened using six MR methods. Assumption checks were conducted for all 309 regulators to determine the most suitable analytical tools, with the IVW method being selected as the primary approach due to the absence of heterogeneity and weak instruments. Following multiple test adjustments using the false discovery rate (FDR) *P*-value threshold, eight metabolic exposures were identified as statistically significant at a threshold of P_{FDR}< 0.05 (Figure 2). It is noteworthy that exposure factors associated with CeD and RA, represented by SNPs 3 and 6, were incorporated into the results (Table 2). Despite the limited number of SNPs, which may lead to reduced statistical power or the presence of weak instrumental variables, subsequent statistical analysis confirmed that these two exposure factors met the criteria for strong instrumental variables, with their statistical power values aligning with the standard requirements for exposure factors. The statistical robustness of our findings aligns with the standard requirements for exposure factors, resulting in the retention of the results. These associations encompassed five metabolites from the lipid pathways, two from the lipid metabolism pathways, one from the amino acid pathways, and two from the xenobiotic pathways. Notably, our results revealed a substantial causal association between a heightened susceptibility to CeD and an elevated level of 1-oleoylglycerophosphoethanolamine (odds ratio [OR] = 11.271, 95% confidence intervals [CI]: 2.053-61.882, P = 0.005, P_{FDR} = 0.032). Furthermore, we observed that the onset of DM could elevate the level of betaine (OR = 0.014, 95% CI: 0.001-0.318, P = 0.007, P_{FDR} = 0.042). Additionally, 1-arachidonoylglycerophosphoethanolamine (OR = 0.411, 95% CI: 0.264-0.642, P = 9.034×10^{-5}, P_{FDR} = 5.420×10^{-4}) and arachidonate

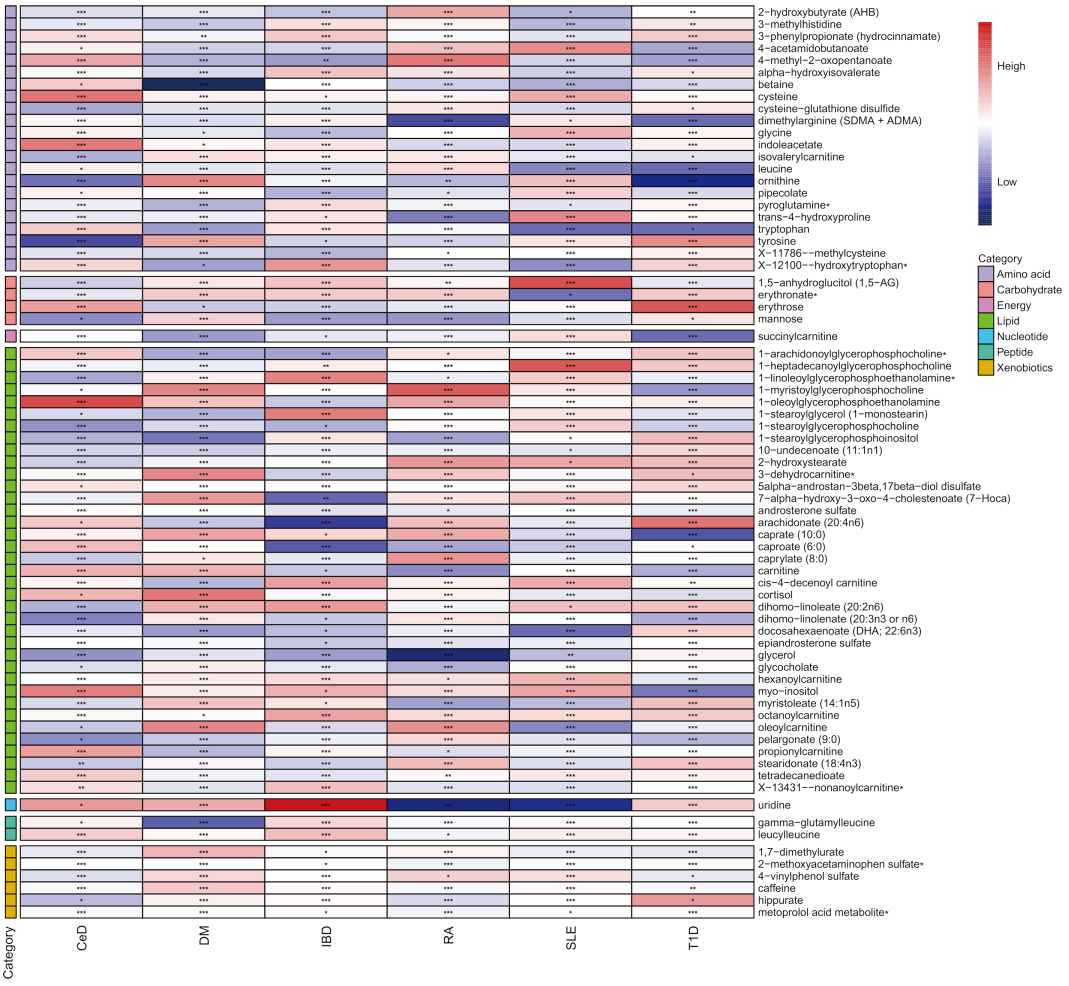

FIGURE 2
Heatmap of mendelian randomized association effect values for known metabolites with significant differences in phenotypic risk for six autoimmune diseases (from fixed effects IVW analysis). (*: P<0.05; **: P<0.01; ***: P<0.001).

10.3389/fimmu.2024.1300457

TABLE 2 Significant MR analysis results in the discovery samples.

Methods	Outcome	Exposure	Category	No. SNP	OR	95% CI	*P*	P_{FDR}
IVW	CeD	1-oleoylglycerophosphoethanolamine	Lipid	3	11.271	2.053-61.882	**0.005**	**0.032**
Weighted Median					10.380	1.255-85.843	0.030	0.060
MR-Egger					1.076	0.000-3.156	0.684	0.684
Simple Mode					21.886	1.015-471.939	0.144	0.215
Weighted Mode					7.261	0.516-102.194	0.238	0.286
MR-PRESSO					11.271	1.393-91.160	0.023	0.060
IVW	DM	betaine	Amino acid	22	0.014	0.001-0.318	**0.007**	**0.042**
Weighted Median					0.119	0.002-0.456	0.028	0.056
MR-Egger					0.002	0.000-3.585	0.121	0.242
Simple Mode					0.282	0.000-466.990	0.741	0.741
Weighted Mode					0.119	0.000-121.643	0.553	0.664
MR-PRESSO					0.014	0.000-0.422	0.014	0.042
IVW	IBD	1-arachidonoylglycerophosphoethanolamine	Lipid	26	0.411	0.264-0.642	**9.034×10^{-5}**	**5.420×10^{-4}**
Weighted Median					0.352	0.180-0.686	0.002	0.004
MR-Egger					0.143	0.044-0.465	0.004	0.004
Simple Mode					0.598	0.160-2.226	0.450	0.450
Weighted Mode					0.207	0.080-0.535	0.003	0.004
MR-PRESSO					0.411	0.253-0.669	3.511×10^{-4}	0.001
IVW	IBD	arachidonate (20:4n6)	Lipid	20	0.352	0.195-0.635	**5.132×10^{-4}**	**0.002**
Weighted Median					0.285	0.148-0.549	1.750×10^{-4}	0.001
MR-Egger					0.216	0.081-0.579	0.007	0.008
Simple Mode					0.596	0.124-2.856	0.525	0.525
Weighted Mode					0.255	0.128-0.509	0.001	0.002
MR-PRESSO					0.352	0.179-0.693	0.003	0.004
IVW	RA	1-myristoylglycerophosphocholine	Lipid	6	1.009	1.004-1.014	**0.001**	**0.003**
Weighted Median					1.010	1.003-1.017	0.005	0.010
MR-Egger					1.013	1.000-1.026	0.129	0.129
Simple Mode					1.010	1.000-1.020	0.105	0.126
Weighted Mode					1.010	1.002-1.018	0.050	0.075
MR-PRESSO					1.009	1.004-1.014	0.001	0.003
IVW	RA	glycerol	Lipid	18	0.991	0.986-0.997	**0.005**	**0.031**

(Continued)

TABLE 2 Continued

Methods	Outcome	Exposure	Category	No. SNP	OR	95% CI	*P*	P_{FDR}
Weighted Median					0.993	0.986-1.000	0.048	0.096
MR-Egger					1.000	0.988-1.012	0.972	0.972
Simple Mode					0.996	0.985-1.007	0.451	0.542
Weighted Mode					0.995	0.987-1.002	0.166	0.249
MR-PRESSO					0.991	0.985-0.998	0.012	0.037
IVW	SLE	2-methoxyacetaminophen sulfate	Xenobiotics	97	0.945	0.920-0.971	**4.008×10^{-5}**	**1.477×10^{-4}**
Weighted Median					0.943	0.907-0.980	0.003	0.006
MR-Egger					0.921	0.853-0.995	0.038	0.056
Simple Mode					0.903	0.811-1.006	0.066	0.079
Weighted Mode					0.935	0.862-1.014	0.104	0.104
MR-PRESSO					0.945	0.920-0.971	4.924×10^{-5}	1.477×10^{-4}
IVW	T1D	glycerol 2-phosphate	Xenobiotics	21	3.382	1.897-6.027	**3.599×10^{-5}**	**2.159×10^{-4}**
Weighted Median					1.980	0.894-4.382	0.092	0.184
MR-Egger					1.226	0.410-3.668	0.718	0.718
Simple Mode					1.591	0.412-6.144	0.505	0.607
Weighted Mode					1.801	0.683-4.749	0.244	0.366
MR-PRESSO					3.382	1.757-6.509	2.654×10^{-4}	0.001

The bold font is the P-value of IVW algorithm, the main analysis method used in this study, and the P-value after FDR correction.

(20:4n6) (OR = 0.352, 95% CI: 0.195-0.635, $P = 5.132\times10^{-4}$, P_{FDR} = 0.002) were found to be elevated in IBD patients. The causal effect of RA on 1-myristoylglycerophosphocholine was estimated at 1.009 (95% CI: 1.004-1.014, P = 0.001, P_{FDR} = 0.003), while glycerol was estimated at 0.991 (OR = 0.991, 95% CI: 0.986-0.997, P = 0.005, P_{FDR} = 0.031). A positive association was observed between 2-methoxyacetaminophen sulfate and SLE (OR = 0.945, 95% CI: 0.920-0.971, $P = 4.008\times10^{-5}$, $P_{FDR} = 1.477\times10^{-4}$). Conversely, glycerol 2-phosphate exhibited a negative association with T1D (OR = 3.382, 95% CI: 1.897-6.027, $P = 3.599\times10^{-5}$, P_{FDR} = 2.159×10^{-4}). It is important to note that the values of OR of 1-myristoylglycerophosphocholine, glycerol, and 2-methoxyacetaminophen sulfate are very close to 1, implying a limited clinical impact despite their statistical significance. This discrepancy can potentially be attributed to substantial variation in the independent variable. Therefore, it is imperative to conduct further *in vivo* investigations to ascertain the clinical relevance of these three exposure factors.

Sensitivity analyses

To mitigate the horizontal pleiotropy of MR estimates, sensitivity analyses were conducted. A series of six tests were implemented for metabolites associated with multiple SNPs54t, including fixed-/random-effects IVW test, weighted median method, and MR-Egger regression test. The results of these sensitivity analyses for eight metabolites and their causal relationships with ADs are detailed in Table 2, demonstrating statistically significant findings. Notably, robust causality was frequently observed to exhibit statistical significance in two additional MR tests (P< 0.05), specifically the weighted median test and the MR-PRESSO test. All eight pairs of associations are considered robust (Table 2). Furthermore, an evaluation for potential horizontal pleiotropy in all these associations was undertaken using the MR-Egger intercept term and the MR-PRESSO global test (Supplementary Table 3). Heterogeneity among SNPs related to each metabolite was assessed using Cochrane's Q test. In instances where heterogeneity was detected (P< 0.05), the random-effects IVW test was employed to offer a more conservative yet robust estimate. Additionally, scatter plots (Figure 3) and funnel plots (Figure 4) were utilized to rule out potential outliers and horizontal pleiotropy for all identified metabolites. Furthermore, the LOO analysis did not reveal substantial variation in estimates of causality between the eight metabolites and ADs, suggesting that none of the identified causal relationships were influenced by any single instrumental variable (Supplementary Figure 1).

Moreover, the significant metabolites identified in the initial discovery stage were successfully replicated in independent replication datasets. The replication MR analysis followed the same rigorous methodology as applied in the discovery samples, ensuring consistency and reliability in the findings.

Replication and meta-analysis

To enhance the robustness of the estimates, validated metabolites showing significant causal links with ADs were subjected to validation in independent replication samples (Supplementary Table 2). As anticipated, similar patterns were observed for the identified metabolites in replicated GWAS data for ADs. Notably, beyond SLE and T1D, statistical significance persisted for other AD-related metabolites even following FDR correction ($P< 0.05$). The meta-analysis further confirmed the impact of eight blood metabolites on ADs (Figure 5). Specifically, genetic predisposition for elevated levels of betaine (OR 0.02, 95% CI: 0.002-0.16, $P = 0.0004$), 1-arachidonoylglycerophosphoethanolamine (OR 0.50, 95% CI: 0.37-0.67, $P< 0.0001$), arachidonate (20:4n6) (OR 0.43, 95% CI: 0.29-0.66, $P< 0.0001$), glycerol (OR 0.99, 95% CI: 0.987-0.995, $P< 0.0001$), and 2-methoxyacetaminophen sulfate (OR 0.96, 95% CI: 0.93-0.98, $P = 0.0006$) was associated with reduced susceptibility to ADs. Conversely, genetic predisposition for higher levels of 1-oleoylglycerophosphoethanolamine (OR 12.39, 95% CI: 3.29-46.75, $P = 0.0002$), 1-myristoylglycerophosphocholine (OR 1.0089, 95% CI: 1.0051-1.0126, $P< 0.0001$), and glycerol 2-phosphate (OR 3.45, 95% CI: 2.24-5.31, $P< 0.0001$) was associated with increased susceptibility to ADs. Importantly, the Steiger test results confirmed the accuracy of the selected IVs, with a P-value significantly below 0.05.

Metabolic pathway analysis

Although shared causal metabolites were identified across the six ADs, it is noteworthy that five out of the eight significantly associated metabolites were lipid compounds. This finding suggests the potential role of lipids as key components among plasma metabolites associated with ADs. Analysis based on the eight identified metabolites revealed enrichment of six metabolic pathways in the KEGG and SMPDB databases, which could play a role in the pathogenesis of ADs (Supplementary Tables 5, 6). Within the KEGG database, these metabolites were primarily enriched in pathways such as glycerolipid metabolism, galactose metabolism, glycine, serine, and threonine metabolism, biosynthesis of unsaturated fatty acids, glycerophospholipid metabolism, and arachidonic acid pathways. Particularly noteworthy was the significant enrichment of glycerolipid metabolism pathway with a P-value below 0.05, indicating its potential relevance to common ADs. In contrast, analysis using the SMPDB database showed enrichment of metabolites in pathways including betaine, glycerolipid, galactose, methionine, glycine, serine, and arachidonic acid metabolism.

Discussion

The early-stage symptoms of ADs often go unnoticed, with the detection of antibodies being relatively costly (43). As a result, patients are frequently diagnosed when they have already reached an advanced and irreversible stage of the disease. Early screening for ADs can serve as a proactive measure, alerting individuals at risk to consider lifestyle adjustments and prioritize efforts to prevent

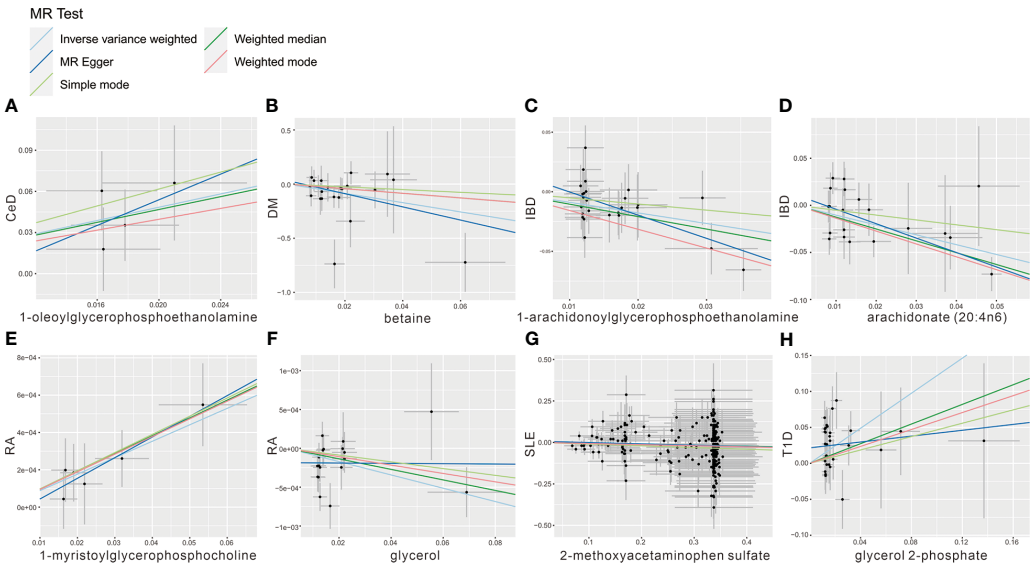

FIGURE 3
Scatter plot showing the genetic associations of seven metabolites on the risk of 6 AD phenotypes. **(A)** 1-oleoylglycerophosphoethanolamine on CeD, **(B)** betaine on DM, **(C)** 1-arachidonoylglycerophosphoethanolamine on IBD, **(D)** arachidonate (20:4n6) on IBD, **(E)** 1-myristoylglycerophosphocholine on RA, **(F)** glycerol on RA, **(G)** 2-methoxyacetaminophen sulfate on SLE, **(H)** glycerol 2-phosphate on T1D.

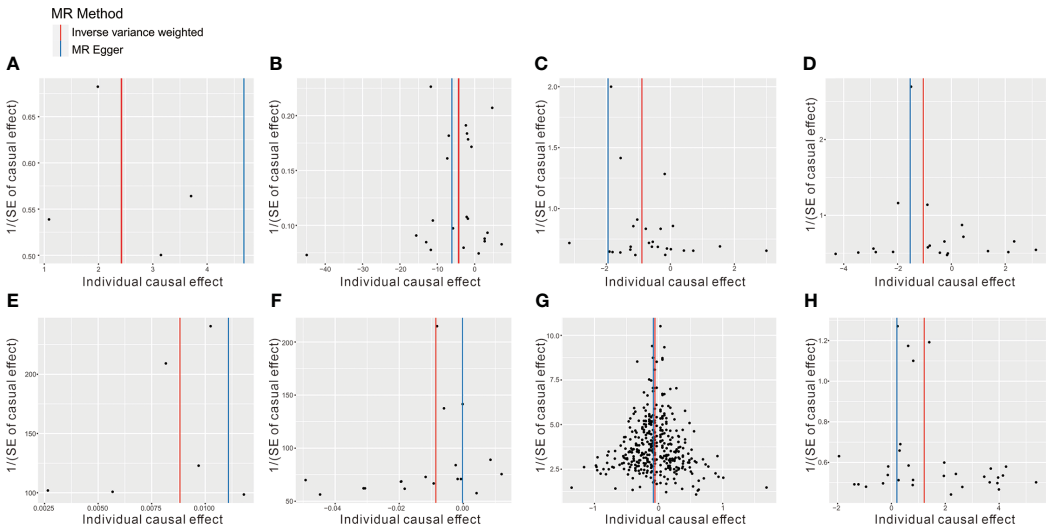

FIGURE 4
The funnel plot represents IVs for each significant causal association between metabolites and OA phenotypes. **(A)** 1-oleoylglycerophosphoethanolamine on CeD, **(B)** betaine on DM, **(C)** 1-arachidonoylglycerophosphoethanolamine on IBD, **(D)** arachidonate (20:4n6) on IBD, **(E)** 1-myristoylglycerophosphocholine on RA, **(F)** glycerol on RA, **(G)** 2-methoxyacetaminophen sulfate on SLE, **(H)** glycerol 2-phosphate on T1D.

disease progression (44). Serum metabolites, which are relatively easy to obtain and can be detected using less invasive methods, can serve as biomarkers for the early screening of ADs. However, prior MR studies examining the relationship between ADs and serum metabolites were limited to specific GWAS samples, lacking replication and integrated analyses (45). Therefore, in order to obtain more robust results, MR and meta-analyses were conducted to evaluate the association between serum metabolites and ADs.

Blood, recognized as a reliable source for assessing metabolite levels, contains numerous detectable metabolites and can be easily obtained in substantial sample sizes, facilitating the screening of circulating risk markers for AD. This two-sample MR study represents a significant advancement in elucidating the causal relationship between 73 metabolites and six AD phenotypes. Eight of these metabolites exhibited strong associations that persisted even after correction for multiple testing, underscoring their promise as dependable biomarkers or targets for therapeutic intervention. These results were substantiated through sensitivity analyses, bolstering their reliability. This study provides further analytical perspectives on the impact of gene-environment interactions in the development of ADs. Delving into the functional implications of these metabolites within metabolic pathways may pave the way for future precision medicine strategies. Furthermore, this study in question affirmed the presence of an AD-specific metabolic profile and identified critical metabolites and metabolic pathways causally associated with the development of ADs.

Over the past decade, numerous studies have underscored the close relationship between AD onset and human metabolism. This association is evident not only through its co-occurrence with various symptoms of metabolic disorders but also due to the emergence of metabolite-related dysfunctions within immune cells in metabolomics studies (46–49). Furthermore, research has demonstrated that intracellular metabolism can significantly impact the state of immune cells, suggesting potential avenues for developing novel therapeutic targets to counter dysfunctional antigen-induced immune responses in ADs, which are closely linked to blood metabolite concentrations. Published research has illuminated the role of L-Arginine in regulating T cell metabolism, thereby influencing T cell differentiation and outcomes (50). Additionally, studies have revealed the protective function of Selenium-GPX4 on follicular helper T cells (51). Notably, in the study, five out of the eight metabolites identified as causally associated with the pathogenesis of ADs belong to the category of lipid metabolites, including 1-oleoylglycerophosphoethanolamine, 1-arachidonoylglycerophosphoethanolamine, arachidonate (20:4n6), 1-myristoylglycerophosphocholine, and glycerol. Circulating lipids play a significant role in immune cell function. Lipid uptake or efflux influences cellular lipid burden and function, which is particularly notable in autoimmunity, where dyslipidemia and cardiovascular complications are common. The metabolism of lipids is crucial in a range of ADs (52–54). Elevations in both cell membrane glycosphingolipids and cholesterol are associated with heightened T cell and B cell receptor signaling, leading to activation and inflammation. Immune cells generate lipoxins, resolvins, and protectins through the enzymatic conversion of omega-3 fatty acids, playing a role in resolving inflammation and restoring tissue homeostasis. Their levels are linked to reduced joint pain in patients with RA and are decreased in experimental models of RA with persistent joint inflammation (52).

Lysophospholipids, characterized by a single fatty acid, play a role in regulating the five primary indicators of inflammation: *rubor* (redness), *tumor* (swelling), *calor* (fever), *dolor* (pain), and *functio laesa* (loss of function) (55). Currently, research mainly focuses on lysophospholipic acid (LPA) and sphingosine 1-phosphate (S1P) among lysophospholipids. Advances in lysophospholipid research

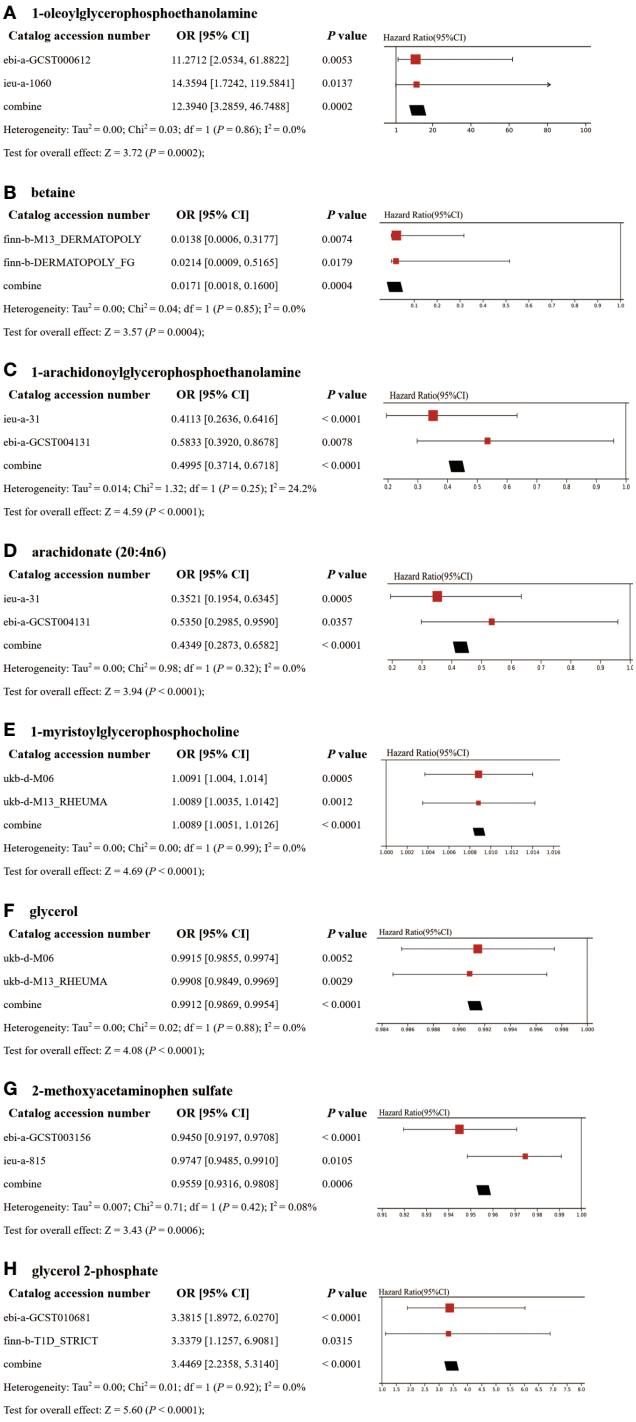

FIGURE 5
Meta-analysis of significantly associated (IVW derived P< 0.05) between metabolites and CeD **(A)**, DM **(B)**, IBD **(C–D)**, RA **(E–F)**, SLE **(G)**, and T1D **(H)**. 95% CI, 95% confidence interval; OR, odds ratio.

have led to the development of novel treatment strategies for ADs, with numerous therapies currently in the early stages of development for various conditions, including fibrotic disorders, vascular diseases, and cancer. Among the two types of lysophospholipids, our research results indicate that 1-oleoylglycerophosphoethanolamine plays a protective role in CeD, while 1-myristoylglycerophosphocholine provides protection in RA. Several observational and experimental studies have reported the involvement of lysophospholipids in regulating immune cells. Lysophospholipids are involved in the resolution processes that counteract the protective mechanisms of normal inflammation. For example, lysophospholipids can influence the activity of traditional regulators of vascular permeability, such as histamine, serotonin, and bradykinin, to positively or negatively control vasodilation,

vasoconstriction, and vascular leakage. G-protein-coupled S1PRs expressed by endothelial cells mediate vasodilation and inhibit vascular leakage by promoting the assembly of adherens junctions. On the other hand, vascular smooth muscle expresses Gq- and G12/13-coupled S1PRs and LPARs, which induce vasoconstriction and promote vascular leakage under inflammatory conditions. Additionally, lysophospholipids also regulate hematopoietic and immune cells during inflammation. Platelet aggregation, neutrophil phagocytosis, macrophage fate switching, innate immunity, natural killer cell release into circulation, and the trafficking and tissue residence of adaptive (T and B) cells are all regulated by lysophospholipid signaling via G protein-coupled receptors (GPCRs), impacting inflammatory and resolution responses (55). Although the two metabolites identified in this study have not been extensively investigated, they hold great research potential considering the function of relatively mature lysophospholipids in the immune process.

Moreover, our study identified two arachidonic acids, 1-arachidonoylglycerophosphoethanolamine and arachidonate (20:4n6), which showed a significant causal association with the onset and progression of IBD, highlighting their potential role in promoting susceptibility to this condition. Arachidonic acid is converted into active metabolites by enzymes such as cyclooxygenase (COX), lipoxygenase, and cytochrome P450 (CYP). Downstream eicosanoid signaling can directly impact the metabolism of immune cell subsets by regulating PPAR, controlling the liver X receptor (LXR), and mediating anti-inflammatory effects. Prostaglandin signaling can either stimulate or inhibit the anti-inflammatory ability of PPARγ to counteract NF-κB in various immune cells (52). Additionally, eicosanoids produced by arachidonic acid metabolism are crucial mediators of inflammation, and some of their metabolic network proteins have become important targets for anti-inflammatory drug design (56). Among these metabolites, prostaglandin E2 (PGE2) is the most widely studied in IBD, with elevated levels observed in individuals with active ulcerative colitis (57). Recent research has highlighted the involvement of the 12-lipoxygenase pathway, one of the metabolic pathways of AA, in intestinal inflammation (58). Although the pro-inflammatory effect of arachidonic acid in the pathogenesis of IBD is established, the clinical utilization of non-steroidal anti-inflammatory drugs (NSAIDs) to block its metabolites suggests that its mechanism of action needs further investigation (59). Moreover, while 1-arachidonoylglycerophosphoethanolamine is associated with dermatologic diseases, and arachidonate (20:4n6) is linked to various ADs, their potential role in IBD has not been previously documented. Given the close relationship between lipid metabolites and the development of IBD, further research on these two metabolites may represent a promising avenue for future investigation.

Another significant finding from our study is the detrimental effect of 2-methoxyacetaminophen sulfate in SLE, while glycerol 2-phosphate demonstrates a protective effect in T1D. It is noteworthy that both of these metabolites are classified as xenobiotics, which are foreign substances not naturally present in the body. Exogenous metabolism, as a crucial pathway in the body, plays a vital role in regulating and detoxifying such chemicals to prevent potential harm caused by environmental substances. Specifically, 2-methoxyacetaminophen belongs to the class of acetamides and is a paracetamol sulfate derivative with a methoxy group substitution at position 3 (60). On the other hand, glycerol 2-phosphate is a bacterial metabolite produced during a metabolic reaction within Escherichia coli (61). The discovery of xenobiotics further emphasizes the intricate relationship between ADs, heredity, and the environment. It highlights the need for future research on ADs to move beyond solely focusing on individual genetic or environmental factors in isolation. Instead, it suggests that the pathogenesis of ADs likely arises from complex interactions between genes and the environment.

Furthermore, the study findings indicated that betaine serves as a pathogenic risk factor for DM. Betaine is acknowledged for its essential roles as an osmoprotectant and methyl group donor in physiological processes. Numerous pieces of evidence have highlighted the anti-inflammatory properties of betaine in various conditions, including obesity, diabetes, cancer, and Alzheimer's disease (62). Surprisingly, limited research has explored the impact of betaine on DM specifically. Given the well-known anti-inflammatory attributes of betaine, there is a clear necessity for further investigation to uncover the precise mechanisms through which betaine influences the development of DM.

In this study, we identified metabolic pathways that play a causal role in the development of ADs. Some of these pathways have been extensively studied experimentally and are well-documented to contribute to the pathogenesis of ADs. Moreover, our analysis of KEGG and SMPDB data revealed a robust association between the pathogenesis of ADs and glycerolipid metabolism, as well as galactose metabolism pathways. Furthermore, it was observed that the differentiation and function of immune cells involved in the inflammatory response are intricately linked to the process of glycerol and lactose metabolism (63–65). These findings suggest that targeting this interconnected metabolic network could offer a promising approach for intervening in the autoimmune state and ultimately treating ADs.

The present study offers several notable advantages. Firstly, its main strength lies in the broad range of genetic variables considered to investigate the association between blood metabolites and various phenotypes of ADs. Specifically, this study encompassed a comprehensive panel of 486 metabolites, excluding those yet to be identified. Additionally, genetic variables for each AD were sourced from two separate datasets, and a meta-analysis was conducted to combine the analytical outcomes from these dual databases. This approach enabled a relatively comprehensive and systematic analysis of the metabolic profile associated with the development of ADs. Secondly, the utilization of the MR Design in this study significantly mitigated issues related to reverse causality and residual confounding factors. The extensive sensitivity analysis effectively accounted for potential influences of variable polymorphisms. Consequently, the inference of a causal relationship between metabolites and the risk of ADs in this study is considered robust.

However, the study also has certain limitations. Firstly, the MR analysis was based on blood metabolomics data, and although it identified some serum metabolites with a causal relationship to ADs, further clinical empirical studies are needed to identify more promising biomarkers and potential drug targets. Secondly, the metabolite data predominantly originated from European

populations, limiting the generalizability of these findings to different ethnic groups. Thirdly, while this study encompassed a relatively comprehensive metabolite profile, the functions and mechanisms of certain metabolites in the context of disease remain incompletely understood. This limitation affects the full interpretation of the results of this MR analysis.

Conclusion

In summary, this study presents a systematic MR and meta-analysis utilizing GWAS data to evaluate the causal relationship between serum metabolites and various AD phenotypes. It offers preliminary evidence for the impact of circulatory metabolic disorders on AD risk. By employing the IVW method and conducting multiple sensitivity analyses, robust causal relationships were established between eight metabolites and six AD phenotypes. Furthermore, the analysis of metabolic pathways revealed that these eight metabolites are enriched in six significant metabolic pathways. Our findings suggest that elevated levels of lipid metabolites may contribute to the development of ADs. This implies that specific metabolites and genetic susceptibilities may serve as biomarkers for the risk of ADs, potentially enabling earlier diagnosis and more effective treatment options.

Data availability statement

The original contributions presented in the study are included in the article/Supplementary Material. Further inquiries can be directed to the corresponding authors.

Author contributions

WW: Conceptualization, Data curation, Software, Writing – original draft, Writing – review & editing. MH: Data curation, Investigation, Methodology, Writing – original draft. WG: Investigation, Methodology, Supervision, Writing – review & editing. JF: Data curation, Supervision, Writing – review & editing. XZ: Methodology, Software, Writing – review & editing. CL: Formal analysis, Supervision, Validation, Writing – review & editing. LW: Investigation, Software, Supervision, Writing – original draft, Writing – review & editing.

Funding

The author(s) declare that financial support was received for the research, authorship, and/or publication of this article. This research was supported by the National Natural Science Foundation of China (82373680, 82273728 and 82273729).

Acknowledgments

We appreciate all the consortium studies for making the summary association statistics data publicly available.

Conflict of interest

The authors declare that the research was conducted in the absence of any commercial or financial relationships that could be construed as a potential conflict of interest.

Publisher's note

Supplementary material

The Supplementary Material for this article can be found online at: https://www.frontiersin.org/articles/10.3389/fimmu.2024.1300457/full#supplementary-material

References

1. Wang L, Wang FS, Gershwin ME. Human autoimmune diseases: A comprehensive update. *J Intern Med*. (2015) 278:369–95. doi: 10.1111/joim.12395

2. Zhou Z, Liu H, Yang Y, Zhou J, Zhao L, Chen H, et al. The five major autoimmune diseases increase the risk of cancer: epidemiological data from a large-scale cohort study in China. *Cancer Commun (Lond)*. (2022) 42:435–46. doi: 10.1002/cac2.12283

3. Miller FW. The increasing prevalence of autoimmunity and autoimmune diseases: an urgent call to action for improved understanding, diagnosis, treatment, and prevention. *Curr Opin Immunol*. (2023) 80:102266. doi: 10.1016/j.coi.2022.102266

4. Brown GJ, Cañete PF, Wang H, Medhavy A, Bones J, Roco JA, et al. Tlr7 gain-of-function genetic variation causes human lupus. *Nature*. (2022) 605:349–56. doi: 10.1038/s41586-022-04642-z

5. Adil Harroud, Pernilla Stridh, Jacob L McCauley, Janna Saarela, Aletta M R van den Bosch, Hendrik J Engelenburg. Locus for severity implicates cns resilience in progression of multiple sclerosis. *Nature*. (2023) 619:323–31. doi: 10.1038/s41586-023-06250-x

6. Li Y, Ma C, Liao S, Qi S, Meng S, Cai W, et al. Combined proteomics and single cell rna-sequencing analysis to identify biomarkers of disease diagnosis and disease exacerbation for systemic lupus erythematosus. *Front Immunol*. (2022) 13:969509. doi: 10.3389/fimmu.2022.969509

7. Rafii MS, Aisen PS. Detection and treatment of alzheimer's disease in its preclinical stage. *Nat Aging*. (2023) 3:520–31. doi: 10.1038/s43587-023-00410-4

8. Frazzei G, van Vollenhoven RF, de Jong BA, Siegelaar SE, van Schaardenburg D. Preclinical autoimmune disease: A comparison of rheumatoid arthritis, systemic lupus erythematosus, multiple sclerosis and type 1 diabetes. *Front Immunol*. (2022) 13:899372. doi: 10.3389/fimmu.2022.899372

9. Smolen JS. Insights into the treatment of rheumatoid arthritis: A paradigm in medicine. *J Autoimmun*. (2020) 110:102425. doi: 10.1016/j.jaut.2020.102425

10. Lazar S, Kahlenberg JM. Systemic lupus erythematosus: new diagnostic and therapeutic approaches. *Annu Rev Med*. (2023) 74:339–52. doi: 10.1146/annurev-med-043021-032611

11. Martí ILAA, Reith W. Arginine-dependent immune responses. *Cell Mol Life Sci*. (2021) 78:5303–24. doi: 10.1007/s00018-021-03828-4

12. Patel CH, Leone RD, Horton MR, Powell JD. Targeting metabolism to regulate immune responses in autoimmunity and cancer. *Nat Rev Drug Discovery*. (2019) 18:669–88. doi: 10.1038/s41573-019-0032-5

13. Lim SA, Su W, Chapman NM, Chi H. Lipid metabolism in T cell signaling and function. *Nat Chem Biol*. (2022) 18:470–81. doi: 10.1038/s41589-022-01017-3

14. Gerriets VA, Rathmell JC. Metabolic pathways in T cell fate and function. *Trends Immunol*. (2012) 33:168–73. doi: 10.1016/j.it.2012.01.010

15. Mehla K, Singh PK. Metabolic regulation of macrophage polarization in cancer. *Trends Cancer*. (2019) 5:822–34. doi: 10.1016/j.trecan.2019.10.007

16. Rhoads JP, Major AS, Rathmell JC. Fine tuning of immunometabolism for the treatment of rheumatic diseases. *Nat Rev Rheumatol*. (2017) 13:313–20. doi: 10.1038/nrrheum.2017.54

17. Bhargava P, Fitzgerald KC, Calabresi PA, Mowry EM. Metabolic alterations in multiple sclerosis and the impact of vitamin D supplementation. *JCI Insight*. (2017) 2. doi: 10.1172/jci.insight.95302

18. Cocco E, Murgia F, Lorefice L, Barberini L, Poddighe S, Frau J, et al. (1)H-nmr analysis provides a metabolomic profile of patients with multiple sclerosis. *Neurol Neuroimmunol Neuroinflamm*. (2016) 3:e185. doi: 10.1212/nxi.0000000000000185

19. Baker SA, Rutter J. Metabolites as signalling molecules. *Nat Rev Mol Cell Biol*. (2023) 24:355–74. doi: 10.1038/s41580-022-00572-w

20. Birney E. Mendelian randomization. *Cold Spring Harb Perspect Med*. (2022) 12. doi: 10.1101/cshperspect.a041302

21. Shin SY, Fauman EB, Petersen AK, Krumsiek J, Santos R, Huang J, et al. An atlas of genetic influences on human blood metabolites. *Nat Genet*. (2014) 46:543–50. doi: 10.1038/ng.2982

22. Huang C, Shi M, Wu H, Luk AOY, Chan JCN, Ma RCW. Human serum metabolites as potential mediators from type 2 diabetes and obesity to covid-19 severity and susceptibility: evidence from mendelian randomization study. *Metabolites*. (2022) 12. doi: 10.3390/metabo12070598

23. Gu Y, Jin Q, Hu J, Wang X, Yu W, Wang Z, et al. Causality of genetically determined metabolites and metabolic pathways on osteoarthritis: A two-sample mendelian randomization study. *J Transl Med*. (2023) 21:357. doi: 10.1186/s12967-023-04165-9

24. Xiao G, He Q, Liu L, Zhang T, Zhou M, Li X, et al. Causality of genetically determined metabolites on anxiety disorders: A two-sample mendelian randomization study. *J Transl Med*. (2022) 20:475. doi: 10.1186/s12967-022-03691-2

25. Ge A, Sun Y, Kiker T, Zhou Y, Ye K. A metabolome-wide mendelian randomization study prioritizes potential causal circulating metabolites for multiple sclerosis. *J Neuroimmunol*. (2023) 379:578105. doi: 10.1016/j.jneuroim.2023.578105

26. Liu JZ, van Sommeren S, Huang H, Ng SC, Alberts R, Takahashi A, et al. Association analyses identify 38 susceptibility loci for inflammatory bowel disease and highlight shared genetic risk across populations. *Nat Genet*. (2015) 47:979–86. doi: 10.1038/ng.3359

27. Hom G, Graham RR, Modrek B, Taylor KE, Ortmann W, Garnier S, et al. Association of systemic lupus erythematosus with C8orf13-blk and itgam-itgax. *N Engl J Med*. (2008) 358:900–9. doi: 10.1056/NEJMoa0707865

28. Dubois PC, Trynka G, Franke L, Hunt KA, Romanos J, Curtotti A, et al. Multiple common variants for celiac disease influencing immune gene expression. *Nat Genet*. (2010) 42:295–302. doi: 10.1038/ng.543

29. de Lange KM, Moutsianas L, Lee JC, Lamb CA, Luo Y, Kennedy NA, et al. Genome-wide association study implicates immune activation of multiple integrin genes in inflammatory bowel disease. *Nat Genet*. (2017) 49:256–61. doi: 10.1038/ng.3760

30. Bentham J, Morris DL, Graham DSC, Pinder CL, Tombleson P, Behrens TW, et al. Genetic association analyses implicate aberrant regulation of innate and adaptive immunity genes in the pathogenesis of systemic lupus erythematosus. *Nat Genet*. (2015) 47:1457–64. doi: 10.1038/ng.3434

31. Trynka G, Hunt KA, Bockett NA, Romanos J, Mistry V, Szperl A, et al. Dense genotyping identifies and localizes multiple common and rare variant association signals in celiac disease. *Nat Genet*. (2011) 43:1193–201. doi: 10.1038/ng.998

32. Verbanck M, Chen CY, Neale B, Do R. Detection of widespread horizontal pleiotropy in causal relationships inferred from mendelian randomization between complex traits and diseases. *Nat Genet*. (2018) 50:693–8. doi: 10.1038/s41588-018-0099-7

33. Palmer TM, Lawlor DA, Harbord RM, Sheehan NA, Tobias JH, Timpson NJ, et al. Using multiple genetic variants as instrumental variables for modifiable risk factors. *Stat Methods Med Res*. (2012) 21:223–42. doi: 10.1177/0962280210394459

34. Pierce BL, Ahsan H, Vanderweele TJ. Power and instrument strength requirements for mendelian randomization studies using multiple genetic variants. *Int J Epidemiol*. (2011) 40:740–52. doi: 10.1093/ije/dyq151

35. Gill D, Brewer CF, Monori G, Trégouët DA, Franceschini N, Giambartolomei C, et al. Effects of genetically determined iron status on risk of venous thromboembolism and carotid atherosclerotic disease: A mendelian randomization study. *J Am Heart Assoc*. (2019) 8:e012994. doi: 10.1161/jaha.119.012994

36. Burgess S, Butterworth A, Thompson SG. Mendelian randomization analysis with multiple genetic variants using summarized data. *Genet Epidemiol*. (2013) 37:658–65. doi: 10.1002/gepi.21758

37. Bowden J, Davey Smith G, Haycock PC, Burgess S. Consistent estimation in mendelian randomization with some invalid instruments using a weighted median estimator. *Genet Epidemiol*. (2016) 40:304–14. doi: 10.1002/gepi.21965

38. Bowden J, Davey Smith G, Burgess S. Mendelian randomization with invalid instruments: effect estimation and bias detection through egger regression. *Int J Epidemiol*. (2015) 44:512–25. doi: 10.1093/ije/dyv080

39. O'Connor LJ, Price AL. Distinguishing genetic correlation from causation across 52 diseases and complex traits. *Nat Genet*. (2018) 50:1728–34. doi: 10.1038/s41588-018-0255-0

40. Hemani G, Tilling K, Davey Smith G. Orienting the causal relationship between imprecisely measured traits using gwas summary data. *PloS Genet*. (2017) 13:e1007081. doi: 10.1371/journal.pgen.1007081

41. Balduzzi S, Rücker G, Schwarzer G. How to perform a meta-analysis with R: A practical tutorial. *Evid Based Ment Health*. (2019) 22:153–60. doi: 10.1136/ebmental-2019-300117

42. Hemani G, Zheng J, Elsworth B, Wade KH, Haberland V, Baird D, et al. The mr-base platform supports systematic causal inference across the human phenome. *Elife*. (2018) 7. doi: 10.7554/eLife.34408

43. Konforte D, Diamandis EP, van Venrooij WJ, Lories R, Ward MM. Autoimmune diseases: early diagnosis and new treatment strategies. *Clin Chem*. (2012) 58:1510–4. doi: 10.1373/clinchem.2012.189480

44. López-Nevado M, González-Granado LI, Ruiz-García R, Pleguezuelo D, Cabrera-Marante O, Salmón N, et al. Primary immune regulatory disorders with an autoimmune lymphoproliferative syndrome-like phenotype: immunologic evaluation, early diagnosis and management. *Front Immunol*. (2021) 12:671755. doi: 10.3389/fimmu.2021.671755

45. Yu XH, Cao RR, Yang YQ, Lei SF. Identification of causal metabolites related to multiple autoimmune diseases. *Hum Mol Genet*. (2022) 31:604–13. doi: 10.1093/hmg/ddab273

46. Raza IGA, Clarke AJ. B cell metabolism and autophagy in autoimmunity. *Front Immunol*. (2021) 12:681105. doi: 10.3389/fimmu.2021.681105

47. Wójcik P, Gęgotek A, Žarković N, Skrzydlewska E. Oxidative stress and lipid mediators modulate immune cell functions in autoimmune diseases. *Int J Mol Sci*. (2021) 22. doi: 10.3390/ijms22020723

48. Wang G, Su Z, Li H, Xiao L, Li C, Lian G. The role of metabolism in th17 cell differentiation and autoimmune diseases. *Int Immunopharmacol*. (2022) 103:108450. doi: 10.1016/j.intimp.2021.108450

49. Wang Z, Long H, Chang C, Zhao M, Lu Q. Crosstalk between metabolism and epigenetic modifications in autoimmune diseases: A comprehensive overview. *Cell Mol Life Sci*. (2018) 75:3353–69. doi: 10.1007/s00018-018-2864-2

50. Geiger R, Rieckmann JC, Wolf T, Basso C, Feng Y, Fuhrer T, et al. L-arginine modulates T cell metabolism and enhances survival and anti-tumor activity. *Cell*. (2016) 167:829–42.e13. doi: 10.1016/j.cell.2016.09.031

51. Yao Y, Chen Z, Zhang H, Chen C, Zeng M, Yunis J, et al. Selenium-gpx4 axis protects follicular helper T cells from ferroptosis. *Nat Immunol*. (2021) 22:1127–39. doi: 10.1038/s41590-021-00996-0

52. Robinson G, Pineda-Torra I, Ciurtin C, Jury EC. Lipid metabolism in autoimmune rheumatic disease: implications for modern and conventional therapies. *J Clin Invest*. (2022) 132. doi: 10.1172/jci148552

53. Chandrashekara S, Dhote SV, Anupama KR. The differential influence of immunological process of autoimmune disease on lipid metabolism: A study on ra and sle. *Indian J Clin Biochem*. (2019) 34:52–9. doi: 10.1007/s12291-017-0715-9

54. Lei Y, Yang J, Li H, Zhong H, Wan Q. Changes in glucose-lipid metabolism, insulin resistance, and inflammatory factors in patients with autoimmune thyroid disease. *J Clin Lab Anal*. (2019) 33:e22929. doi: 10.1002/jcla.22929

55. Kano K, Aoki J, Hla T. Lysophospholipid mediators in health and disease. *Annu Rev Pathol*. (2022) 17:459–83. doi: 10.1146/annurev-pathol-050420-025929

56. de Boer SY, van Berge Henegouwen GP. [Eicosanoids and the gastrointestinal tract]. *Ned Tijdschr Geneeskd*. (1989) 133:870–3. doi: 10.1016/0016-5085(95)90296-1

57. Vong L, Ferraz JG, Panaccione R, Beck PL, Wallace JL. A pro-resolution mediator, prostaglandin D(2), is specifically up-regulated in individuals in long-term remission from ulcerative colitis. *Proc Natl Acad Sci U.S.A*. (2010) 107:12023–7. doi: 10.1073/pnas.1004982107

58. Mrsny RJ, Gewirtz AT, Siccardi D, Savidge T, Hurley BP, Madara JL, et al. Identification of hepoxilin A3 in inflammatory events: A required role in neutrophil migration across intestinal epithelia. *Proc Natl Acad Sci U.S.A.* (2004) 101:7421–6. doi: 10.1073/pnas.0400832101

59. Felder JB, Korelitz BI, Rajapakse R, Schwarz S, Horatagis AP, Gleim G. Effects of nonsteroidal antiinflammatory drugs on inflammatory bowel disease: A case-control study. *Am J Gastroenterol.* (2000) 95:1949–54. doi: 10.1111/j.1572-0241.2000.02262.x

60. Mrochek JE, Katz S, Christie WH, Dinsmore SR. Acetaminophen metabolism in man, as determined by high-resolution liquid chromatography. *Clin Chem.* (1974) 20:1086–96. doi: 10.1093/clinchem/20.8.1086

61. Yang K, Wang M, Metcalf WW. Uptake of glycerol-2-phosphate *via* the ugp-encoded transporter in escherichia coli K-12. *J Bacteriol.* (2009) 191:4667–70. doi: 10.1128/jb.00235-09

62. Zhao G, He F, Wu C, Li P, Li N, Deng J, et al. Betaine in inflammation: mechanistic aspects and applications. *Front Immunol.* (2018) 9:1070. doi: 10.3389/fimmu.2018.01070

63. Langston PK, Nambu A, Jung J, Shibata M, Aksoylar HI, Lei J, et al. Glycerol phosphate shuttle enzyme gpd2 regulates macrophage inflammatory responses. *Nat Immunol.* (2019) 20:1186–95. doi: 10.1038/s41590-019-0453-7

64. Ji Y, Gao Y, Chen H, Yin Y, Zhang W. Indole-3-acetic acid alleviates nonalcoholic fatty liver disease in mice via attenuation of hepatic lipogenesis, and oxidative and inflammatory stress. *Nutrients.* (2019) 11. doi: 10.3390/nu11092062

65. Leontiadis GI, Longstreth GF. Evolutionary medicine perspectives: helicobacter pylori, lactose intolerance, and 3 hypotheses for functional and inflammatory gastrointestinal and hepatobiliary disorders. *Am J Gastroenterol.* (2022) 117:721–8. doi: 10.14309/ajg.0000000000001681

Frontiers in Immunology

Explores novel approaches and diagnoses to treat immune disorders.

The official journal of the International Union of Immunological Societies (IUIS) and the most cited in its field, leading the way for research across basic, translational and clinical immunology.

Discover the latest Research Topics

See more →

Frontiers

Avenue du Tribunal-Fédéral 34
1005 Lausanne, Switzerland
frontiersin.org

Contact us

+41 (0)21 510 17 00
frontiersin.org/about/contact